STABILITY ANALYSIS OF PWM INVERTER-FED SYNCHRONOUS MOTORS

A thesis

submitted to the Department of Electrical and Electronic Engineering
in partial fulfilment of the requirements for the degree

of

DOCTOR OF PHILOSOPHY IN ELECTRICAL AND ELECTRONIC ENGINEERING
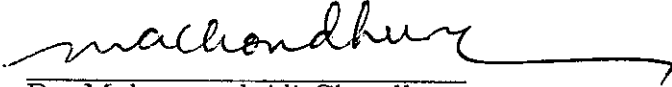
by

Md. Bashir Uddin

JANUARY, 1996

DEPARTMENT OF ELECTRICAL AND ELECTRONIC ENGINEERING
BANGLADESH UNIVERSITY OF ENGINEERING AND TECHNOLOGY
DHAKA

DECLARATION

I do hereby declare that this work has been done by me and neither this thesis nor any part thereof has been submitted elsewhere for the award of any degree or diploma except for publication.

Countersigned:
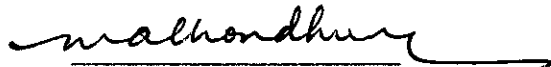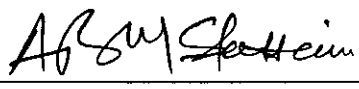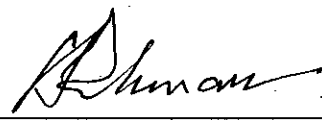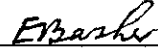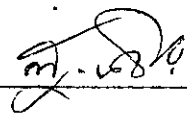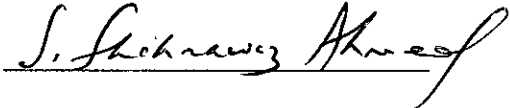
Dr. Mohammad Ali Choudhury

(Supervisor)

Md. Bashir Uddin

i

The thesis titled " Stability Analysis of PWM Inverter-Fed Synchronous Motors" submitted by Md. Bashir Uddin Roll number 901301F, session 1988-1989 to the Department of Electrical and Electronic Engineering of Bangladesh University of Engineering and Technology has been accepted as satisfactory for the partial fulfillment of the requirements for the degree of Doctor of Philosophy in Electrical and Electronic Engineering.

Board of Examiners

Dr. Mohammad Ali Choudhury
Associate Professor
Department of Electrical and Electronic Engineering
Bangladesh University of Engineering and Technology

Chairman
(*Supervisor*)

Dr. A. B. M. Siddique Hossain
Professor and Head of the
Department of Electrical and Electronic Engineering
Bangladesh University of Engineering and Technology

Member
(*Ex - officio*)

Dr. Syed Fazl - I Rahman
Professor
Department of Electrical and Electronic Engineering
Bangladesh University of Engineering and Technology

Member

Dr. Enamul Basher
Professor
Department of Electrical and Electronic Engineering
Bangladesh University of Engineering and Technolgy

Member

Dr. S. M. Lutful Kabir
Associate Professor.
Department of Electrical and Electronic Engineering
Bangladesh University of Engineering and Technology

Member

Dr. S. Shahnawaz Ahmed
Associate Professor
Department of Electrical and Electronic Engineering
Bangladesh University of Engineering and Technology

Member

Dr. K. M. Waliuzzaman
Professor
Department of Electrical and Electronic Engineering
Islamic Institute of Technology, Dhaka, Bangladesh and
former Professor of BIT Rajshahi, Bangladesh

Member
(*External*)

Dr. M. Azizur Rahman FIEEE, FIEE, FIEB
University Research Professor
Faculty of Science and Engineering
Memorial University of Newfoundland, Canada

Member
(*External*)

ACKNOWLEDGEMENTS

TABLE OF CONTENTS

Chapter 3: STABILITY ANALYSIS OF SYNCHRONOUS MOTORS

Chapter 4: STABILITY ANALYSIS OF PWM INVERTER-FED
             SYNCHRONOUS MOTOR OPERATION

LIST OF SYMBOLS

A   Slope of rising section of the carrier wave

A   State transition matrix

B   Slope of falling section of the carrier wave

B   Inverse matrix of co-efficient of the derivatives of **X**

E   Co-efficient matrix of the derivatives of **X**

E_c Magnitude of the carrier triangular wave

E_m Maximum voltage of modulating wave in SPWM

e_{xfd} Fictitious field voltage

f   Frequency

f_c Frequency of the carrier wave

f_m Frequency of the modulating wave

F   Co-efficient matrix of **X**

g   Gate function

H   Rotor inertia constant in second

I_s RMS value of the stator line current

I_a RMS current flowing through phase a

I_b RMS current flowing through phase b

I_c RMS current flowing through phase c

i_{ds} Direct axis stator current

i_{qs} Quadrature axis stator current

i_{kd} Direct axis damper current

i_{kq} Quadrature axis damper current

i_{fd} Field current

I   Identity matrix

K_i Constant of proportionality

L_d Direct axis synchronous inductance

L_q Quadrature axis synchronous inductance

L_{md} Direct axis mutual inductance

L_{mq} Quadrature axis mutual inductance

L_{is} Stator Leakage inductance

L_{kd} Sum of the direct axis damper and mutual inductance

L_{kq} Sum of the quadrature axis damper and mutual inductance

L_{fd} Sum of the field and mutual inductance

m   Modulation index

m(t)   Triangular sine modulated wave for multiple cycles

$m_T(t)$ Triangular sine modulated wave for one cycle

N   Number of pulse per cycle of modulating wave in triangular sine modulation

N_p Number of pulses in one cycle

p	Operator d/dt
R_s	Stator resistance
R_{kd}	Direct axis damper resistance
R_{kq}	Quadrature axis damper resistance
R_{fd}	Field resistance
S	Slope of the carrier wave
s(t)	Delta modulated wave for multiple cycles
$s_T(t)$	Delta modulated wave for one cycle
t	Time in second
t_i	Starting time of i-th pulse
t_{i+1}	Starting time of (i+1)th pulse
T	Period of one cycle
T_e	Electrical torque
T_L	Load torque
V_a	RMS voltage across phase a
V_b	RMS voltage across phase b
V_c	RMS voltage across phase c
V_s	RMS stator phase voltage
V	Maximum stator phase voltage
V_{f1}	Fundamental voltage of filter output
V_m	Maximum voltage of modulating wave
V_{m1}	Fundamental RMS voltage of modulator output
V_r	Reference sine wave in volt
v_{ds}	Direct axis stator voltage
v_{qs}	Quadrature axis stator voltage
v_{os}	0-axis stator voltage
v_{kd}	Direct axis damper voltage
v_{kq}	Quadrature axis damper voltage
v_{fd}	Field voltage
$\frac{V}{f}$	Volt/hertz
x_1, x_2	Intersecting points of modulating and carrier wave in SPWM
X_{ls}	Stator leakage reactance
X_d	Direct axis synchronous reactance
X_q	Quadrature axis synchronous reactance
X_{md}	Direct axis mutual inductive reactance
X_{mq}	Quadrature axis mutual inductive reactance
X_{kd}	Direct axis damper reactance
X_{kq}	Quadrature axis damper reactance
X_{fd}	Field reactance
Y_d	Direct-axis elements of admittance matrix
Y_q	Quadrature-axis elements of admittance matrix
Z_d	Direct axis impedance

Z_q Quadrature axis impedance

Z_s Input impedance

$Z_{d(oc)}$ Direct axis open-circuit impedance

$Z_{d(sc)}$ Direct axis short-circuit impedance

(Z+1)Number of cycles of the input signal to be simulated

δ Torque angle

δ_i Width of i-th pulse in SPWM

Δ Small increment

ΔV Window width in volt

λ Roots of the characteristic equation of A

λ_{ds} Directs axis flux linkage

λ_{qs} Quadrature axis flux linkage

λ_{os} 0-axis flux linkage

λ_{kd} Direct axis damper flux linkage

λ_{kq} Quadrature axis damper flux linkage

λ_{fd} Field flux linkage

ω Angular frequency of modulating wave

ω_b Base angular speed in rad/s

ω_e Synchronous speed in electrical rad/s

ω_r Rotor speed in electrical rad/s

ψ_{ds} Direct axis flux linkage per second

ψ_{qs} Quadrature axis flux linkage per second

ψ_{os} 0-axis flux linkage per second

ψ_{kd} Direct axis damper flux linkage per second

ψ_{kq} Quadrature axis damper flux linkage per second

ψ_{fd} Field flux linkage per second

θ Power factor angle

θ_e Position of synchronous reference axis

θ_i Middle position of i-th pulse

θ_r Rotor position

τ Time constant

$\tau_d{}'$ Direct axis transient time constant

$\tau_d{}''$ Direct axis subtransient time constant

LIST OF FIGURES

LIST OF TABLES

ABSTRACT

AC drives with variable loads operate at maximum efficiency when they are operated at adjustable speed. Speed variation of ac drives can most effectively be attained through change of supply frequency. Normal electromechanical frequency conversions do not meet the criteria of stiff frequency operation (i.e. frequency deviates with drive condition without any desirable control). Modern static converters, specially the inverters and the cycloconverters provide solution to the stiff frequency source. Pulse width modulated (PWM) inverters in this respect also allow one to change voltage and frequency of the supply in one conversion stage requiring minimum filters or no filters at all between a supply and the motor. This thesis aims at the stability analysis of conventional synchronous motors fed from PWM inverters. Particular emphasis is given to the stability study of motors supplied by inverters having open loop v/f control.

This thesis contributes in two major areas. These are the determination of switching points of PWM waveforms using a simplified technique and formulation of a new operating strategy for maintaining stability of synchronous motors fed from pulse width modulated inverters. This strategy at the same time enhances the load bearing capability of synchronous motors without loosing the synchronism.

New formulations in the form of algebraic equation have been proposed to find the switching waveforms of PWM converters. The approach is completely new and different from conventionally used simulation and numerical techniques, and provides a method of easier and computationally fast analysis of sine PWM waveforms. In the present thesis the proposed technique is utilized in the analysis of triangular sine PWM and delta sine PWM inverter waveforms for subsequent use in the stability analysis of inverter-fed synchronous motors.

Stability analysis of synchronous motors has been carried out extensively in this work considering the variable-voltage variable-frequency supply. The analysis is based on the small signal perturbation and eigenvalue search techniques. In the formulation of linear differential equations small signal perturbation of all the pos-

sible variables are considered. It has been established in this thesis that normal control scheme with rated v/f to ensure constant air gap flux is not appropriate for maintaining stability of synchronous motors in low frequency range. This research proposes a new control scheme with v/f ratio other than its rated value to maintain stability of synchronous motors fed from variable-voltage variable-frequency sources. The results of the analysis have also been substantiated by time domain analyses and experiments. A suitable modulation scheme is proposed in the thesis for an inverter-fed synchronous motor to obtain the desired v/f ratio in open-loop control to maintain the motor stability. The scheme has been developed from the results of inverter waveform analysis and the stability analysis of the synchronous motor.

Accurate representation of a machine by its parameters is necessary for the stability investigations. During this research, problems were encountered in measuring the required parameters from tests. It was found that available test methods were not equally applicable for large and small machines. Parameter estimation of synchronous machines is a topic of continuous research even today. Many of the methods proposed in recent years are computationally involved, requires costly instrumentation and are based on assumptions which are not valid under various operating conditions. A simple test method based on input impedance measurement has been developed. This method is applicable for finding the parameters of synchronous machines of any size.

CHAPTER 1

INTRODUCTION
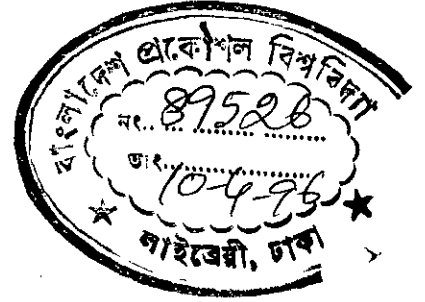
1.1 Introduction

Technological advancements in the field of solid-state static converters have widened the field of application of synchronous motors. Static converters having the capability to change voltage and frequency of available utility supply have extended the scope of synchronous motors to contribute significantly in adjustable-speed drive systems [1,2]. In some applications inverter-fed synchronous motors provide certain features that make them preferable to other motor drives [3]. Synchronous motors respond more quickly to change in load torque than any other ac motors. They can be used where simultaneous speed control of a number of motors are required. The variable-speed synchronous motor drive provides the means of simple precise position control [4]. Since a synchronous motor can conveniently be operated at nearly unity power factor the resulting commutation problem of converters is greatly alleviated. The operation of synchronous motors at nearly unity power factor decreases the armature copper loss and hence reduces inverter size [5,6]. Therefore, an inverter-fed synchronous motor has advantages of higher energy conversion than its counter-parts. In large installations where even a fraction of efficiency increase would save substantial amount of energy, synchronous motors are the better choice [7]. Synchronous motors supplied by static-converters make it possible to achieve good dynamic behaviour in high power range [8] of drive systems.

There are many problems associated with variable frequency drives which are still being investigated. The stability problem is one of the concerns in the design of

1

a synchronous motor drive system. As a result, the phenomenon of stability of synchronous motor drives has received a great deal of attention in the past and will continue to receive attention in future. In general, instability of a synchronous motor supplied from a voltage source inverter results either from inherent instability of the motor or from its interaction with the source for a given operating condition [9,10]. Motor parameters, source parameters, load characteristics and operating conditions all affect the system stability [11,12]. Use of solid-state converters improves the performance of synchronous motor drives and adds new dimensions to the stability study with other performance criteria of synchronous motors. Stability study requires investigation of solid-state inverter waveforms, inverter-motor-load modeling and solution of models by computer aided fast numerical techniques [13]. Each of these steps is involved and complicated in nature.

A synchronous motor fed from a pulse width modulated (PWM) inverter system must be operated within the range of stability limit to ensure reliable performance. The system instability might occur in the form of sustained speed oscillations or of complete loss of synchronism. The stability depends on system parameters and terminal constraints and the cause of instability of the inverter-fed synchronous motor may be minimized by introducing appropriate system damping through modification of these quantities. In some instances, it may be convenient to modify the system parameters so as to improve stability. The modification of system parameters of motor-inverter system is only possible in design and construction stage. However, in other applications it may be desirable to introduce system damping by controlling the effective value of the voltage applied to the stator [14]. It has been found that during low frequency operation a synchronous motor is lightly damped [5] which can cause sustained speed oscillations or lead to pulling out of step. The stability of a synchronous motor drive with simple frequency control [9] was analysed. It is possible to obtain stable, well damped response from such a drive provided that the steady-state torque does not change rapidly and the rate of change of frequency is

limited. At low frequencies there is a tendency towards greater instability, which can be explained qualitatively by observing that low frequency operation is equivalent to the operation at rated frequency with added armature resistance. The fact that increased armature resistance results in a more lightly damped-electromechanical system has been demonstrated by several authors [15].

The advent of solid-state inverters with improved modulation techniques extends the facilities of control of the voltage and frequency. One approach to improve the stability of synchronous motor is to introduce positive damping by simultaneous adjustment of the applied stator voltage and frequency. As this method uses control of both the voltage and the frequency the effective damping may be higher than the conventional methods for stabilizing the synchronous motor operation. Modern pulse width modulation technique as applied to the static inverter waveform modulation can meet the criteria needed for controlling voltage and frequency simultaneously.

The analysis of stability control can be carried out by employing the theory of small perturbation to the governing equations of synchronous motors. This analysis stems from the logical inference that in constant volt/hertz mode of synchronous motor operation the maximum torque limit can be enhanced by increasing the amplitude of the applied stator voltage and by decreasing frequency of the supply. Therefore, simultaneous increase in voltage and decrease in frequency can boost up the maximum torque limit which should be higher than that caused by either voltage change or frequency change individually.

1.2 Review of Sine PWM Techniques for Inverter Operation

Pulse width modulated (PWM) inverters are popular in ac drive systems. Normal voltage source inverters (VSI) and current source inverters (CSI) have the inconve-

niences of generating square waves at the output of the inverter containing undesired low frequency harmonics. They also need double power conversion process for simultaneous voltage and frequency control. These problems can be reduced by using pulse width modulated operation of VSIs or CSIs. In pulse width modulation technique the switches of power converters are operated at high frequencies according to a particular modulation mode so as to produce pulses of varying widths at the output of an inverter. The earliest modulation techniques applied to inverter operation are single pulse modulation and multiple pulse modulation [16-20]. These techniques are capable of providing inverter output voltages with low harmonic contents. As investigations continued single pulse and multiple pulse modulation techniques were replaced by the sine pulse width modulation [20,21]. Asynchronous and synchronous sine pulse width modulation schemes were used for switching the power converters [22]. For drive applications the fixed frequency modulation was found problematic at different operating frequencies. In order to overcome the drawbacks of ordinary sine pulse width modulation, variable ratio PWM scheme was introduced. Presently, three distinct sinusoidal pulse width modulation schemes are in use for inverter operation [22-26]. They are the (1) natural sampling method, (2) regular sampling method, and (3) optimal switching technique. In the first method a sine wave is compared with a high frequency triangular wave to determine the switching points of modulated waves. In the regular sampling technique, the sine wave is replaced by a sampled or a stepped sine wave and the switching points are determined from the crossover points of the carrier triangular wave with the stepped sine wave [27-29]. The third approach uses optimized switching technique based on certain performance criteria [30-32]. Due to the developments of microprocessor technology, the implementation of optimized pulse width modulation for switching inverters has become feasible [33-36]. Two types of PWM strategies have been used recently for inverter operation. They are bang-bang sampled PWM technique and the delta modulation (DM) technique. The principle of bang-bang sampling is based on the

4

motor output current hysteresis comparison with a reference waveform to generate the modulated waveforms [37-40]. The current hysteresis controller governs the converter switching pattern to maintain the mean value of the load current at the required value.

Delta modulation technique allows easy implementation retaining all the features of triangular carrier wave modulated sine PWM technique. It uses sine and carrier wave comparison to generate switching waveforms as that of triangular modulation [41,42]. Delta modulation technique is capable of operating in both PWM and square wave modes of operation. The closed loop arrangement of the delta modulator ensures that the polarity of the pulses are adjusted by the sign of the error signal which causes the locally decoded waveform to track the input signal. The primary delta modulation circuit consists of single integrator in its feedback path. Double integrator, multiple integrator or their counterparts in digital form have also been used in the feedback path for more precision in digitization [43]. Some investigators replaced the integrator of the feedback loop by RC network [44] giving rise to exponential delta modulated encoders. To suit the delta modulation technique for uncorrelated signal, sigma delta modulation was introduced [45,46]. This type of DM uses an integrator to integrate the input signal prior to DM coding. For using variable step size quantization to compete with pulse code modulation adaptive delta modulation (ADM) was suggested [47,48]. Two other kinds of delta modulation schemes encountered in literature are companded delta modulation and asynchronous delta modulation [49,50]. The companded DM technique uses compression of large signal levels as compared to the smaller ones. The asynchronous delta modulation systems have digital output quantized in amplitude but not in time. The rectangular wave delta modulation (RWDM) is an asynchronous DM technique which has been used for operation of single phase and three phase voltage source PWM inverters [51-53]. Introduction of tuned filter in the feedback path of RWDM has led to the benefit of waveform optimization by varying modu-

lation parameters [54,55], which allows the reduction of low order harmonics easily. Though various PWM techniques have been developed to meet the requirements of power converters, the switching point determination, analysis of harmonics of voltage and current waveforms and drive performances remained complicated and tedious.

1.3 Review of Stability Analysis of Conventional Synchronous Machines

1.3.1 Review of Machine Modeling

In the past, stable operation of synchronous machine had been the subject of numerous research. Study of the behaviour of synchronous machine requires deriving machine equations valid for general operating conditions. Classically, the theory of synchronous machine was presented in terms of traveling air-gap flux, current and emf waves [56]. This has the advantage of close adherence to physical realities within the machine and serves excellently the limited purpose of explaining the elementary steady-state operating characteristics. This approach becomes almost impractical when it becomes necessary to study the behaviour of the machine under transient conditions and its interactions with external network. The initial works on this subject dealt with formulating sets of differential equations having time varying coefficients. The equations, though linear for constant speed, but become nonlinear as speed variation is encountered and require numerical solution by computer [57]. However, it is possible to simplify these equations by a special technique which was introduced by Andre Blondel in 1904 and is known as the 'two-reaction theory' [58]. A simplification of synchronous machine modeling was obtained by the introduction of this theory. The method was examined in detail by Doherty and Nickle [69]. In the late 1920s, R.H. Park introduced a modified approach to electric machine analysis [60-61]. He formulated a change of variables which in effect replaced the

6

variables (voltages, currents, and flux linkages) associated with the stator windings of a synchronous machine by variables associated with fictitious windings rotating with the rotor. The rotor circuits of Park's model was modified by I.M. Canay in 1969 [62]. It was shown by Canay that the usual method for calculation of field current or field voltage did not agree with measurements. He proposed a synchronous machine model based on equivalent circuit with representation of field and damper circuit through introduction of a characteristic reactance which was independent of rotor reference frame quantities, replacing the armature leakage reactance.

1.3.2   Review on Determination of Machine Constants

Machine parameters are necessary in the formulation of modeling and control purposes of a machine. Design data and dimension of a machine govern these parameters significantly. Some of the parameters necessary for steady-state, transient and dynamic performance study can be obtained directly from design data. However, many of the parameters are to be found by tests and computational techniques on data obtained from tests. The test methods for cylindrical rotor and salient-pole machines are available in standard text books [63,64] and in recognized standards [65-67]. Among these tests the synchronous-impedance method, Old AIEE method, Potier triangle method, the magnetomotive-force method, ASA method, etc. are conventionally used for finding stator parameters required in steady-state analysis. Transient and dynamic performances, specially the stability analysis of synchronous machine, however, require the steady-state stator circuit parameters, magnetic coupling, and the rotor circuit parameters. The short-circuit test, in which the three terminals of an unloaded synchronous machine are short-circuited simultaneously, is a well established method to identify machines' transient characteristics and various time constants [68,69]. This method provides the information from which the parameters of the field winding and damper winding in the d-axis can be determined. There has been a general lack of procedure to find information on quadrature axis

7

parameters [70]. In small machines where stator resistance cannot be neglected compared to its leakage reactance, the short-circuit test method does not produce correct results [71]. In many cases it was thought that two rotor circuits in addition to the field winding circuit might better identify the direct axis equivalent circuit used in these studies. Similarly in the quadrature axis it has been felt that certain types of rotor design could call for as many as three equivalent rotor circuits, acknowledging the fact that no field winding exists in the quadrature axis. The identification of additional parameters is troublesome considering conventional short-circuit test data. The advent of digital computers made it possible to examine various models for greater accuracy of representation. One possible method by which the above problems could be alleviated is use of frequency response method to derive the accurate machine parameters [72]. A number of approaches were considered and measurements were carried out under loaded [73,74] and stand-still [75-79] conditions. The theory and practical details of this method for direct and quadrature axes model have been developed [80-82]. The stand-still frequency response test method requires costly and unconventional instrumentation. It has been practically realized that it is very difficult, if not impossible, to carry out these tests at higher current levels (50% - 100% of the rated current) for large machines due to the lack of large power supplies at low frequencies [83,84]. During test performance it has been noticed that application of variable field current in the measurement, quadrature axis mutual inductance changes more significantly than direct axis inductance [85]. Though frequency response method is a very useful tool in parameter identification for synchronous machines the difficulties of this method has led to researches on time domain identification of synchronous machine parameters from stand-still measurements. Recently a set of stand-still measurements for time-domain identification of linear model parameters for direct and quadrature axes of synchronous machine is proposed [86-88]. This method uses the topologies same as used in frequency response method and requires rigorous computation. The research and investigation

in this area are still continuing [89-94] and it is expected that newer test methods to identify synchronous machine parameters will be proposed in future.

1.3.3 Review of Stability Study

Stable operation of synchronous machines is an important subject of research. The articles of Nickle and Pierce [95], Wagner [96], Prescott and Richardson [97], Park [60,61], Lauder [98], Kron [99] etc. on this subject were to insure efficient and economic design and satisfactory operating conditions considering stability aspect of synchronous machines. The analysis of synchronous machine operation is complex and the number of variables under study is so large that the physical aspects of the problem have tended to become submerged completely in mathematical manipulation. The first of the major steps by which the designers were extricated from this maze of mathematical transformations was due to Park whose generalized two-reaction theory was applicable directly to the analysis of synchronous machine operations. The next major step was the application of the Kron's tensor analysis [100] by which the multiple mathematical equations could be handled in groups rather than individually. Calculations were still complex and time-consuming to permit their application to routine design problems. A solution to these difficulties appeared in the form of generalized equivalent circuits presented by Kron [100-102]. Applying Kron's formulae and equivalent circuits calculation of torque developed by a machine becomes easier. In the next phase, stability of conventional synchronous machine was assessed through observing the nature of torque developed by a machine. Two types of electrical torque are considered responsible for influencing the stability. These are the damping torque and synchronizing torque. Damping torque is defined as the torque in-phase with rotor speed while the synchronizing torque is in-phase with rotor angle. The operation of a synchronous machine is endangered when damping torque developed during hunting of the machine becomes negative. Reduction of synchronizing torque also affects the stable operation. As a result,

stability studies of synchronous machines were concentrated towards the investigation of the magnitude and characteristics of these torque. Literature survey on this area shows that a series of papers were published for evaluation of damping and synchronizing torque of ac machines [103-110]. It has been known for a long time that high armature resistance tends to produce a component of negative damping in synchronous motor or generator operating in parallel with other synchronous machines [95]. On the other hand, if the armature resistance becomes extremely high it contributes towards a positive torque [96]. In a study the starting problem of electrically connected synchronous machines in rest [111] neglecting rotor resistance showed that in some cases oscillations may be sufficiently amplified after synchronizing, to cause loss of synchronism. Later, a study with the inclusion of rotor resistance proved that damper windings were essential to prevent negative damping during the starting period [107]. A stability study of synchronous machine operation has been made by applying Routh's criterion to the linearized equations describing behaviour for small perturbations about a steady state operating point in reference [15]. In the study the stability boundaries have been examined in a torque vs. armature resistance plane for various machine parameters and constraints. The effect of frequency, load torque, rotor inertia, stator resistance , and other machine parameters and constraints have been included in the analysis.

1.4 Review of Stability Analysis of Variable-Speed Synchronous Machines

Application of static converter in synchronous motor drives has extended the scope of research on performance analysis, particularly in the field of stability of synchronous motor drives. In the synchronous machine family, stability analysis was first carried out on reluctance-synchronous machine in variable frequency operation [10]. In this analysis the equations which describe the behaviour of a reluctance

synchronous machine have been established and method of small displacement technique has been employed to linearize the motor equations. In a subsequent work several methods of stabilizing the reluctance machine during operation at low speeds were proposed [14]. The work showed that the system damping could be introduced in a synchronous reluctance machine by adjusting the effective value of the applied voltage in accordance with the change of speed. The report also suggested a control system which would continuously adjust the amplitude of the source voltage by employing controlled rectifiers. To investigate the feasibility of the synchronous machine as variable speed device, a detailed study has been carried out over a wide range of frequency in constant volt/hertz mode in reference [5]. The approach of analysis is similar to that as followed in the stability study of reluctance synchronous machine. The study reveals that when a synchronous machine is lightly damped it may be unstable at low speeds. However, a well-designed synchronous machine may generally be stable over all regions of operation. In this paper the authors also detailed the results of the effect of varying the excitation and the amplitude of the applied voltage on stability. The stability has been found to improve as a result of an increase in the amplitude of the stator voltage and decrease in the field excitation. The influence on stability of the machine due to changes of machine parameters were also investigated [5]. Steady-state properties and stability aspects of a variable-speed synchronous motor using current source inverter have been derived from an equivalent circuit model in reference [4]. The analysis shows that the motor should exhibit no spontaneous sustained oscillations when operated within its steady-state torque limits. This has been shown to be true even if the motor has saliency. The analysis also shows that the field winding enhances the damping of forced oscillations under loaded condition and quadrature axis damper winding is required to provide damping at no load. The stability behaviour of a synchronous motor drive was studied with simple frequency control in reference [9]. The study reveals that it is possible to obtain stable, well-damped response from

11

a drive provided that the steady-state load torque does not change rapidly and the rate of change of supply frequency is limited. If, however, the mechanical load torque contains transients and if quick response in speed is required, simple frequency control is inadequate. A step application of rated torque may readily result in loss of synchronism. Incorporation of power factor control can change the operating point stability of a synchronous motor drive which was investigated using a supply of current source inverter in reference [112]. In the study the direct axis damper windings have been found to be most effective in achieving stable operation. The size of the stable operating region remains relatively insensitive to damper resistance. Imperfections in the current source inverter has little effect on the stability boundaries but reduce the damping in the stable region.

1.5   Objectives of the Thesis

Stability of a synchronous motor is an important factor during its operation. Steady-state and dynamic stability studies are standard practices in the design and operation of a synchronous machine fed from utility power supply. Advent of solid-state static converters in variable-speed operation has regenerated the studies in all types of ac motors. Objectives of such studies aim at finding suitable operating conditions for motors in stable region when fed from static converters i.e., inverters, cycloconverters and controlled ac/ac converters. Synchronous motors are not exception to this. However, such an study in complete form is involved and tedious. As a result, investigations are usually carried out individually and the results of a number of studies are put together to formulate a control strategy.

So far stability study of static converter-fed variable-speed synchronous motors are carried out either in constant voltage mode or in constant volt/hertz mode. Constant voltage mode is not a practical situation in variable-speed ac drives. Constant volt/hertz mode is adopted to maintain constant air-gap flux in ac machines. How-

12

ever, constant volt/hertz mode at the rated value of v/f is not advantageous for stable operation of a synchronous motor, specially in low frequency range. In view of this, one of the main objectives of this research is to find a proper volt/hertz relationship that would result in an improved stable operation of synchronous motor fed from a PWM inverter. Analysis of a conventional synchronous motor fed from a PWM inverter having variable voltage and variable frequency operation has been undertaken in this thesis. Stability analysis of inverter-fed motors involves several steps. Identification of inverter fundamental voltage through harmonic analysis, choice of proper motor model with correct parameters of the motor and formulation and solution of linearized motor equations are necessary for this purpose.

Performance of inverter-fed synchronous motors can be studied with the knowledge of inverter voltages and the machine models. Representation of inverter voltages in mathematical form and finding the various voltage components of harmonics require solution of switching points of converter voltages. The analytical means of determining switching points of conventional triangular sine pulse width modulated and delta modulated inverter waveforms until now requires numerical solution or simulation. In this thesis, simplified techniques can be developed in the form of solution of algebraic equations to find the switching points of sine PWM inverter waveforms. The developed equations can be used in the harmonic analysis to find the fundamental voltage of inverters in order to incorporate the results in stability analysis.

Stability analysis of the conventional synchronous motor is carried out using machine model based on d-q axes transformation. Park's model can conveniently be used to obtain the performance equations of the synchronous motor. The equations are then linearized by employing small-signal perturbation theory. The stability is assessed by computing eigenvalues of the synchronous motor using a standard eigenvalue routine [114]. The results of the stability analysis obtained by eigen-

value technique can be justified by time domain simulation of the performance of the synchronous motor. The time responses due to change of voltage, frequency and load can be found from the solution of simultaneous differential equations by Runge-Kutta method.

Variable-voltage, variable-frequency ac drives are usually operated at a constant volt/hertz mode in order to maintain constant air-gap flux over the entire operating range. It is an established fact that in constant volt/hertz mode synchronous motor becomes lightly damped or may even become unstable during low frequency operation. Stability study described in this thesis stems mainly from the instability occurring at low frequency operation. The stability investigation of utility-fed synchronous motor reveals that an increase of applied voltage to the stator improves the stability while a decrease in frequency increases positive damping during normal operation of the synchronous motor. A combination of voltage and frequency other than constant volt/hertz improves the motor stability even at low frequency range of operation. Stability is investigated for different volt/hertz ratio. For a synchronous motor when incorporated with such a control, the variation of air-gap flux must be kept within its allowable linear range of operation.

In stability investigation of a synchronous motor the parameters of the machine have a significant role in obtaining accurate results. To determine the parameters of synchronous machines a modified input impedance measurement method has been developed. The modified method is simpler, requires commonly used instrumentation and is valid for all size of conventional synchronous machines.

1.6   Thesis Organization

Chapter 1 contains the introduction of the thesis and provides an idea of the proposed research described in five chapters. Various advantages and requirements of synchronous motor drives and basic concepts of their stability aspects are discussed

at the beginning of chapter 1. Literature reviews on PWM techniques, synchronous machine modeling including parameter estimation, and stability analysis of synchronous motor are presented in this chapter. Objectives of the present research are also incorporated.

Methods of simplified switching point determination of triangular sine pulse width modulation and delta modulation for inverter switching are proposed in chapter 2. Results of harmonic analysis of single-phase and three-phase inverter waveforms based on the proposed techniques are presented in chapter 2. The last section of chapter 2 includes the analysis of three-phase voltage waveforms of a PWM inverter. Expressions of line-to-line voltage, line-to-neutral voltage and d-q axes voltage are derived in this section by incorporating the proposed switching point formulation of pulse width modulation technique. The practical waveforms of a three-phase PWM inverter are presented to validate the results of theoretical waveform analyses.

Development of the synchronous machine model, particularly the Park's model is presented in chapter 3. Machine parameters required for this model have been determined by a modified test method outlined in Appendix B. The Park's synchronous machine model is then linearized employing small signal perturbation theory for subsequent stability analysis. Chapter 3 also investigates the influence of the change of terminal quantities on the stability of the synchronous motor fed from variable-voltage variable-frequency supply.

The results of chapter 3 leads to the formulation of volt/hertz relationships required for improved stable operation of PWM inverter-fed synchronous motors. The formulation of proposed volt/hertz relationship is presented in chapter 4 of this thesis. The analysis, theoretical and experimental verifications are presented in chapter 4. The new volt/hertz relationship proposed in this thesis is different from that used to maintain constant air-gap flux of the motor. It has been shown that the new technique would perform better in terms of stability of the experimental motor.

This chapter also illustrates the choice of PWM control strategy of an inverter to obtain the proposed volt/hertz control on the basis of the results of chapter 2. It has been shown that delta modulated inverters with proper parameter selection would provide the desired volt/hertz control by inverters in a very simple manner. The selection of modulator parameters for inverter control to achieve the proposed volt/hertz control is outlined in this chapter as well.

Chapter 5 of this thesis describes the salient features of the work and summarizes the contributions of this research with certain suggestions for future work on the subject.

CHAPTER 2

ANALYSIS OF STATIC PWM INVERTER WAVEFORMS

2.1 Introduction

A new approach for simplification of the analytical method of studying pulse width modulated (PWM) waveforms for triangular sine modulation and delta modulation is described in this chapter. Of various types of inverter waveform modulations, triangular sine pulse width modulation and delta modulation are extensively used in power converter applications. The analysis of pulse width modulation technique requires the knowledge of switching points of modulated waveforms. Analytical methods for determining switching points have been simplified for both the triangular sine modulation and delta modulation. The constant of proportionality encountered in the equation for switching point determination of triangular sine pulse width modulation is formulated based on certain approximations without loss of accuracy. The transcendental equation involved in determining the switching points of the delta modulated converter waveforms has been replaced by a simple algebraic equation.

The features of the PWM techniques as applied to the operation of inverters are investigated and summarized. Spectrum analysis has been carried out for modulated inverter waveforms. Analysis of $d - q$ axes inverter waveforms is provided in this chapter. The results of waveform analysis are subsequently used in the stability analysis of the PWM inverter-fed synchronous motor. Through harmonic analysis, proper choice of modulation parameters has been made for stability analysis.

17

2.2 Pulse Width Modulation Techniques

Modulation of static-converter waveforms is a common method of harmonic minimization and simultaneous voltage and frequency control. High frequency carrier modulation reduces filter size in converter applications. Sine pulse width modulation is the most common technique for obtaining switching waveforms of different types of static power converters. Triangular sine pulse width modulation and delta modulation are two common techniques used for generating modulated control signal for power converters.

Sinusoidal PWM technique also known as triangular modulation is very popular in industrial applications and is extensively reviewed in the literature. The principle of sinusoidal PWM technique is illustrated in Fig. 2.1. The sine modulating wave is compared with a triangular carrier wave, and the points of intersections of two waves determine the switching points of the inverter power devices. The frequency and amplitude of the modulating wave can be varied to obtain variable voltage and variable frequency output. On the other hand delta modulation is the simplest method for modulating an analog signal to its digital form. This is also a PWM scheme suitable for waveform modulation of power converters. The basic delta modulator consists of a comparator/quantizer and an integrator as shown in Fig. 2.2. The comparator at the input of this block compares the input signal with the stepwise approximation of the input signal. The quantizer quantizes the error signal according to the sign of the error signal to produce the positive and negative pulses of the modulated wave. The function of the integrator in the modulator is to reconstruct the input signal from the output modulated signal. Thus input to the integrator is the modulated waveform. The integrator acts as a low-pass filter and estimates the modulating signal. The waveforms of delta modulation scheme are illustrated in Fig. 2.3.

(a)

(b)
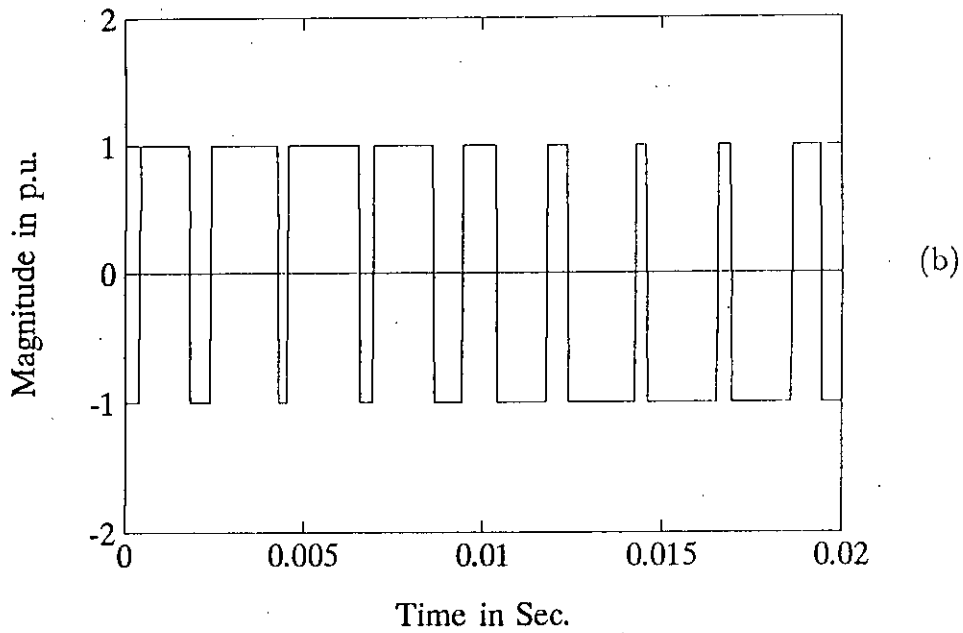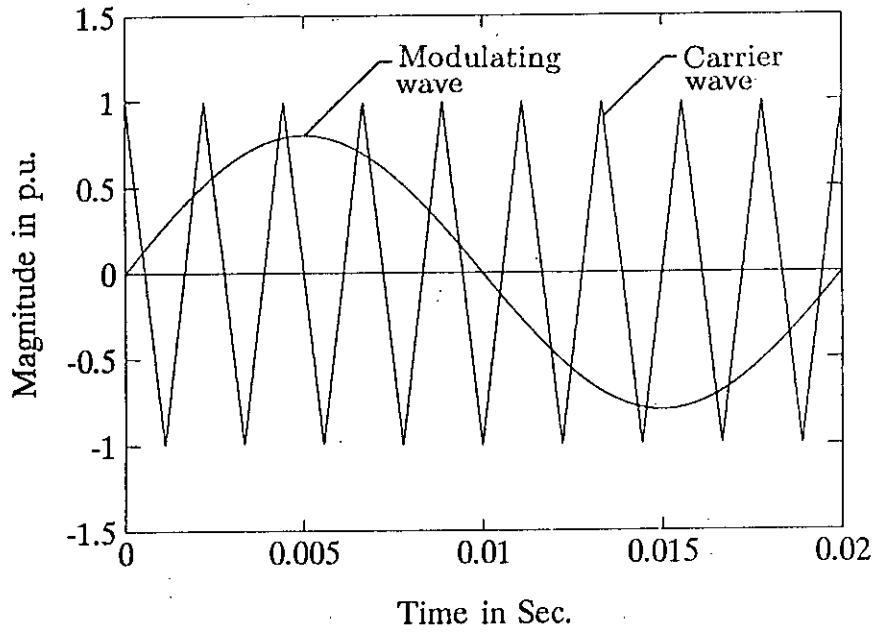
Figure 2.1:   Illustration of triangular sine pulse width modulation:
(a) modulating wave and triangular carrier wave;
(b) modulated wave.
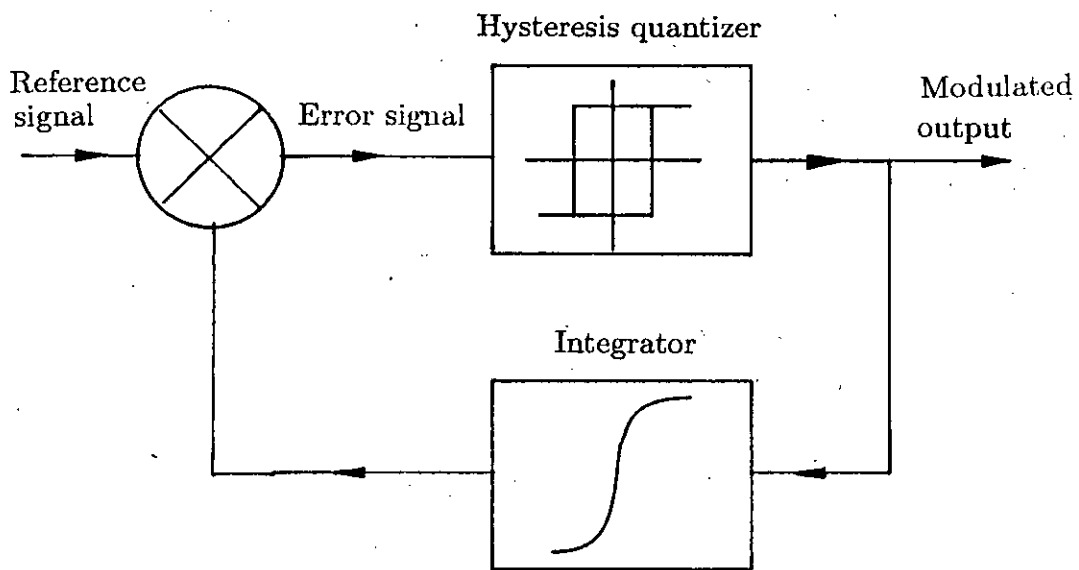
Figure 2.2:   Block diagram of delta modulation technique.

(a)

(b)
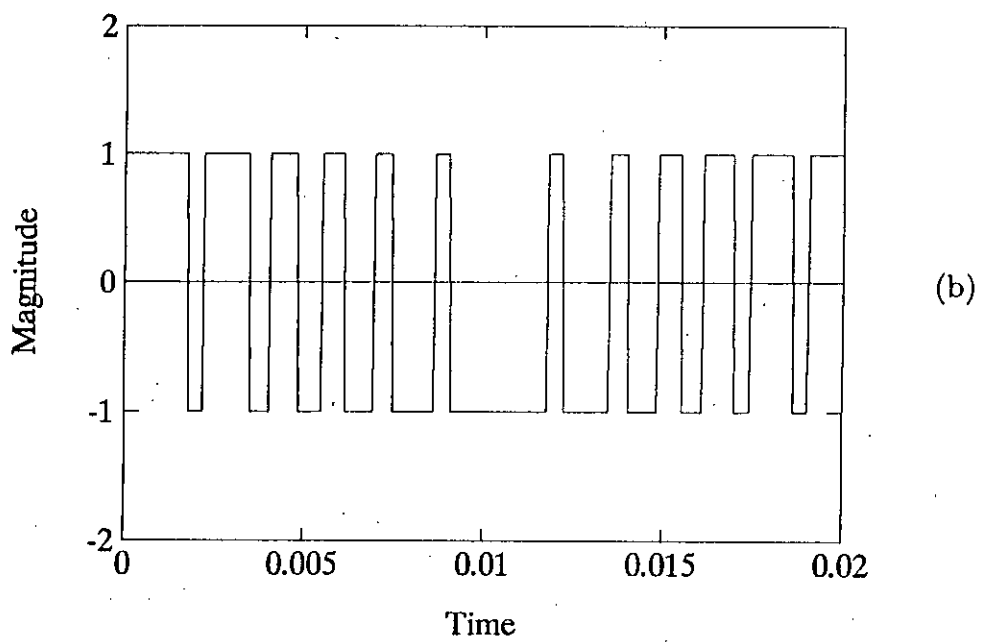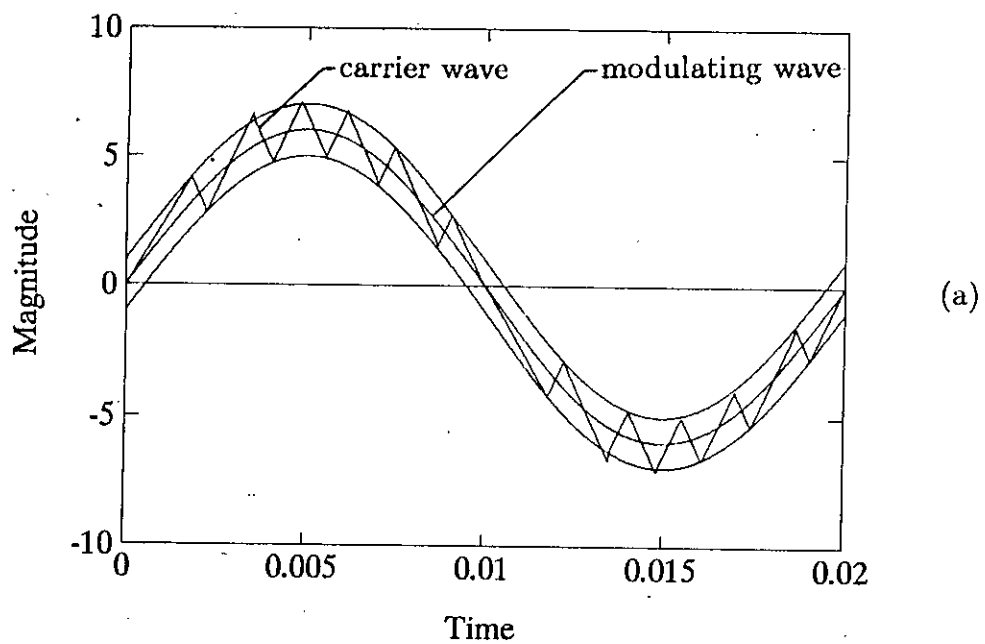
Figure 2.3:   Illustration of delta modulation technique:
(a) modulating wave and carrier wave;
(b) modulated wave.

21

2.3 Proposed Method of Determining Switching Points of Triangular Sine Modulated Inverter Waveforms

The method of determining the switching points for a typical triangular sine pulse width modulation is described with the help of Fig. 2.4.

The number of pulse per cycle of modulating wave is determined by the following relation:

$$N = \frac{f_c}{f_m} \tag{2.1}$$

where,

f_m = frequency of modulating sine wave

f_c = frequency of triangular wave

Let θ_i be the middle point of the i-th pulse produced by the intersection of two waves at the points x_1 and x_2 as shown in Fig. 2.4. θ_i can be expressed as,

$$\theta_i = \frac{2i - 1}{N}\pi \tag{2.2}$$

Also, assuming the slope of the triangular wave to be S where,

$$S = \frac{E_c}{\frac{\pi}{2N}} \tag{2.3}$$

Expression for the slope can be written as,

$$S = \frac{2NE_c}{\pi} \tag{2.4}$$

where, E_c = magnitude of the triangular carrier wave

Determination of the switching points of the triangular modulation shown in Fig. 2.4 is based on the following observations [20]:
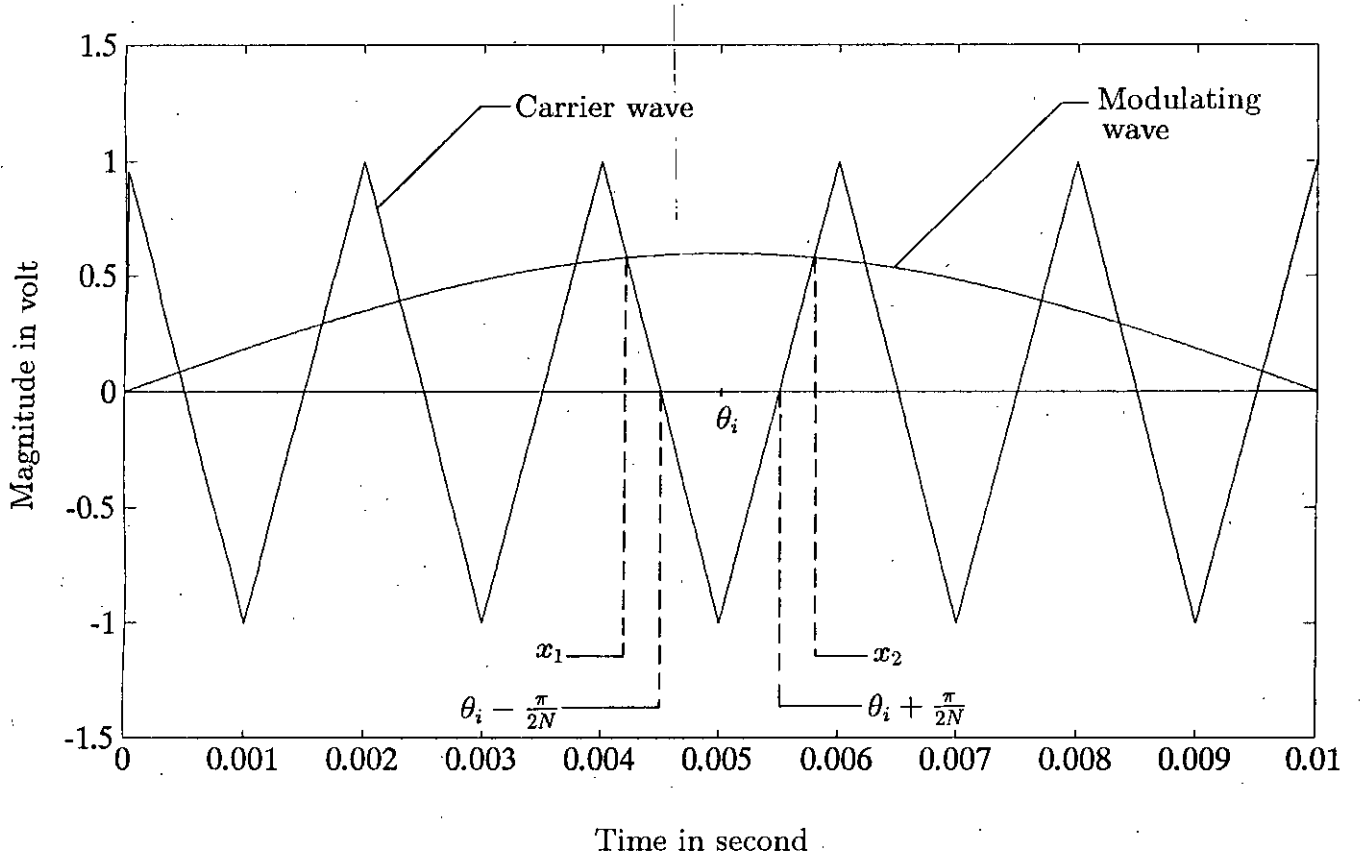
Figure 2.4: Enlarged diagram of triangular sine pulse width modulation.

- Pulse widths are directly proportional to the instantaneous value of $E_m \sin \theta_i$ at θ_i

- Pulse widths are inversely proportional to the magnitude of E_c

These relations can mathematically be expressed as,

$$x_2 - x_1 = \delta_i \quad \propto \quad E_m \sin \theta_i \tag{2.5}$$

$$\delta_i \quad \propto \quad \frac{1}{E_c} \tag{2.6}$$

$$\delta_i \quad = \quad K_i \frac{E_m \sin \theta_i}{E_c} \tag{2.7}$$

$$\delta_i \quad = \quad K_i m \sin \theta_i \tag{2.8}$$

where,

δ_i = width of the i-th pulse

m = modulation index = $\frac{E_m}{E_c}$

K_i = constant of proportionality.

Though equation (2.8) is a simple one, no quantitative value of K_i was available [23]. In the following analysis a definite expression for K_i is suggested. From Fig. 2.4, an equation of the slope for any falling section of the triangular wave can be written as,

$$S \quad = \quad \frac{E_m \sin x_1}{\left(\theta_i - \frac{\pi}{2N}\right) - x_1} \tag{2.9}$$

$$E_m \sin x_1 \quad = \quad S\left[-x_1 + \left(\theta_i - \frac{\pi}{2N}\right)\right] \tag{2.10}$$

Similarly, the equation of the slope for any rising section of the triangular wave can be written as,

$$E_m \sin x_2 = S\left[x_2 - \left(\theta_i + \frac{\pi}{2N}\right)\right] \tag{2.11}$$

Solving the transcendental equations (2.10) and (2.11) by numerically would give switching points x_1 and x_2. But the proposed method provides a simpler solution as follows:

Combining equations (2.10) and (2.11) and replacing $(x_2 - x_1)$ by δ_i, one obtains,

$$E_m (\sin x_1 + \sin x_2) = S\delta_i - \frac{\pi}{N}S \qquad (2.12)$$

$$S\delta_i = E_m (\sin x_1 + \sin x_2) + \frac{\pi}{N}S \qquad (2.13)$$

$$\delta_i = \frac{E_m}{S} (\sin x_1 + \sin x_2) + \frac{\pi}{N} \qquad (2.14)$$

Since equations (2.8) and (2.14) represent the same quantity, substituting the expression of δ_i from equation (2.8) in (2.14) one obtains,

$$K_i m \sin \theta_i = \frac{E_m}{S}(\sin x_1 + \sin x_2) + \frac{\pi}{N} \qquad (2.15)$$

$$K_i = \frac{1}{m \sin \theta_i} \left[\frac{E_m}{S}(\sin x_1 + \sin x_2) + \frac{\pi}{N} \right] \qquad (2.16)$$

With a fair accuracy, $E_m (\sin x_1 + \sin x_2)$ can be approximated by $2E_m \sin \theta_i$. This assumption is valid for regularly sampled sine wave modulation where the reference signal is a stepped sine wave. Substituting $E_m (\sin x_1 + \sin x_2)$ by $2E_m \sin \theta_i$ in equation (2.16), one obtains,

$$K_i = \frac{1}{Sm \sin \theta_i} \left(2E_m \sin \theta_i + \frac{\pi S}{N} \right) \qquad (2.17)$$

$$K_i = \frac{2E_m}{Sm} + \frac{\pi}{N} \frac{1}{m \sin \theta_i} \qquad (2.18)$$

Replacing S by equation (2.4) and the modulation index m by $\frac{E_m}{E_c}$, equation (2.18) becomes

$$K_i = \frac{\pi}{N} + \frac{\pi}{N} \frac{1}{m \sin \theta_i} \qquad (2.19)$$

$$K_i = \frac{\pi}{N} \left(1 + \frac{1}{m \sin \theta_i} \right) \qquad (2.20)$$

Once the value of K_i is known, the pulse width can be determined using equation (2.8) as,

$$\delta_i = K_i m \sin \theta_i \qquad (2.21)$$

25

Substituting equation (2.20), equation (2.21) becomes

$$\delta_i = \frac{\pi}{N} \left(1 + \frac{1}{m \sin \theta_i}\right) m \sin \theta_i \qquad (2.22)$$

or,

$$\delta_i = \frac{\pi}{N} \left(1 + m \sin \theta_i\right) \qquad (2.23)$$

However, the pulse width can directly be written without the constant of proportionality obtained from equation (2.14). Substituting $E_m (\sin x_1 + \sin x_2)$ by $2E_m \sin \theta_i$, one obtains,

$$\delta_i = \frac{\pi}{N} + \frac{2E_m \sin \theta_i}{S} \qquad (2.24)$$

or,

$$\delta_i = \frac{\pi}{N} + \frac{2E_m \sin \theta_i}{\frac{2E_c N}{\pi}} \qquad (2.25)$$

or,

$$\delta_i = \frac{\pi}{N} + \frac{\pi m \sin \theta_i}{N} \qquad (2.26)$$

or,

$$\delta_i = \frac{\pi}{N} \left(1 + m \sin \theta_i\right) \qquad (2.27)$$

If the pulse widths are known, the switching points can easily be found as,

$$x_1 = \theta_i - \frac{\delta_i}{2} \qquad (2.28)$$

$$x_2 = \theta_i + \frac{\delta_i}{2} \qquad (2.29)$$

Once the switching instances of the modulated wave are determined for certain modulation index, number of pulse per cycle and operating frequency, the modulated wave and inverter output wave can be represented analytically as described in the following section. These may be used for inverter waveform study and subsequent application in the stability study of the synchronous motor.

The switching points of triangular sine pulse width modulation obtained by the proposed simplified method are compared with the results of the natural intersection of

modulating wave and triangular carrier wave as well as with those of transcendental equation solution by the Newton-Raphson method. Three set of results have been shown graphically in Fig. 2.5 and in tabular form as in Table 2.1. A modulating signal of 30 Hz, carrier wave of 510 Hz and modulation index of 0.8 are used for the comparison. The comparison of the results shows that the switching points of the proposed method have close agreement in middle zone and insignificant difference in the two ends of each half wave of the modulating signal. The small difference found from comparison of the results have insignificant effect on fundamental voltage of the inverter.

2.4 Triangular Sine PWM Inverter Waveform Analysis

Switching of single phase inverters can be done in such a way that the output waveform appears like a modulated wave as shown in Fig. 2.6. The switching waveform can be represented by the following expressions.

For one cycle:

$$m_T(t) = \sum_{i=0,1,2...}^{\frac{N_p}{2}} \left[g(t, t_{2i}, t_{2i+1}) - g(t, t_{2i} + \frac{T}{2}, t_{2i+1} + \frac{T}{2}) \right] \qquad (2.30)$$

For multiple cycles:

$$m(t) = \sum_{A=0,T,2T...}^{ZT} \sum_{i=0,1,2...}^{\frac{N_p}{2}} \left[g(t, t_{2i} + A, t_{2i+1} + A) - g(t, t_{2i} + \frac{T}{2} + A, t_{2i+1} + \frac{T}{2} + A) \right]$$
$$(2.31)$$

where,

N_p is the number of pulses in one cycle

T is the period of one cycle

$A = 0, T, 2T...$etc. $(Z + 1)$ is the number of cycle of the input signal to be simulated

t_{2i} is the starting position of $(i + 1)$-th pulse

t_{2i+1} is the end position of $(i + 1)$-th pulse

27
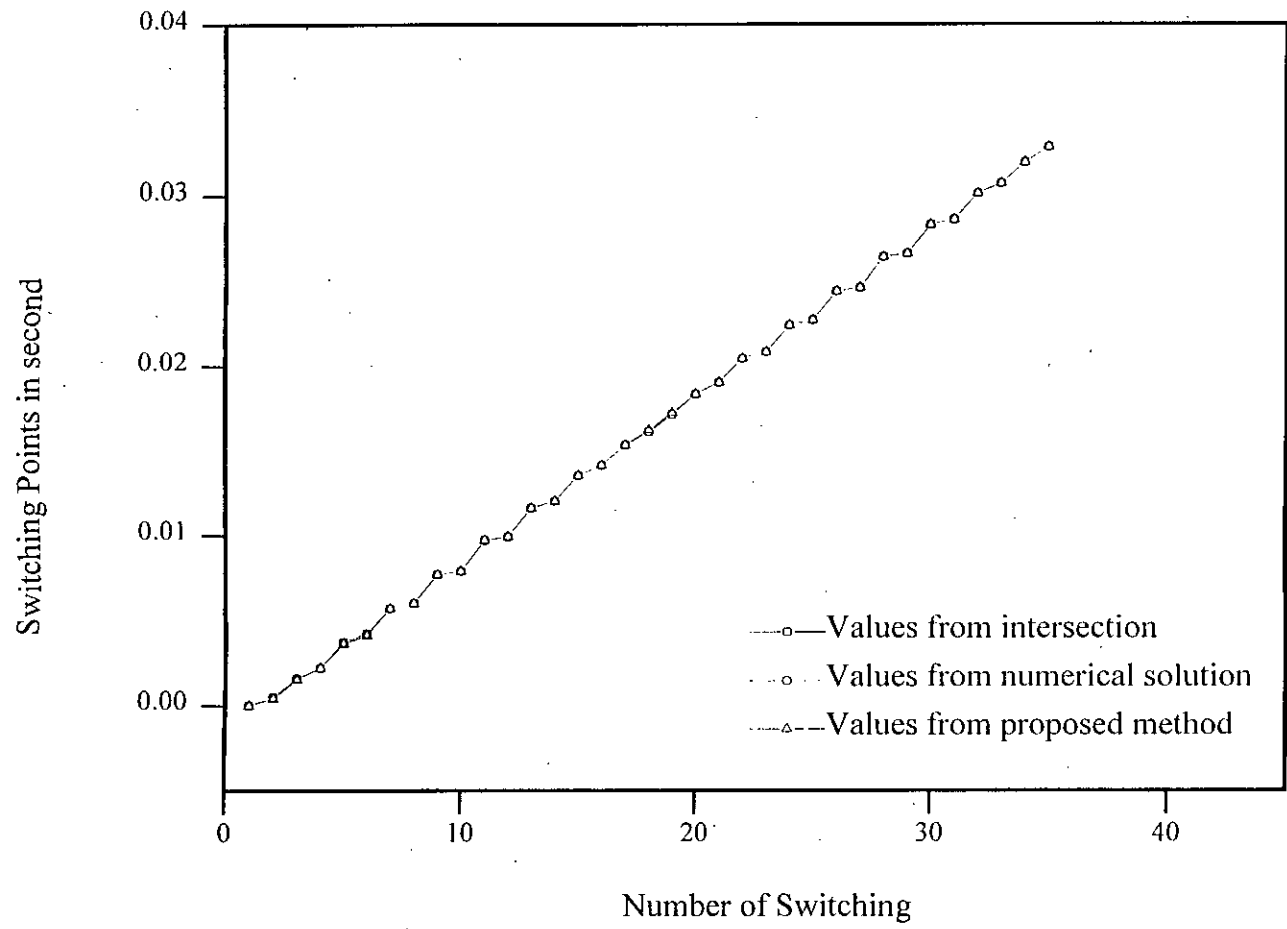
Figure 2.5: Switching points of Triangular SPWM waveforms.

Table 2.1: Comparison of switching points of triangular SPWM

No.	A (sec)	B (sec)	C (sec)
1	0.0000	0.0000	0.0000
2	0.0005	0.0005	0.0004
3	0.0016	0.0016	0.0015
4	0.0023	0.0023	0.0022
5	0.0037	0.0037	0.0036
6	0.0042	0.0042	0.0041
7	0.0057	0.0057	0.0057
8	0.0060	0.0060	0.0060
9	0.0077	0.0077	0.0077
10	0.0079	0.0079	0.0079
11	0.0097	0.0097	0.0097
12	0.0099	0.0099	0.0099
13	0.0116	0.0116	0.0116
14	0.0120	0.0120	0.0120
15	0.0135	0.0135	0.0135
16	0.0141	0.0141	0.0141
17	0.0153	0.0153	0.0153
18	0.0161	0.0161	0.0162
19	0.0171	0.0171	0.0172
20	0.0183	0.0183	0.0183
21	0.0190	0.0190	0.0190
22	0.0204	0.0204	0.0204
23	0.0208	0.0208	0.0208
24	0.0224	0.0224	0.0224
25	0.0227	0.0227	0.0227
26	0.0244	0.0244	0.0244
27	0.0246	0.0246	0.0246
28	0.0264	0.0264	0.0264
29	0.0266	0.0266	0.0266
30	0.0283	0.0283	0.0283
31	0.0286	0.0286	0.0286
32	0.0301	0.0301	0.0301
33	0.0307	0.0307	0.0307
34	0.0319	0.0319	0.0319
35	0.0328	0.0328	0.0328

A: Values from intersection

B: Values from numerical solution

C: Values from proposed method

Switching points of a single phase triangular modulated PWM inverter can be obtained from equation (2.28) and (2.29) and converted to one cycle or multiple cycles of a single phase inverter waveform using equations (2.30) and (2.31).

Analysis of triangular sine PWM inverter waveforms is usually performed on parameter variations of modulation index and number of pulse per cycle of the modulating wave. Simulated waveforms of a single phase inverter for 30 Hz operation are shown in Fig. 2.6 for constant number of pulse per cycle. Corresponding spectra of the waveforms are shown in Fig. 2.7. Typical spectral variation of the triangular modulated inverter waves for variation of modulating index, carrier frequency and operating frequency are shown in Figs. 2.8 ,2.9 and 2.10, respectively. Figs. 2.11 and 2.12 illustrate the practical SPWM waveforms generated by natural comparison method. The necessary simulated waveforms and their spectra of single phase SPWM inverters are shown in Figs. A.1 to A.6 in Appendix A. Features of modulation of inverter waveforms are evident from these illustrations. The results of triangular modulated waveform analysis can be summarized as follows:

- Increase in carrier frequency causes dominant harmonics to occur at higher frequency. This is advantageous, because higher frequency dominant harmonics would require small filters for smoothing the converter waveform. However, the increase in carrier frequency is limited by the switching frequency of the static devices used in the converters. Number of switching per second of these device increases with the increase of carrier frequency. As a result, the carrier frequency increase is limited by the highest switching frequency of the static device in the converter. The highest switching frequency in the static devices vary from device to device resulting in the variation of cost of the converter.

- Increase of modulation index m (other parameters remaining constant) causes an increase in fundamental output voltage. Increase of voltage with modulation index is linear. Thus variation of modulation index provides a means for voltage

30
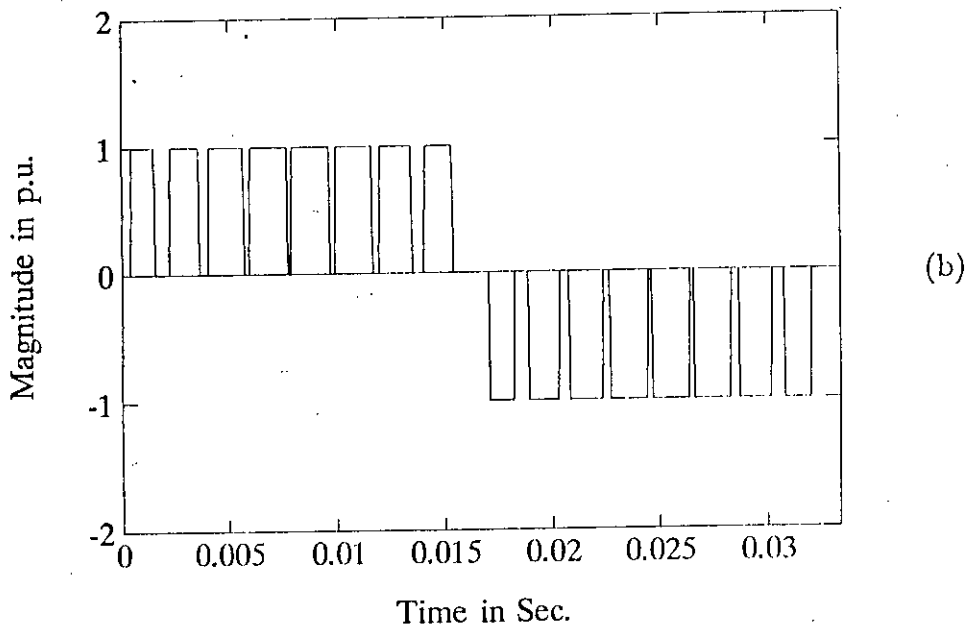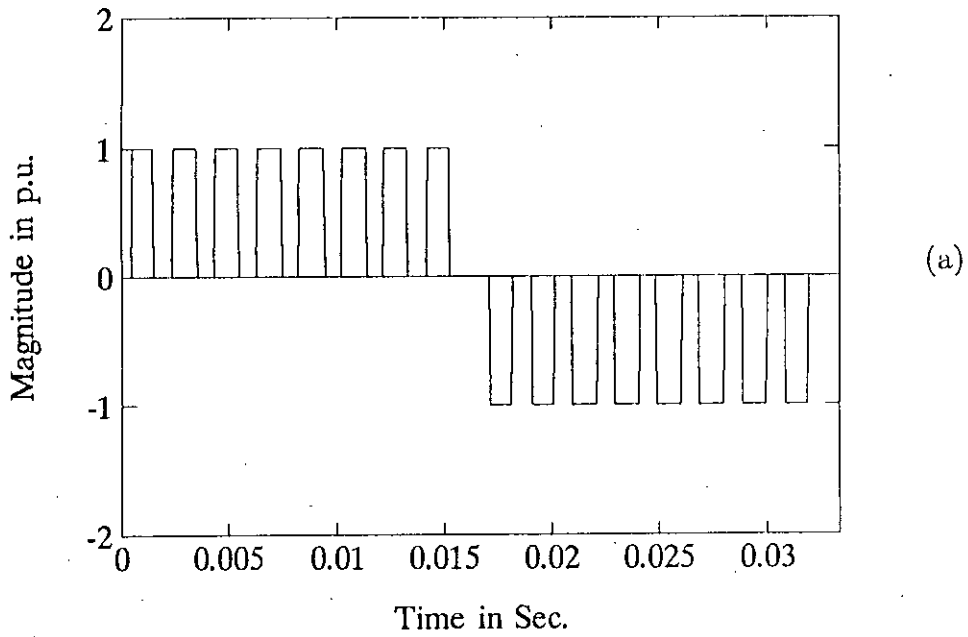
Figure 2.6: Simulated single-phase triangular SPWM inverter waveforms for $f = 30$ Hz: (a) $m = 0.2$; (b) $m = 0.8$. (no. of pulse/cycle constant)
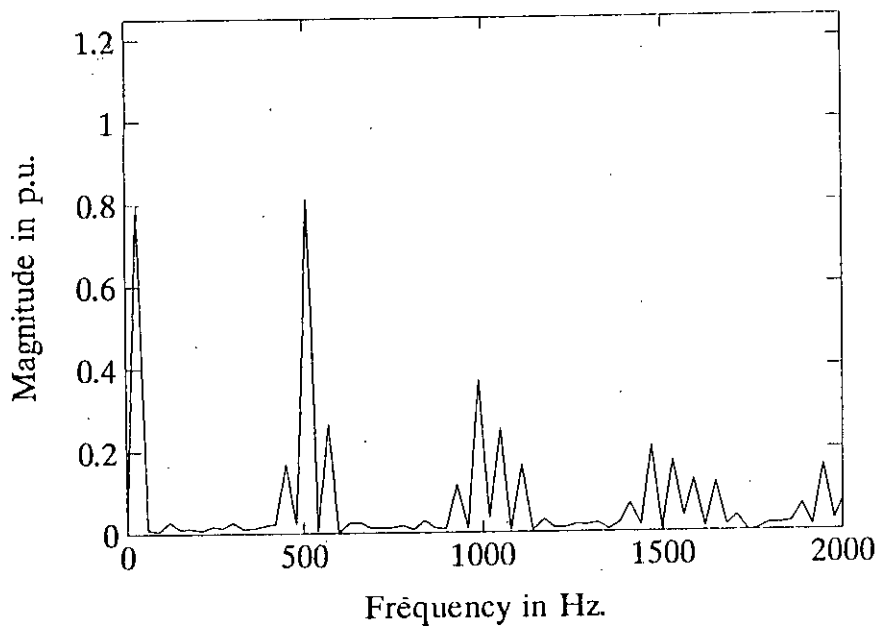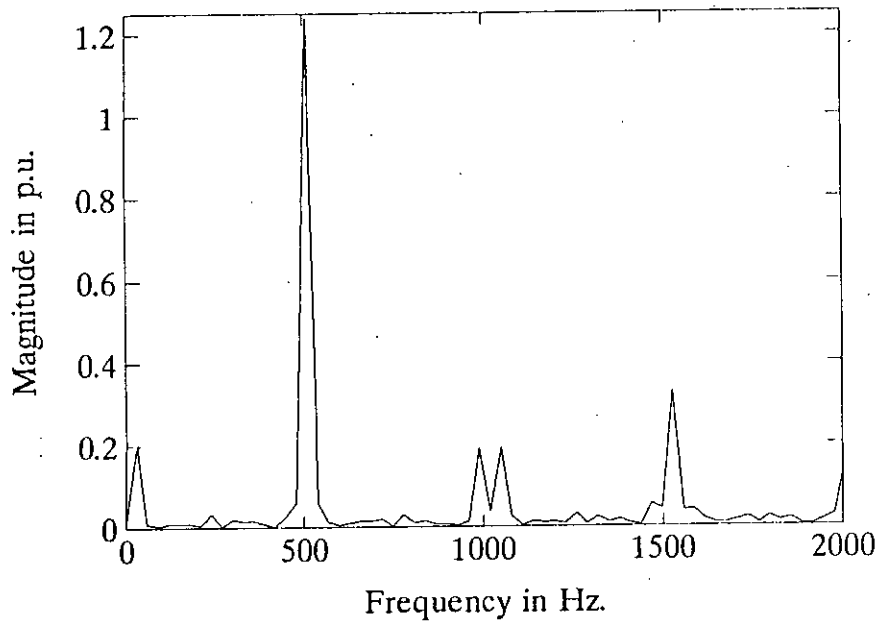
Figure 2.7: Spectrum corresponding to simulated SPWM waveforms of Fig. 2.6:(a) $m = 0.2$; (b) $m = 0.8$. (no. of pulse/cycle constant)
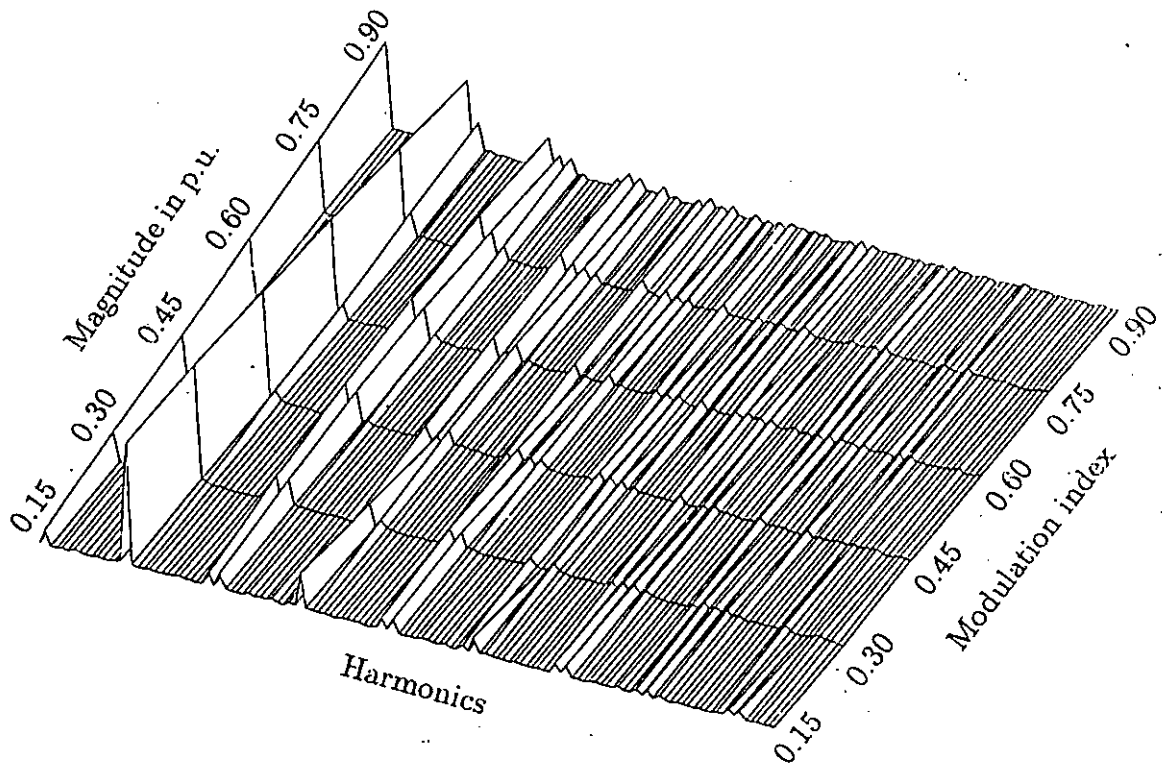
Figure 2.8: Spectral variations of triangular SPWM inverter waveforms for modulation index varying from 0.15 to 0.9 volts. (frequency and no. of pulse/cycle constant)
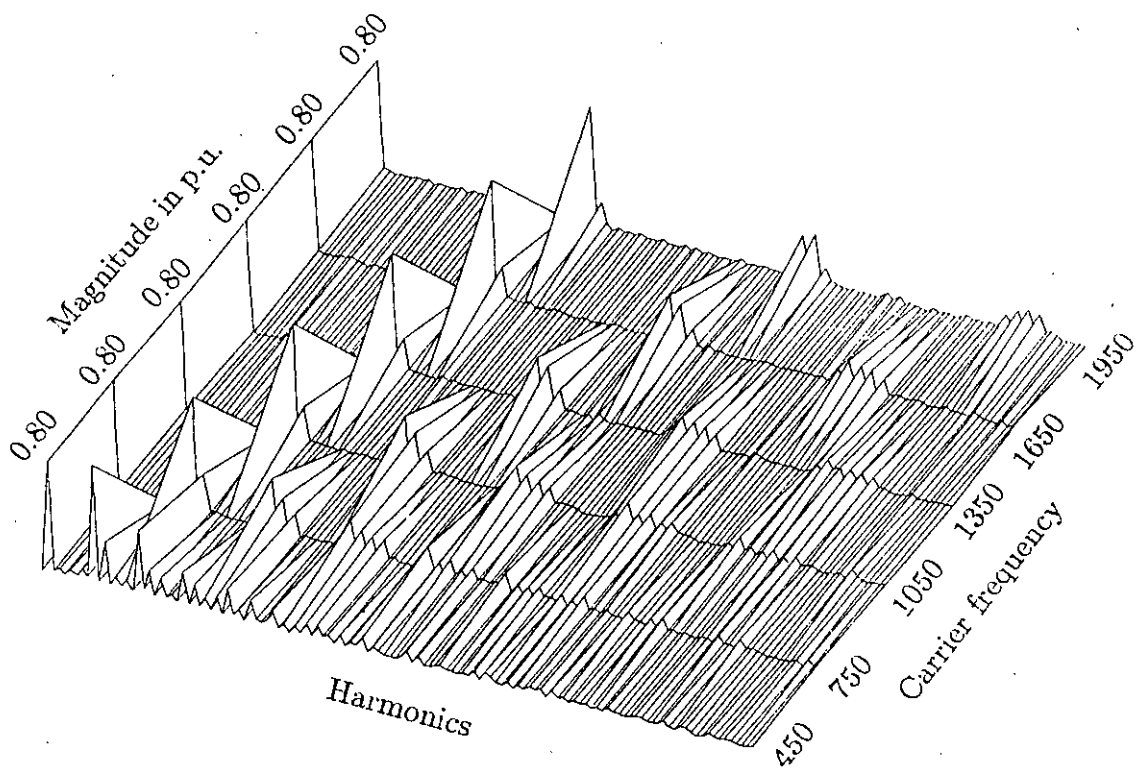
Figure 2.9: Spectral variations of triangular SPWM inverter waveforms for carrier frequency varying from 450 to 1950 Hz. (modulation index and no. of pulse/cycle constant)
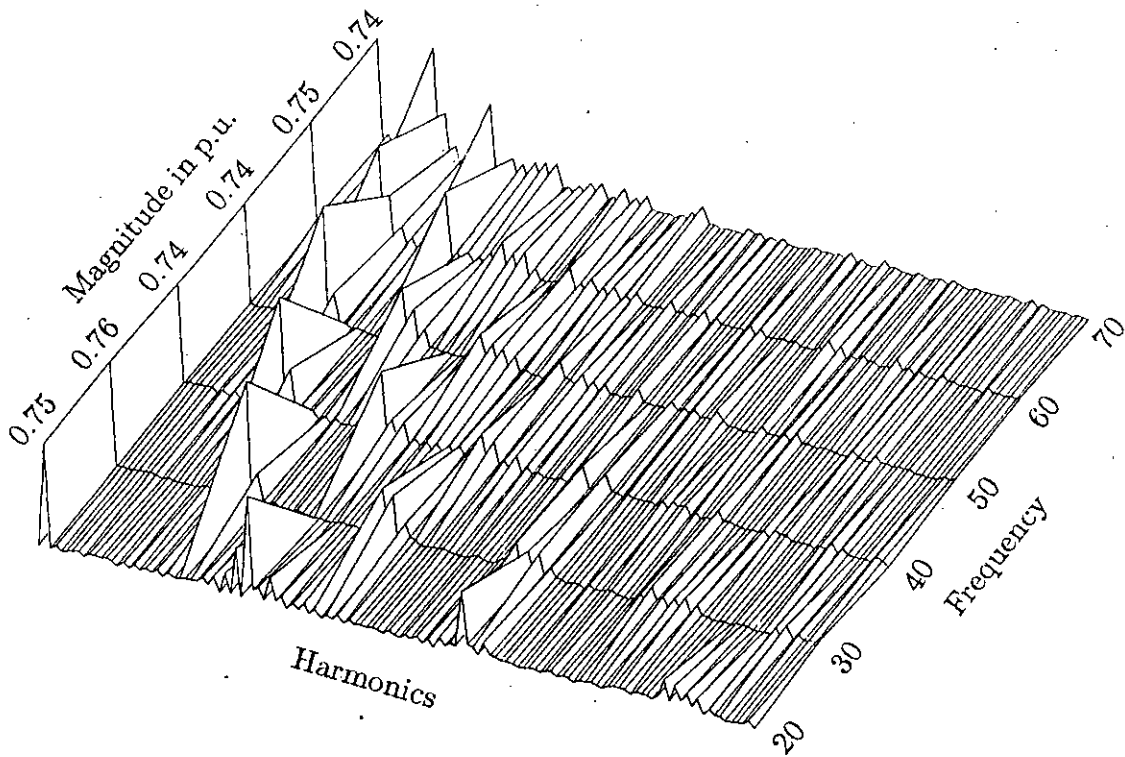
Figure 2.10: Spectral variations of triangular SPWM inverter waveforms for operating frequency varying from 20 to 70 Hz. (modulation index and no. of pulse/cycle constant)
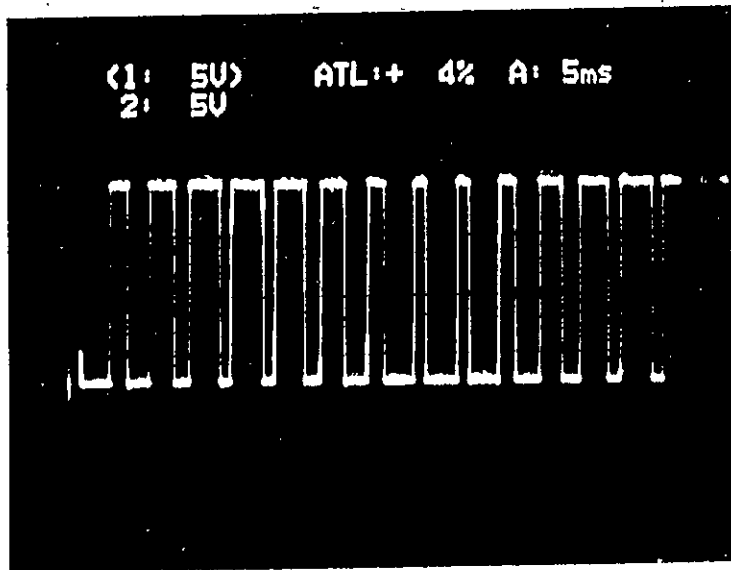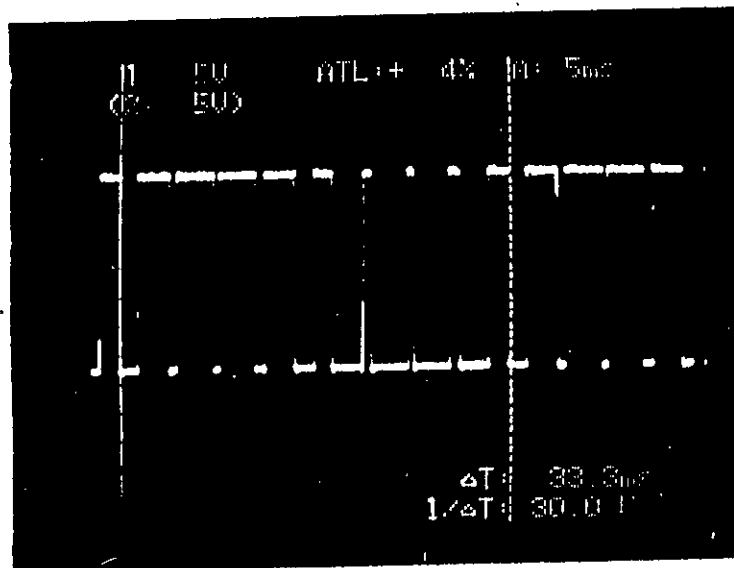
Figure 2.11:   Practical waveforms of single phase triangular SPWM
inverter for $f = 30$ Hz:
(a) $m = 0.5$ and $N = 9$; (b) $m = 0.8$ and $N = 9$.

(a)

(b)
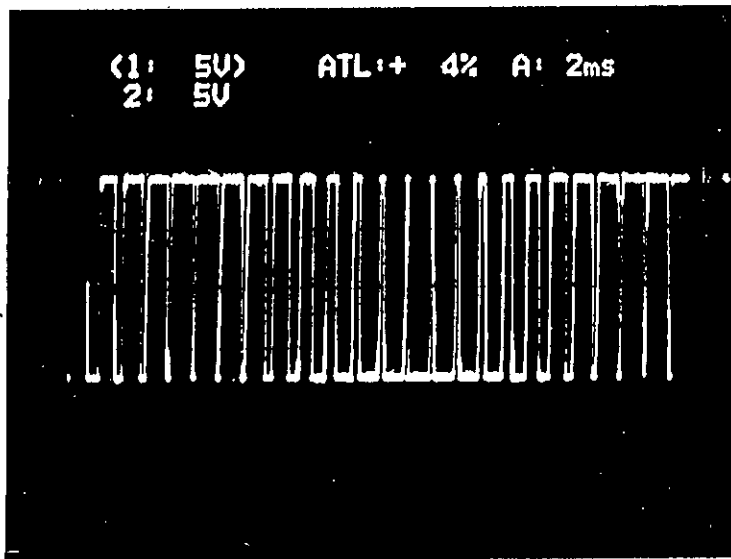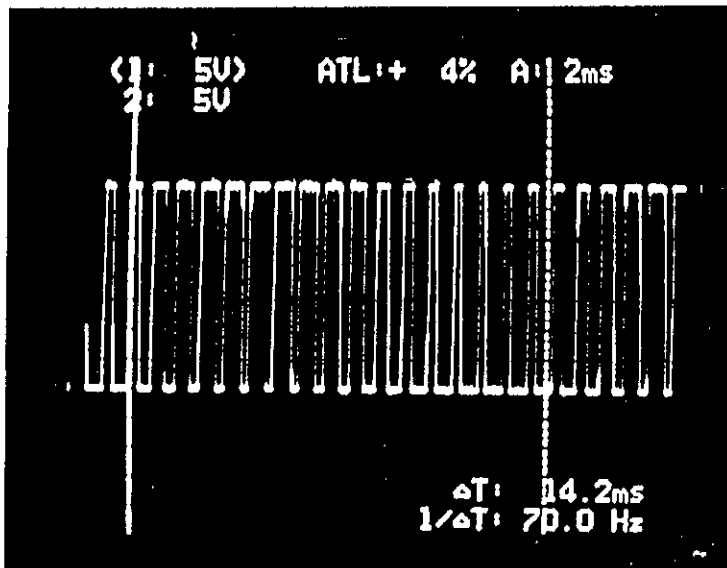
Figure 2.12:   Practical waveforms of single phase triangular SPWM
inverter for $f = 70$ Hz:
(a) $m = 0.5$ and $N = 17$; (b) $m = 0.8$ and $N = 17$.

variation in application where controllable voltage is desired.

- An ac drive requires simultaneous voltage control and carrier frequency control. Carrier frequency adjustment is necessary to maintain the switching frequency within the devices switching limit and to control switching loss within an allowable range. Voltage control is necessary to maintain constant torque operation ($\frac{v}{f}$=const). Under these conditions the waveforms of the inverter gradually turn into square wave mode of operation and the spectra of waveform contain dominant harmonics which are low order multiples of the fundamental.

2.5 Proposed Method of Determining Switching Points of Delta Modulated Inverter Waveforms

The method of determining switching points for typical delta modulated waveforms is explained with the help of Fig. 2.13.

For any rising section of the carrier wave, equation can be written as [113],

$$A = \frac{2\Delta V + V_m(\sin \omega t_i - \sin \omega t_{i-1})}{(t_i - t_{i-1})} \tag{2.32}$$

$$2\Delta V + V_m(\sin \omega t_i - \sin \omega t_{i-1}) = A(t_i - t_{i-1}) \tag{2.33}$$

where,

A is the slope of any rising section of the carrier wave, t_i and t_{i-1} are the switching points of the i-th pulse for leading and trailing edges of the rising section of the carrier wave, respectively and ΔV is the window width as shown in Fig. 2.13.

Similarly, the equation of the slope for any falling section of the carrier wave can be written as [113],

$$B = \frac{2\Delta V + V_m(\sin \omega t_i - \sin \omega t_{i-1})}{(t_i - t_{i-1})} \tag{2.34}$$

$$2\Delta V + V_m(\sin\omega t_i - \sin \omega t_{i-1}) = B(t_i - t_{i-1}) \tag{2.35}$$

38
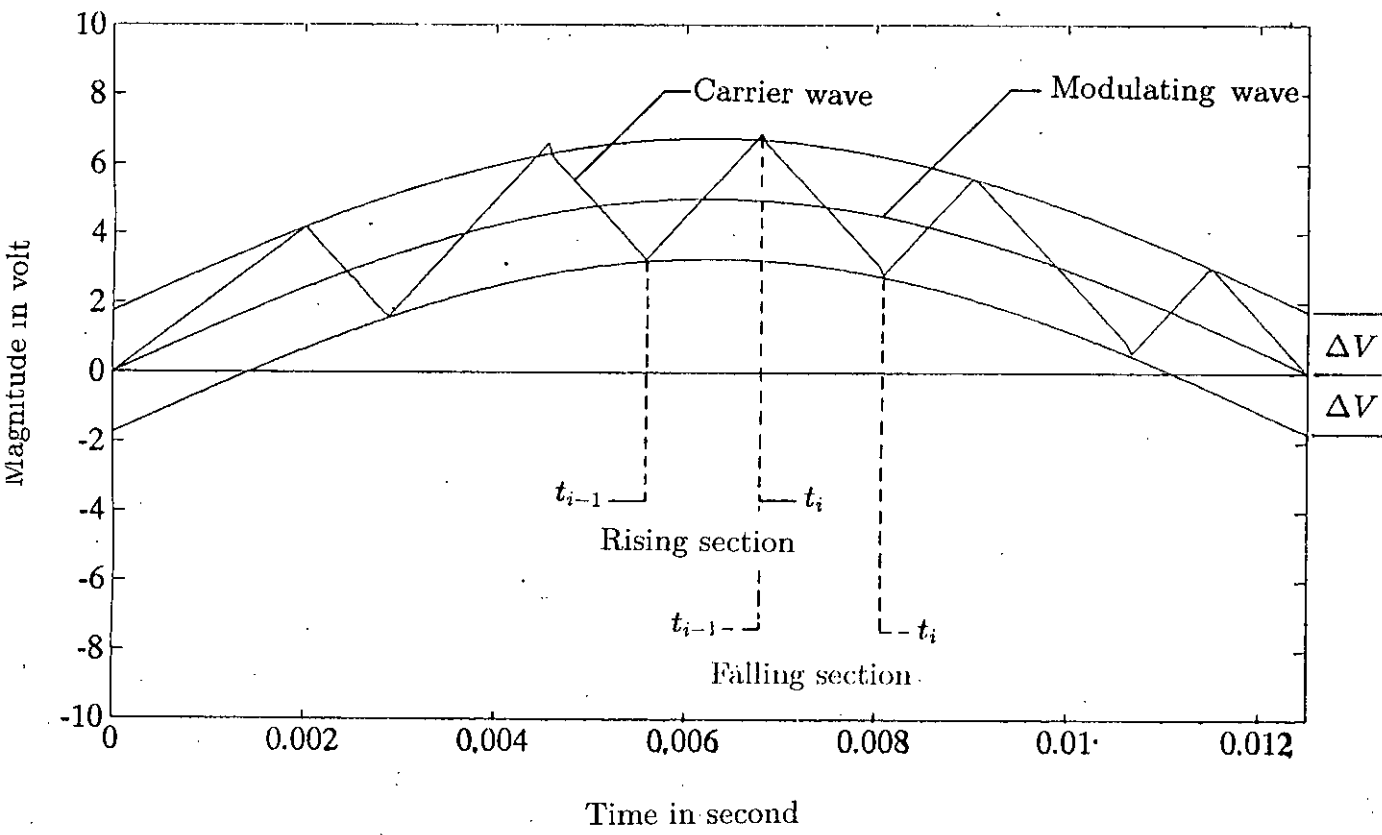
Figure 2.13: Enlarged diagram illustrating the delta modulation technique.

where, B is the slope of the falling section of the carrier wave.

Switching points can be determined by solving equations (2.33) and (2.35) as reported previously [113]. But these equations are transcendental in nature and computational time required for solution of these equations is quite substantial.

These transcendental equations for determining the switching points of delta modulation can be simplified with fair degree of approximation within the operating range of converters. The simplification of these equations can be made through replacing $V_m(\sin \omega t_i - \sin \omega t_{i-1})$ by $(t_i - t_{i-1}) \times$ slope of $V_m \sin \omega t$ in equation (2.33) to give,

$$2\Delta V + (t_i - t_{i-1}) \times \text{slope of } V_m \sin \omega t = A(t_i - t_{i-1}) \tag{2.36}$$

Since the slope of $V_m \sin \omega t$ at $t = t_{i-1}$ is $\omega V_m \cos \omega t_{i-1}$, equation (2.36) can be written as,

$$2\Delta V + (t_i - t_{i-1})\omega V_m \cos \omega t_{i-1} = A(t_i - t_{i-1}) \tag{2.37}$$

$$t_i = t_{i-1} + \frac{2\Delta V}{A - \omega V_m \cos \omega t_{i-1}} \tag{2.38}$$

Similarly, for falling edge equation (2.35) can be modified to,

$$2\Delta V - (t_i - t_{i-1})\omega V_m \cos \omega t_{i-1} = B(t_i - t_{i-1}) \tag{2.39}$$

$$t_i = t_{i-1} + \frac{2\Delta V}{B + \omega V_m \cos \omega t_{i-1}} \tag{2.40}$$

A general equation of switching point determination of the delta modulated wave can be written, which represents both equations (2.38) and (2.40). The first switching point is $t_1 = 0$, and the subsequent switching points can be expressed by a general expression as,

$$t_i = t_{i-1} + \frac{2\Delta V}{S + (-1)^{i-1} V_m \omega \cos \omega t_{i-1}} \tag{2.41}$$

where,

$S = A$, slope of rising section for $i =$ even

$S = B$, slope of falling section for $i =$ odd

40

Equation (2.41) is a simple algebraic equation and requires the knowledge of preceding switching point for finding the present switching point. Once the switching instances of the modulated wave are determined for certain reference voltage, operating frequency, window width and slope, the modulated wave and inverter output wave can be repre-sented analytically as described in the following section. These may be used for inverter waveform analysis and subsequent application in the stability study of the synchronous motor.

The switching points of delta modulation wave obtained by the proposed simplified method are compared with the results of the intersection of carrier wave with upper and lower bands as well as with those of transcendental equation solution by the Newton-Raphson method. Three set of results are shown graphically in Fig. 2.14 and in tabular form as in Table 2.2. A modulating signal having maximum amplitude of 8 volts, operating frequency of 30 Hz, window width 1.0 volt and slope 3000 volt/sec are used for comparison. The comparison shows that the switching points of the proposed method have close agreement with the other two methods and insignificant difference in the results found from comparison virtually has no influence on the fundamental voltage of the inverter.

2.6   Delta Modulated Inverter Waveform Analysis

The modulated waveform of a rectangular wave delta modulator as shown in Fig. 2.3 can be used to switch an inverter to produce the same waveform at the output of the inverter. In order to achieve this, the positive pulses are used to gate one pair of active devices, whereas, the negative pulses are used to gate the other pair in a single phase inverter. The switching waveform can be represented by the following expressions.

For one cycle:

$$s_T(t) = \sum_{i=1,2,3\ldots}^{N_p} (-1)^{i+1} \left[g(t, t_i, t_{i+1}) \right] \qquad (2.42)$$

41
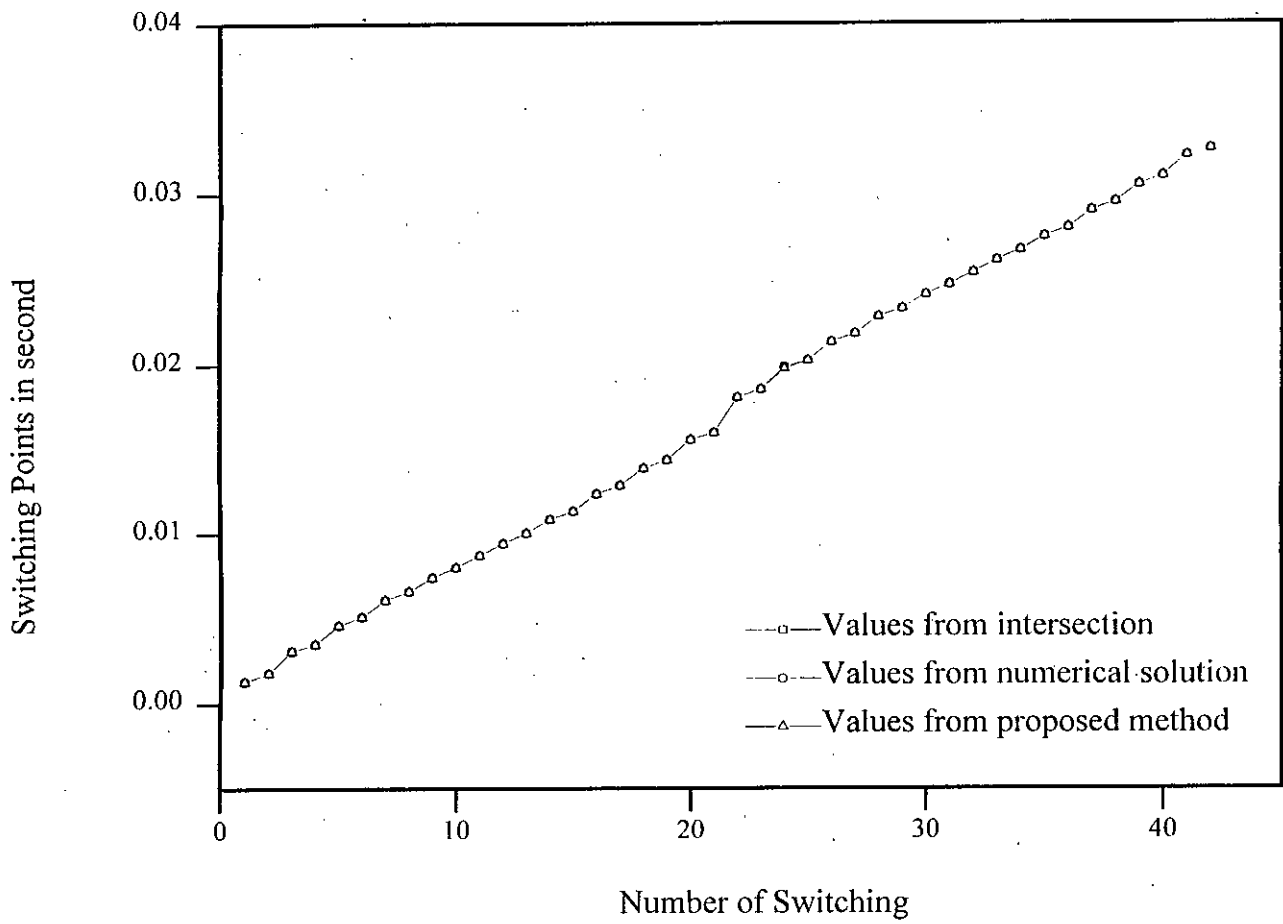
Figure 2.14: Switching points of delta modulated waveforms.

42

Table 2.2: Comparison of switching points of delta modulation

No.	A (sec)	B (sec)	C (sec)
1	0.0013	0.0013	0.0013
2	0.0018	0.0018	0.0018
3	0.0031	0.0031	0.0031
4	0.0035	0.0035	0.0035
5	0.0046	0.0046	0.0046
6	0.0051	0.0051	0.0051
7	0.0061	0.0061	0.0061
8	0.0066	0.0066	0.0066
9	0.0074	0.0074	0.0074
10	0.0080	0.0080	0.0080
11	0.0087	0.0087	0.0087
12	0.0094	0.0094	0.0094
13	0.0100	0.0100	0.0100
14	0.0108	0.0108	0.0108
15	0.0113	0.0113	0.0113
16	0.0123	0.0123	0.0123
17	0.0128	0.0128	0.0128
18	0.0138	0.0138	0.0138
19	0.0143	0.0143	0.0143
20	0.0155	0.0155	0.0155
21	0.0159	0.0159	0.0159
22	0.0180	0.0180	0.0180
23	0.0185	0.0185	0.0185
24	0.0198	0.0198	0.0197
25	0.0202	0.0202	0.0202
26	0.0213	0.0213	0.0213
27	0.0218	0.0218	0.0218
28	0.0228	0.0228	0.0228
29	0.0233	0.0233	0.0233
30	0.0241	0.0241	0.0241
31	0.0247	0.0247	0.0247
32	0.0254	0.0254	0.0254
33	0.0261	0.0261	0.0261
34	0.0267	0.0267	0.0267
35	0.0275	0.0275	0.0275
36	0.0280	0.0280	0.0280
37	0.0290	0.0290	0.0290
38	0.0295	0.0295	0.0295
39	0.0305	0.0305	0.0305
40	0.0310	0.0310	0.0310
41	0.0322	0.0322	0.0322
42	0.0326	0.0326	0.0326

A: Values from intersection; B: Values from numerical solution; C: Values from proposed method

43

For multiple cycles:

$$s(t) = \sum_{A=0,T,2T...}^{ZT} \sum_{i=1,2,3...}^{N_p} (-1)^{i+1} [g(t, t_i + A, t_{i+1} + A)] \qquad (2.43)$$

where,

N_p is the number of pulses in one cycle

T is the period of one cycle

$A = 0, T, 2T...$etc.

$(Z + 1)$ is the number of cycle of the input signal to be simulated

t_i is the starting position of i th pulse

t_{i+1} is the starting position of $(i + 1)$th pulse

From the knowledge of switching points as obtained by solution of equation (2.41) and using equations (2.42) and (2.43), the inverter output can be simulated for harmonic studies. The analysis of the delta PWM inverter waveform is usually done on harmonic determination with variation of modulator parameters, such as window width, slope, magnitude of reference wave and frequency. Simulated delta modulated single phase inverter waveforms for 30 Hz operation are shown in Fig. 2.15. The spectra of these waveforms are shown in Fig. 2.16. Results of parametric variations of the modulator on the waveform spectra are shown in Figs. 2.17, 2.18, 2.19 and 2.20 for reference voltage, frequency, window width and slope variations. Figs. 2.21, 2.22, 2.23 and 2.24 are the practical waveforms showing the effect of parameter variations. In each of the experimental waveforms the upper wave represents the carrier signal while the lower one is the modulated output. The necessary simulated waveforms and their spectra of single phase delta modulated inverters are shown in Figs. A.7 to A.16 in Appendix A. Features of the delta modulated waveforms are evident from spectral illustrations and are summarized below:

- With all other parameters remaining constant, the fundamental of the DM inverter output voltage increases with frequency maintaining an almost constant v/f. In

44

(a)

(b)
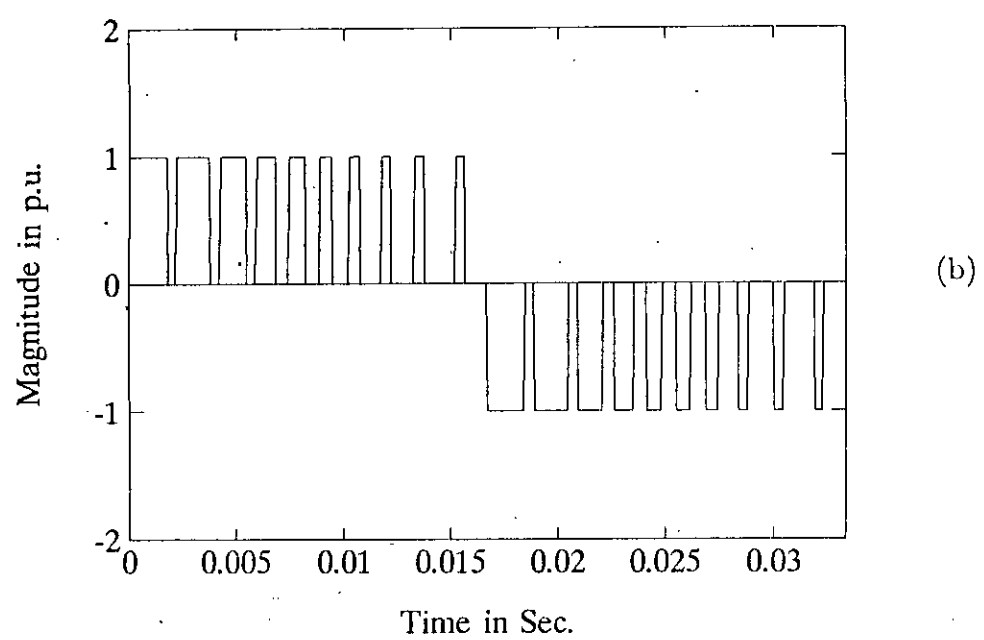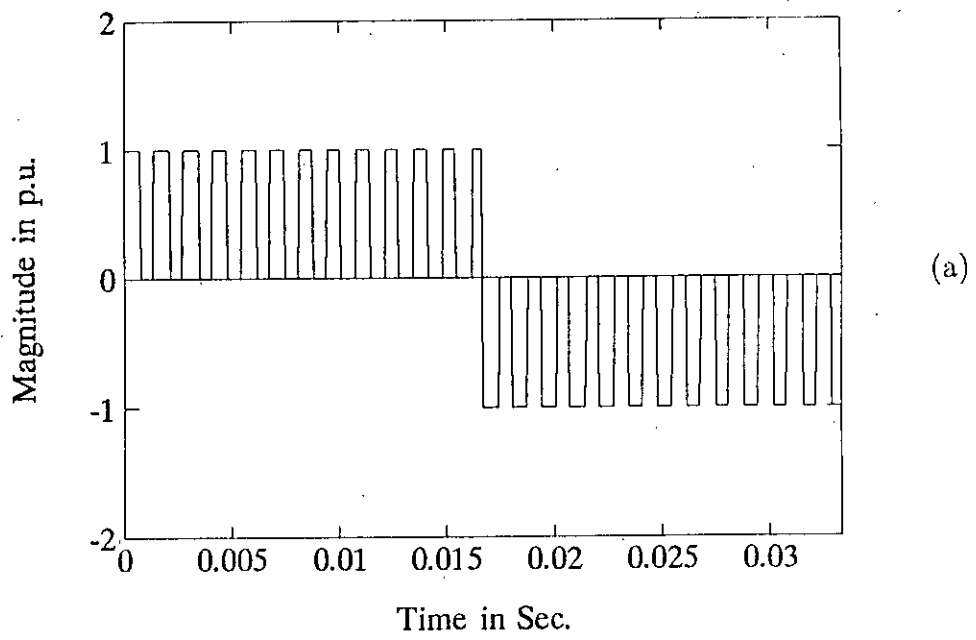
Figure 2.15:   Simulated single-phase DM inverter waveforms
for $f = 30$ Hz: (a) $V_m = 2$; (b) $V_m = 10$.
(slope and window width constant)

45

(a)

(b)
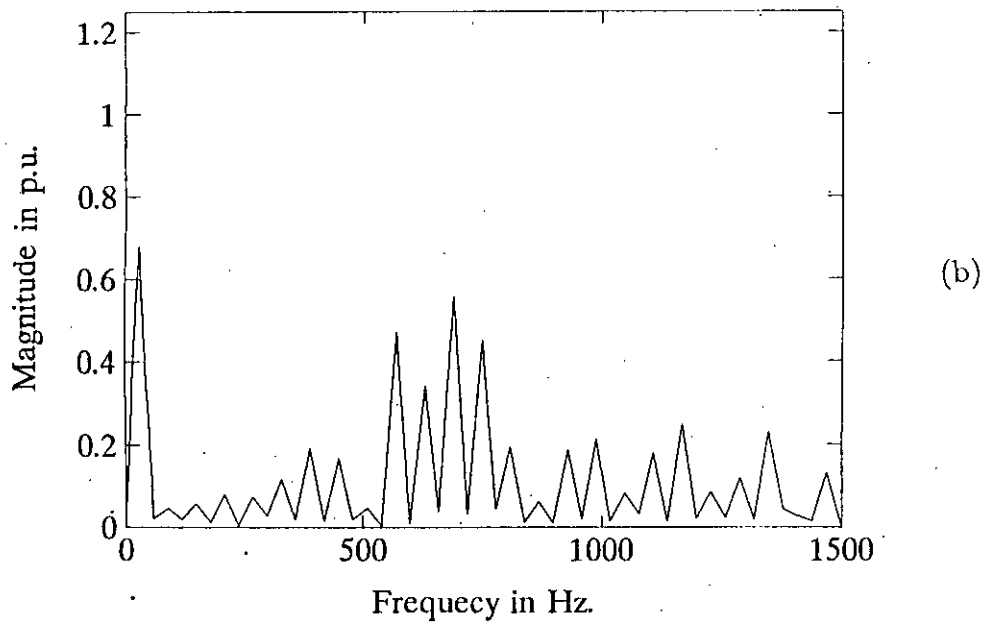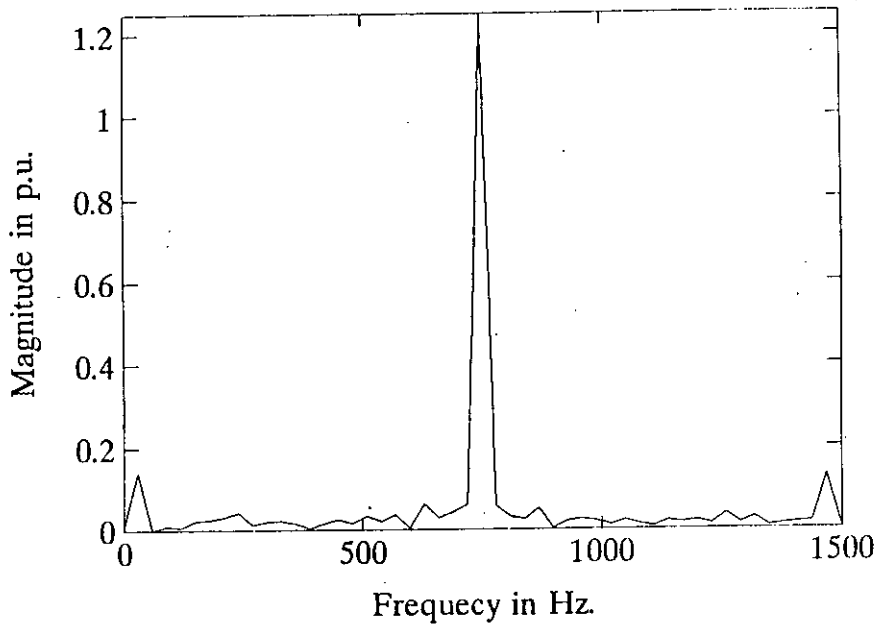
Figure 2.16: Spectrum corresponding to simulated DMPWM waveforms of Fig. 2.15:(a) $V_m = 2$; (b) $V_m = 10$. (slope and window width constant)
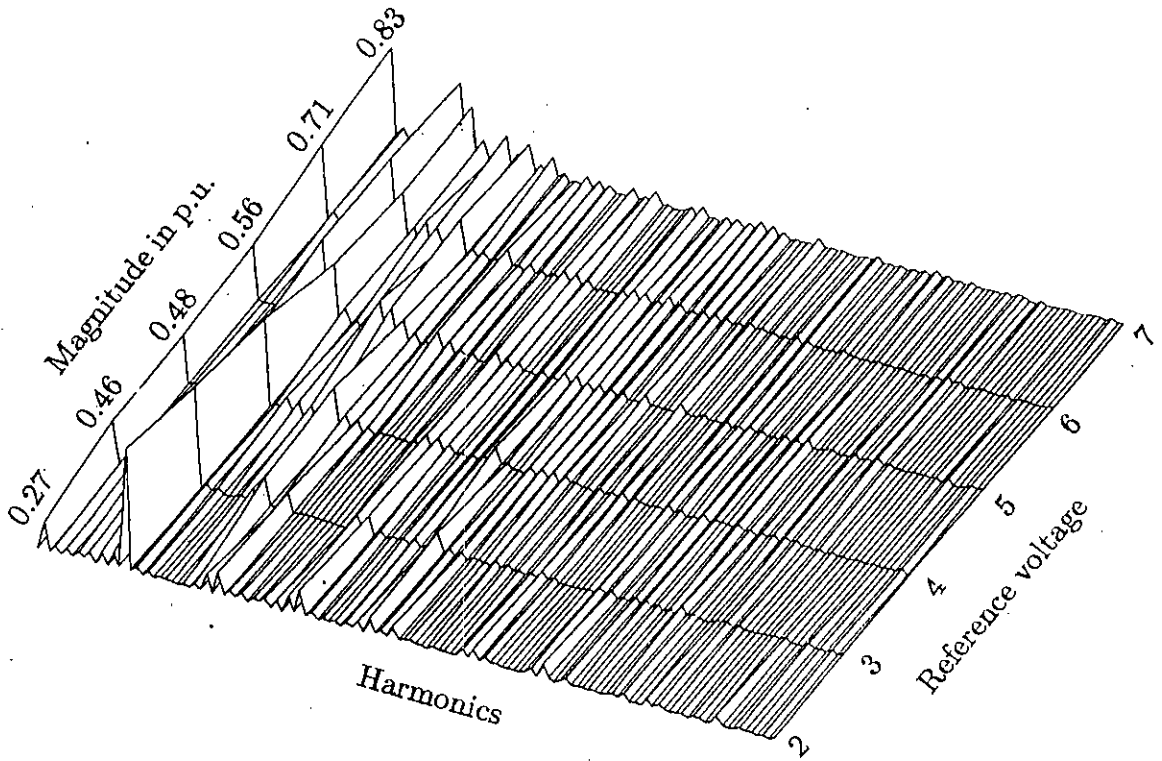
Figure 2.17: Spectral variations of DM inverter waveforms for
reference voltage varying from 2 to 7 volts.
(slope, window width and frequency constant)

47
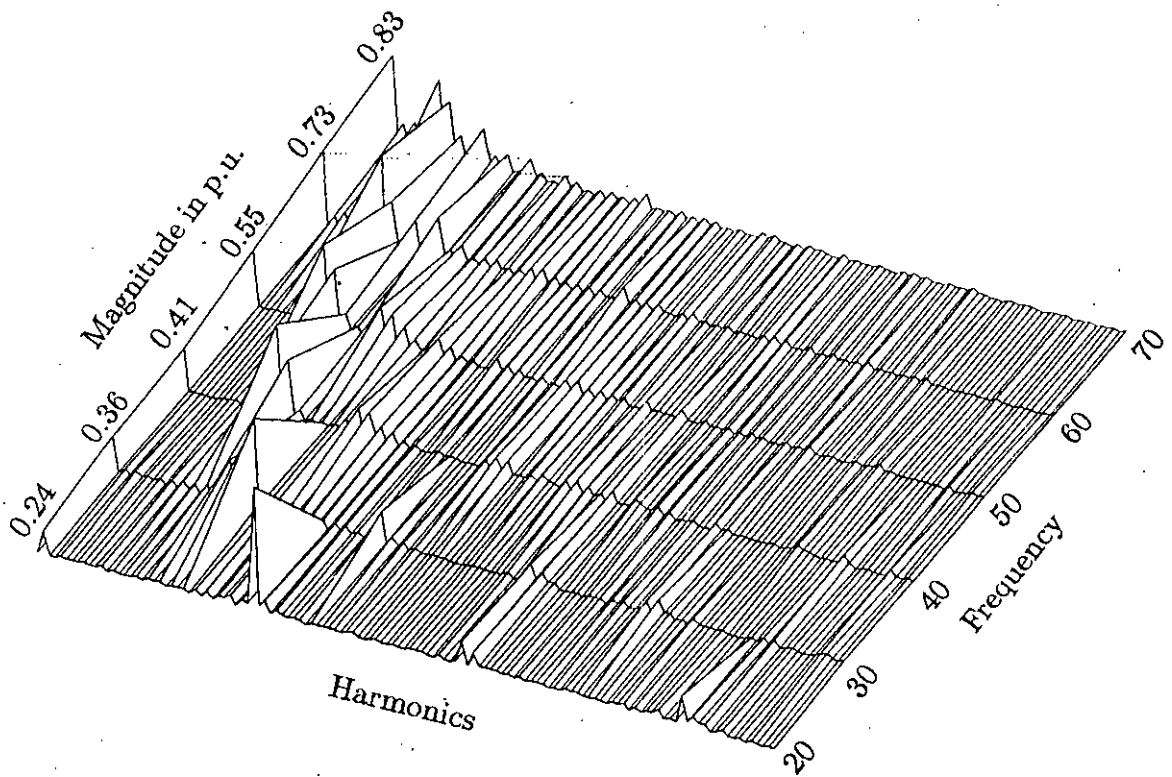
Figure 2.18: Spectral variations of DM inverter waveforms for operating frequency varying from 20 to 70 Hz. (slope, window width and reference voltage constant)
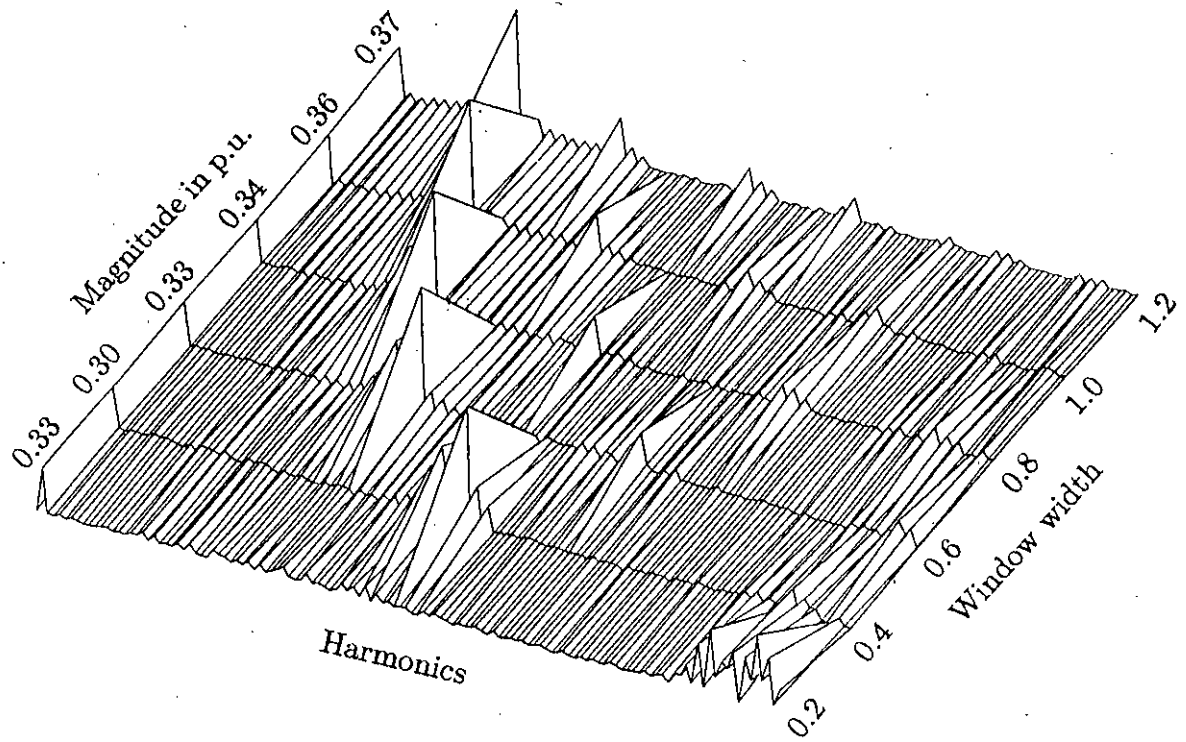
Figure 2.19: Spectral variations of DM inverter waveforms for
window width varying from 0.2 to 1.2 volts.
(slope, reference voltage and frequency constant)
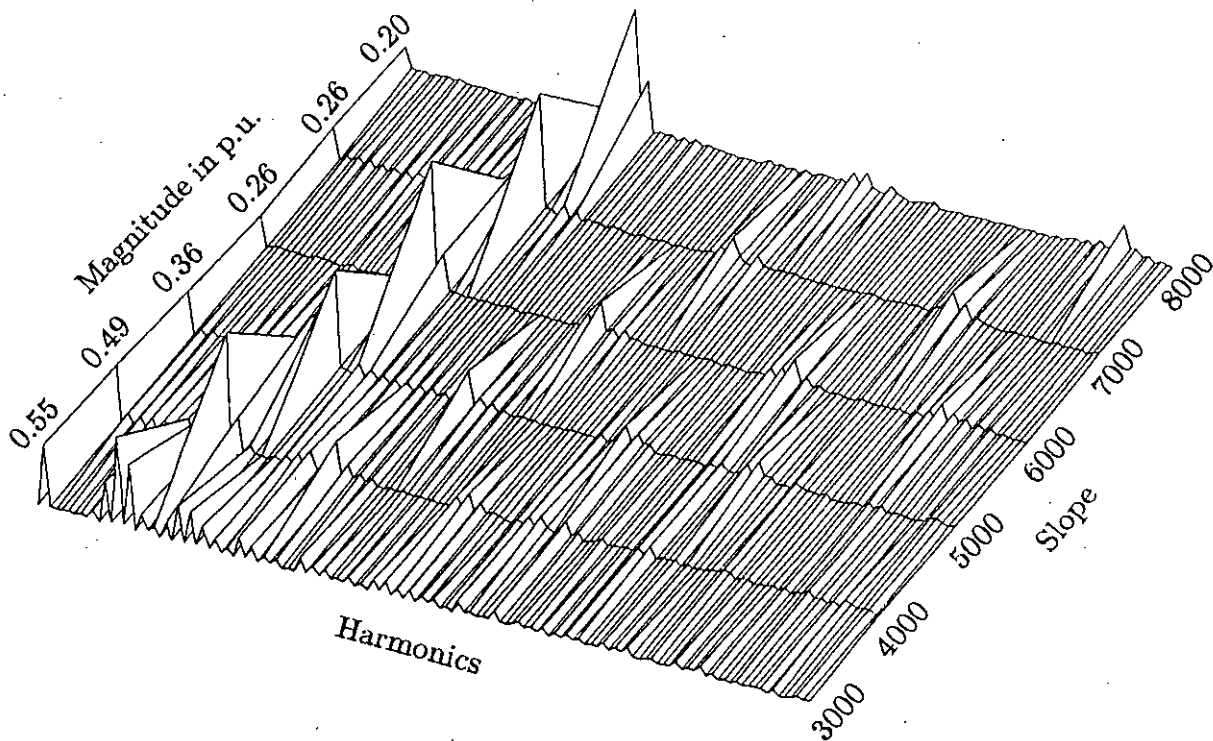
Figure 2.20: Spectral variations of DM inverter waveforms for
              slope varying from 2000 to 7000 volts/sec.
              (window width, reference voltage and frequency con-
              stant)
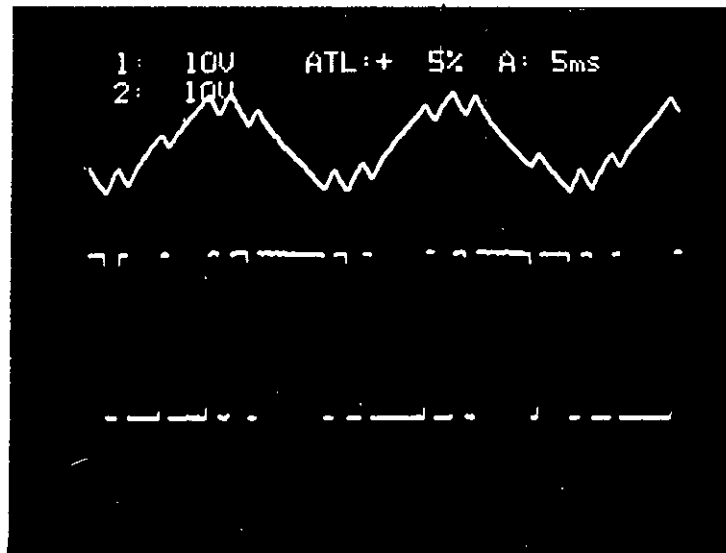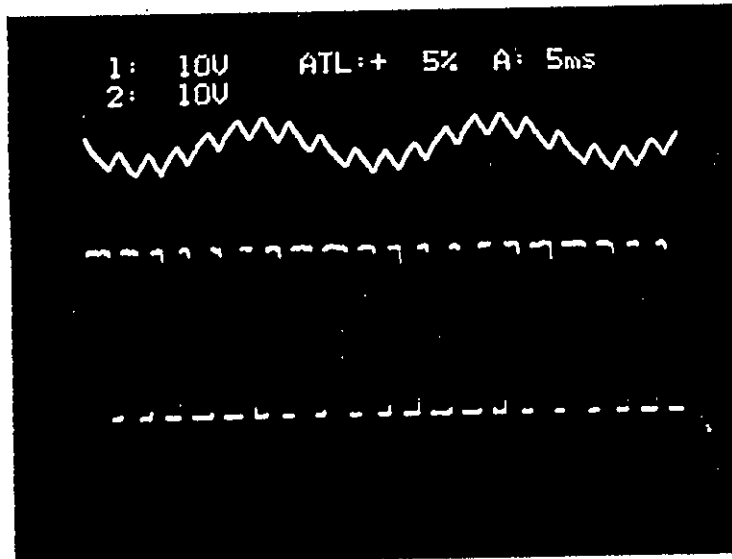
Figure 2.21: Practical waveforms of delta modulation for reference voltage variation.
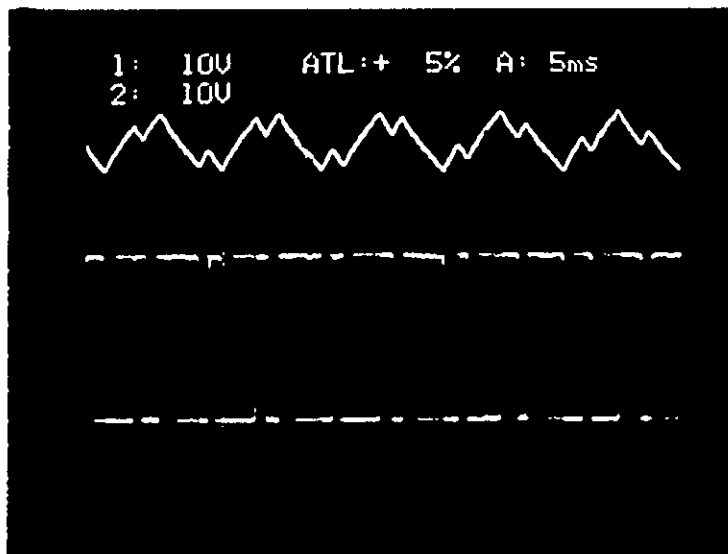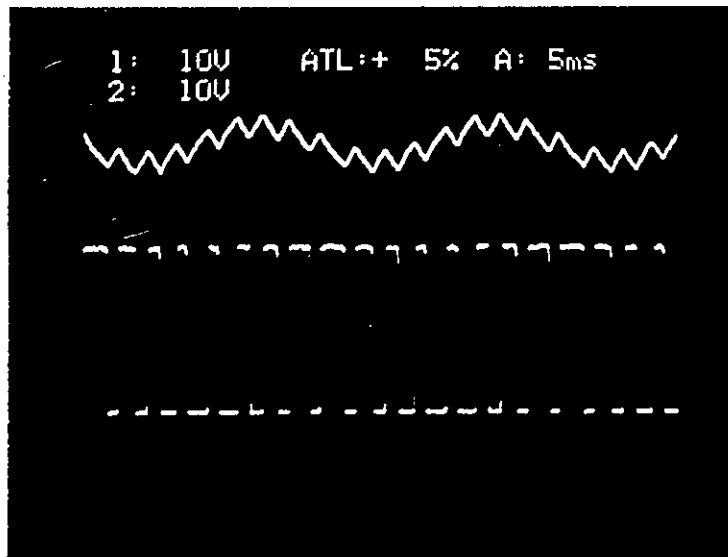
Figure 2.22: Practical waveforms of delta modulation for frequency variation.
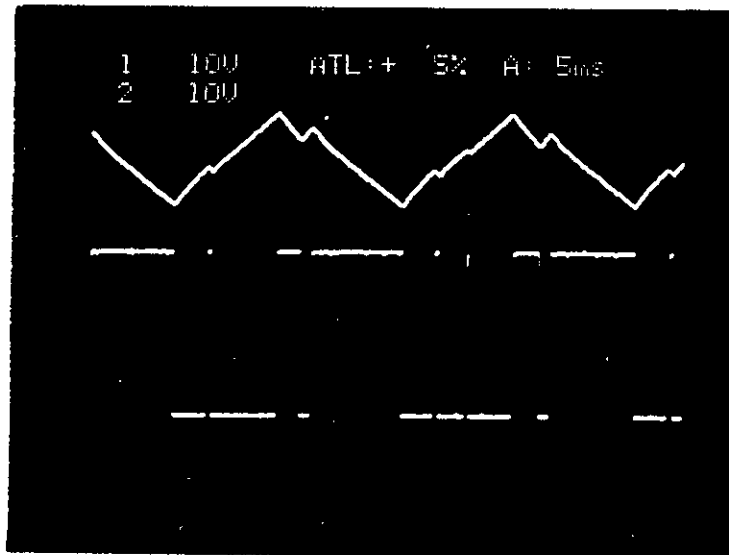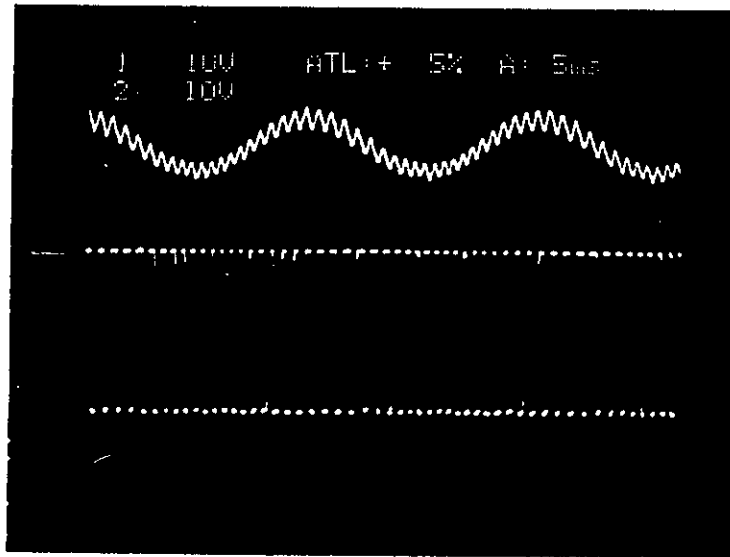
Figure 2.23: Practical waveforms of delta modulation for window width variation.
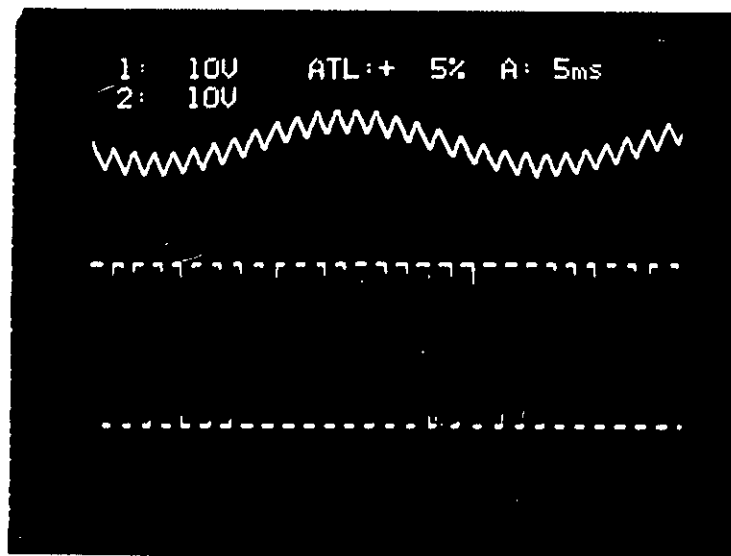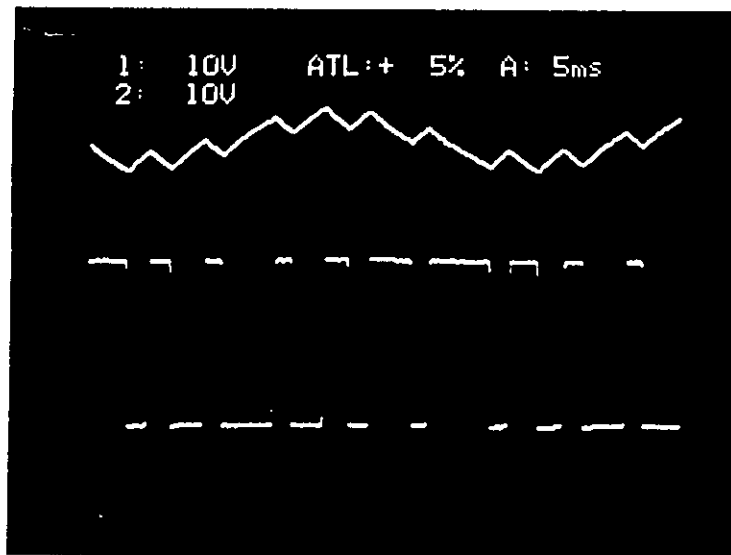
Figure 2.24:   Practical waveforms of delta modulation
                for slope variation.

doing so the number of pulses per cycle are reduced and pulse widths are increased. Hence an automatic v/f = constant is maintained in DM inverter and also pulse dropping occurs with increase in operating frequency of the inverter. The v/f = constant feature is essential for the operation of ac drives. The pulse dropping is also necessary for keeping the switching frequency of static devices of the inverter within their allowable operating ranges.

- Due to pulse dropping and pulse width increasing natures with increase of operating frequency, the inverter waveform gradually turns to square wave mode of operation and maintains this mode of operation at higher operating frequency. In the square wave mode of operation a DM switched inverter exhibits constant voltage characteristics.

- During low frequency operation, the inverter waveforms contain high frequency dominant harmonics. During high frequency operation, the low order harmonics begins to appear in the inverter waveforms.

- Parameters like window width and slope of the modulator determine available fundamental voltage and magnitude of harmonics contained in the inverter waveforms. Higher slope and smaller window width basically increase the oscillating frequency of the estimated wave, and thus moves the dominant harmonics to higher frequencies. These parameters can be varied on-line to achieve harmonics at desired range and level.

- Magnitude of the reference wave also significantly controls the available fundamental voltage of the inverter. Increase in magnitude of the reference wave (while all other parameters are maintained constant) increases the available fundamental voltage of the inverter.

- One significant aspect of the delta modulated inverter is that it controls the excursion of current when feeding inductive loads. This is due to hysteresis band

55

of the modulator imposed by the hysteresis quantizer. As a result, the current of the inductive load is always bound by a limit. This limiting characteristic of the load current within a band is inherently achieved in delta modulation. If such current control is desired in other modulation techniques, extra control circuits are necessary.

One of the fundamental features of the delta modulation i.e., $v/f =$ constant control can also be explained from the modulator operation.

If V_{m1} is the fundamental voltage of modulator output, then considering the filter input/output relationship we have,

$$\frac{V_{l1}}{V_{m1}} \simeq \frac{1}{\omega\tau} \tag{2.44}$$

where, τ is the time constant. But fundamental component of the filter output is equal to magnitude of the input reference sine wave. Hence $V_{l1} = V_r$. Equation (2.44) can be rewritten as,

$$\frac{V_{m1}}{\omega} = V_{l1}\tau = V_r\tau \tag{2.45}$$

As long as the magnitude of the reference sine wave and modulator's filter time constant are maintained constant (which is true if the values of modulator's components are not changed), then the product $V_r\tau$ is constant. Hence

$$\frac{V_{m1}}{f} = 2\pi V_r\tau = \text{constant} \tag{2.46}$$

2.7 Three Phase PWM Inverter Waveform Analysis

In order to investigate the stability of a synchronous motor fed from a 3-phase PWM inverter, it is essential to represent inverter output voltages as line-to-line, line-to-neutral and $d-q$ axes mathematically. Knowing the representation of the switching waveforms, by proper phase staggering ($+120^o$, -120°) and addition of scaled waves, output voltages of three phase PWM inverter can be obtained. The method for obtaining inverter

output voltages is illustrated in Fig. 2.25 for square wave mode of operation. Line to line voltages of three phase inverter are obtained by the addition of scaled modulated wave with phase shifted scaled modulated wave.

To represent inverter output voltages in various forms a switching function $m(t)$ as obtained from a modulated waveforms of Fig. 2.6 is necessary and $m(t)$ can be defined by following expressions.

For one cycle:

$$m_T(t) = \sum_{i=0,1,2..}^{\frac{N_p}{2}} \left[g(t, t_{2i}, t_{2i+1}) - g(t, t_{2i} + \frac{T}{2}, t_{2i+1} + \frac{T}{2}) \right] \qquad (2.47)$$

For multiple cycles:

$$m(t) = \sum_{A=0,T,2T..}^{ZT} \sum_{i=0,1,2..}^{\frac{N_p}{2}} \left[g(t, t_{2i} + A, t_{2i+1} + A) - g(t, t_{2i} + \frac{T}{2} + A, t_{2i+1} + \frac{T}{2} + A) \right] \qquad (2.48)$$

Three phase PWM inverter waveforms are obtained by multiplying time addition of phase staggered switching waves and gating the resultant waves by the line to line voltage waveform of unity magnitude of square wave mode of operation. Gating by line to line voltage of square mode of operation is necessary because inverter line voltages can not be more than V_{dc} in either direction. The analytical expressions for line to line voltages in terms of switching waveforms shown in Fig. 2.25 are obtained as,

$$V_{ab} = \frac{1}{2} V_{dc} \left[m(t) + m(t + \frac{T}{6}) \right] u(t) s_1 \qquad (2.49)$$

$$V_{bc} = \frac{1}{2} V_{dc} \left[m(t - \frac{T}{6}) + m(t - \frac{T}{3}) \right] u(t) s_2 \qquad (2.50)$$

$$V_{ca} = \frac{1}{2} V_{dc} \left[m(t - \frac{T}{2}) + m(t + \frac{T}{3}) \right] u(t) s_3 \qquad (2.51)$$

where, $V(t) = V_{ab}, V_{bc}, V_{ca}$ line to line voltages of the inverter.
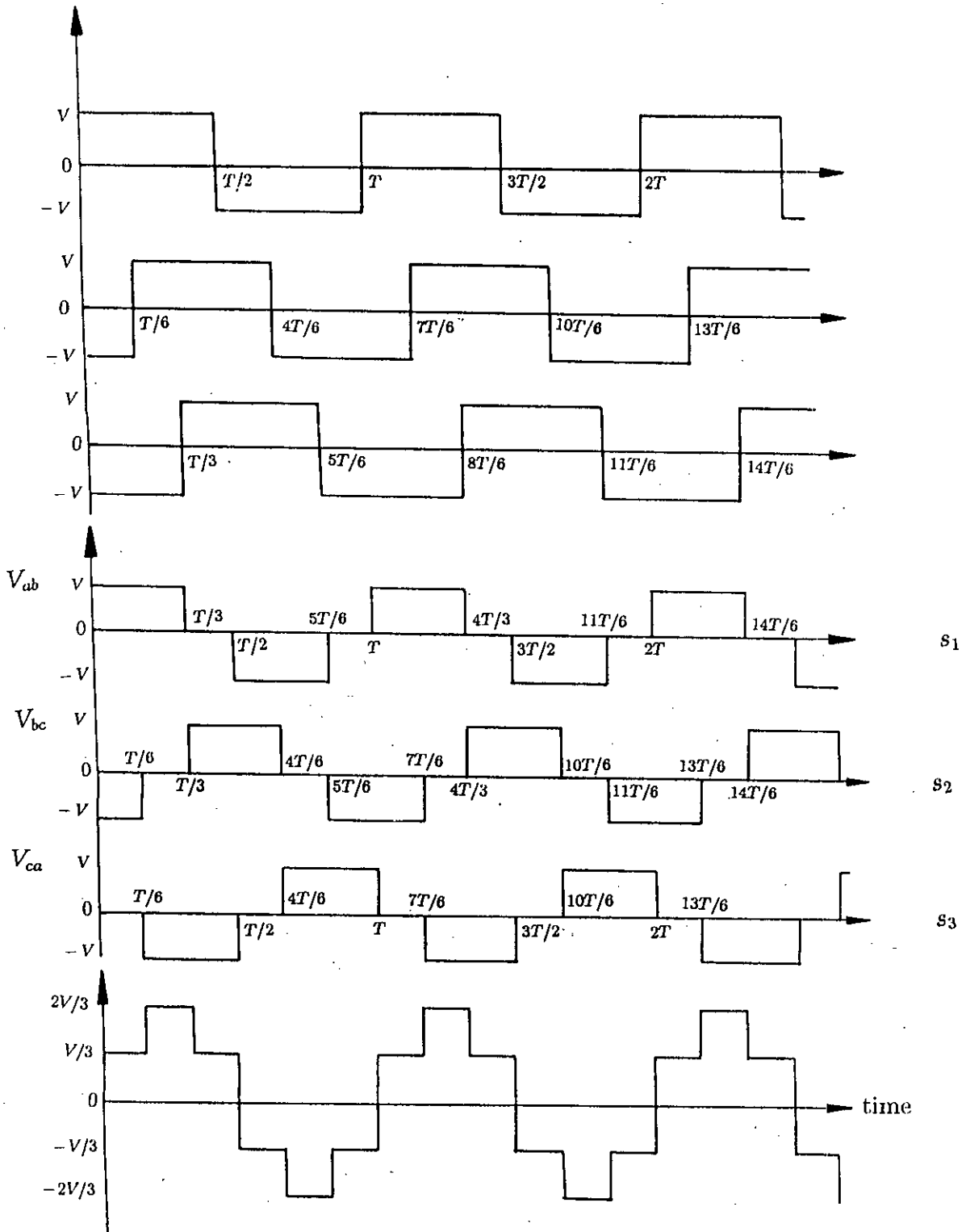
Figure 2.25: Illustration of obtaining three-phase inverter output from switching waveforms.

Since,

$$m\left(t - \frac{T}{2}\right) = -m\left(t\right) \tag{2.52}$$

$$m\left(t - \frac{T}{3}\right) = -m\left(t + \frac{T}{6}\right) \tag{2.53}$$

$$m\left(t + \frac{T}{3}\right) = -m\left(t - \frac{T}{6}\right) \tag{2.54}$$

Equations (2.49) to (2.51) can be written as,

$$V_{ab} = \frac{1}{2}V_{dc}\left[m(t) + m(t + \frac{T}{6})\right]u(t)s_1 \tag{2.55}$$

$$V_{bc} = \frac{1}{2}V_{dc}\left[m(t - \frac{T}{6}) - m(t + \frac{T}{6})\right]u(t)s_2 \tag{2.56}$$

$$V_{ca} = \frac{1}{2}V_{dc}\left[-m(t) + m(t - \frac{T}{6})\right]u(t)s_3 \tag{2.57}$$

In equations (2.55) to (2.57), s_1, s_2 and s_3 are line to line voltage waveforms of unity magnitude in the square wave mode of operation. The line to neutral voltages of the inverter are given by following expressions,

$$V_{an} = \frac{1}{3}\left(V_{ab} - V_{ca}\right) \tag{2.58}$$

$$V_{bn} = \frac{1}{3}\left(V_{bc} - V_{ab}\right) \tag{2.59}$$

$$V_{cn} = \frac{1}{3}\left(V_{ca} - V_{bc}\right) \tag{2.60}$$

where, V_{an}, V_{bn} and V_{cn} are line to neutral voltages of the inverter.

The expressions for line to neutral voltages of the inverter can be written in terms of switching waveforms as,

$$V_{an} = \frac{V_{dc}}{6}\left[\left(m(t) + m(t + \frac{T}{6})\right)s_1 - \left(-m(t) - m(t - \frac{T}{6})\right)s_3\right]u(t) \tag{2.61}$$

$$V_{bn} = \frac{V_{dc}}{6}\left[\left(m(t - \frac{T}{6}) - m(t + \frac{T}{6})\right)s_2 - \left(m(t) + m(t + \frac{T}{6})\right)s_1\right]u(t) \tag{2.62}$$

59

$$V_{cn} = \frac{V_{dc}}{6} \left[\left(-m(t) - m(t - \frac{T}{6}) \right) s_3 - \left(m(t - \frac{T}{6}) - m(t + \frac{T}{6}) \right) s_2 \right] u(t) \qquad (2.63)$$

For machine performance analysis using $d - q$ transformation, we require direct and quadrature axis voltages V_d and V_q [13], which also refers to α β transformation. The reference voltages can be written as,

$$\begin{bmatrix} V_q \\ V_d \end{bmatrix} = \frac{2}{3} \begin{bmatrix} 1 & -\frac{1}{2} & -\frac{1}{2} \\ 0 & -\frac{\sqrt{3}}{2} & +\frac{\sqrt{3}}{2} \end{bmatrix} \begin{bmatrix} V_{ab} \\ V_{bc} \\ V_{ca} \end{bmatrix} \qquad (2.64)$$

$$V_q = \frac{1}{3} [2V_{ab} - V_{bc} - V_{ca}] \qquad (2.65)$$

$$V_d = -\frac{1}{\sqrt{3}} [V_{bc} - V_{ca}] \qquad (2.66)$$

By substitution of equations (2.55) to (2.57) in equations (2.65) to (2.66), V_d and V_q can be expressed as,

$$V_q = \frac{V_{dc}}{6} \left[2 \left(m(t) + m(t + \frac{T}{6}) \right) s_1 - \left(m(t - \frac{T}{6}) - m(t + \frac{T}{6}) \right) s_2 \right]$$
$$\left[- \left(-m(t) + m(t - \frac{T}{6}) \right) s_3 \right] u(t) \qquad (2.67)$$

$$V_d = -\frac{V_{dc}}{2\sqrt{3}} \left[\left(m(t - \frac{T}{6}) - m(t + \frac{T}{6}) \right) s_2 - \left(-m(t) + m(t - \frac{T}{6}) \right) s_3 \right] u(t) \qquad (2.68)$$

Typical voltage waveforms for V_{ab}, V_{an}, V_q and V_d are shown in Figs. 2.26 and 2.27. for modulation index of $m = 0.2$ and carrier frequency of 1.2 kHz. Figs. 2.28 (a) - (e) illustrate practical waveforms of line to neutral voltage obtained from a PWM inverter for 20, 30, 40, 50 and 60 Hz operation with pulse dropping characteristics as inverter goes into higher operating frequency. Figs. 2.29 (a) - (c) show practical waveforms of line to neutral voltage at constant 50 Hz operation of PWM inverter illustrating the trend of change in carrier frequency. Typical spectra of 3-phase PWM inverter waveforms are shown in Figs. 2.30 and 2.31.

An attempt has been made to simulate the above mentioned situation and to produce same voltage waveforms practically while maintaining same operating conditions. The practical waveforms shown in Figs. 2.28 and 2.29 are found to have close agreement with the theoretically obtained waveforms.
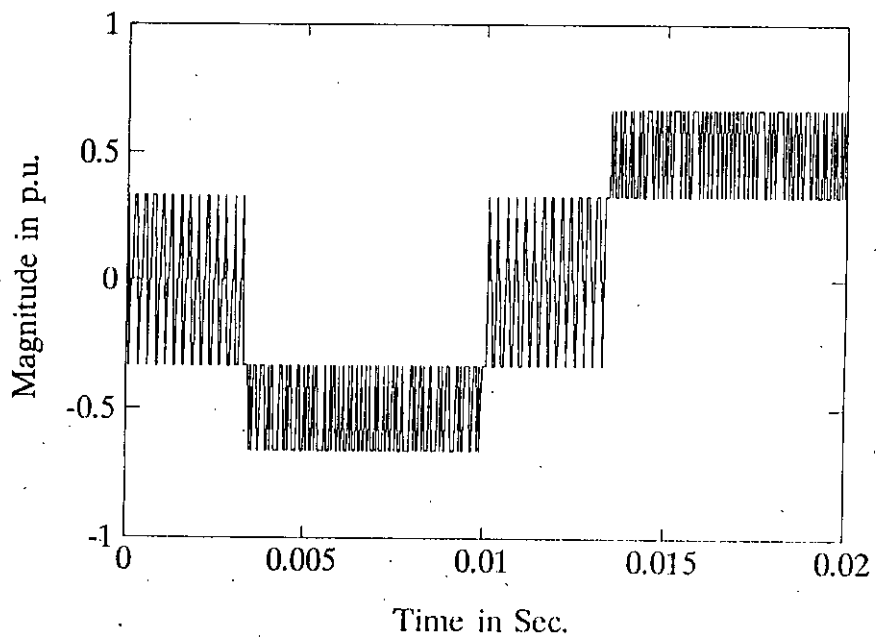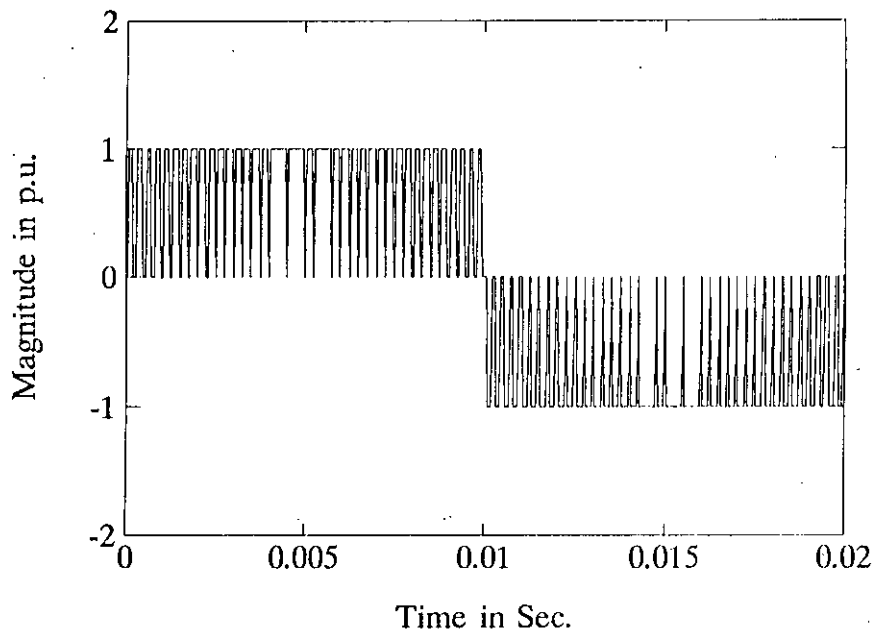
Figure 2.26: Simulated waveforms of three phase PWM inverter for $f = 50$ Hz, $m = 0.8$ and $N = 80$: (a) line voltage; (b) phase voltage.
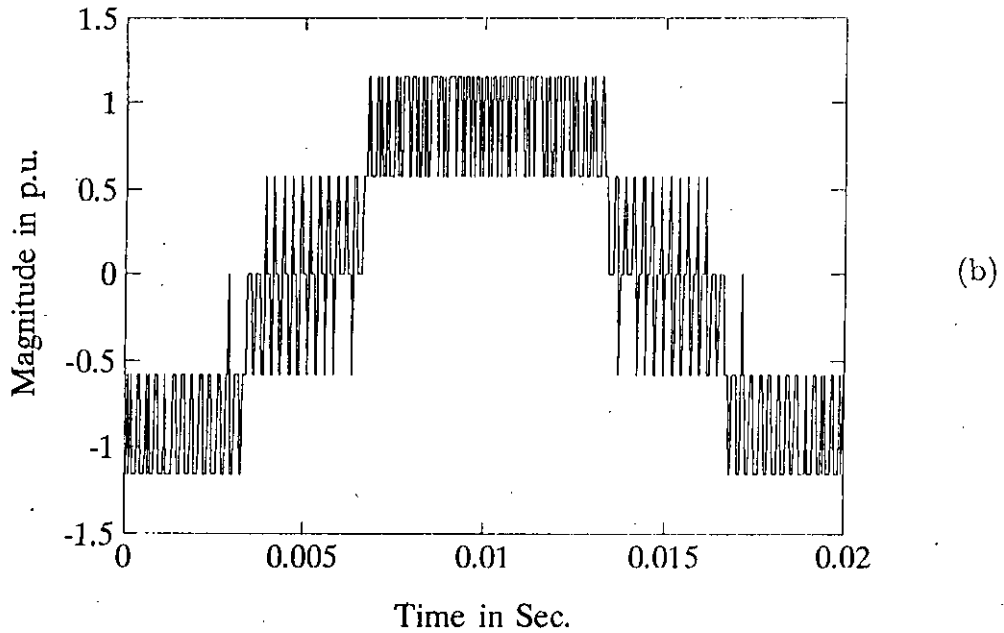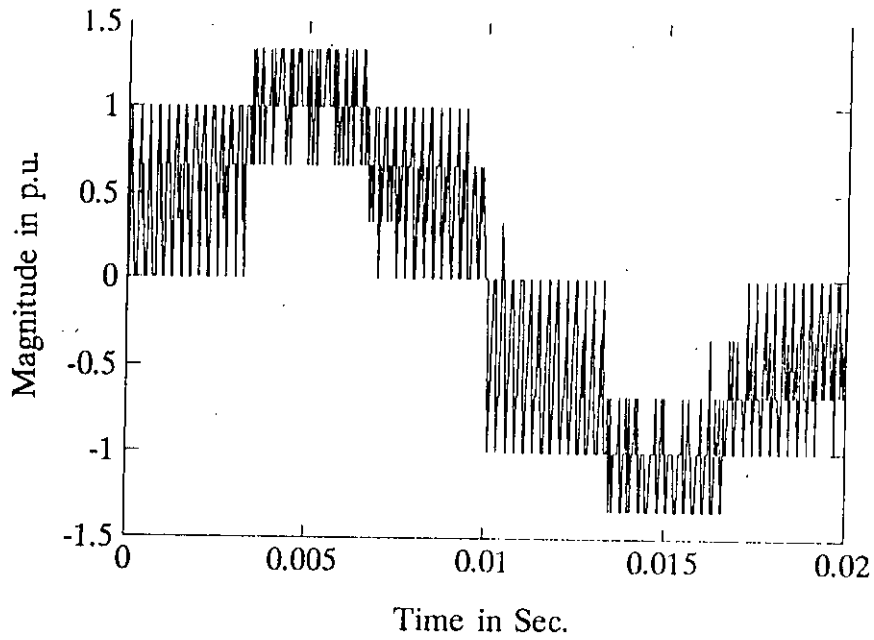
Figure 2.27: Simulated waveforms of three phase PWM inverter for $f = 50$ Hz, $m = 0.8$ and $N = 80$: (a) d-axis voltage; (b) q-axis voltage.
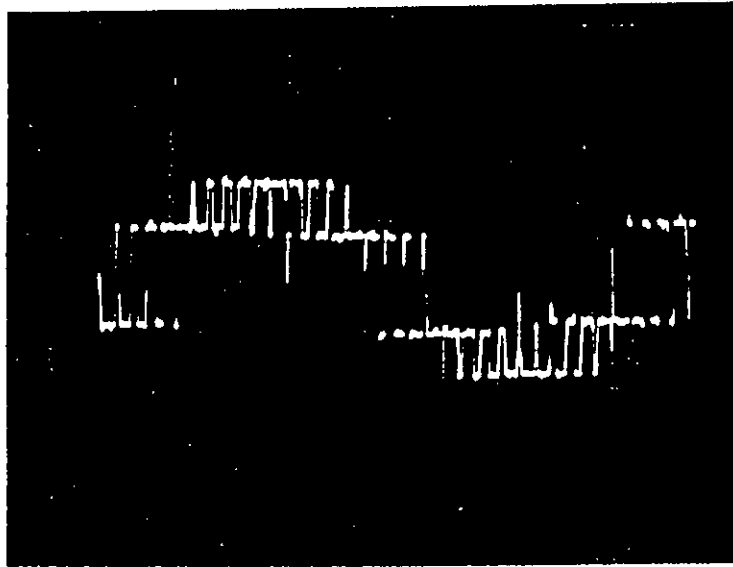
(a)
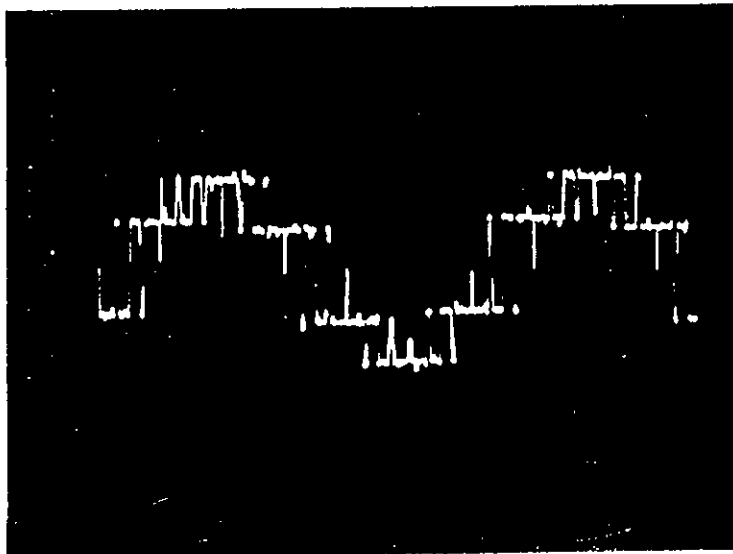
(b)

Figure 2.28   Practical waveforms of phase voltage of three phase
              PWM inverter for the modulating frequency:
              (a) 20 Hz; (b) 30 Hz.

64
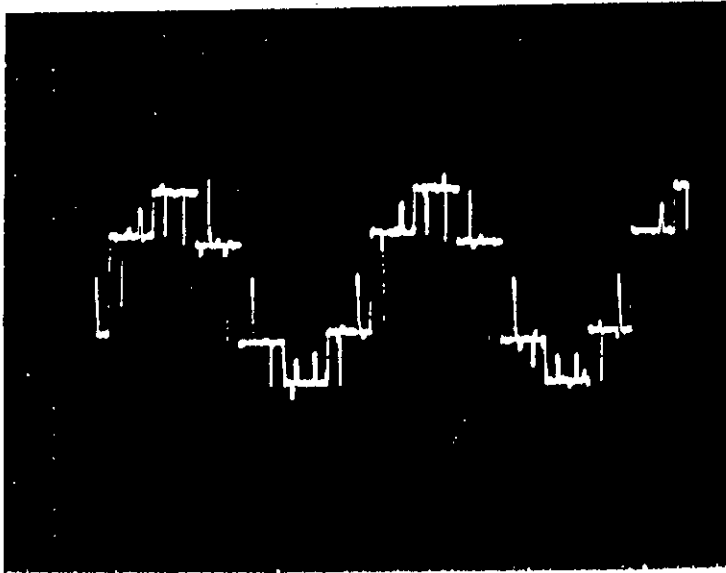
(c)
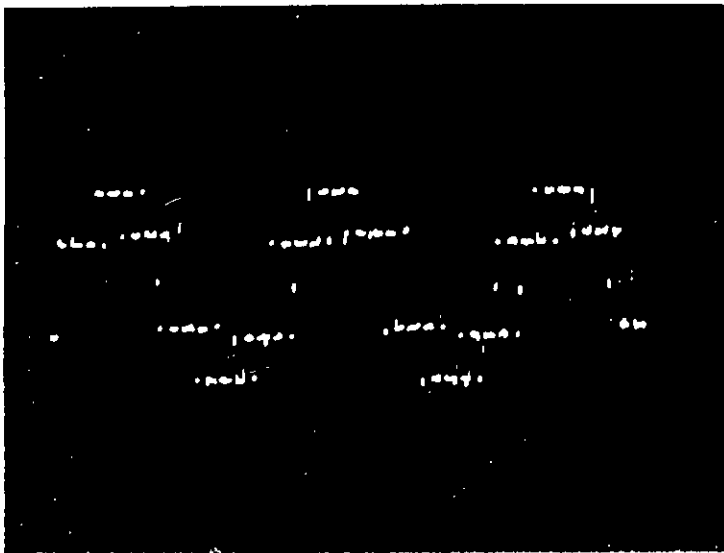
(d)

Figure 2.28 Practical waveforms of phase voltage of three phase
PWM inverter for the modulating frequency:
(c) 40 Hz; (d) 50 Hz.
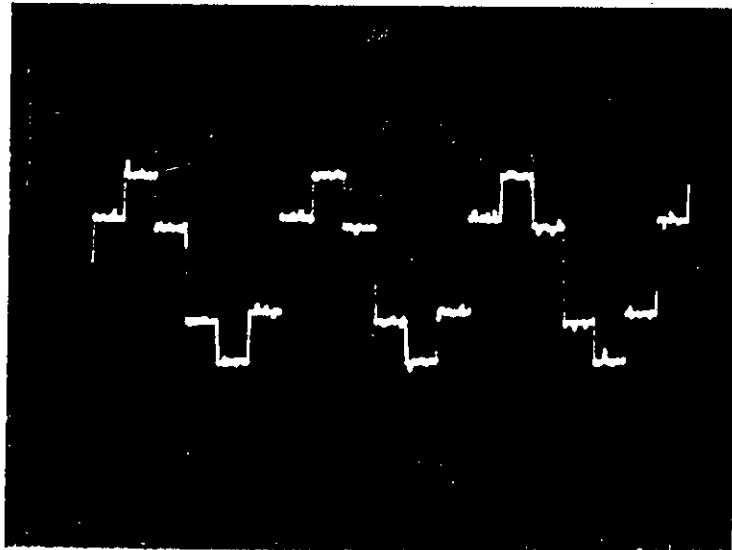
(e)

Figure 2.28   Practical waveforms of phase voltage of three phase
             PWM inverter for the modulating frequency:
             (e) 60 Hz.
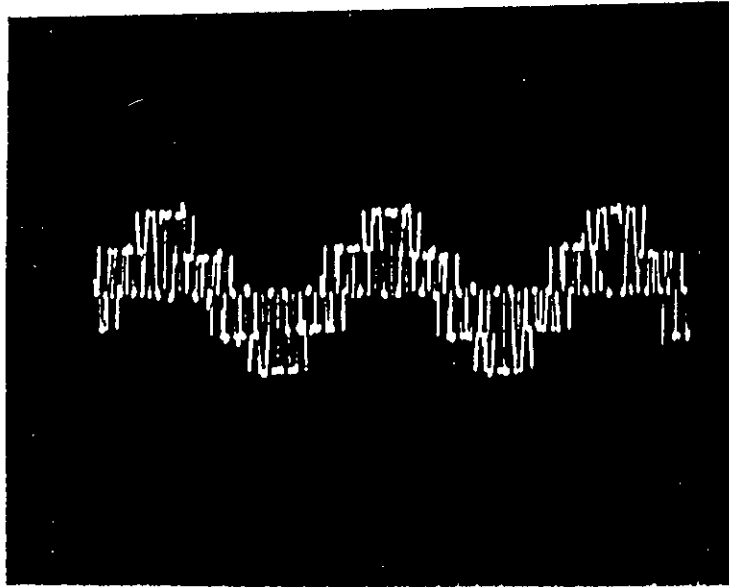
(a)
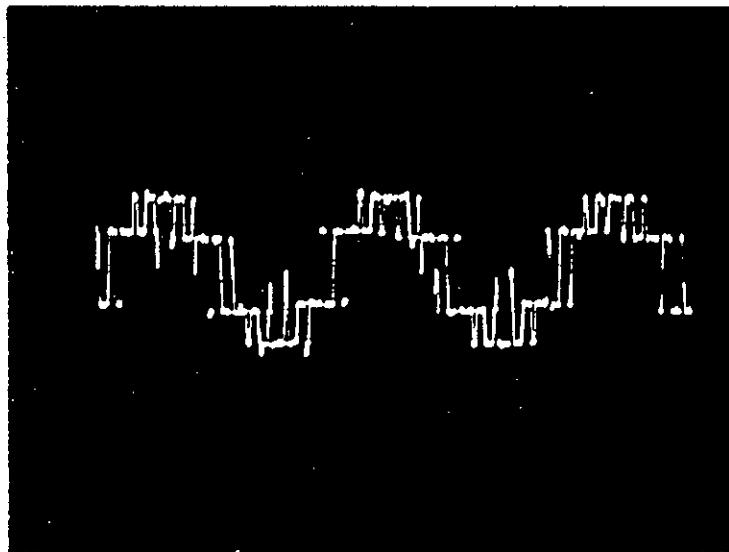
(b)

Figure 2.29   Practical waveforms of phase voltage of three phase
PWM inverter for $(N_1 < N_2 < N_3)$:
(a) N_1 pulses;   (b) N_2 pulses.
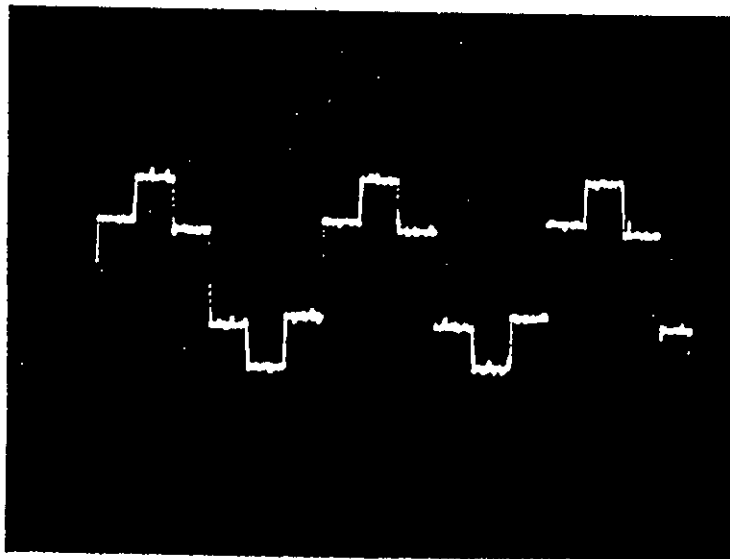
(c)

Figure 2.29   Practical waveforms of phase voltage of three phase
PWM inverter for $(N_1 < N_2 < N_3)$:
(c) N_3 pulses.

(a)

(b)
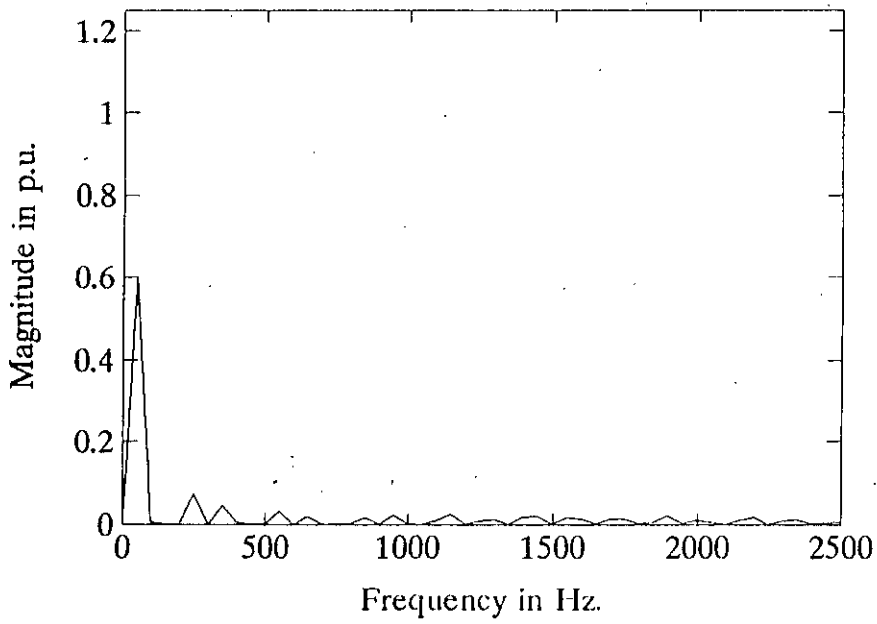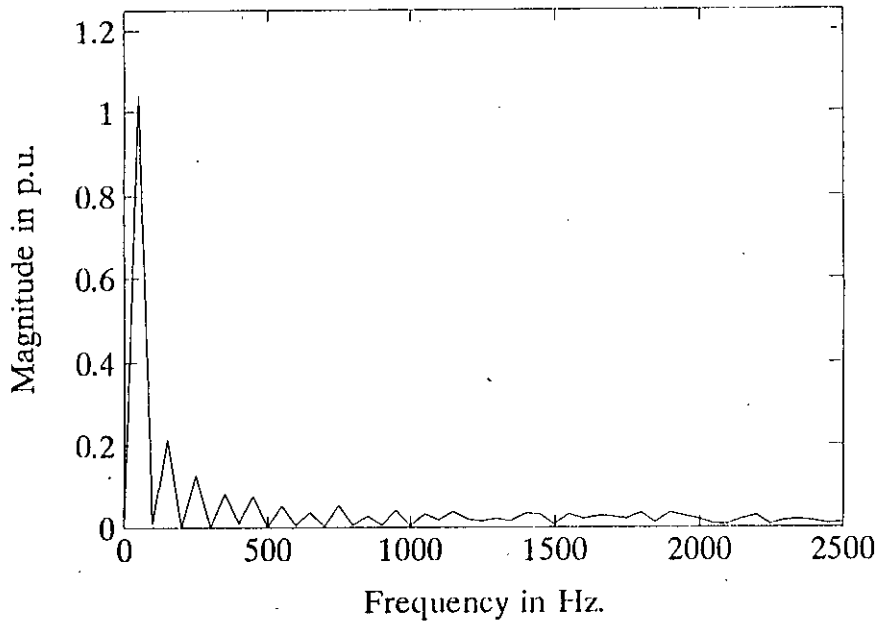
Figure 2.30:   Spectrum of line and phase voltages
for $f = 50$ Hz, $m = 0.8$ and $N = 80$:
(a) line voltage;   (b) phase voltage.

69

(a)

(b)
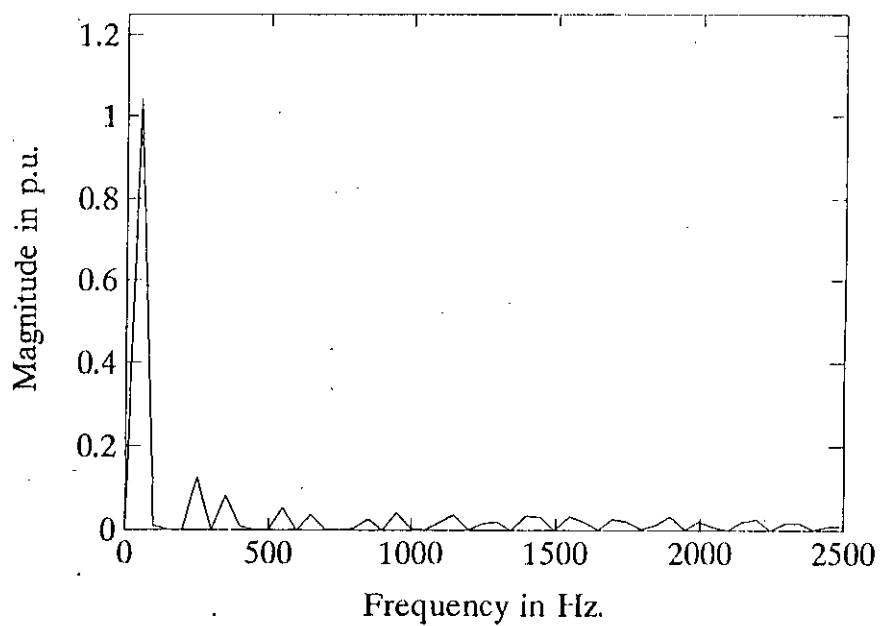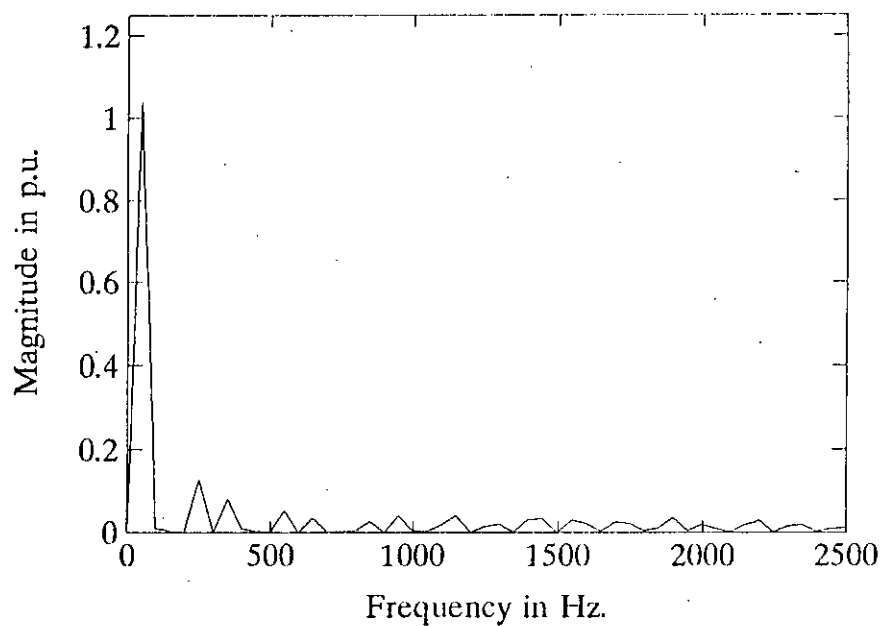
Figure 2.31:   Spectrum of d-axis and q-axis voltages
               for $f = 50$ Hz, $m = 0.8$ and $N = 80$:
               (a) d-axis; (b) q-axis voltage.

CHAPTER 3

STABILITY ANALYSIS OF SYNCHRONOUS MOTORS

3.1 Introduction

Stability of a conventional synchronous motor is its ability to return to normal stable operation after being subjected to a disturbance. Instability of a synchronous motor is experienced in the form of loss of synchronism. Momentary load change or disturbance torque exceeding the motor's limiting torque angle swing results in loss of synchronism. Study of synchronous motor stability both theoretically and experimentally is important for design and operation of the motor and for its control. The mathematical formulations in the form of differential equations are necessary for studying stability of synchronous motor. The differential equations which describe the behaviour of synchronous motors are in general nonlinear. However, considerable insight regarding the stability can be gained from the linearized version of these equations. Linearization approximates the equations by small signal deviation around a steady-state operating point. This involves a set of linearized equations derived in rotor reference frame of the synchronous motor by assuming that each variable is composed of a steady-state or bias component and a small time varying component or perturbation. Each of the two term variables can be substituted for corresponding original variable and second order perturbations are neglected. A set of linear differential equations result in small signal perturbation variables around a steady-state operating point of the synchronous motor. Using the linear set of equations, various methods have so far been used for stability

assessment of ac machines including that of conventional synchronous motors. Of these methods eigenvalue determination and transfer function formulation applying Routh's or Nyquist criteria of classical control theory are common.

In this chapter linearization of synchronous motor equations for sinusoidal excitation having variable voltage and variable frequency characteristics are used to study the effects of operating constraints on motor stability. Eigenvalue determination of the machine equations by state matrix solution has been used to study the stability of the synchronous motor. The method requires the knowledge of elements contained in the state matrix for the steady-state operating conditions. Effects of terminal constraints on the stability are investigated by varying one quantity, while holding the others constant. The results on stability obtained by eigenvalue search technique are substantiated by time domain simulation of torque, torque angle and speed etc.

3.2 Synchronous Machine Models

In order to understand the behaviour of a synchronous machine under both the steady-state and dynamic conditions, machine equations valid for general operating conditions are required. Classically, the theory of synchronous machine was presented in terms of traveling air-gap flux, current and mmf waves. This theory has the advantage of close adherence to the physical realities within the machine and serves the purpose of explaining elementary steady-state operating characteristics. However, the approach becomes extremely impractical when it is necessary to study the behaviour of a machine under transient and dynamic conditions. In modeling, a synchronous machine is considered of containing four basic windings i.e., three symmetrically placed stator windings and a rotor winding. An actual machine contains one or more damper windings. With full knowledge of all circuit parameters, sets of circuit equations can be formulated to obtain all information related to both the transient and dynamic studies. In such a situation general differential equations, which represents the dynamic behaviour are linear with

time-varying coefficients [56]. Under influence of electrodynamical torque, change of speed makes these differential equations nonlinear. The two drawbacks of representing synchronous machine characteristics by straightforward differential equations are thus time-varying machine parameters and nonlinear dynamic machine equations.

Blondel two reaction-theory introduced by Andre Blondel of France and subsequent developments carried out by Doherty, Nickele, Park and others [58,59,60] simplified the differential equations of ac machines to a great extent. The technique involves transformation of voltage, current, flux and other variables to a reference frame where these components are represented by direct axis (d), quadrature axis (q) and zero axis (o) components. These transformations result in new inductances referred to as $d-q-o$ axis machine inductances. The transformation reduces the complexity of machines analysis in two ways:

1. The differential equations have a set of constant parameters instead of time-varying parameters.

2. Transformed equations contain comparatively few terms and transformed currents are weakly coupled to each other than actual stator currents.

If the power supply is a balanced three phase, the $d - q$ axes theory is a standard analytical tool for dynamic modeling of ac machines. Several steady-state and dynamic machine models based on two-reaction theory are available. Of these models, the Park's $d - q$ axes model [60,61] is considered to be one of the most practical model of synchronous machines, because of the presence of rotating field winding and saliency of rotor poles.

3.2.1 Park's Model

The Park's model [60,61] is based on transformation of stator variables of synchronous machine to a reference frame fixed in the rotor. As a result, the time-varying inductances

73

from the voltage equations disappear. The parameters of rotor winding in Park's model are referred to the stator quantities by multiplying the rotor quantities by a constant of proportionality based on turns ratio. The voltage equations describing the behaviour of a synchronous machine are [80],

$$v_{qs} = R_s i_{qs} + \omega_r \lambda_{ds} + p\lambda_{qs} \tag{3.1}$$

$$v_{ds} = R_s i_{ds} - \omega_r \lambda_{qs} + p\lambda_{ds} \tag{3.2}$$

$$v_{os} = R_s i_{os} + p\lambda_{os} \tag{3.3}$$

$$v_{kq} = R_{kq} i_{kq} + p\lambda_{kq} \tag{3.4}$$

$$v_{fd} = R_{fd} i_{fd} + p\lambda_{fd} \tag{3.5}$$

$$v_{kd} = R_{kd} i_{kd} + p\lambda_{kd} \tag{3.6}$$

where, λ represents flux linkage, p is the operator d/dt, ω_r is the rotor angular speed. The expression of flux linkages are related to the currents by,

$$\lambda_{qs} = L_q i_{qs} + L_{mq} i_{kq} \tag{3.7}$$

$$\lambda_{ds} = L_d i_{ds} + L_{md}(i_{fd} + i_{kd}) \tag{3.8}$$

$$\lambda_{os} = L_{ls} i_{os} \tag{3.9}$$

$$\lambda_{kq} = L_{kq} + L_{mq} i_{qs} \tag{3.10}$$

$$\lambda_{fd} = L_{fd} i_{fd} + L_{md}(i_{ds} + i_{kd}) \tag{3.11}$$

$$\lambda_{kd} = L_{kd} i_{kd} + L_{md}(i_{ds} + i_{fd}) \tag{3.12}$$

where, L denotes the inductance with appropriate subscripts for direct and quadrature axes . L_{md} and L_{mq} are the $d-q$ axes magnetizing inductances, respectively. These well-established equations are derived using the following assumptions:

- Each stator winding is described so as to produce a sinusoidal wave of magneto-motive force.

- Stator slots produce negligible variations in the rotor inductances.

74

- Saturation of magnetic circuits and eddy currents are neglected.

- The damper circuit may be represented by a single equivalent winding in each axis.

- Direct axis mutual inductance between the field and the armature is same.

Based on the assumptions above and the voltage equations (3.1) to (3.6) and flux linkage equations (3.7) to (3.12), the equivalent circuits of a synchronous machine are represented as shown in Fig. 3.1. These equivalent circuits are the representation of Park's model for synchronous machines.

Since machine parameters are usually given in ohms or in per unit, it is convenient to express the voltage and flux linkage equations in terms of reactances rather than inductances. Hence, equations (3.1) to (3.12) are rewritten as [80],

$$v_{qs} = R_s i_{qs} + \frac{\omega_r}{\omega_b}\psi_{ds} + \frac{p}{\omega_b}\psi_{qs} \tag{3.13}$$

$$v_{ds} = R_s i_{ds} - \frac{\omega_r}{\omega_b}\psi_{qs} + \frac{p}{\omega_b}\psi_{ds} \tag{3.14}$$

$$v_{os} = R_s i_{os} + \frac{p}{\omega_b}\psi_{os} \tag{3.15}$$

$$v_{kq} = R_{kq} i_{kq} + \frac{p}{\omega_b}\psi_{kq} \tag{3.16}$$

$$v_{fd} = R_{fd} i_{fd} + \frac{p}{\omega_b}\psi_{fd} \tag{3.17}$$

$$v_{kd} = R_{kd} i_{kd} + \frac{p}{\omega_b}\psi_{kd} \tag{3.18}$$

where, $\psi = \omega_b \lambda$, represents flux linkage per second and ω_b is base angular speed used to calculate the inductive reactances. The flux linkages per second are,

$$\psi_{qs} = X_q i_{qs} + X_{mq} i_{kq} \tag{3.19}$$

$$\psi_{ds} = X_d i_{ds} + X_{md}(i_{fd} + i_{kd}) \tag{3.20}$$

$$\psi_{os} = X_{ls} i_{os} \tag{3.21}$$

$$\psi_{kq} = X_{kq} + X_{mq} i_{qs} \tag{3.22}$$

75
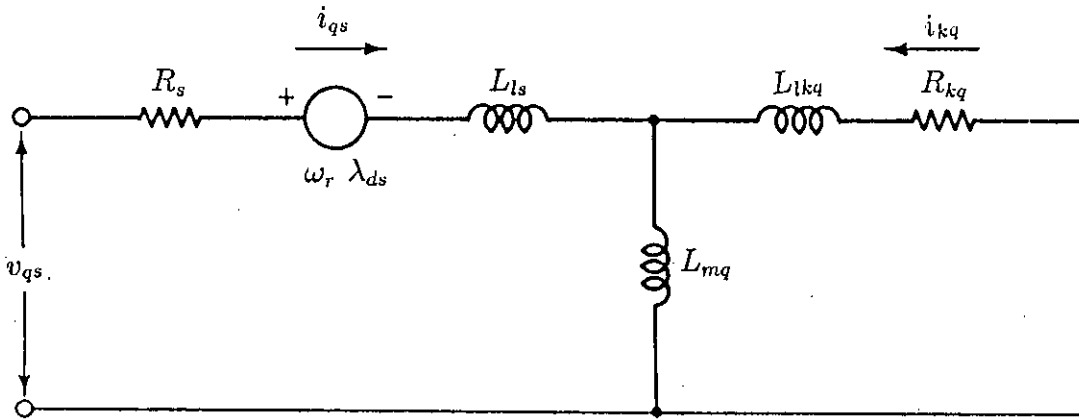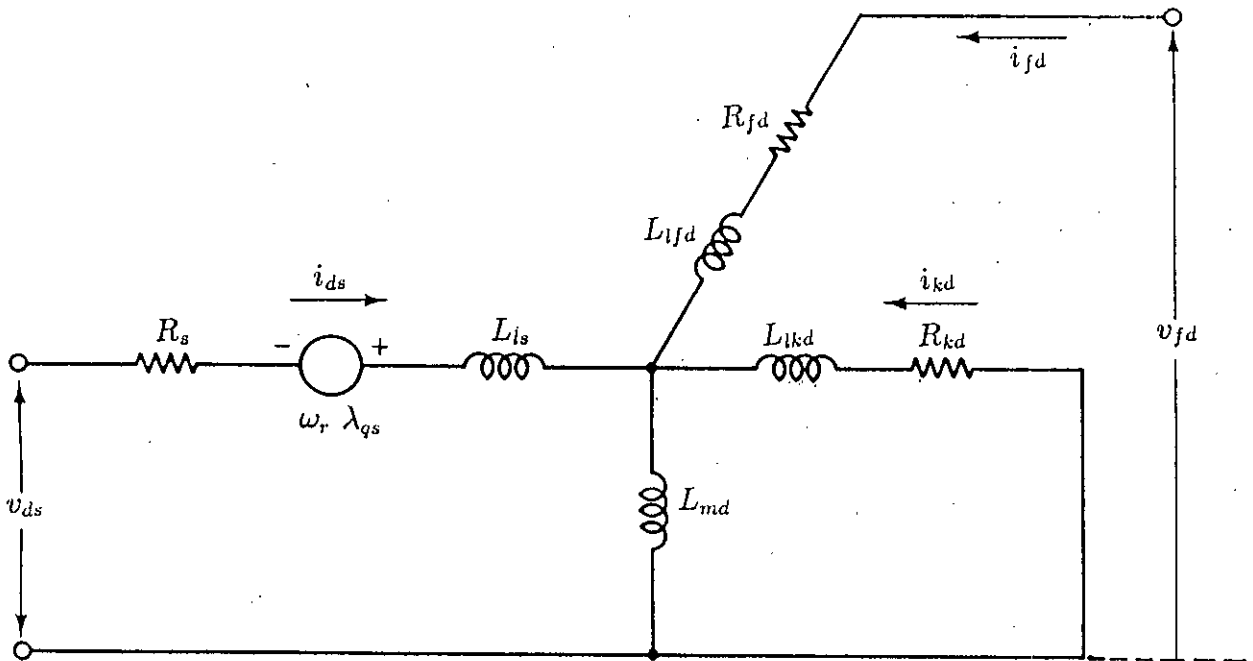
Figure 3.1: Park's equivalent circuits of synchronous machine:
(a) quadrature-axis equivalent circuit;
(b) direct-axis equivalent circuit.

$$\psi_{fd} = X_{fd}i_{fd} + X_{md}(i_{ds} + i_{kd}) \tag{3.23}$$

$$\psi_{kd} = X_{kd}i_{kd} + X_{md}(i_{ds} + i_{fd}) \tag{3.24}$$

where, X denotes the inductive reactance with appropriate d, q subscripts.

For convenience of per unitizing field variables, the field voltage v_{fd} is replaced by the following relation [80],

$$e_{xfd} = v_{fd}\frac{X_{md}}{R_{fd}} \tag{3.25}$$

Substituting this relationship into equation (3.17) the expression for field voltage becomes,

$$e_{xfd} = \frac{X_{md}}{R_{fd}}(R_{fd}i_{fd} + \frac{p}{\omega_b}\psi_{fd}) \tag{3.26}$$

To obtain voltage equations in terms of currents as state variables, the flux linkages per second equations (3.19) to (3.24) are substituted into equations (3.13) to (3.18). The field voltage equation (3.26) is used instead of equation (3.17). The resulting voltage equations are expressed in matrix form as,

$$\begin{bmatrix} v_{qs} \\ v_{ds} \\ v_{0s} \\ v_{kq} \\ e_{xfd} \\ v_{kd} \end{bmatrix} = \begin{bmatrix} R_s + \frac{p}{\omega_b}X_q & \frac{\omega_r}{\omega_b}X_d & 0 & \frac{p}{\omega_b}X_{mq} & \frac{\omega_r}{\omega_b}X_{md} & \frac{\omega_r}{\omega_b}X_{md} \\ -\frac{\omega_r}{\omega_b}X_q & R_s + \frac{p}{\omega_b}X_d & 0 & -\frac{\omega_r}{\omega_b}X_{mq} & \frac{p}{\omega_b}X_{md} & \frac{p}{\omega_b}X_{md} \\ 0 & 0 & R_s + \frac{p}{\omega_b}X_{ls} & 0 & 0 & 0 \\ \frac{p}{\omega_b}X_{mq} & 0 & 0 & R_{kq} + \frac{p}{\omega_b}X_{kq} & 0 & 0 \\ 0 & \frac{X_{md}}{R_{fd}}(\frac{p}{\omega_b}X_{md}) & 0 & 0 & \frac{X_{md}}{R_{fd}}(R_{fd} + \frac{p}{\omega_b}X_{fd}) & \frac{X_{md}}{R_{fd}}(\frac{p}{\omega_b}X_{md}) \\ 0 & \frac{p}{\omega_b}X_{md} & 0 & 0 & \frac{p}{\omega_b}X_{md} & R_{kd} + \frac{p}{\omega_b}X_{kd} \end{bmatrix} \begin{bmatrix} i_{qs} \\ i_{ds} \\ i_{0s} \\ i_{kq} \\ i_{fd} \\ i_{kd} \end{bmatrix}$$
$$\tag{3.27}$$

where,

$$X_q = X_{ls} + X_{mq} \tag{3.28}$$

$$X_d = X_{ls} + X_{md} \tag{3.29}$$

$$X_{kq} = X_{lkq} + X_{mq} \tag{3.30}$$

$$X_{fd} = X_{lfd} + X_{md} \tag{3.31}$$

$$X_{kd} = X_{lkd} + X_{md} \tag{3.32}$$

The reactances X_q and X_d are generally referred to as q—axis and d—axis reactances, respectively. The flux linkages per second may be expressed from equation (3.19) to

77

(3.24) as,

$$
\begin{bmatrix} \psi_{qs} \\ \psi_{ds} \\ \psi_{0s} \\ \psi_{kq} \\ \psi_{fd} \\ \psi_{kd} \end{bmatrix} = \begin{bmatrix} X_q & 0 & 0 & X_{mq} & 0 & 0 \\ 0 & X_d & 0 & 0 & X_{md} & X_{md} \\ 0 & 0 & X_{ls} & 0 & 0 & 0 \\ X_{mq} & 0 & 0 & X_{kq} & 0 & 0 \\ 0 & X_{md} & 0 & 0 & X_{fd} & X_{md} \\ 0 & X_{md} & 0 & 0 & X_{md} & X_{kd} \end{bmatrix} \begin{bmatrix} i_{qs} \\ i_{ds} \\ i_{0s} \\ i_{kq} \\ i_{fd} \\ i_{kd} \end{bmatrix} \tag{3.33}
$$

If flux linkages per second are selected as state variables it is convenient to express equation (3.33) as,

$$
\begin{bmatrix} \psi_{qs} \\ \psi_{kq} \end{bmatrix} = \begin{bmatrix} X_q & X_{mq} \\ X_{mq} & X_{kq} \end{bmatrix} \begin{bmatrix} i_{qs} \\ i_{kq} \end{bmatrix} \tag{3.34}
$$

and,

$$
\begin{bmatrix} \psi_{ds} \\ \psi_{fd} \\ \psi_{kd} \end{bmatrix} = \begin{bmatrix} X_d & X_{md} & X_{md} \\ X_{md} & X_{fd} & X_{md} \\ X_{md} & X_{md} & X_{kd} \end{bmatrix} \begin{bmatrix} i_{ds} \\ i_{fd} \\ i_{kd} \end{bmatrix} \tag{3.35}
$$

Solving the above equations for currents yields,

$$
\begin{bmatrix} i_{qs} \\ i_{kq} \end{bmatrix} = \begin{bmatrix} Y_{q(1,1)} & Y_{q(1,2)} \\ Y_{q(2,1)} & Y_{q(2,2)} \end{bmatrix} \begin{bmatrix} \psi_{qs} \\ \psi_{kq} \end{bmatrix} \tag{3.36}
$$

and,

$$
\begin{bmatrix} i_{ds} \\ i_{fd} \\ i_{kd} \end{bmatrix} = \begin{bmatrix} Y_{d(1,1)} & Y_{d(1,2)} & Y_{d(1,3)} \\ Y_{d(2,1)} & Y_{d(2,2)} & Y_{d(2,3)} \\ Y_{d(3,1)} & Y_{d(3,2)} & Y_{d(3,3)} \end{bmatrix} \begin{bmatrix} \psi_{ds} \\ \psi_{fd} \\ \psi_{kd} \end{bmatrix} \tag{3.37}
$$

where, Y_q and Y_d are the elements of admittance matrix obtained by inversion of matrix equations (3.34) and (3.35).

Rearranging the matrix equation (3.27) in terms of flux linkages per second one obtains,

$$
\begin{bmatrix} v_{qs} \\ v_{ds} \\ v_{0s} \\ v_{kq} \\ v_{fd} \\ v_{kd} \end{bmatrix} = \begin{bmatrix} R_s Y_{q(1,1)} + \frac{p}{\omega_b} & \frac{\omega_r}{\omega_b} & 0 & R_s Y_{q(1,2)} & 0 & 0 \\ -\frac{\omega_r}{\omega_b} & R_s Y_{d(1,1)} + \frac{p}{\omega_b} & 0 & 0 & R_s Y_{d(1,2)} & R_s Y_d(1,3) \\ 0 & 0 & \frac{R_s}{X_{ls}} + \frac{p}{\omega_b} & 0 & 0 & 0 \\ R_{kq} Y_{q(2,1)} & 0 & 0 & R_{kq} Y_{q(2,2)} + \frac{p}{\omega_b} & 0 & 0 \\ 0 & R_{fd} Y_{d(2,1)} & 0 & 0 & R_{fd} Y_{d(2,2)} + \frac{p}{\omega_b} & R_{fd} Y_{d(2,3)} \\ 0 & R_{kd} Y_{d(3,1)} & 0 & 0 & R_{kd} Y_{d(3,2)} & R_{kd} Y_{d(3,3)} + \frac{p}{\omega_b} \end{bmatrix} \begin{bmatrix} \psi_{qs} \\ \psi_{ds} \\ \psi_{0s} \\ \psi_{kq} \\ \psi_{fd} \\ \psi_{kd} \end{bmatrix} \tag{3.38}
$$

It is important to note that each of the $q-$axis and $d-$axis voltage equations contains two derivatives of currents when currents are selected as state variables. But it is shown

from equation (3.38), when flux linkages per second are selected as state variables, both the q—axis and d—axis voltage equations contain only one derivative of ψ. It is more convenient to implement a computer simulation of a synchronous motor with flux linkages per second as state variables rather than with currents.

The expression for the instantaneous electromagnetic torque is obtained by employing the principle of arbitrary displacement assuming current as state variable. The per unit torque can be expressed [80] as,

$$T_e = X_{md}(i_{ds} + i_{fd} + i_{kd})i_{qs} - X_{mq}(i_{qs} + i_{kq})i_{ds} \qquad (3.39)$$

The per unit relationship between the torque and the rotor speed can be written as,

$$T_e = 2Hp\frac{\omega_r}{\omega_b} + T_L \qquad (3.40)$$

where, H represents the rotor inertia and T_L is the load torque.

The position θ_e of the reference axis at any instant is,

$$\theta_e = \omega_e t \qquad (3.41)$$

and the rotor position θ_r and its speed ω_r are expressed as,

$$\theta_r = \omega_e t + \delta \qquad (3.42)$$

$$\omega_r = \omega_e + p\delta \qquad (3.43)$$

$$\delta = \frac{\omega_b}{p}\left(\frac{\omega_r - \omega_e}{\omega_b}\right) \qquad (3.44)$$

where, δ is known as torque angle, the value of which is negative for motor action. The equations of a synchronous machine are used in various performance studies such as steady-state, dynamic performance and stability analysis etc.

3.3 Linearization

3.3.1 Motor Model

The equations of the synchronous motor and their derived versions as used in various performance study, have been outlined in section 3.2. These equations are based on equivalent circuits of the motor as shown in Fig. 3.1. For balanced operating conditions the o quantities of the dqo variables may be omitted from all the voltage and flux linkage equations. The $d - q$ axes stator voltages in the rotor reference frame are function of the torque angle δ and are expressed [80] as,

$$v_{qs} = \sqrt{2}v_s \cos\delta \tag{3.45}$$

$$= V\cos\delta \tag{3.46}$$

$$v_{ds} = \sqrt{2}v_s \sin\delta \tag{3.47}$$

$$= V\sin\delta \tag{3.48}$$

Substituting equations (3.46) and (3.48) into equation (3.27), the voltage equations of synchronous motor in the rotor reference frame modifies to,

$$
\begin{bmatrix}
V\cos\delta \\
V\sin\delta \\
v_{kq} \\
e_{xfd} \\
v_{kd}
\end{bmatrix}
=
\begin{bmatrix}
R_s + \frac{p}{\omega_b}X_q & \frac{\omega_r}{\omega_b}X_d & \frac{p}{\omega_b}X_{mq} & \frac{\omega_r}{\omega_b}X_{md} & \frac{\omega_r}{\omega_b}X_{md} \\
-\frac{\omega_r}{\omega_b}X_q & R_s + \frac{p}{\omega_b}X_d & -\frac{\omega_r}{\omega_b}X_{mq} & \frac{p}{\omega_b}X_{md} & \frac{p}{\omega_b}X_{md} \\
\frac{p}{\omega_b}X_{mq} & 0 & R_{kq} + \frac{p}{\omega_b}X_{kq} & 0 & 0 \\
0 & \frac{X_{md}}{R_{fd}}\left(\frac{p}{\omega_b}X_{md}\right) & 0 & \frac{X_{md}}{R_{fd}}\left(R_{fd} + \frac{p}{\omega_b}X_{fd}\right) & \frac{X_{md}}{R_{fd}}\left(\frac{p}{\omega_b}X_{md}\right) \\
0 & \frac{p}{\omega_b}X_{md} & 0 & \frac{p}{\omega_b}X_{md} & R_{kd} + \frac{p}{\omega_b}X_{kd}
\end{bmatrix}
\begin{bmatrix}
i_{qs} \\
i_{ds} \\
i_{kq} \\
i_{fd} \\
i_{kd}
\end{bmatrix}
\tag{3.49}
$$

where, the reactances are defined by equations (3.28) to (3.32).

3.3.2 Steady-State Operating Characteristics

The theoretical treatment regarding synchronous motor stability requires values of all the variables in steady state condition. During balanced steady-state operation the rotor windings do not experience a change of flux linkages, hence current is not flowing in the short-circuited damper windings. The field voltage and its current remain constant. In this mode of operation, since the machine rotates at a constant speed, the time rate of

change in rotor angle $p\theta_r$ is a constant. Therefore, the equations for the steady-state operation are obtained by neglecting the terms having time derivatives from differential equations (3.49). The steady-state version of equations are derived as follows.

$$v_{qs0} = R_s i_{qs0} + \frac{\omega_{r0}}{\omega_b} X_d i_{ds0} + \frac{\omega_{r0}}{\omega_b} X_{md} i_{fd0} \tag{3.50}$$

$$v_{ds0} = R_s i_{ds0} - \frac{\omega_{r0}}{\omega_b} X_q i_{qs0} \tag{3.51}$$

$$e_{xfd0} = X_{md} i_{fd0} \tag{3.52}$$

$$\psi_{qs0} = X_q i_{qs0} \tag{3.53}$$

$$\psi_{ds0} = X_d i_{ds0} + X_{md} i_{fd0} \tag{3.54}$$

$$\psi_{fd0} = X_{md}(i_{ds0} + i_{fd0}) \tag{3.55}$$

Here the steady-state values, about which small changes occur, are indicated by suffix 0. The quantities mentioned in the above equations are defined by equations (3.19) to (3.24) and (3.28) to (3.32). During steady-state conditions, the electrical angular speed of the rotor ω_{r0} is constant and equals to ω_e. The steady-state torque T_{e0} and torque angle δ_0 are defined as,

$$T_{e0} = X_{md}(i_{ds0} + i_{fd0})i_{qs0} - X_{mq}i_{qs0}i_{ds0} \tag{3.56}$$

$$\delta_0 = \theta_{r0} - \omega_e t \tag{3.57}$$

It is clear that the frequency ratio $\frac{\omega_e}{\omega_b}$ depends upon the value of the electrical angular velocity of the applied stator voltages.

3.3.3 Linearization for Small Perturbations

Stability of synchronous motors governed by non-linear equations can be assessed without complete solution, when the motor is subjected to a small disturbance. For small variation relative to a given steady-state condition, the non-linear differential equations can be approximately converted into linear ones. Such linearized equations can conveniently be used for studying the stability of synchronous motors.

81

The method of analyzing the small changes is applied to the motor equations for studying stability by imagining a sudden change in any of the applied quantities, v_{qs}, v_{ds}, v_{kq}, v_{fd}, v_{kd}, T_L or f and finding the resulting change in i_{qs}, i_{ds}, i_{kq}, i_{fd}, i_{kd}, ω_r or δ.

In order to illustrate the method, let us assume that a motor variable f_i changes from a steady value f_{i0} to a slightly different value $f_{i0} + \Delta f_i$, where Δf_i is the small excursion of this motor variable about its steady value. Applying the small signal perturbation theory to equations (3.46), (3.48) and (3.49) and expressing all the variables in perturbed form,

$$V \cos(\delta_0 + \Delta\delta) = V(\cos\delta_0 - \sin\delta_0 \Delta\delta) \tag{3.58}$$

$$= V \cos\delta_0 - V \sin\delta_0 \Delta\delta \tag{3.59}$$

$$V \sin(\delta_0 + \Delta\delta) = V(\sin\delta_0 + \cos\delta_0 \Delta\delta) \tag{3.60}$$

$$= V \sin\delta_0 + V \cos\delta_0 \Delta\delta \tag{3.61}$$

$$V \cos\delta_0 - V \sin\delta_0 \Delta\delta = (R_s + \frac{p}{\omega_b}X_q)(i_{qs0} + \Delta i_{qs}) + \frac{\omega_{r0} + \Delta\omega_r}{\omega_b}X_d(i_{ds0} + \Delta i_{ds})$$
$$+ \frac{p}{\omega_b}X_{mq}(i_{kq0} + \Delta i_{kq}) + \frac{\omega_{r0} + \Delta\omega_r}{\omega_b}X_{md}(i_{fd0} + \Delta i_{fd}) + \frac{\omega_{r0} + \Delta\omega_r}{\omega_b}X_{md}(i_{kd0} + \Delta i_{kd}) \tag{3.62}$$

$$V \sin\delta_0 + V \cos\delta_0 \Delta\delta = -\frac{\omega_{r0} + \Delta\omega_r}{\omega_b}X_q(i_{qs0} + \Delta i_{qs}) + (R_s + \frac{p}{\omega_b}X_d)(i_{ds0} + \Delta i_{ds})$$
$$- \frac{\omega_{r0} + \Delta\omega_r}{\omega_b}(i_{kq0} + \Delta i_{kq}) + \frac{p}{\omega_b}X_{md}(i_{fd0} + \Delta i_{fd}) + \frac{p}{\omega_b}X_{md}(i_{kd0} + \Delta i_{kd}) \tag{3.63}$$

$$v_{kq0} + \Delta v_{kq} = \frac{p}{\omega_b}X_{mq}(i_{qs0} + \Delta i_{qs}) + (R_{kq} + \frac{p}{\omega_b}X_{kq})(i_{kq0} + \Delta i_{kq}) \tag{3.64}$$

$$e_{xfd0} + \Delta e_{xfd} = \frac{X_{md}}{R_{fd}}(\frac{p}{\omega_b}X_{md})(i_{ds0} + \Delta i_{ds}) + \frac{X_{md}}{R_{fd}}(R_{fd} + \frac{p}{\omega_b}X_{fd})(i_{fd0} + \Delta i_{fd})$$
$$+ \frac{X_{md}}{R_{fd}}(\frac{p}{\omega_b}X_{md})(i_{kd0} + \Delta i_{kd}) \tag{3.65}$$

$$v_{kd0} + \Delta v_{kd} = \frac{p}{\omega_b}X_{md}(i_{ds0} + \Delta i_{ds}) + \frac{p}{\omega_b}X_{md}(i_{fd0} + \Delta i_{fd}) + (R_{kd} + \frac{p}{\omega_b}X_{kd})(i_{kd0} + \Delta i_{kd}) \tag{3.66}$$

The quantities v_{qs0}, v_{ds0}, v_{fd0}, i_{qs0}, i_{ds0}, i_{fd0}, ω_{r0} and δ_0 describe the steady-state operating points and can be determined using the equations presented in section 3.3.2. It is to be noted that under steady-state conditions, damper windings do not experience any change of flux linkages. Thus the induced damper currents (i_{kq0}, i_{kd0}) are zero and they will not be included in final linearized equations.

Similarly, applying the small perturbation theory to the torque expressions of equations

(3.39) and (3.40), the linearized torque equations can be obtained as,

$$
\begin{aligned}
T_{e0} + \Delta T_e &= X_{md}[\Delta i \sin(\delta_0 + \theta) + I \sin(\delta_0 + \theta) + I \cos(\delta_0 + \theta)\Delta\delta + I_{fd0} + \Delta i_{fd} + \Delta i_{kd}] \\
&\quad [\Delta i \cos(\delta_0 + \theta) + I \cos(\delta_0 + \theta) - I \sin(\delta_0 + \theta)\Delta\delta] \\
&\quad - X_{mq}[\Delta i \cos(\delta_0 + \theta) + I \cos(\delta_0 + \theta) - I \sin(\delta_0 + \theta)\Delta\delta + \Delta i_{kq}] \\
&\quad [\Delta i \sin(\delta_0 + \theta) + I \sin(\delta_0 + \theta) + I \cos(\delta_0 + \theta)\Delta\delta] \qquad (3.67)
\end{aligned}
$$

and,

$$
T_{e0} + \Delta T_e = 2Hp\frac{\omega_{r0} + \Delta\omega_r}{\omega_b} + T_{L0} + \Delta T_L \qquad (3.68)
$$

Small controlled changes in the frequency of the applied stator voltages, as in variable-speed drive system, may be taken into account analytically by replacing ω_e with $\omega_{e0} + \Delta\omega_e$ in the expression for δ in equation (3.43),

$$
p(\delta_0 + \Delta\delta) = \omega_{r0} + \Delta\omega_r - \omega_{e0} - \Delta\omega_e \qquad (3.69)
$$

Under steady-state condition, the rotor of the synchronous motor rotates at synchronous speed, hence equation (3.69) becomes,

$$
p\Delta\delta = \Delta\omega_r - \Delta\omega_e \qquad (3.70)
$$

If the steady-state expressions are canceled from both sides of equations (3.62) - (3.69) and if the square or the products of small changes are neglected, the differential equations are linear. Combining these equations yields a linearized model of synchronous motor equations in matrix form as,

$$
\begin{bmatrix} 0 \\ 0 \\ \Delta v_{kq} \\ \Delta e_{xfd} \\ \Delta v_{kd} \\ \Delta T_L \\ \Delta \omega_e \end{bmatrix}
=
\begin{bmatrix}
R_s + \frac{p}{\omega_b}X_q & \frac{\omega_{r0}}{\omega_b}X_d & \frac{p}{\omega_b}X_{mq} & \frac{\omega_{r0}}{\omega_b}x_{md} & \frac{\omega_{r0}}{\omega_b}x_{md} & a_{16} & V\sin\delta_0 \\
-\frac{\omega_{r0}}{\omega_b}X_q & R_s + \frac{p}{\omega_b}X_d & -\frac{\omega_{r0}}{\omega_b}X_{mq} & \frac{p}{\omega_b}X_{md} & \frac{p}{\omega_b}X_{md} & -X_q I_{qs0} & -V\cos\delta_0 \\
\frac{p}{\omega_b}X_{mq} & 0 & R_{kq} + \frac{p}{\omega_b}X_{kq} & 0 & 0 & 0 & 0 \\
0 & \frac{X_{md}}{R_{fd}}(\frac{p}{\omega_b}X_{md}) & 0 & \frac{X_{md}}{R_{fd}}(R_{fd} + \frac{p}{\omega_b}X_{fd}) & \frac{X_{md}}{R_{fd}}(\frac{p}{\omega_b}X_{md}) & 0 & 0 \\
0 & \frac{p}{\omega_b}X_{md} & 0 & \frac{p}{\omega_b}X_{md} & R_{kd} + \frac{p}{\omega_b}X_{kd} & 0 & \frac{p}{\omega_b}a_{57} \\
a_{61} & a_{62} & X_{mq}I_{ds0} & X_{md}I_{qs0} & X_{md}I_{qs0} & -2Hp & 0 \\
0 & 0 & 0 & 0 & 0 & \omega_b & -p
\end{bmatrix}
\begin{bmatrix} \Delta i_{qs} \\ \Delta i_{ds} \\ \Delta i_{kq} \\ \Delta i_{fd} \\ \Delta i_{kd} \\ \frac{\Delta \omega_r}{\omega_b} \\ \Delta\delta \end{bmatrix}
$$

$$(3.71)$$

Where a_{ij} are defined as,

$$a_{16} = X_d I_{ds0} + X_{md} I_{fd0}$$

$$a_{61} = (X_{md} - X_{mq}) I_{ds0} + X_{md} I_{fd0}$$

$$a_{62} = (X_{md} - X_{mq}) I_{qs0}$$

It is easy to sort out the derivative terms and write equation (3.71) in the state variable form as,

$$\mathbf{E}p\mathbf{x} = \mathbf{F}\mathbf{x} + \mathbf{u} \tag{3.72}$$

where,

u vector represents input state variables

x vector represents output state variables

Both the state variables **u** and **x** can be expressed in matrix form as,

$$(\mathbf{x})^T = \left[\Delta i_{qs}, \ \Delta i_{ds}, \ \Delta i_{kq}, \ \Delta i_{fd}, \ \Delta i_{kd}, \ \frac{\Delta \omega_r}{\omega_b}, \ \Delta \delta \right] \tag{3.73}$$

$$(\mathbf{u})^T = [\Delta v_{qs}, \ \Delta v_{ds}, \ \Delta v_{kq}, \ \Delta e_{xfd}, \ \Delta v_{kd}, \ \Delta T_L, \ \Delta \omega_e] \tag{3.74}$$

where, superscript T denotes transposed matrix form.

F and **E** are the coefficients matrix of **x** and its derivatives, respectively.

E matrix can be written as,

$$\mathbf{E} = \frac{1}{\omega_b} \begin{bmatrix} X_q & 0 & X_{mq} & 0 & 0 & 0 & 0 \\ 0 & X_d & 0 & X_{md} & X_{md} & 0 & 0 \\ X_{mq} & 0 & X_{kq} & 0 & 0 & 0 & 0 \\ 0 & \frac{X_{md}}{2R_{fd}} & 0 & \frac{X_{md}}{R_{fd}}(X_{fd}) & \frac{X_{md}}{2R_{fd}} & 0 & 0 \\ 0 & X_{md} & 0 & X_{md} & X_{kd} & 0 & 0 \\ 0 & 0 & 0 & 0 & 0 & -2H\omega_b & 0 \\ 0 & 0 & 0 & 0 & 0 & 0 & -1 \end{bmatrix} \tag{3.75}$$

Similarly, the **F** matrix can be written as,

$$\mathbf{F} = - \begin{bmatrix} R_s & \frac{\omega_{r0}}{\omega_b}X_d & 0 & \frac{\omega_{r0}}{\omega_b}X_{md} & \frac{\omega_{r0}}{\omega_b}X_{md} & a_{16} & V\sin\delta_0 \\ -\frac{\omega_{r0}}{\omega_b} & R_s & -\frac{\omega_{r0}}{\omega_b} & 0 & 0 & -X_q I_{qs0} & -V\cos\delta_0 \\ 0 & 0 & R_{kq} & 0 & 0 & 0 & 0 \\ 0 & 0 & 0 & X_{md} & 0 & 0 & 0 \\ 0 & 0 & 0 & 0 & R_{kd} & 0 & 0 \\ a_{61} & a_{62} & X_{md}I_{qs0} & X_{md}I_{qs0} & 0 & 0 & \\ 0 & 0 & 0 & 0 & 0 & \omega_b & 0 \end{bmatrix} \qquad (3.76)$$

In linear analysis it is convenient to express the linear differential equations in the form as,

$$p\mathbf{x} = \mathbf{A}\mathbf{x} + \mathbf{B}\mathbf{u} \qquad (3.77)$$

Equation (3.77) is the state form of the linear differential equations. It is commonly referred to as the state-space equation.

Equation (3.71) may be written as,

$$p\mathbf{x} = (\mathbf{E})^{-1}\mathbf{F}\mathbf{x} + (\mathbf{E})^{-1}\mathbf{u} \qquad (3.78)$$

which is in the form of equation (3.77), where, **A** and **B** are given as,

$$\mathbf{A} = (\mathbf{E})^{-1}\mathbf{F} \qquad (3.79)$$

$$\mathbf{B} = (\mathbf{E})^{-1} \qquad (3.80)$$

It is to be noted that $(\mathbf{E})^{-1}$ is the inverse of **E** matrix of coefficients.

3.4 Eigenvalues for Stability Analysis

The method of eigenvalue determination is a convenient means for predicting the stability of a system in linearized mode. Eigenvalues provide the range of stability as well as the oscillating frequency of state variables of a system.

The linear differential equations for synchronous motors are derived in state variable form where **u** vector represents the forcing functions of the motor. If **u** is set to zero,

85

the general solution of the force free linear differential equation (3.77) becomes,

$$\mathbf{x} = \mathbf{K}e^{\mathbf{A}t} \tag{3.81}$$

Where, $\mathbf{K}$ is a vector determined from the initial conditions. The exponential $e^{\mathbf{A}t}$ represents the unforced response of the system, which is known as state transition matrix. Stability is assured if all elements of the transition matrix approach zero asymptotically as time approaches infinity. Asymptotic behaviour of all elements of the matrix occurs, whenever all of the roots of the characteristic equation of $\mathbf{A}$ is defined by,

$$\det(\mathbf{A} - \lambda\mathbf{I}) = 0 \tag{3.82}$$

In equation (3.82) $\mathbf{I}$ is the identity matrix and λ are the roots of the characteristic equation of $\mathbf{A}$ referred to as eigenvalues. Eigenvalues may either be real or complex. When complex, they occur as conjugate pairs signifying a mode of oscillation of the state variables. Negative real parts correspond to the state variables or oscillations of state variables which decrease exponentially with time indicating the system to be stable. Positive real parts refer to an exponential increase with time, indicating an unstable condition.

3.5 Methods of Stability Studies

The linearized form of state matrix equations which have been illustrated in section 3.4 offer a convenient means of predicting the stability of synchronous motor. All the machine parameters and the terminal constraints used in stability studies of this research are in per unit values which are given in Table 3.1. These values have been determined for the synchronous machine using the modified method of parameter estimation proposed in Appendix B. A change of supply frequency is taken into account by change in the value of the angular speed, ω_e throughout this study. The rated frequency is assumed to be 50 Hz which is denoted by ω_b as the base angular speed, the per unit system employed is based on the operation at this frequency. Thus, the ratio $\frac{\omega_e}{\omega_b}$ can be

Table 3.1:   Synchronous Machine Parameters

Parameters	Values in p.u.
Stator resistance, R_s	0.06211
Stator leakage reactance, X_{ls}	0.0606
Q-axis mutual reactance, X_q	0.4875
D-axis mutual reactance, X_d	0.4875
Q-axis damper resistance, R_{kq}	0.0380
Q-axis damper reactance, X_{lkq}	0.0548
D-axis damper resistance, R_{kd}	0.0264
D-axis damper reactance, X_{lkd}	0.0590
Field circuit resistance, R_{fd}	0.0448
Field circuit reactance, X_{lfd}	0.5548

interpreted as the steady-state operating speed expressed in per unit. The influence of various machine parameters and terminal constraints on the stability of a synchronous motor can be examined by determining the eigenvalues of the characteristic equation of A of the state transition matrix. The value of each of the motor quantities are varied in a number of steps. Prior to the determination of eigenvalues of the state matrix, the values of steady-state operating points contained in the state matrix have been determined using equations (3.50) to (3.57). The seventh-order equations of the synchronous motor yield seven eigenvalues in each step of calculation. For variation of each quantity seven sets of eigenvalues are obtained. Since the real parts of the eigenvalues are the determining criteria for stability, imaginary parts are not shown in the results, only the real parts are presented in graphical form. Each graphical representation illustrates the effects of change on relative stability of the synchronous motor. The straight line parallel to the x-axis passing through zero value of the ordinate forms the boundary between stable and unstable region of operation. The lower part of the boundary represents the stable region and the upper part signifies the unstable region of operation. The eigenvalues are obtained by using a standard eigenvalue computer routine [114]. A cross check of the computed eigenvalues has also been done by the popular software MATLAB [115].

3.6 Effects of Terminal Quantities on Stability

The investigation of the relative stability due to the variation of terminal quantities is important in the formation of a convenient basis of stability analysis of synchronous motor drives. This study is intended to explore the criteria for stability improvement of synchronous motors in constant volt/hertz mode of operation. The analyses for variable-voltage and variable-frequency operation are carried out for finding proper choice of volt/hertz ratio in a variable-speed synchronous motor drive. In order to investigate the stability for each operating point seven sets of eigenvalues are computed

88

from the seventh order characteristic equation of state transition matrix. Each of the eigenvalues is examined and the plots of only the dominant eigenvalues will be presented for observations.

The stability study in constant volt/hertz mode of operation of a synchronous motor has significant aspect when the motor is operated at variable speed. The results of the study are presented by plots of eigenvalues against normalized frequency. In this investigation it is assumed that the amplitude of the stator applied voltage decreases linearly with decrease in frequency. In order to investigate the stability of a synchronous motor it is necessary to vary the frequency at all operating speeds and at all practical steady-state torque angles. Since we are concerned with the investigation of stability, the transitions of eigenvalues from stable region to unstable region are important. Therefore, the study is mainly focused near the boundary of stable and unstable regions.

The excursion of eigenvalues computed for the rated values of machine variables and parameters in constant volt/hertz mode are shown in Fig. 3.2. In each step of computation the applied voltage is decreased linearly with frequency. The results of this plot show that synchronous machines become unstable at low frequency. The eigenvalues are found to cross the boundary at low frequency of 0.305 p.u. (15.25 Hz) at the stator voltage of 0.305 p.u. indicating unstable operation below the frequency of 15.25 Hz.

The influence of the amplitude of the applied stator voltage on stability is illustrated in Fig. 3.3 by two additional curves in Fig. 3.2. The curves are obtained by increasing the stator voltage to 1.1 and 1.15 per unit. The two additional curves demonstrate that the stability of the synchronous motor is improved as a result of increase in the applied stator voltage [5].

To establish that the eigenvalue method of stability analysis conforms with real situation, the machine performance with changes in voltage and frequency have been studied in time domain as well. For time domain simulation the set of equations (3.34) to (3.40) and (3.43) have been solved using the fourth order Runge-Kutta method with an in-
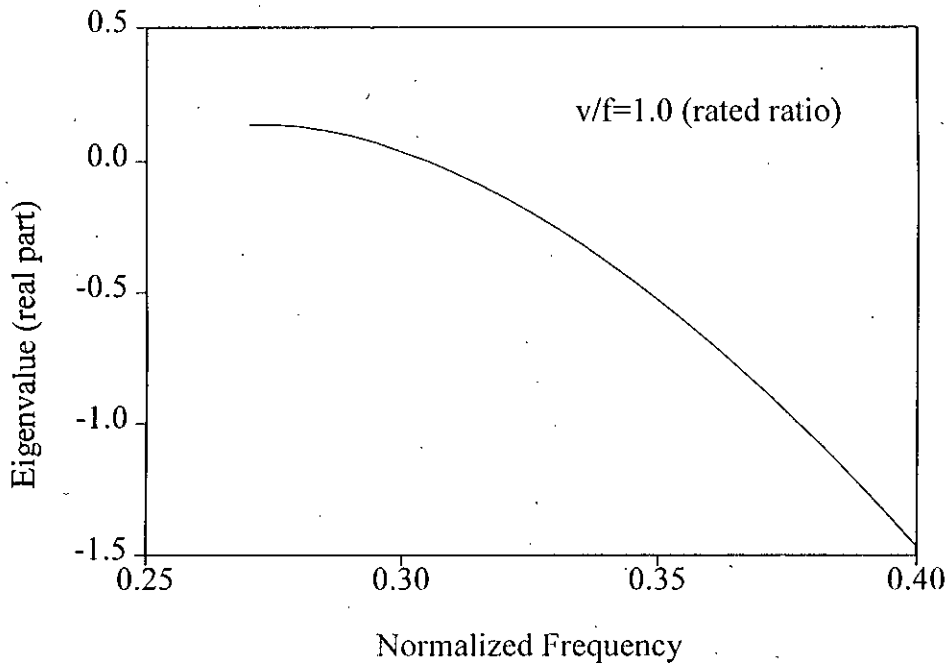
Figure 3.2: Illustration of stability of synchronous motor for rated v/f operation.
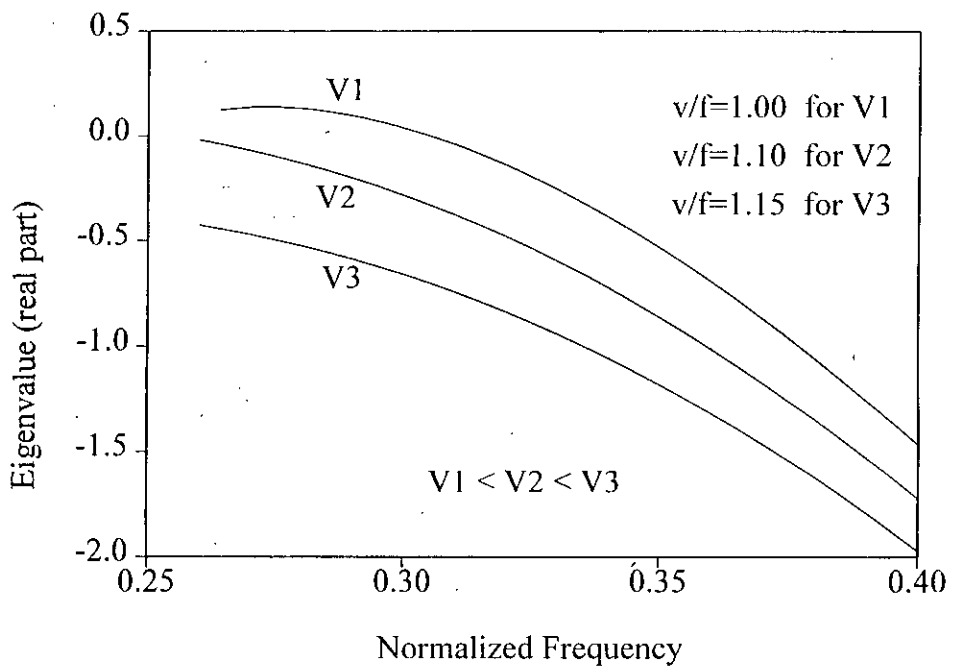

Figure 3.3: Effect of increase of stator voltage on stability of synchronous motor.

terval of 10^{-4} second. The results of the stability study in time domain are shown in Figs. 3.4 - 3.7 for a reduction of voltage and frequency to 0.305 p.u. Sustained oscillations are observed in the traces of torque and torque angle versus time as shown in Figs. 3.4 - 3.5, respectively for the change of voltage and frequency to 0.305 p.u. The change of voltage and speed from their rated values to 0.305 p.u. which cause sustained oscillations are also depicted in Figs. 3.6 and 3.7, respectively. When the stator voltage and frequency are both decreased to 0.28 p.u. the motor under investigation becomes completely unstable which is evident in torque and torque angle variations as shown in Figs. 3.8 and 3.9, respectively. A positive damping can be introduced by increasing the applied stator voltage keeping the frequency unchanged. This phenomenon is illustrated in Figs. 3.10 and 3.11. The effect of increasing the stator voltage for improving stability is observed in these Figures, where, the oscillations of torque and torque angle have been significantly damped. The increase of the stator voltage is shown in Fig. 3.12 and Fig 3.13 represents the trace of speed versus time where the frequency remains at 0.305 p.u. The results substantiate the observations made by eigenvalue method that the stability of the synchronous motor can be improved by increasing the stator voltage.

When the torque angle increases as a result of additional load and exceeds the limit cycle, the stability of the synchronous motor may be improved by reducing the supply frequency. Power demanded by the load is reduced as a result of reduction of frequency and consequently, instability is avoided. The improvement of stability is demonstrated in Fig. 3.14 by showing the excursions of eigenvalues for frequencies of 1.0, 0.90 and 0.85 p.u. while all other variables are kept unchanged. It can therefore be inferred that a change of frequency may be utilized to restore stable operation of the synchronous motor.

From the study of constant volt/hertz mode it has been observed that applied voltage, and frequency have significant effects on stability of the synchronous motor. It may be mentioned at this stage that during operation the applied stator voltage and frequency
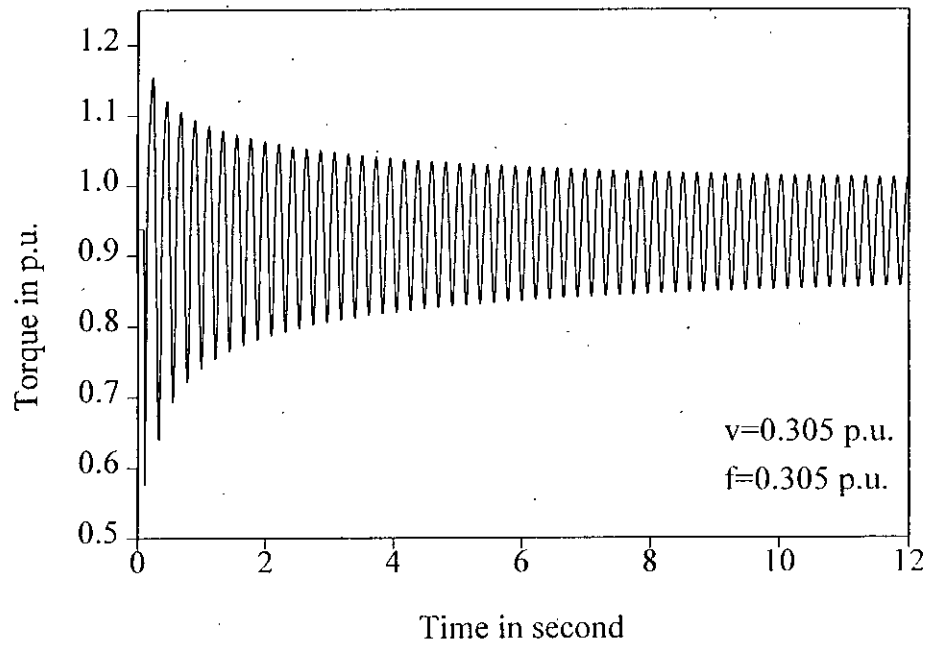
Figure 3.4: Torque vs. time characteristic of synchronous motor showing sustained oscillation.
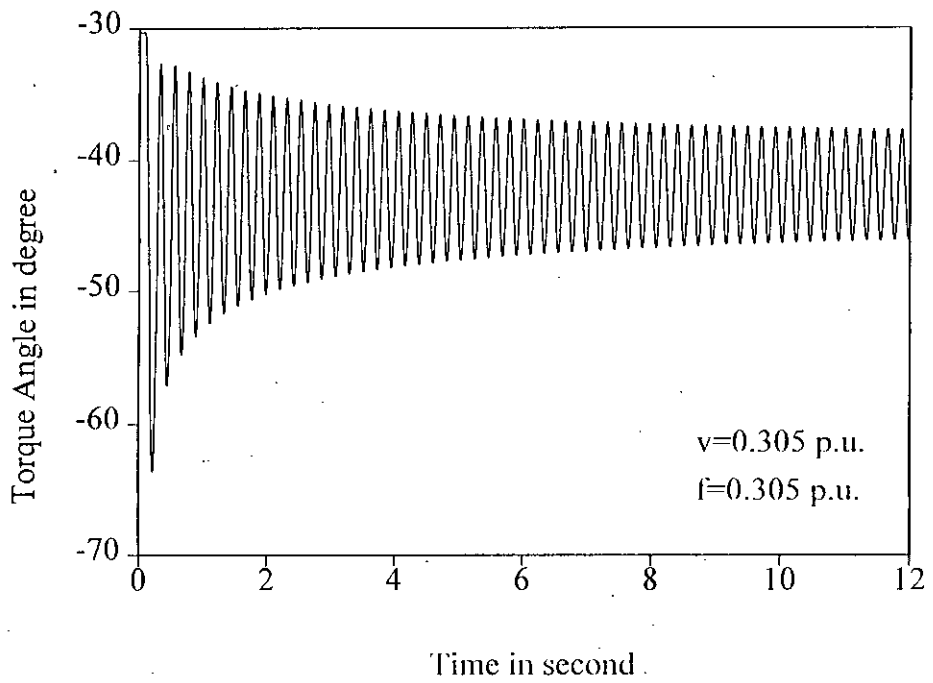
Figure 3.5: Torque angle vs. time characteristic of synchronous motor showing sustained oscillation.

Figure 3.6: Stator voltage vs. time characteristic of synchronous motor for sustained oscillation.
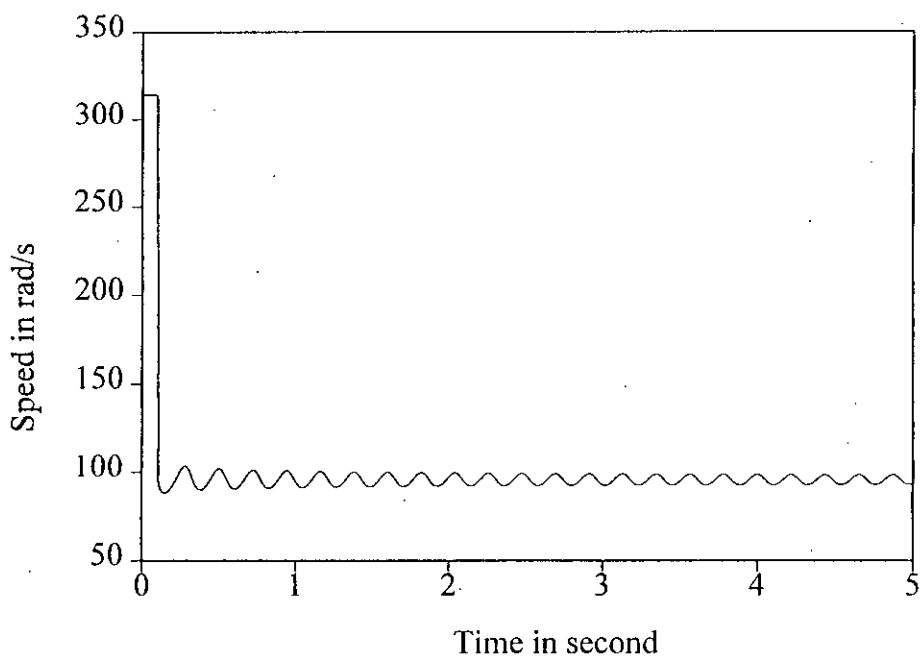
Figure 3.7: Speed vs. time characteristic of synchronous motor for sustained oscillation.
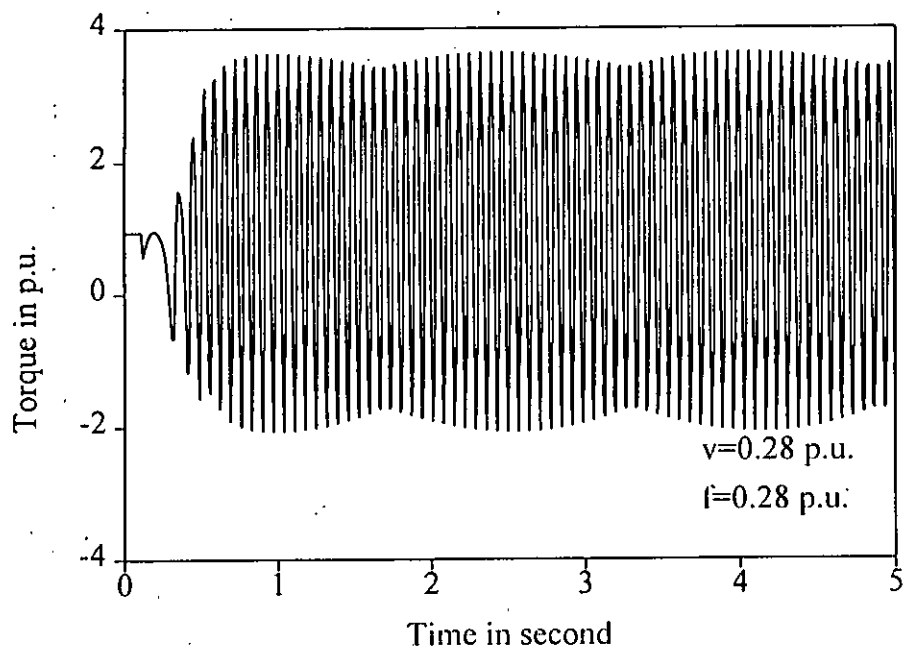
Figure 3.8: Torque vs. time characteristic of synchronous motor for an unstable operation.
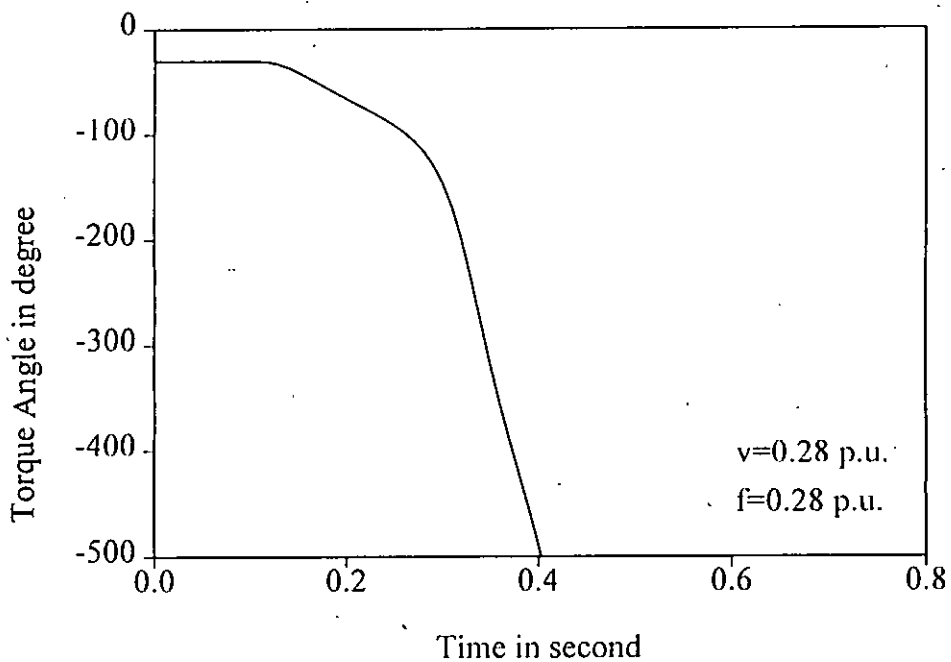
Figure 3.9: Torque angle vs. time characteristic of synchronous motor for an unstable operation.

94
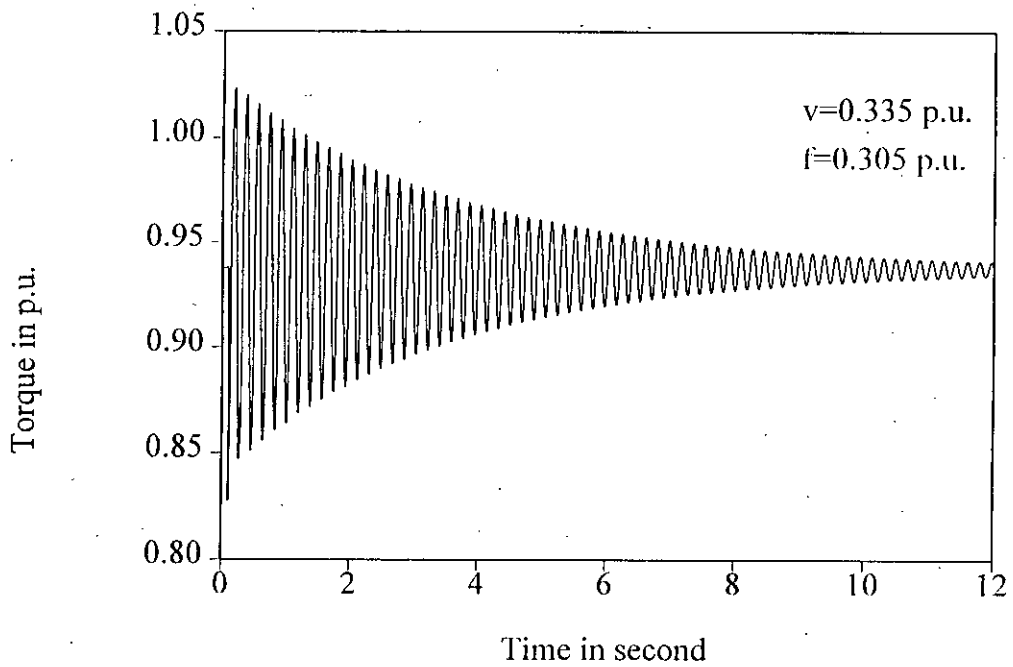
Figure 3.10: Torque vs. time characteristic of synchronous motor showing damped oscillation for increased stator voltage.
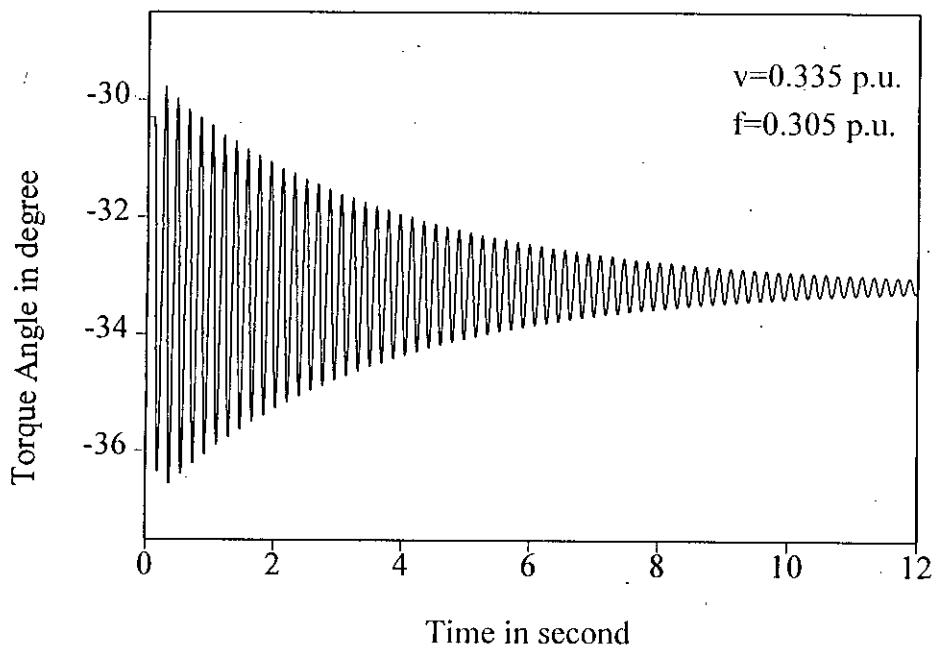
Figure 3.11: Torque angle vs. time characteristic of synchronous motor showing damped oscillation for increased stator voltage.
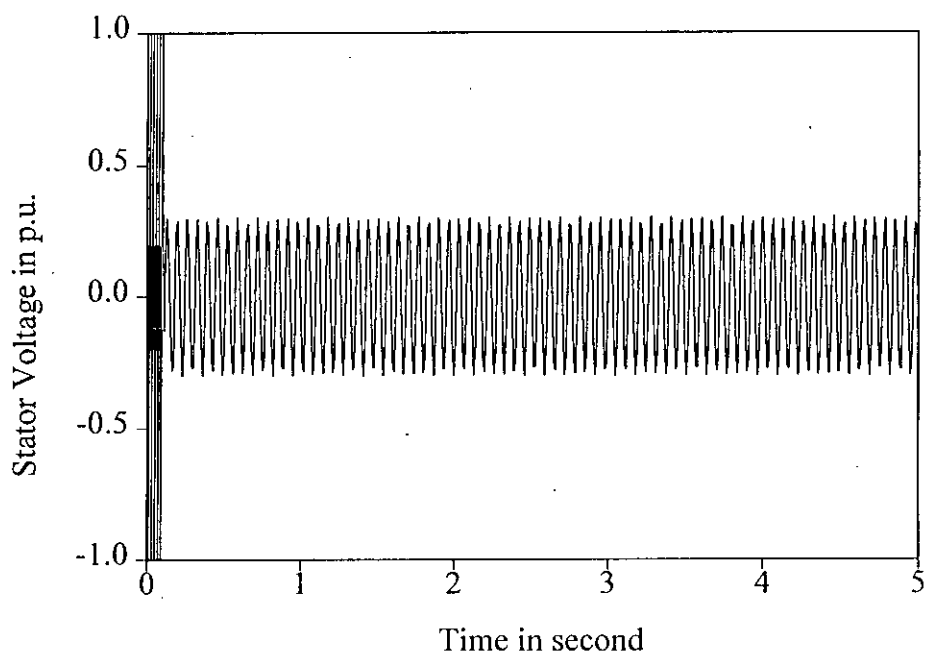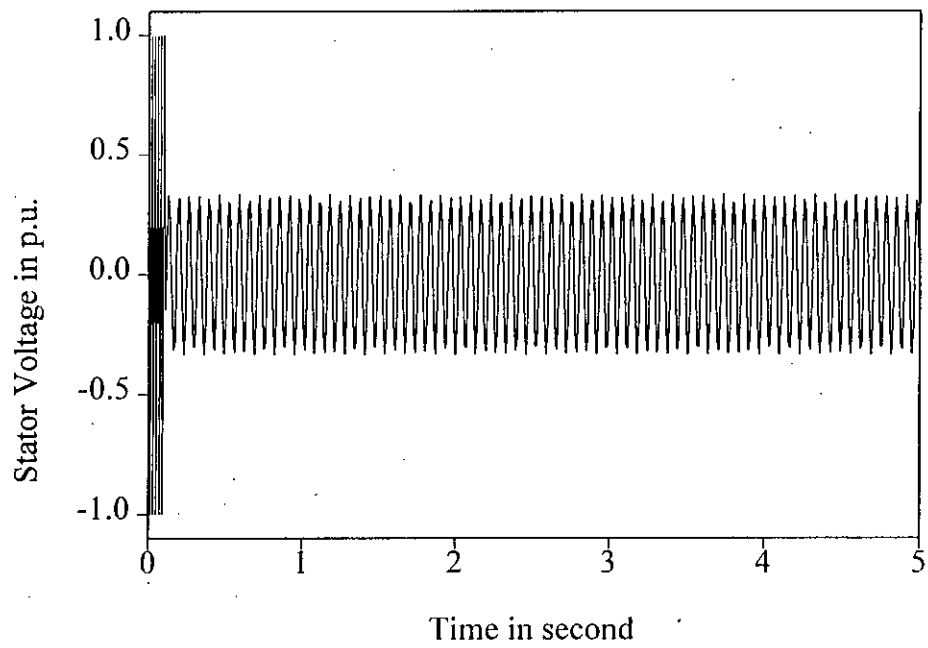
Figure 3.12: Stator voltage vs. time characteristic of synchronous motor for damped oscillation.
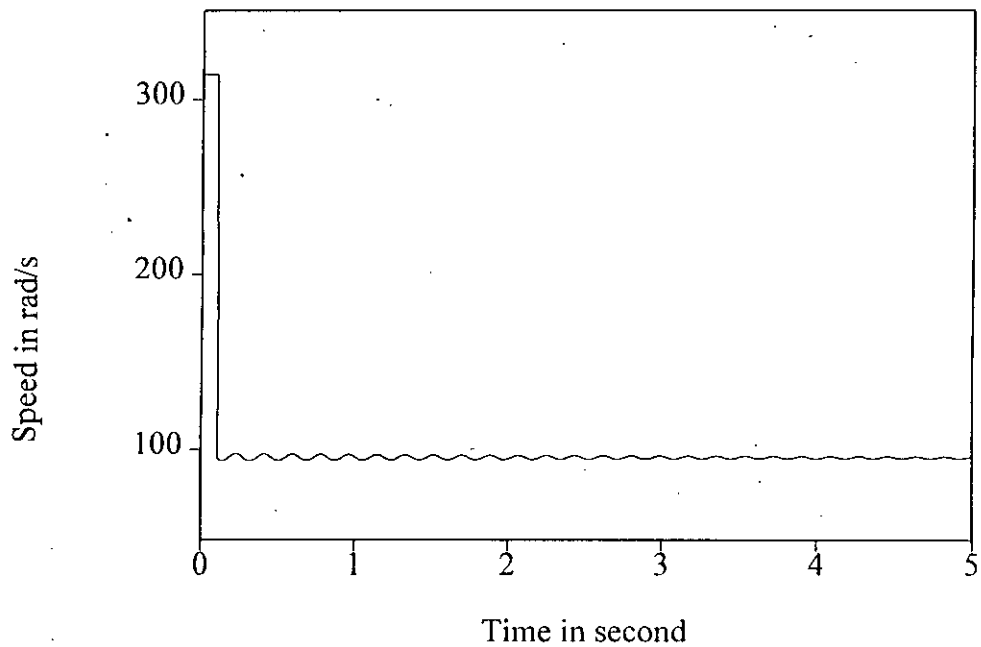
Figure 3.13: Speed vs. time characteristic of synchronous motor for damped oscillation.
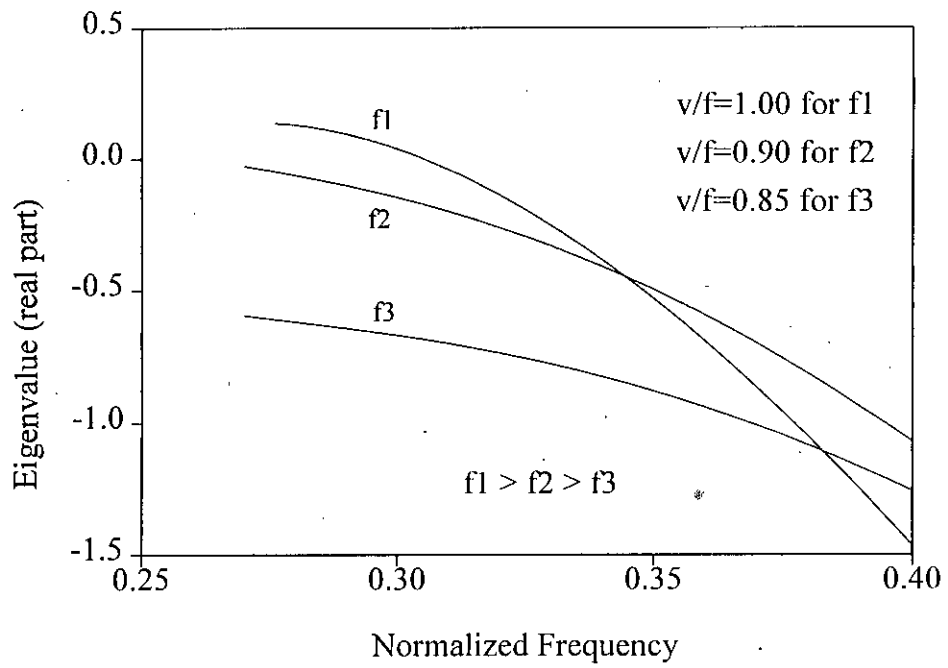
Figure 3.14: Effect of decrease of frequency on stability of synchronous motor.

are the two quantities that can be externally controlled to maintain stability of the machine. Observation reveals that the stability of a synchronous machine improves with higher stator voltage as shown in Fig. 3.3. However, such voltage increase cannot be done beyond certain range due to insulation and other related causes. It is noted that stability also improves with decrease in frequency as shown in Fig. 3.14. Therefore, from the study in constant volt/hertz mode it may be concluded that it is possible to improve the stability of the synchronous motor by increasing the applied stator voltage and decreasing frequency simultaneously.

CHAPTER 4

STABILITY ANALYSIS OF PWM INVERTER-FED SYNCHRONOUS MOTOR OPERATION

4.1 Introduction

The adjustable speed synchronous motors are generally operated in constant torque mode so that the air gap flux is kept at a fixed value. Fixed air gap-flux operation calls for maintaining constant volt/hertz ratio of rated voltage to rated frequency which can conveniently be obtained from a static inverter. But it is found that during low frequency operation a synchronous motor can demonstrate sustained oscillations and may pull out of step in rated volt/hertz mode of operation. A sudden change of load or any sort of disturbance may cause sustained speed oscillations. In these cases the regions of instability occur even with balanced sinusoidal applied stator voltage. Incorporation of damping to the system can ensure stable operation in such adverse circumstances. An appropriate damping may be introduced by simultaneous adjustment of stator voltage and frequency of synchronous motors. During the investigation of stability of synchronous motor it has been found that proper choice of volt/hertz ratio other than the ratio of rated voltage to frequency can improve the stability of the motor within the linear range of operation. A relation between applied stator voltage and frequency can be developed to improve the stability of a synchronous motor. This chapter is intended to describe the relationship between voltage and frequency to achieve stable operation over low frequency range. The study of loading effect on stability and necessary criteria

to maintain stability are also presented in this chapter. The influence on motor stability due to variations of inputs like voltage, frequency and load torque are considered. The stability of the synchronous motor operation is assessed by employing eigenvalue method which gives information about stability properties of a system. To substantiate the eigenvalue results time domain analyses have been carried out for the proposed volts/hertz control of synchronous motors. The validity of the theoretical results on stability improvement of synchronous motors has been verified by laboratory experiments.

4.2   Principle of Stability Improvement

In constant volt/hertz operation of an inverter-fed synchronous motor the supply frequency is changed with the change of applied stator voltage to maintain rated value of air gap flux. For a fixed power output in the constant volt/hertz operation of a motor any reduction of stator voltage results in an increase of stator current. As a consequence torque is increased. If the stator voltage is continuously decreased torque increases until the point of pull out is reached. The pull out torque occurs at a particular voltage and frequency for a particular motor. The motor cannot be operated below this frequency in the rated volt/hertz mode without loss of stability.

An increase only in the applied voltage to the stator increases the maximum torque limit and can stabilize the operation even at the boundary of stability. On the other hand, for same output a decrease in frequency can increase maximum torque limit of the motor at the cost of lowering the speed in constant volt/hertz mode. Simultaneous adjustment of voltage and frequency can improve the stability as well as enlarge the region of stable range of operation of synchronous motors. This phenomenon can be explained with the help of steady-state torque-frequency characteristics as shown in Fig. 4.1. Curve A represents torque versus frequency characteristic for the rated volt/hertz ratio. If the volt/hertz ratio is increased 10% above its rated value by decreasing the frequency, the torque characteristic B is obtained indicating higher torque limit than
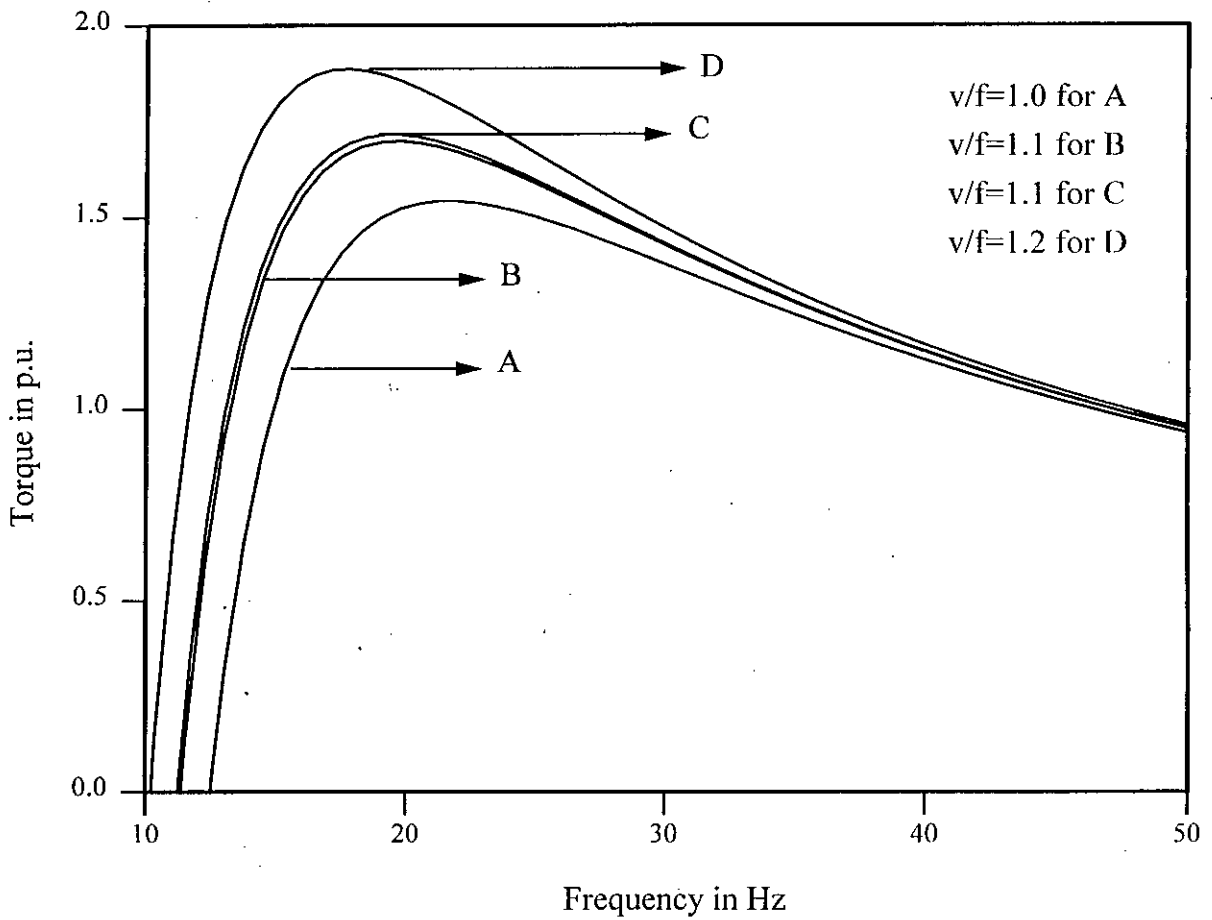
100

Figure 4.1: Steady-state torque vs. frequency characteristics
of synchronous motor.

Curve B: Obtained by decreasing frequency only
Curve C: Obtained by increasing voltage only
Curve D: Obtained by increasing voltage and decreasing frequency

the torque characteristic A at the expense of lowering the speed. Curve C corresponds to the torque characteristic of 10% increased stator voltage while the frequency is at the rated value producing higher torque limit than characteristics A and B. Curve D shows that torque limit has been significantly increased by increasing the stator voltage and decreasing the frequency simultaneously. It is, therefore, evident that the stability of synchronous motors can be improved and the region of stable operation can be enlarged by simultaneous adjustment of stator voltage and frequency.

4.3 Analytical Procedure

PWM inverter waveforms can be used as variable-voltage variable-frequency source to a synchronous motor so as to obtain desired volt/hertz ratio to maintain its stability. The voltage waveforms of line to line, line to neutral and $d - q$ axes etc. of PWM inverters have been analyzed in chapter 2. Using the equations of chapter 2 it is possible to obtain the required voltage equations either by triangular or delta sine PWM technique. It has been observed in chapter 2 that PWM techniques reduce the low order harmonics of inverter output voltages. The frequencies of higher order harmonics, usually of the order of carrier frequency and the multiples of carrier frequency get filtered out by the motor inductances. Hence, neglecting the harmonics, only the fundamental of the inverter output voltages may be transferred to rotor reference frame to be used as applied stator voltage for the analysis. Since motor stability is to be established by small excursion about steady-state operating point, sinusoidal supply voltage representing the fundamental component of the inverter voltage is sufficient for analytical purposes [8,12]. The contribution of the harmonic voltages on electromechanical behaviour is insignificant for most operating conditions and hence they are not considered in the analysis. With the $d - q$ axes voltages thus determined, the linearized motor model of synchronous motor derived in state space form as (3.77),

$$px = \mathbf{A}x + \mathbf{Bu} \qquad (4.1)$$

is used in the stability analysis of this chapter. The analysis consists of establishment of volt/hertz control to maintain stability of a particular synchronous motor by eigenvalue search technique using equations of variable-voltage variable-frequency supply and the motor model in $d - q$ axes. The results of eigenvalue search method and the proposed volt/hertz control is also verified by time domain analyses of torque, torque angle, current, voltage and speed to observe the condition of stability from the variation of these variables with time.

4.4   Volt/Hz control of Synchronous Motors

The variable-voltage variable-frequency operation of synchronous motors has been introduced to increase the controllability of motor performance. Any change of frequency requires corresponding change in stator voltage so as to maintain constant air gap flux in the motor. This mode of operation is usually known as volt/hertz mode and it makes the magnetizing current constant providing constant torque up to the rated stator voltage and frequency of the supply. If the frequency is set to a higher or a lower value, stator voltage is to be increased or decreased proportionately to produce same maximum torque. This control of voltage to frequency ratio is possible in linear region of operation. Beyond the rated value of stator voltage, increase of frequency reduces torque because the magnetizing current is reduced with the reduced volt/hertz ratio. As the frequency is increased further, torque is reduced in the form of rectangular hyperbola, so that the output power remains constant. This mode is known as field weakening mode of operation.

4.5   Proposed Volt/Hz Control for Stability Improvement

Although the adjustable speed synchronous motors are generally operated at the rated volt/hertz ratio, in the context of stability advantages can be gained by operating the motors at volt/hertz ratio other than the rated ratio. An increase in the magnitude of

voltage and decrease in frequency results in significant improvement in stability of the motor operation. The improvement of stability by utilizing this principle is illustrated in Fig. 4.2 in the form of eigenvalue deviation. An unstable operation of synchronous motor for a reduction of voltage and frequency to 0.305 p.u. has been shown by Figs. 3.4 and 3.5 in chapter 3 in the form of oscillations of torque and torque angle respectively. The effect of simultaneous increase of stator voltage and decrease in frequency on stability is demonstrated in Figs. 4.3 to 4.7. These Figures show that an increase of stator voltage by 0.03 p.u. and decrease in frequency by 0.03 p.u. has stabilized the motor operation. The characteristics of variables such as stator current, torque, torque angle, voltage and speed etc. as found from time domain analysis are given to show the stabilized operation. It is evident from the results of Figs. 4.2 to 4.7 that an unstable operation of synchronous motor can be switched to the stable operation by an increase in the stator voltage and decrease of frequency simultaneously.

In many applications the motor load is varying in nature, where the addition of load may exceed the maximum torque level and the motor may pull out of synchronism. In such situations the stable operation of synchronous motors may be maintained by applying the same technique of increasing the stator voltage and decreasing frequency. Figs. 4.8 to 4.11 illustrate the states of instability when the load is increased to 1.52 p.u. for a voltage and frequency of 0.50 p.u. The traces of torque, torque angle, stator voltage and speed demonstrate the results of unstable condition. Such an unstable condition has been stabilized by increasing the stator voltage by 0.01 p.u. and decreasing the frequency by 0.01 p.u. while the load remains at 1.52 p.u. value. This stable operation is indicated by Figs. 4.12 to 4.15 in torque, torque angle, stator voltage and speed variations with time respectively.
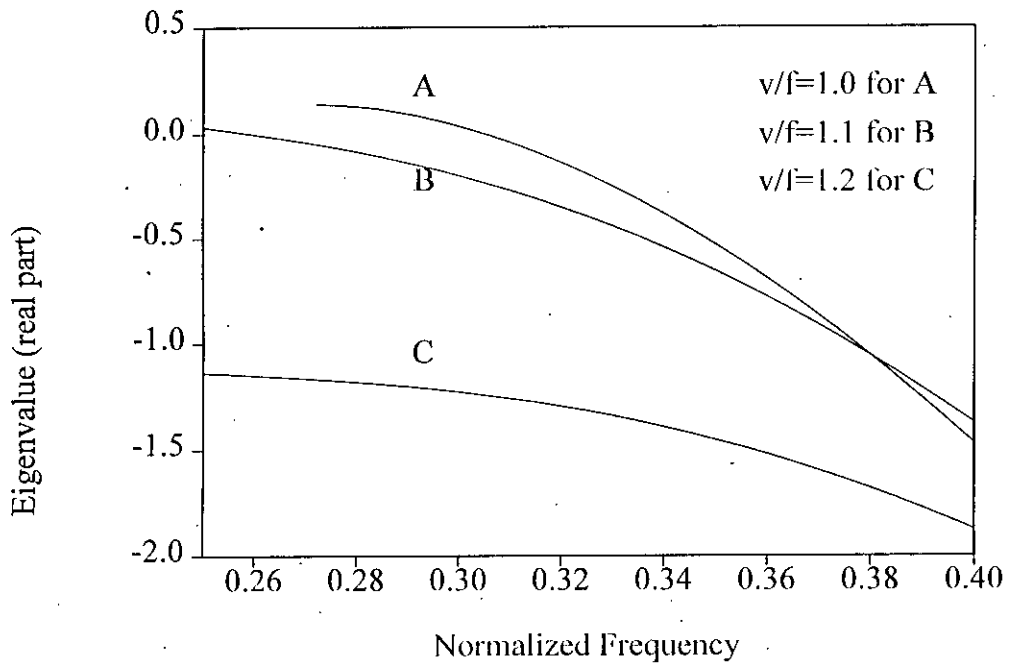
Figure 4.2: Effect of increase in stator voltage and decrease
in frequency on stability at rated load.

Figure 4.3: Stator current vs. time characteristic of synchronous
motor showing stable operation at rated load.

Figure 4.4: Torque vs. time characteristic of synchronous
motor showing stable operation at rated load.

Figure 4.5: Torque angle vs. time characteristic of synchronous
motor showing stable operation at rated load.
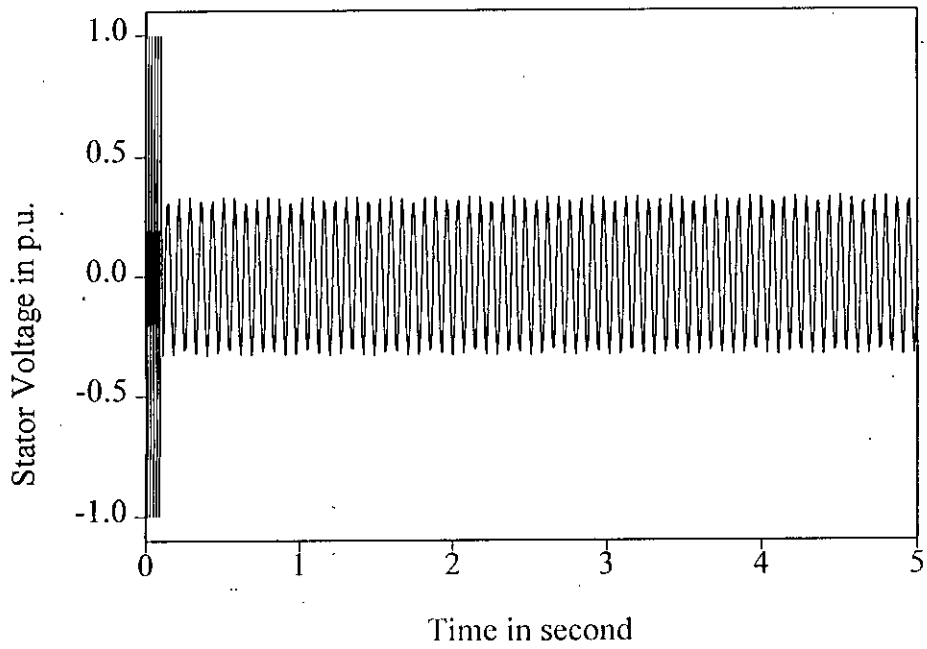
Figure 4.6: Stator voltage vs. time characteristic of synchronous motor for stable operation at rated load.
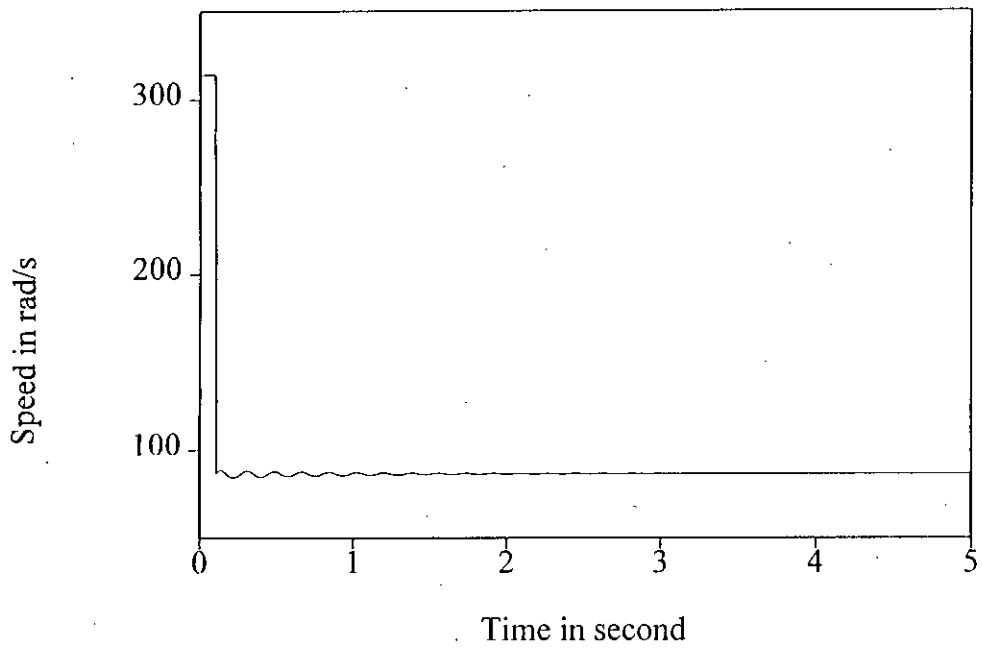
Figure 4.7: Speed vs. time characteristic of synchronous motor for stable operation at rated load.

107

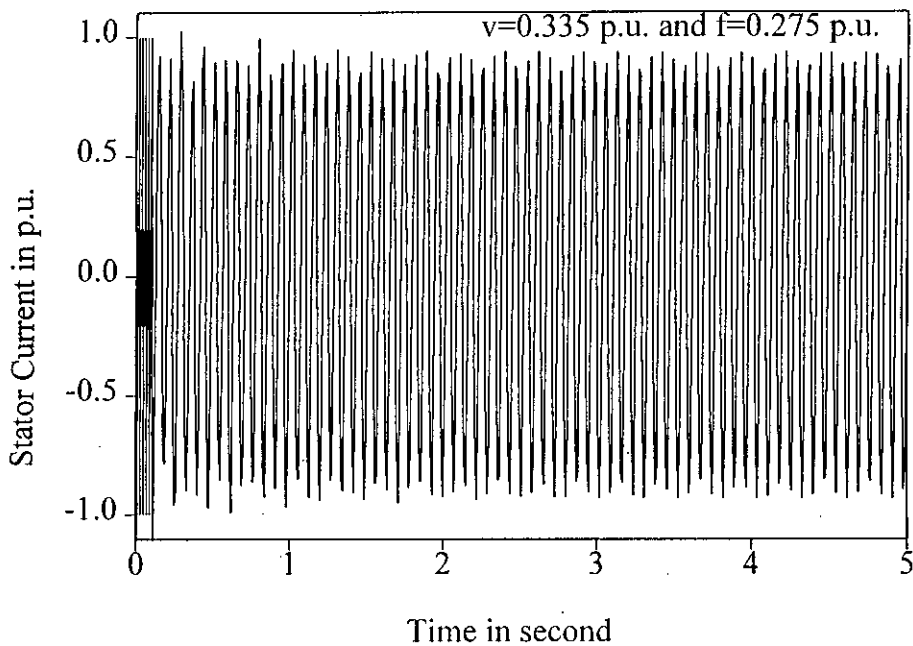Figure 4.8: Torque vs. time characteristic of synchronous motor showing unstable condition for 1.52 p.u. load.

Figure 4.9: Torque Anlge vs. time characteristic of synchronous motor showing unstable condition for 1.52 p.u. load.

Figure 4.10: Stator voltage vs. time characteristic of synchronous
motor for unstable condition caused by 1.52 p.u. load.

Figure 4.11: Speed vs. time characteristic of synchronous motor
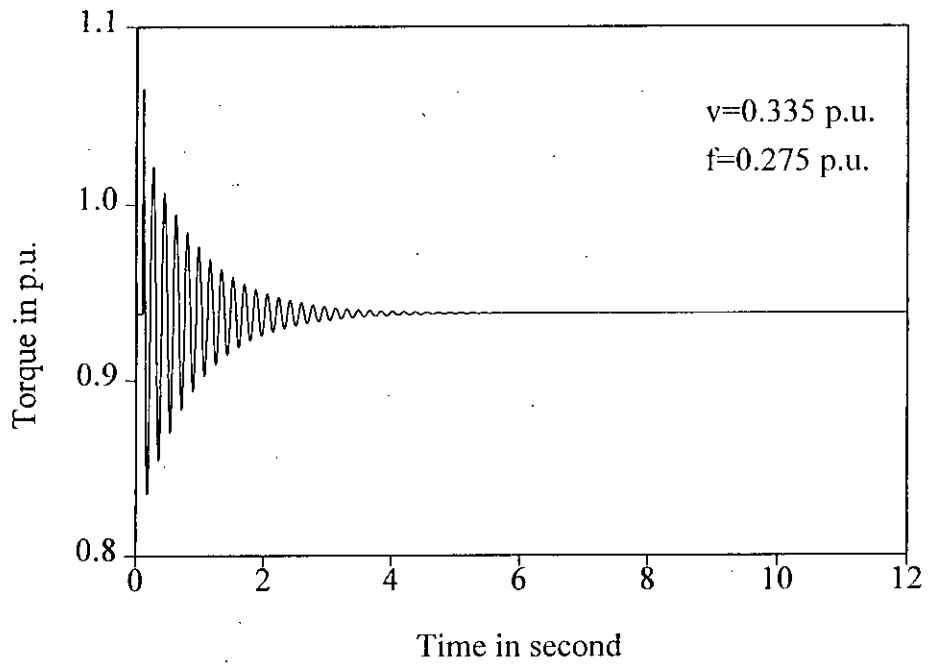for unstable condition cuased by 1.52 p.u. load.

Figure 4.12: Torque vs. time characteristic of synchronous motor showing stable condition for 1.52 p.u. load.
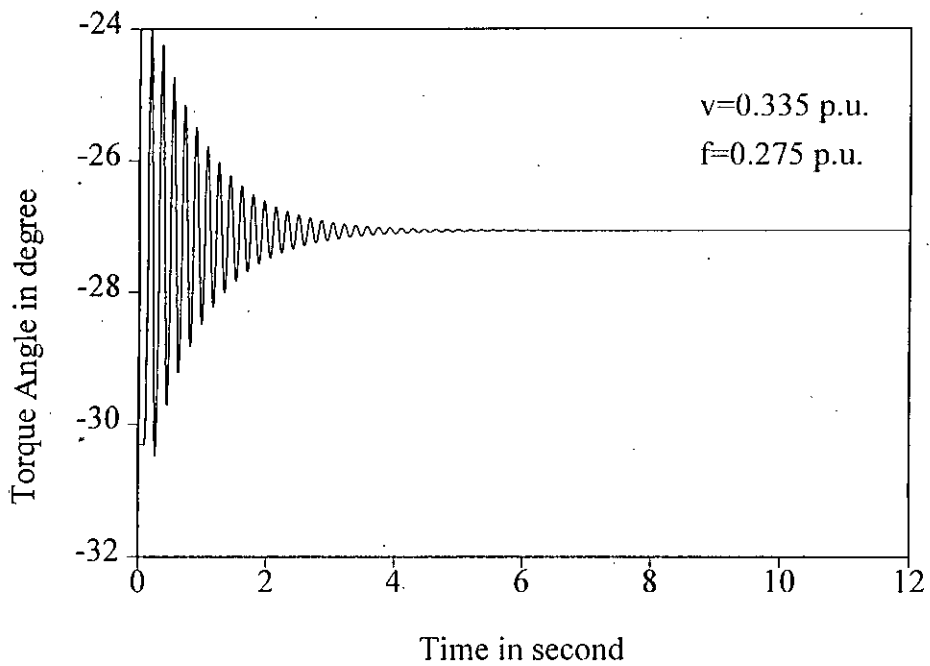

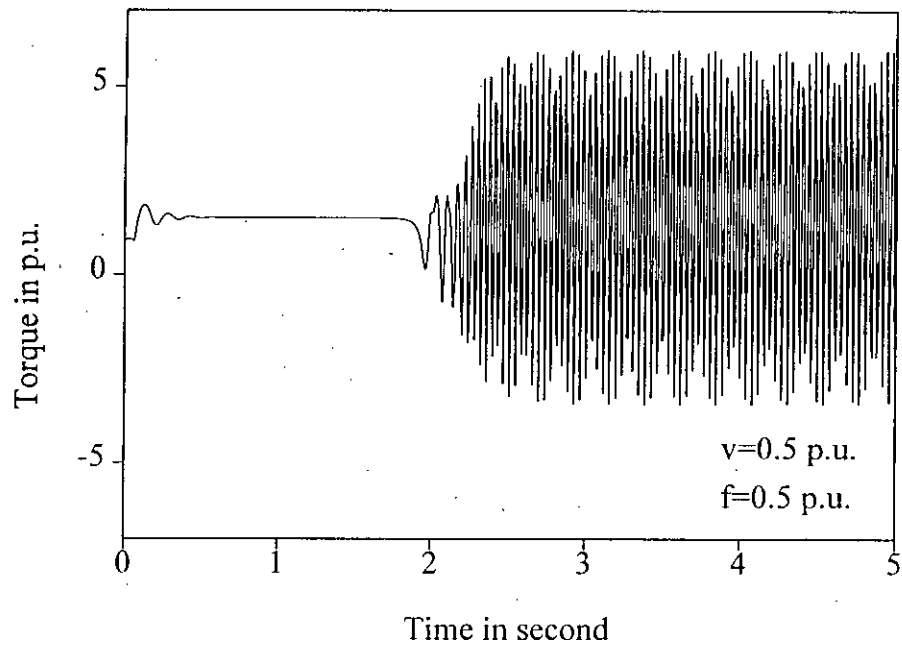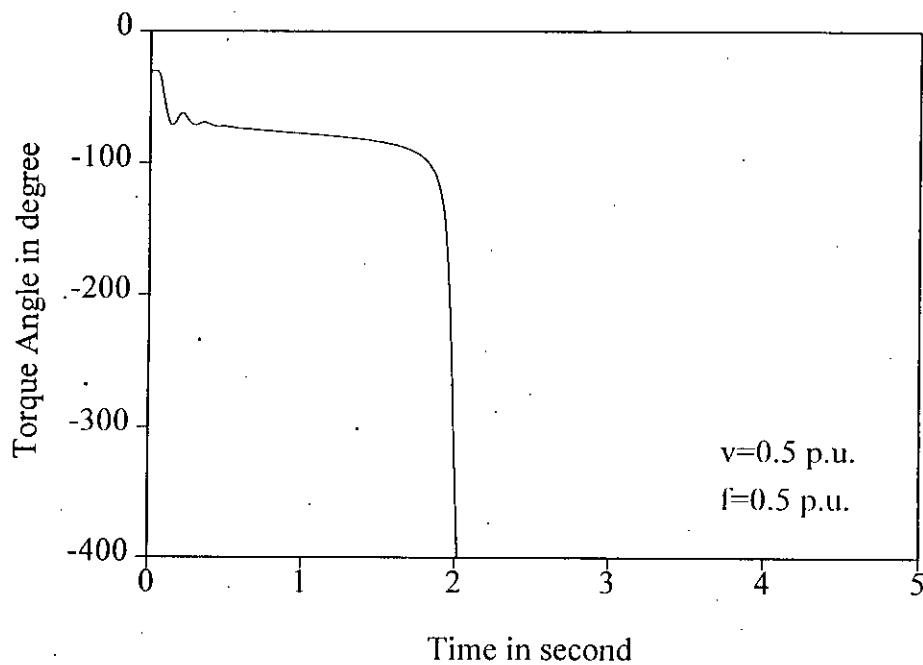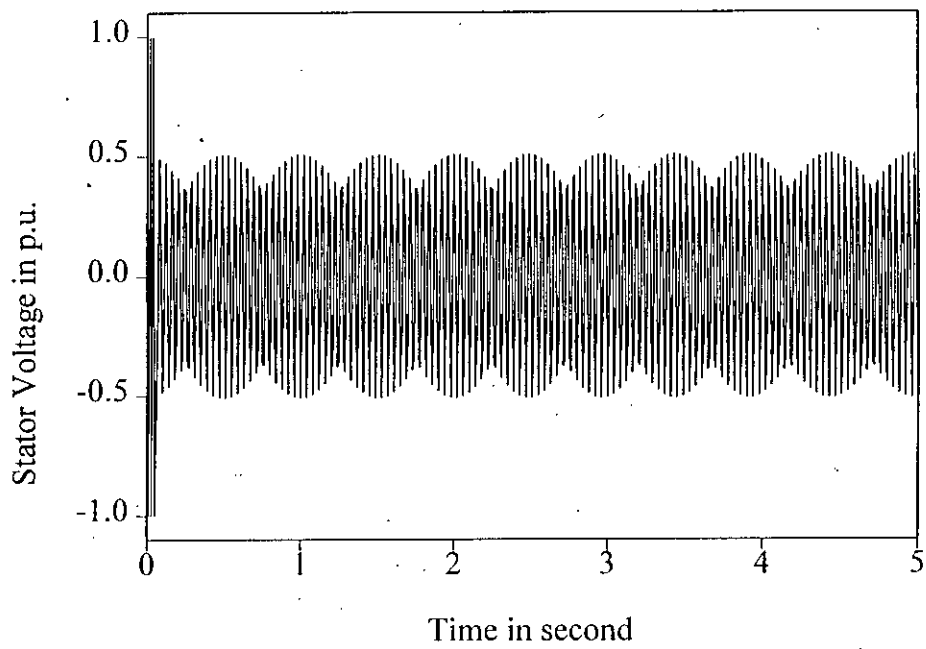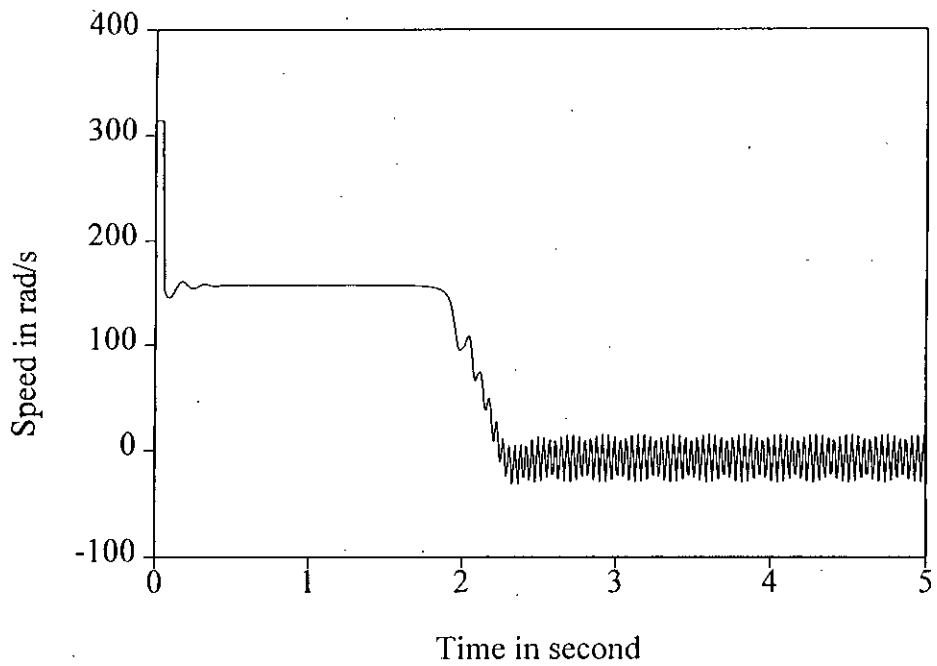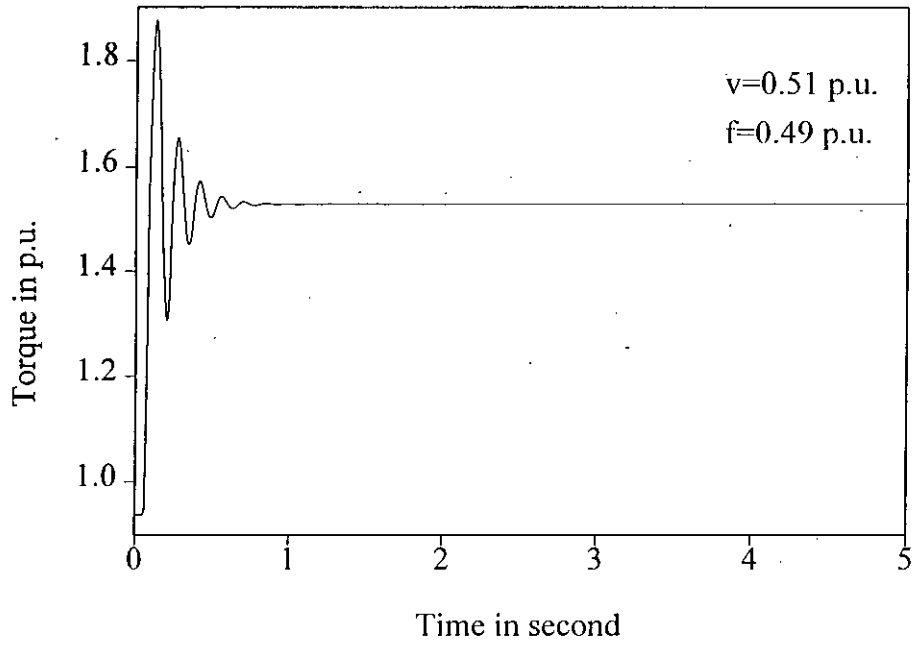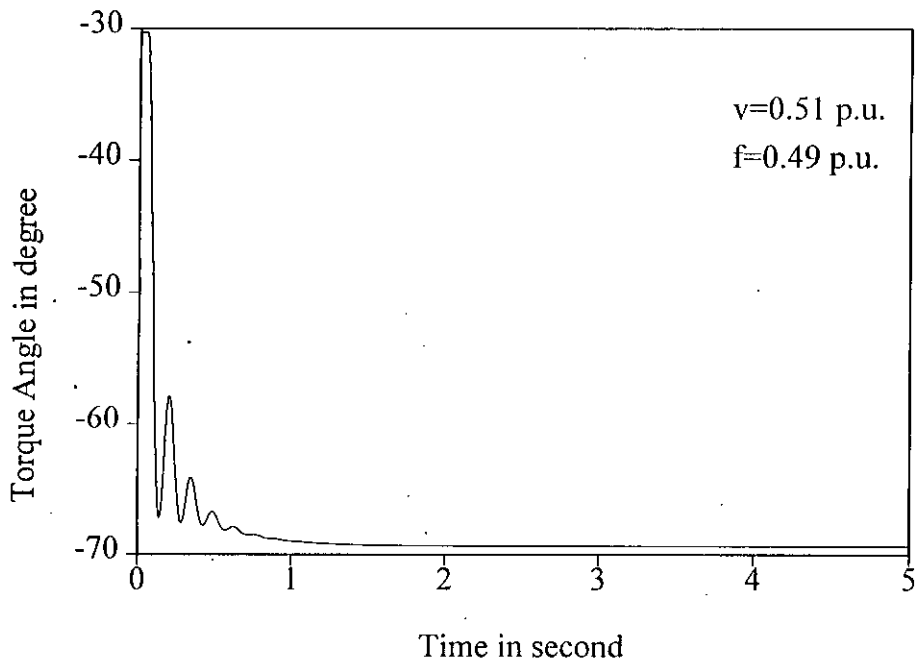Figure 4.13: Torque angle vs. time characteristic of synchronous motor showing stable condition for 1.52 p.u. load.
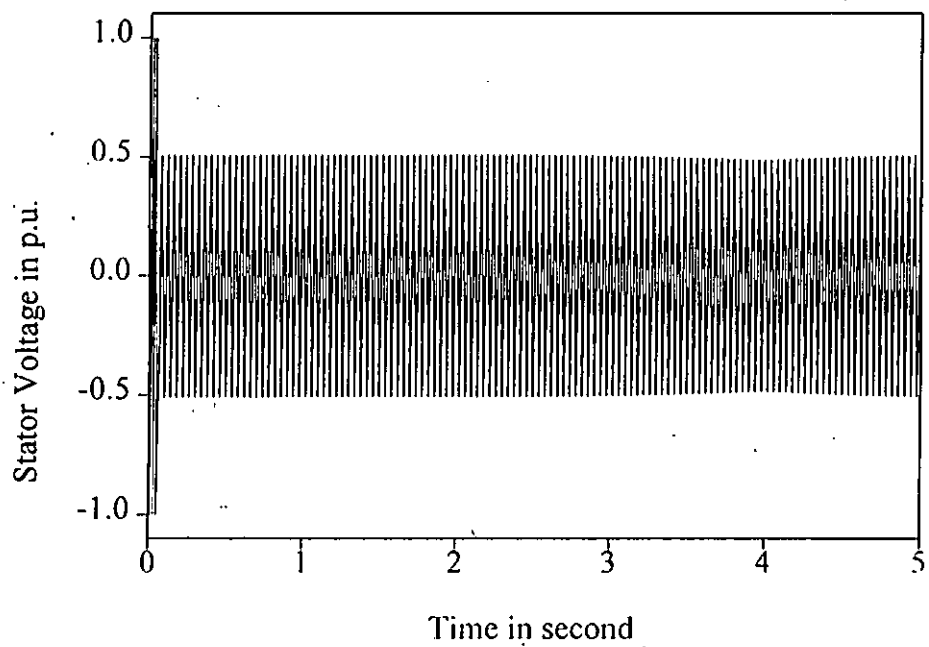
Figure 4.14: Stator voltage vs. time characteristic of stable
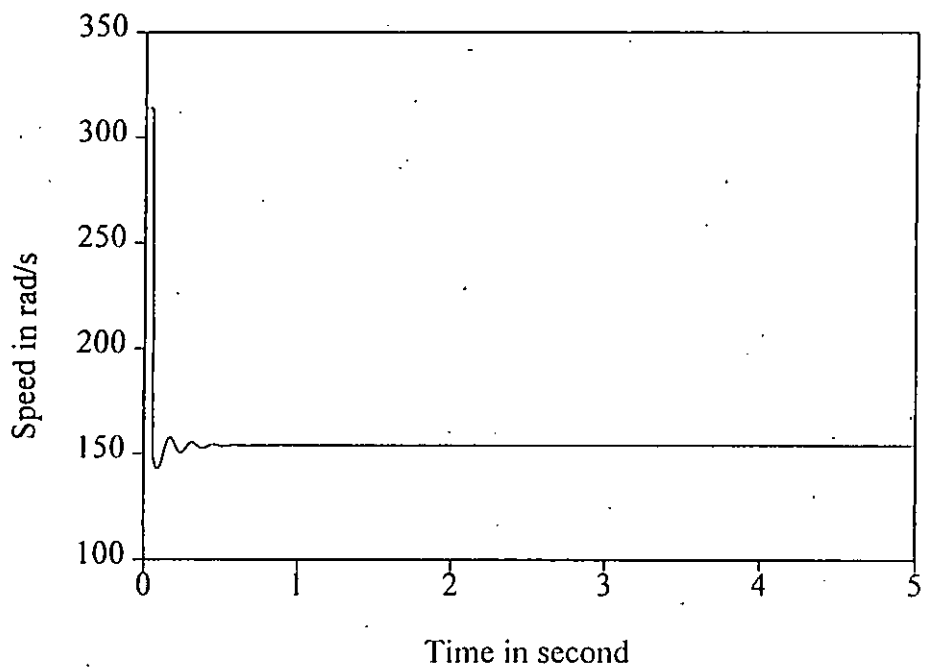condition for 1.52 p.u. load.

Figure 4.15: Speed vs. time characteristic of stable condition
for 1.52 p.u. load.

4.6 Voltage Frequency Relationship for Stable Operation

The linearized equations of synchronous motors are developed in state-space form with perturbation of maximum possible variables. The eigenvalues determined from equation (4.1) indicates the state of motor stability. The effects of change of voltage and frequency are presented in chapter 3 where the general procedure of assessment of stability of synchronous motor using eigenvalue method is described in details. Only the main points related to the development of voltage-frequency relationship for stable operation are illustrated in this section. The analysis carried out for this relationship is restricted to the linear range of operation of synchronous motors.

The conditions of instability of synchronous motor operation in low frequency range at rated volt/hertz has been established in chapter 3. The stability analysis carried out in section 3.6 shows that when the stator voltage and frequency are both decreased towards lower values maintaining volt/hertz ratio at the rated value, the test synchronous motor becomes unstable at frequency of 0.305 p.u. which is known as the boundary frequency. But stable operation is possible below this boundary frequency if the volt/hertz ratio can be maintained above its rated value as evident from the results of section 4.5. In order to develop voltage-frequency relationship for stable operation below the conventional boundary frequency a frequency known as target frequency is selected above which stable operation is desired. The volt/hertz ratio is then increased from its value by fixing the stator voltage at the rated value and the frequency just below the rated value. With this setting, both the voltage and frequency are decreased in a number of steps keeping volt/hertz ratio at a constant value. In each step eigenvaules are evaluated by solving the linearized equations and stability is examined until instability is encountered. In each step it is also observed whether the instability occurs just at the target frequency. If not, volt/hertz ratio is further increased by setting the frequency to another lower value while the stator voltage is kept at the previous value. The same procedure is followed for different settings of frequency to tally whether the instability occurs just

at the target frequency. The voltage to frequency ratio satisfying this condition is a point on the stability boundary. The stator voltage is then fixed to a higher value above the rated one, following the above steps another value of volt/hertz ratio is found on the stability boundary for the same target frequency. Thus for different values of stator voltage a number of voltage to frequency ratios are obtained by which stable operation can be ascertained above a target frequency. The magnitudes of field current and load torque are kept at the rated values throughout this analysis. The marked values of voltage and frequency are plotted in a voltage-frequency plane representing the stability limit for a particular frequency. The motor can be safely operated above this frequency by restricting the operation above this limit. An empirical relationship between voltage and frequency is obtained for stable operation of the test motor. Such voltage-frequency relationships for the motor under investigation in low frequency range are shown in Fig. 4.16 indicating the stability limits. The relationships obtained for three target frequencies are found to be straight lines. The Figure shows that for rated volt/hertz ratio, the motor can be operated above 30.5 percent of rated frequency without loosing the stability as indicated by line A. With volt/hertz ratio increased to 1.043 of the rated value, the minimum speed above which the motor can be operated is 30 percent of rated frequency without loss of stability as represented by line B. With further increase of volt/hertz ratio to 1.079, the minimum speed without loss of stability is 28 percent of the rated frequency as shown by line C. Applying this technique the range of stable operation may be extended towards the lower frequency. The machine under investigation shows that stable operation is not possible below 16 percent of the rated frequency. For the operation below this frequency, developed induced voltage of the machine becomes higher than the applied voltage due to the stator resistance drop of the machine under investigation and hence the machine cannot be operated in stable condition beyond this frequency for any combination of volt/hertz ratio. Every synchronous machine has a minimum such value depending on its parameters.

In section 4.5 it has been illustrated that the instability caused by increasing load can
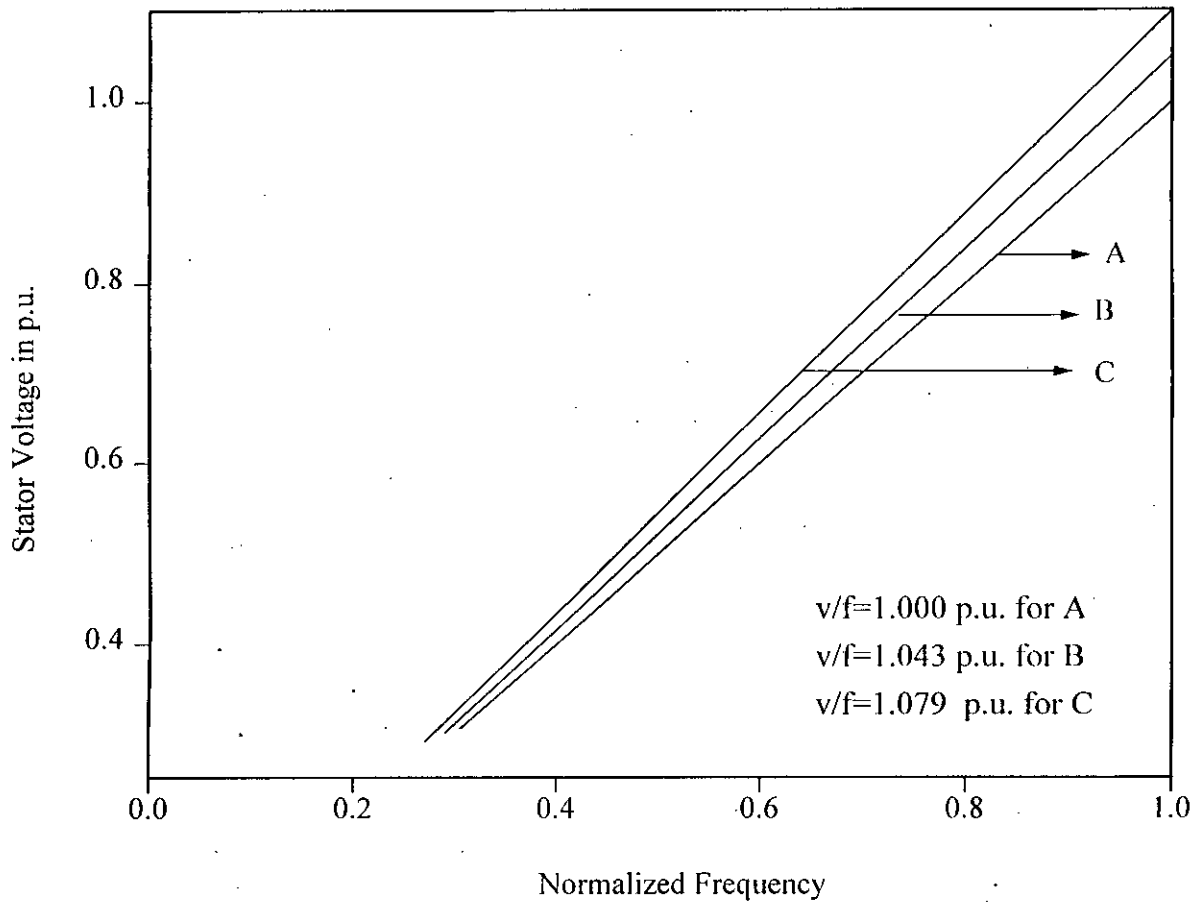
Figure 4.16: Stability limits of synchronous motor in low frequency
range for different v/f ratio at rated load.

114

be stabilized by increasing the stator voltage and decreasing frequency. Applying this principle the load bearing capability of synchronous motors may be increased. Details of this fact is examined to find the voltage frequency relationship for different magnitudes of load torque that can be safely operated. With a particular value of volt/hertz ratio load torque is varied to examine the amount of loading on the motor without loss of stability. The volt/hertz ratio is then set to a higher value by increasing the stator voltage and decreasing frequency to find another value of load for which pull out occurs. This process is continued for different values of volt/hertz ratios. The values of various volt/hertz ratios are plotted against the load torque as shown in Fig. 4.17.

4.7 Experimental Results

The phenomenon of increasing stability of the synchronous motor by increasing stator voltage and decreasing frequency is verified by carrying out laboratory experiments on a 1/4 horse power synchronous machine. Variable-voltage variable-frequency supply is obtained from a motor-generator set. The stator voltage applied to the motor is varied by changing the generator field while the frequency is varied by changing the speed of the motor-generator set.

The motor is supplied with an input of lower range of stator voltage and frequency so as to obtain the operation at rated volt/hertz ratio. Load is then gradually added to the motor until pull out occurs. The stator voltage and frequency are changed for another volt/hertz ratio in such a manner that the motor pulls out at the same load torque as previously observed. This process is continued for different sets of stator voltage and frequency restricting the pull out to occur at the same load torque. Data for stator voltage, frequency and pull-out torque are recorded using an oscilloscope and a dynamometer in each step of volt/hertz ratio. Various voltages and frequencies for a particular value of pull-out torque are plotted to show the stability limit representing the voltage-frequency relationship as shown in Fig. 4.18. Curve A is drawn for the
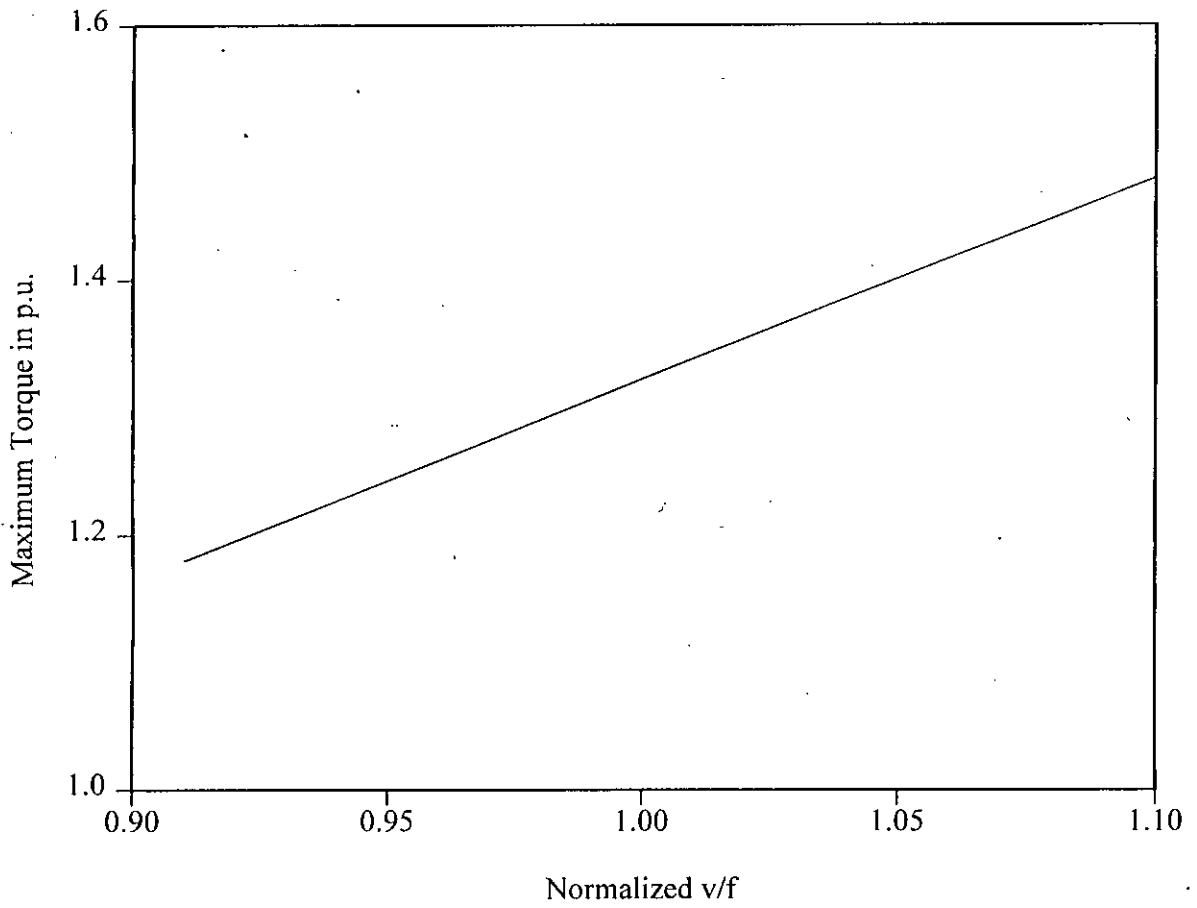
115

Figure 4.17: Enhancement of load bearing capability of synchronous
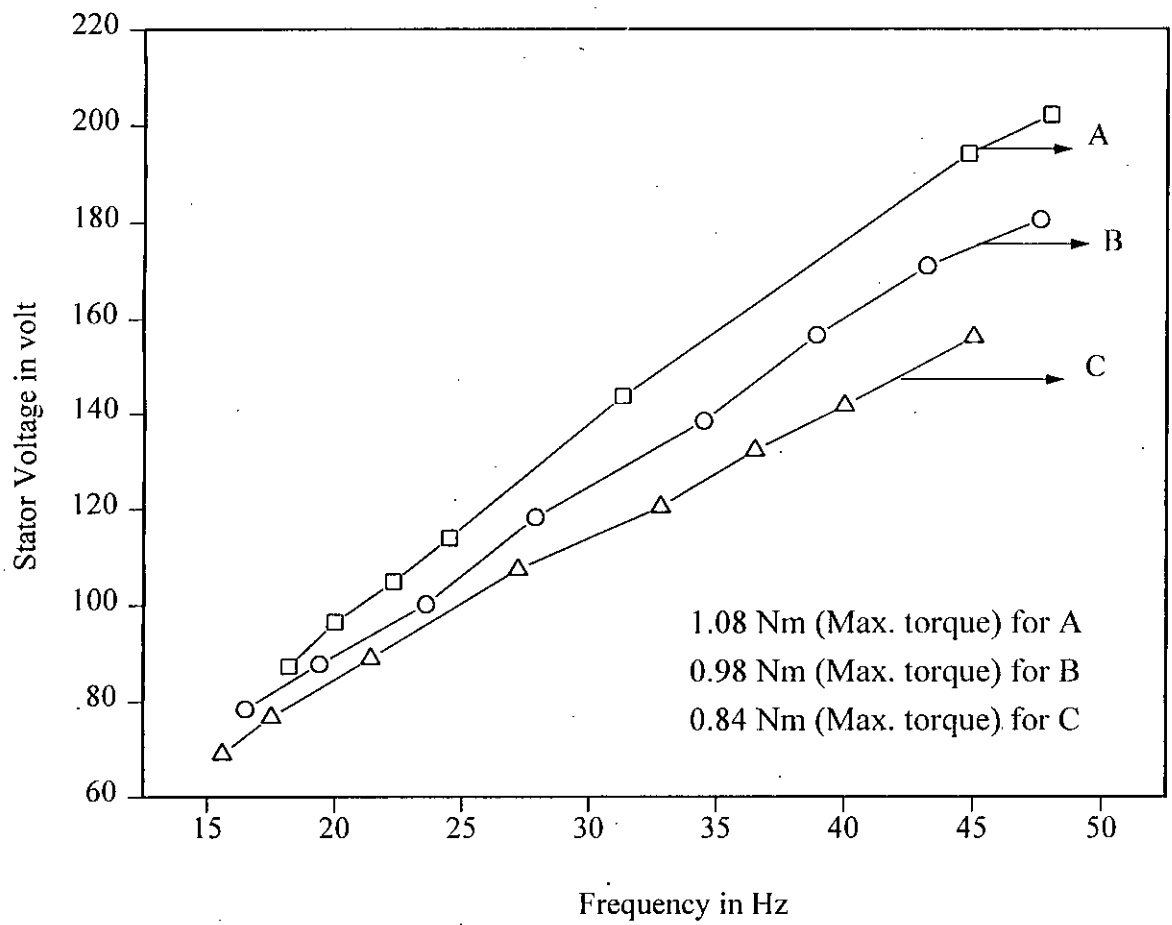motor for increased v/f ratio.

Figure 4.18: Experimental verification of stability limits of synchronous motor.

pull out torque of 0.84 Nm, the slope of which varies from 1.0 at the low frequency range to 0.79 at nearly rated values of voltage and frequency. Curve B demonstrates the voltage-frequency relation for a pull out torque of 0.98 Nm. The slope of volt/hertz for this curve is higher than A and varies from 1.08 at the lowest value of voltage and frequency to 0.88 at the highest value. Curve C is plotted for a pull out torque of 1.08 Nm the slope of which varies from 1.14 to 1.05.

The operation of the synchronous motor for increased volt/hertz ratio proposed in this thesis also enhances the load bearing capability of the synchronous motor at the cost of lowering the speed. Stability improvement by applying this technique can be practically implemented in laboratory. To verify this concept the motor is started with the rated voltage rated frequency signifying rated volt/hertz operation and load is added until pull out is reached. The volt/hertz ratio is then set to a higher value by increasing voltage and decreasing frequency in a number of steps and pull out is observed. The magnitude of volt/hertz and the corresponding pull out torque are measured in each step. Plotting the recorded data the effects of increasing volt/hertz ratio on the pull out torque is graphically illustrated in Fig. 4.19.

4.8 Comments

The voltage-frequency relationships proposed by theoretical analysis are linear in character, whereas, the voltage-frequency relationships obtained by experimental observations are nonlinear in nature. This is an expected result because the theoretical analysis is based on the linearized version of the nonlinear machine equations. As a result, the v/f relationships proposed for stable operation of the motor under investigation have straight line characteristics. On the other hand, the experimental v/f is based on the actual situation where the motor in reality is a nonlinear system. However, as demonstrated in Fig. 4.20, the theoretical results are on the safe operating region. Theoretical and experimental curves coincide in the lower range of the frequency and then the theo-
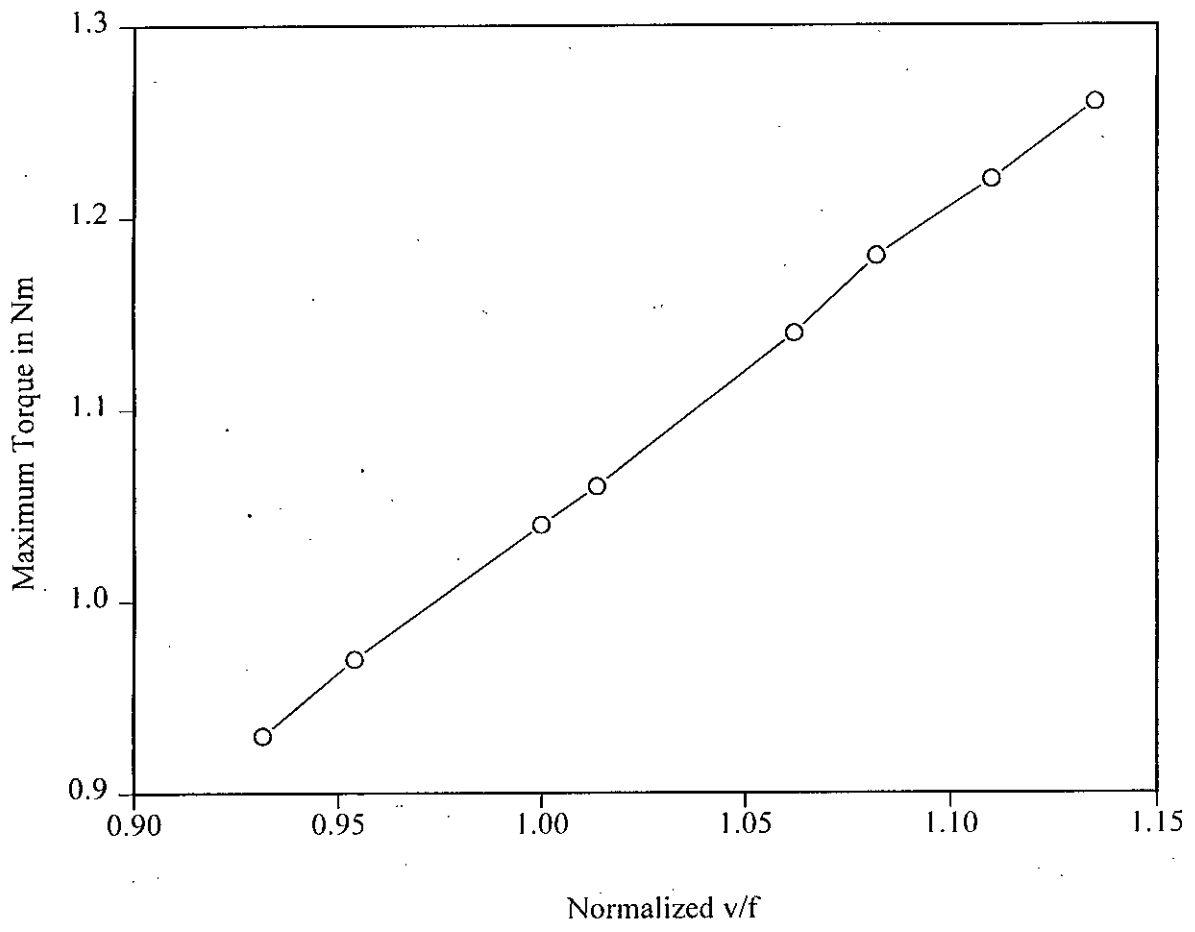
Figure 4.19: Experimental verification of enhanced load bearing capability of synchronous motor for increased v/f ratio.
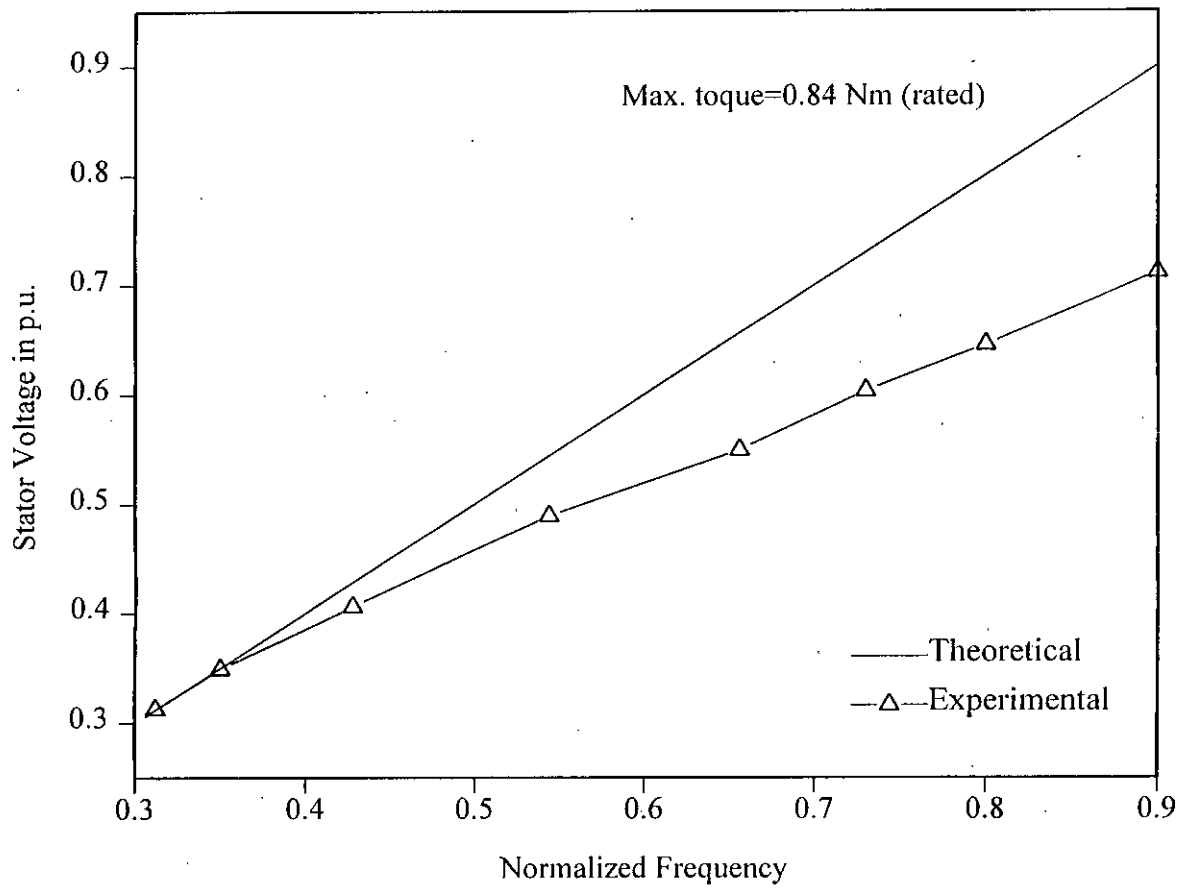
Figure 4.20: Comparison of theoretical and experimental stability
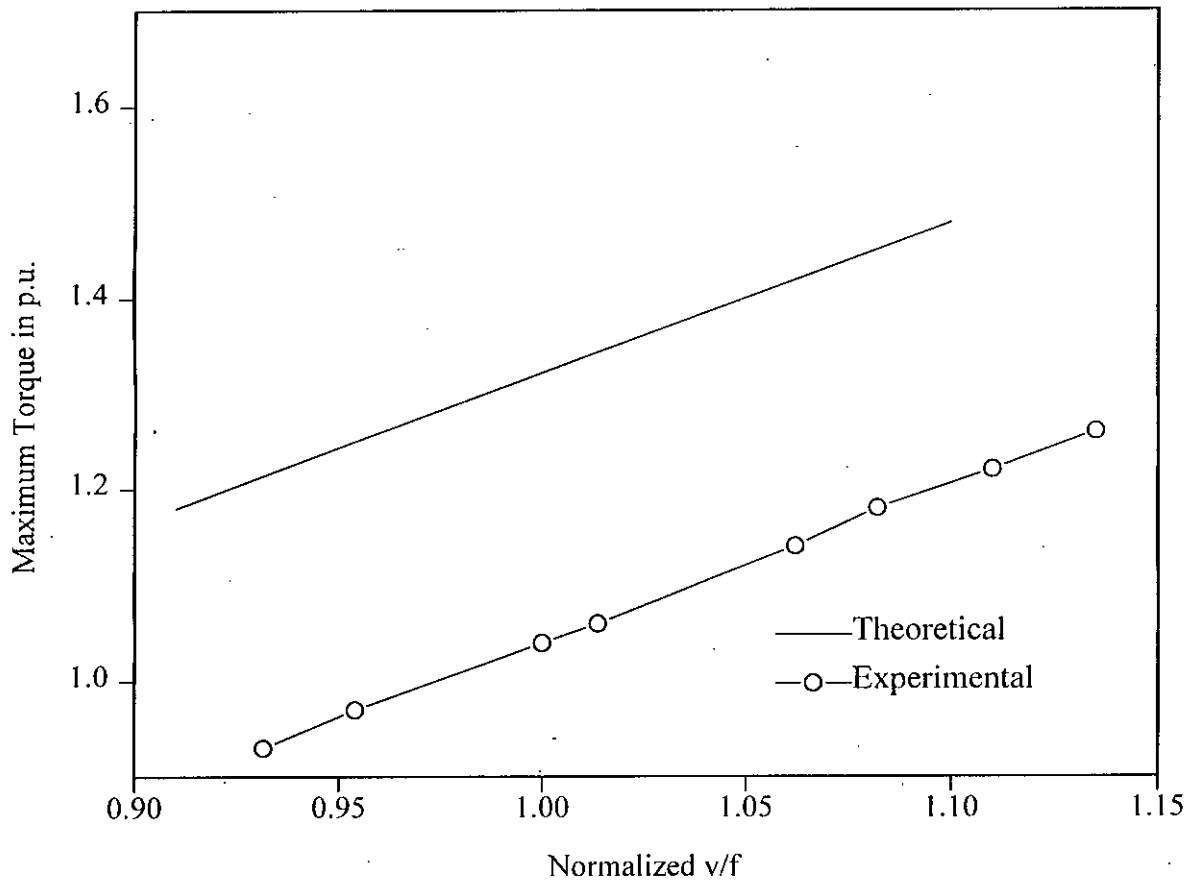limits of synchronous motor.

Figure 4.21: Comparison of theoretical and experimental results
of enhanced load bearing capability.

retical curve gradually deviates from the experimental one in higher frequency range. In proposed v/f operation the motor under investigation is found to be capable of running at about 20% above the maximum allowable load of the rated v/f operation as evident from Fig. 4.19. The improvement of load bearing capability is demonstrated in Fig. 4.21. Theoretical and experimental results in Fig. 4.21 differ from one another due to the fact that the theoretical results are obtained using the formulas which do not account for the losses of the synchronous motor.

4.9 Inverter Control

PWM inverter characteristics of voltage and frequency control can conveniently be used to obtain desired volt/hertz characteristics necessary for stable operation of synchronous motors. It has been shown in chapter 2 that both triangular and delta sine pulse width modulation provide voltage and frequency variation in one conversion stage of an inverter. In triangular carrier modulation the modulation index $(m = \frac{E_m}{E_c})$ controls the output voltage of the inverter, whereas, the carrier frequency changes the harmonic contents of the inverter output waveforms. In delta modulation reference sine wave magnitude, slope and window width can be used to control the output voltage by a variety of parameter combinations. In both the modulation schemes the frequency of the output voltage is changed by the variation of modulating sine wave frequency.

Proper implementation of either modulation scheme will provide desired volt/hertz control of a particular machine for stable operation at various frequencies, particularly, in the low frequency range. It has been established by analysis and by experimentation that the motor under study may be operated in stable condition by maintaining volt/hertz ratio from 1.0 to 1.14. as shown in Fig. 4.18.

In triangular SPWM the output voltage of the inverter depends on the modulation index as illustrated in chapter 2 (for modulation indices of 0.2, 0.3, - - - 0.9 etc. voltage varies at similar per unit values of 0.2, 0.3 - - - 0.9 in terms of line voltage). The desired

volt/hertz ratio can be maintained by changing modulation index with the change of the frequency of the modulating signal. Analog implementation of a such control scheme can be implemented with significant difficulty and added hardware. Such implementation will, however, be easier if computer generated triangular SPWM signals can be made using easy switching point calculation proposed in chapter 2 of this thesis. Significant progress has been made in this respect in a separate research in obtaining On-line PWM waveform generation by the triangular carrier modulation [116] and by delta modulation [117] techniques using the switching point calculation method proposed in this thesis. In triangular carrier modulation it may be opined at this point that for volt/hertz variation above 1, over-modulation ($m > 1$) will be necessary as suggested by results of chapter 2.

In delta modulation scheme, however, the implementation may be either computer controlled or analog circuit controlled. The analog implementation of delta modulator allows change of volt/hertz ratio by incorporating tuned integrator in the modulator [118] as shown in Fig. 4.22. In the delta modulator described in chapter 2 the filter is a normal integrator having approximate input/output relationship as,

$$\frac{V_o}{V_{in}} \simeq \frac{1}{\omega RC} \tag{4.2}$$

$$\simeq \frac{1}{\omega \tau} \tag{4.3}$$

If the expression for normal integrator is used from equation (2.44) of chapter 2, the inverter output voltage can be changed by changing the value of capacitor C (variable) as follows to obtain desired volt/hertz ratio to conform the values of volt/hertz found by analysis and experiments to maintain stability of the machine during low frequency operation,

$$\frac{V_{m1}}{f} = 2\pi V_r \tau = 2\pi V_r RC \tag{4.4}$$

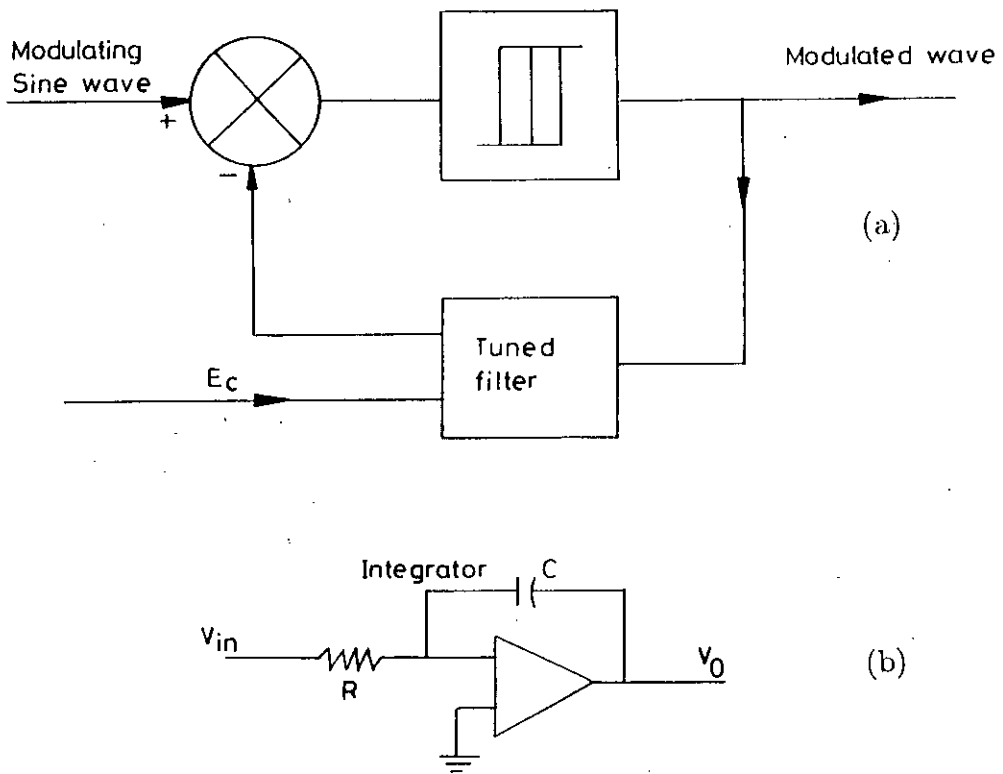Keeping R at a constant value of 100 KΩ,

Figure 4.22: Block diagram of (a) a tuned delta modulator;
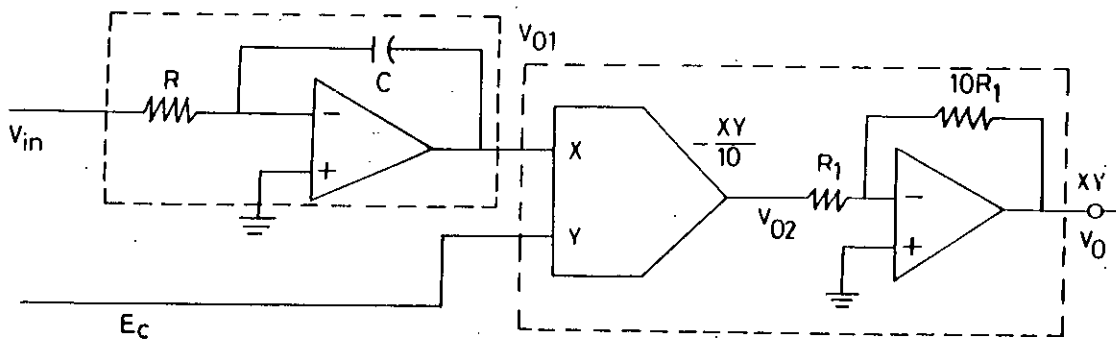(b) a simple integrator circuit

Figure 4.23 A practical tuned delta modulator circuit.

$$C = \left(\frac{V_{m1}}{f}\right)\frac{1}{2\pi V_r R} \tag{4.5}$$

Hence for $\frac{v}{f}$=1.0 and 1.14 etc. required values of C are 0.265 and 0.30 μF respectively. Practically, V_r is taken as 6 volts.

Changing capacitor or resistor of an integrator will require manual control through variable capacitor or resistors. Tuned filter delta modulation will allow one to control the slope of the modulator to provide the same variation by a control signal E_c. From Fig. 4.22, the input/output relation can be obtained as,

For tuned filter

$$\frac{V_o}{V_{in}} = \frac{V_{01}}{V_{in}}\frac{V_{02}}{V_{01}}\frac{V_o}{V_{02}} \tag{4.6}$$

$$= \frac{1}{\omega RC}\left(-\frac{V_{01}E_c}{10V_{01}}\right)(-10) \tag{4.7}$$

$$= \frac{E_c}{\omega RC} = \frac{1}{\left(\frac{RC}{E_c}\right)\omega} \tag{4.8}$$

where, the time constant of the integrator is made as a function of E_c - a control signal. When the modulator incorporates tuned filter, the fundamental of the delta modulated wave to reference signal ratio becomes,

$$\frac{V_{m1}}{V_r} = \frac{V_{I1}}{V_r} \tag{4.9}$$

where V_{m1} and V_{I1} are the fundamental components of modulated wave or integrated input signal. The above relation is also the inverse of ratio of the output to input signal of the tuned filter placed in the modulator circuit.

Hence,

$$\frac{V_r}{V_{m1}} = \frac{E_c}{\omega RC} = \frac{1}{\left(\frac{RC}{E_c}\right)\omega} \tag{4.10}$$

or,

$$\frac{V_{m1}}{f} = 2\pi V_r\left(\frac{RC}{E_c}\right) \tag{4.11}$$

As indicated in required RC variation for variation of v/f from 1.0 to 1.14 in normal filter of delta modulation, manual variation of C from 0.265 μF to 0.3 μF is required with constant R=100 KΩ. This variation can now be obtained by varying the control voltage E_c.

For $\frac{v}{f}$=1.0 with R=100 KΩ and C=0.5 μF

$\frac{1}{E_c} = 1.0 \frac{1}{2\pi} \frac{1}{6} \frac{1}{RC} \Rightarrow E_c = 1.88$ volt

For $\frac{v}{f}$=1.14 with R=100 KΩ and C=0.5 μF

$\frac{1}{E_c} = 1.14 \frac{1}{2\pi} \frac{1}{6} \frac{1}{RC} \Rightarrow E_c = 1.65$ volt

Modulator input frequency can also be controlled with same E_c through proper design of a voltage controlled oscillator and this can be used in the feedback style to maintain machine stability at low speed. A practical tuned delta modulator in its complete form is shown in Fig. 4.23 [119].

The stability criteria for the synchronous motor supplied from volt/hertz controlled sources has been set. The experimental verifications of proposed scheme for stability improvement of the synchronous motor have been carried out using motor generator set The static inverter of voltage source (VSI) or current source (CSI) type can demonstrate better performance. Pulse width modulated inverters in particular can be incorporated in the desired manner to achieve stable operation of synchronous motors.

CHAPTER 5

CONCLUSIONS

5.1 SUMMARY

The stability analysis of inverter-fed synchronous machines have been carried out during this research. The analysis has been aimed at exploring the advantages of simultaneous adjustment of the applied stator voltage and frequency to improve the stability of synchronous motors. The pulse width modulation technique as applied to static inverter provides a tool for simultaneous change of voltage and frequency. Different voltage frequency relationships can conveniently be realized by utilizing PWM techniques. The analysis of the waveforms of PWM inverters have been included in this thesis. The solution method for finding switching points of PWM waveform have been simplified. The simplified method needs the solution of only algebraic equations to determine the switching points of PWM waveforms. The switching points determined from the simplified methods are compared with the actual switching points of PWM inverters waveforms. The results have been found to be satisfactorily accurate.

The direct and quadrature axes parameters of the synchronous motor have been used in the modeling of synchronous machines for stability analysis. The parameter identification has been carried out by a modified method. The modified method is simple and requires inexpensive and conventional instrumentation. The method has been applied on a small size and a medium size machines. The parameters obtained by the modified method are justified by comparing the time constants obtained from short-circuit tests.

Comparison was made for both experimental and simulated short-circuit characteristics of the machines. The results have been found to have close agreement.

The stability analysis has been carried out for utility-fed synchronous motors and PWM inverter-fed synchronous motors. The stability study for the utility-fed motors has been made to form the theoretical basis of the analysis of inverter fed synchronous motors. The effects on stability have been studied for individual variation and simultaneous variation of the applied stator voltage and frequency. Simultaneous adjustment of voltage and frequency can conveniently be realized using modern PWM inverters.

Stability has been examined for the rated volt/hertz ratio and the motor operation is found to be unstable in low frequency range. It has been found that in constant volt/hertz mode of operation of a synchronous motor the maximum torque limit increases either with increased stator voltage or with decreased frequency. Simultaneous increase in stator voltage and decrease in frequency significantly enhance the maximum torque limit. The technique of maximum torque limit improvement would provide effective damping to synchronous motor in case of sustained oscillation or even in normal unstable region of motor operation. The results of the investigation showed that this method of control inherits the features of practical importance which may in some applications offer a convenient means of stabilizing synchronous motors at low-speed operation.

The relationship between voltage and frequency developed in this work for stable operation of synchronous motor depends on the motor parameters and terminal quantities. The relationship is not unique and will vary from motor to motor. The results of the analysis is relative because variation of machine parameters and terminal quantities would change degree of variations of the response. The effects of nonlinearities due to core saturation and eddy currents are not considered in this analysis. Therefore, the observations and conclusions of this thesis are valid for the operation of synchronous motors within the linear range where the machine parameters remain unchanged.

The contributions and achievements of this thesis can be summarized as:

1. Analytical method for determining the switching points of pulse width modulated waveforms was conventionally based on the solution of transcendental equations in both triangular sine pulse width modulation and delta modulation. Algebraic equations are proposed to replace the conventional method of determining the switching points with valid assumptions without loss of accuracy. New simplified equations are derived for both the modulation techniques mentioned above.

2. Stability analysis of the synchronous machine needs the accurate value of machine parameters. In order to meet up the requirements of day-to-day problems of synchronous machine analysis various methods are evolving to determine machine parameters. A modified method for estimation of synchronous machine parameters has been proposed in this thesis. The method is simple and requires only a fixed-frequency utility power supply to carry out the necessary measurements. Conventional instruments such as voltmeter, ammeter, tachometer, oscilloscope etc. are sufficient to record the required measuring data. This test method is applicable for parameter estimation of any size of synchronous machines.

3. PWM switching technique has extended the facility of static converters of controlling both the voltage and the frequency simultaneously for ac drives. A novel method has been proposed to stabilize the operation of a synchronous motor in low frequency range. The stable operation is achieved by introducing the positive damping through increasing the applied stator voltage and decreasing the frequency simultaneously. The application of this new method will enlarge the area of stable range of synchronous motor operation.

4. A control strategy has been suggested to improve the stability through changing the voltage and frequency. Empirical relationships between the applied stator voltage and frequency have been derived to stabilize the motor operation. Since

the instability depends upon the machine parameters, the slope of the proposed voltage-frequency relationship curves will vary from machine to machine.

5. Increase in load beyond certain magnitude causes the synchronous motor to exceed its limit cycle of the torque angle. As a consequence the motor may pull out of step. In such a situation the stable operation can be maintained by applying the technique of increased volt/hertz ratio operation using PWM inverters. The proposed control strategy increases the load bearing capability of synchronous motors by about 20% than its counterpart the rated v/f mode of operation.

5.2 Suggestions for Further Research

The technique of simultaneous adjustment of voltage and frequency can be explored in the control of other ac drives. The change of frequency along with the change of stator voltage other than the rated volt/hertz ratio extends the control flexibility of ac drives which can be effectively applied to other purpose within the allowable range of operation. The stability analysis carried out in this thesis is based on the operation of open-loop system which is a useful guideline for further work in closed-loop control of synchronous motor drives.

Experimental verification requires design and construction of a controller which can provide the facilities of changing voltage and frequency simultaneously according to necessary response to a momentary change of load or any disturbances.

In order to stabilize the operation of variable-speed synchronous motors in low frequency range relationships between the applied stator voltage and frequency are obtained. A computer controlled modulated PWM inverter drive system in closed-loop operation can be implemented for fast and accurate stable system in any future work. In such cases field control can also be incorporated by a controlled rectifier.

REFERENCES

[1] H.Le-Huy and L.A. Dessaint, "An adaptive current control scheme for PWM synchronous motor drives: analysis and simulation", IEEE Trans. on Power Electronics, vol. 4, no. 4, pp. 486-495, October 1989.

[2] P.M. Hart and W.J. Bonwick, "Harmonic Modeling of synchronous machines", IEE Proc. vol. 135, pt. B no. 2, pp. 52-58, March 1988.

[3] G.R. Slemon, J.B. Forsythe, and S.B. Dewan, "Controlled power-angle synchronous motor drive system", IEEE Trans. on Industry Applications, pp. 216-219, March/April 1973.

[4] G.R. Slemon, S.B. Dewan, and J.W.A. Wilson, "Synchronous motor drive with current-source inverter", IEEE Trans. on Industry Applications, vol. IA-10, pp. 412-416, May/June 1974.

[5] T.A. Lipo and P.C. Krause, "Stability analysis of variable frequency operation of synchronous machines", IEEE Trans. on Power Apparatus and Systems, vol. PAS-87, pp. 227-234, January 1968.

[6] B.K. Bose, "Adjustable speed a.c. drive systems", A technology status review, New York: IEEE press 1982.

[7] D.R. Lopez Jaime, "Torque oscillations of synchronous motors under starting conditions", Ph.D. dissertation, University of Pittsburgh, U.S.A 1984.

[8] A. Bellini, A. De. Carli and M. Murgo, "Speed control of synchronous machines", IEEE Trans. Industry General Applications, vol. IGA-7, no. 3, May/June 1971.

[9]   R.A. Turton and G.R. Slemon, "Stability of synchronous motors supplied from current source inverters", IEEE Trans. on Power Apparatus and Systems, vol. PAS-98, no. 1, pp. 181-186, Jan/Feb. 1979.

[10] T.A. Lipo and P.C. Krause, "Stability analysis of a reluctance synchronous machine", IEEE Trans. on Power Apparatus and Systems, vol. 86, pp. 825-834, 1967.

[11] T.A. Lipo, and P.C. Krause, "Stability analysis of a rectifier-inverter induction motor drive", IEEE Trans. on Power Apparatus and Systems, vol. PAS-88, pp. 55-66, Jan. 1969.

[12] G.M. Ong and T.A. Lipo, "Stability behaviour of a synchronous-reluctance machine supplied from a current source inverter", Conf. Record IEEE / IAS, Annual meeting , pp. 484-493, 1975.

[13] B.K. Bose, "Power electronics and ac drives", Englewood Cliffs, NJ: Printice Hall, 1986.

[14] P.C. Krause, "Methods of Stabilizing a Reluctance-Synchronous Machine", IEEE Transactions on Power Apparatus and Systems, Vol. PAS-87, No. 3, March 1968.

[15] E.P. Cornell and D.W. Novotny, "Theoretical and Experimental Analysis of Operating Point Stability of Synchronous Machines", IEEE Summer Power Meeting and EHV conference, Los Angeles, pp. 241-248, July 12-17 1970.

[16] K.G. King, "Variable frequency thyristor inverters for induction motor speed control", Direct Current, pp. 125-132, February, 1965.

[17] A. Kirnick and Heinrick, "Static inverters with neutralization of harmonics", AIEE transactions, vol. 81, pp. 59-68, May, 1962.

[18] F.G. Turnbull, "Selected harmonic reduction in static dc-ac inverters", AIEE transactions, vol. 83, pp. 374-378, July, 1964.

[19] A. Schonung and H. Steinmmler, "Static frequency changer with sub-harmonic control in conjunction with variable speed ac drives", Brown Boveri Review, pp. 555-577. August/September, 1964.

[20] S. Nonaka and H. Okada, "Methods to control pulse widths of three-phase inverters", Journal of IEE, Japan, vol. 86, pp. 71-79, July 1972.

[21] B. Mokrytzki, "Pulse width modulated inverters for ac motor drives", IEEE Trans. on Industry General Applications, vol. IGA-3, pp. 493-503, Nov/Dec. 1967.

[22] D.A. Grant and R. Seinder, "Ratio changing in pulse width modulated inverters", IEE Proc., vol. 128, pt. B, no. 5, pp. 243-248, September 1981.

[23] S.R. Bowes, "New sinusoidal pulse width modulated inverters", IEE Proc. vol. 122, pt. B, no. 11, pp. 1279-1285, 1975.

[24] S.R. Bowes and M.J. Mount, "Microprocessor control of PWM inverters", IEE Proc. vol. 128, pt. B, pp. 293-305, 1981.

[25] R.M. Green and J.T. Boys, "Implementation of pulse width modulated inverter strategies", IEEE trans. on Industry Applications vol. IA-13, pp. 38-39, 1977.

[26] R.D. Adams and R.S. Fox, "Several modulation technique PWM inverter", in Conf. Rec. Industry General Applications, IEEE Fifth Annu. Meet of IEEE Ind. Gen. Appl. Group, pp. 687-693, 1970.

[27] S.R. Bowes and J.C. Clare, "PWM inverter drives", IEE Proc. vol. 130, pt. B, no. 4, pp. 229-240, July 1983.

[28] J. Zubeck, A. Abbodanti and C.J. Nordby, "Pulse width modulated inverter motor drives with improved modulation", IEEE Trans. on Industry Applications vol. IA-11, no. 6, pp. 695-653, 1975.

[29] S.B. Dewan and J.B. Forsythe, "Harmonic analysis of a synchronized pulse width modulated three phase inverter", in Conf. Rec. IGA Sixth Annu. Meet of IEEE Ind. Gen. Appl. Group, pp. 327-332, 1971.

[30] G.S. Buja, and G.B. Indri, "Optimal pulse width modulation for feeding ac motors", IEEE trans. on Industry Applications, vol. IA-13, pp. 38-39, 1977.

[31] T.L. Grant and T.H. Barton, "A highly flexible controller for a pulse width modulated inverters," Conf. Rec. IEEE/IAS Annu. Meet., pp. 486-492, Oct.1978.

[32] P. Bhagwat and V. Stefanovic, "Some New Aspects of the Design of PWM Inverters," Conf. Rec. IEEE/IAS Annu. Meet., pp. 383-388, Oct. 1979.

[33] F.D. Buck, P. Gistellinck and D.D. Backer, "Optimized PWM inverter driven induction motor losses", Proc. IEE, vol. 130, pt. B, no., pp. 310-320, 1983.

[34] S.R. Bowes and S.R. Clements, "Microprocessor based PWM inverters", IEE Proc. vol. 129, pt. B, no. 1, pp. 1-17, January 1982.

[35] B.K. Bose and H.A. Sutherland, "A High Performance Pulse-Width Modulator for an Inverter-Fed Drive System Using a Microcomputer", IEEE Trans. on Industry Applications, Vol. IA-19, pp. 235-243, Mar.-Apr.1983.

[36] A. Pollman, "A digital pulse width modulator employing advanced modulation technique", IEEE conference record on Industry Applications, pp. 116-121, 1982.

[37] W. McMurray, "Modulation of chopping frequency of dc chopper and PWM inverters having hysteresis comparator", IEEE Power Electronics Specialist Conference (PESC) record, pp. 295-299, 1983.

[38] R.G. Palaniappan and J. Vithayathil, "A control strategy for reference wave adaptive current generation", IEEE trans. Industrial Electronics (IE), vol. IE-27, no.2, pp. 92-96, May, 1980.

[39] R.W. Menzis and A.M.A. Mahmoud, "Comparison of optimal PWM techniques with bang bang reference current controller for voltage source inverter motor drives", IEEE conference record on IA, pp. 1205-1212, 1985.

[40] M.A. Rahman, J.E. Quaicoe and M.A. Choudhury, "A comparative study of delta sine PWM inverters", First European conference on Power Electronics and Applications, Brusselts, pp. 63-168, October, 1985.

[41] P.D. Ziogas, "The delta modulation technique in static PWM inverters", IEEE trans. on IA, no. 17, pp. 199-204, 1981.

[42] A. Kawamura and R. Holt, "Instantaneous feedback controlled PWM inverter with adaptive hysteresis", IPEC conference record, Tokyo, pp. 851-857, March, 1983.

[43] P.T. Nielson, "On the stability of double integrator delta modulation", IEEE Trans. on Communication, pp. 364-366, June, 1971.

[44] F.B. Johnson, "Calculating delta modulator performance", IEEE Trans. on Acoustics, AU-16, pp. 121-129, 1968.

[45] D. Slepian, "On delta modulation", Bell System Technical Journal., vol 51, no. 10, pp. 2101-2137, Dec./1971.

[46] N.S. Jayant and P. Noll, "Digital coding of waveforms", Prentice-Hall Inc., pp. 399-415, 1984.

[47] J.E. Abate, "Linear and adaptive delta modulation", Proc. of IEE, vol. 55, no. 3, pp. 298-307, 1967.

[48] A.H. Chowdhury, "On-line optimized converter waveform synthesis by variable step delta modulation", M.Sc. Engg. Thesis, BUET, 1990.

[49] A.A. Cartmate and R. Steele, "Calculating the performance of syllabically companded delta-sigma modulators", Proc. of IEE, pp. 1915-1921, 1965.

[50] P.D. Sharma, "Characteristics of asynchronous delta modulation and binary slope quantized PCM system", Electronic Engineering, pp. 32-37, January, 1968.

[51] M.A. Choudhury and M.A. Rahman, "Starting Performances of Delta-Modulated Inverter-Fed Submersible Induction Motors", IEEE Transactions on Industry Applications, vol 28, No. 3, pp. 685-693, May/June 1992.

[52] M.R. Matin "An analysis of delta modulated inverter for uninterruptible power supplies", M.Sc. Engg. Thesis, BUET, 1991.

[53] M.U. Ahmed, "Analysis of delta modulated switch mode power supply", M.Sc. Engg. Thesis, BUET, 1994.

[54] M.A. Rahman, J.E. Quaicoe, and M.A. Choudhury., "An optimum delta modulation strategy for inverter operation", IEEE PESC conference record, pp. 410-416, 1986.

[55] M.A. Rahman, J.E. Quaicoe, and M.A. Choudhury, "Harmonic minimization in delta modulated inverters using tuned filters", IEEE PESC conference record, pp. 462-468, 1988.

[56]   O.I. Elgerd, "Electrical Energy systems: Theory and Introduction", McGraw Hill, U.S.A. 1971.

[57]   E.W. Kimbark, "Power Stability: Synchronous Machines", Dover Publications, Inc., New York, 1968.

[58]   A. Blondel, Transactions of the St. Louis Electrical Congress, 1904.

[59]   R.E. Doherty and C.A. Nickle, "Synchronous Machines", Trans. A.I.E.E., 49, pp. 650, 1930.

[60]   R.H. Park, "Two-reaction Theory of Synchronous Machines-I", Trans. A.I.E.E., vol. 48, no.2, pp. 716-227, July 1929.

[61]   R.H. Park, "Two-reaction Theory of Synchronous Machines-II"', Trans. A.I.E.E., 52, p.52, 1933.

[62]   I.M. Canay, "Causes of Discrepancies on Calculation of Rotor Quantities and Exact Equivalent Diagrams of the Synchronous Machine", IEEE Trans, PAS-88, no. 7, pp. 1114-1120, July, 1969.

[63]   A.F. Puchstein, T.C. Lloyd and A.G. Conrad, "Alternating Current Machines", John Wiley & Sons, Inc. New York 1954.

[64]   Westinghouse Electrical Transmission and Distribution Reference Book, Fourth Edition, Fifth Printing, 1964.

[65]   IEEE Standard 115-1983, IEEE Guide: Test procedures for Synchronous Machines, 1983.

[66]   IEEE Std 115A, "IEEE Trial Use Standard Procedure for Obtaining Synchronous Machine Parameters Standstill Frequency Response Testing", Supplement to ANSI/IEE Std 115-1983.

[67] British Standard Institution, SL-26, June 1985.

[68] R.E. Doherty, "A Simplified Method of Analysing Short-Circuit Problems', Trans. A.I.E.E., 42, pp. 841, 1923.

[69] B. Adkins and R.G. Harley, "The general theory of AC machines: Application to practical problems", Chapman and Hall, London 1975,

[70] IEEE Joint W/G "Supplementary Definitions Associated Test Method for Obtaining Parameters for Synchronous Machine Stability Constants" - IEEE Trans. on Power Apparatus and Systems, vol. PAS-99, pp. 1625-1633, July/Aug 1981.

[71] "Synchronous Machine Stability Constants -Requirements and Realizations" - Joint Working Group Paper A77-210-8, presented at PES Winter Meeting, 1977.

[72] S.K. Sen and B. Adkins, "The Application of the Frequency Response Method to Electrical Machines", Proc IEE, 103C, pp. 378, 1956.

[73] G. Manchur, D.C. Lee, M.E. Coultes, J.D. Griffin, W. Watson, Generator Models Established by Frequency Response Tests on a 555 MVA Machine, IEEE Trans. on Power Apparatus and Systems, vol. 91, No. 5. pp. 2077-2084, September/October 1972.

[74] T. Sugiyama, T. Nishiwaki, S. Tukeda and S. Abe, "Measurements of synchronous machine parameters under operating conditions", IEEE Trans. Power Apparatus and Systems, vol. PAS-101, no. 4, pp. 895-904, April 1982.

[75] M.E. Coultes, "Standstill Frequency Response Tests," in IEEE Symposium Publication 83TH 101-6-PWR, pp. 26-30, Feb. 1983.

[76] "IEEE Standard Procedure for Obtaining Synchronous Machine Parameters by Standstill Frequency Response Testing", IEEE Std. 115A, 1985.

[77] "IEEE Standard Procedures for Obtaining Synchronous Machines Parameters by Stand-still Frequency Response Testing", IEEE Standard 115A, 1987.

[78] E. Eitelberg and R.G. Harley, "Estimating Synchronous Machine Electrical Parameters from Frequency Response Tests", IEEE Transactions on Energy Conversion, Vol. EC-2, No. 1, pp. 132-138, March 1987.

[79] I. Kamwa, P. Viarouge, H.Le-huy and J. Dickinson, "A Frequency-Domain Maximum Likelihood Estimation of Synchronous Machine High-Order Models Using SSFR Test Data", IEEE Transactions on Energy Conversion, Vol. 7, No. 3, pp. 525-536, September 1992.

[80] P.C. Krause., "Analysis of electric machinery", McGraw-Hill, New York, 1986.

[81] M.E. Coultes and W. Watson, "Synchronous Machine Models by Standstill Frequency Response Tests", IEEE Transactions on Power Apparatus and Systems, vol. PAS-100, No. 4, pp. 1480-1488, April 1981.

[82] P.L. Dandeno and A.T. Poray: "Development of Detailed Turbogenerator Equivalent Circuits from Standstill Frequency Response Measurements", IEEE Trans on Power Apparatus and Systems, Vol. PAS-100, No. 4, pp. 1646-1655, 1981.

[83] IEEE test procedures for synchronous machines, IEEE Machine Committee, no. 115, March 1965.

[84] R.P. Schultz, W.D. Jones, and D.N. Ewart, "Dynamic Models of Turbogenerators Derived from Solid Rotor Equivalent Circuits", IEEE Trans. Vol. PAS-92, No. 3, p. 926-933 (Discussion).

[85] G. Shackshaft and R. Neilson, "Results of Stability Tests on an Under excited 120 MW Generators", PROC. IEE Vo. 119, No. 2, pp. 175-188.

[86] E.S. Boje, J.C. Balda, R.G. Harley and R.C. Beck, "Time-domain identification of synchronous machine parameters from simple stand-still tests", IEEE Trans. on Energy Conversion vol. 5, no. 1, pp. 164-175, March 1990.

[87] E.S. Boje, "Linear Model Identification for Multivariable Continuous to Practical Systems", M.Sc. Engg. Thesis, University of Natal, July 1986.

[88] I. Kamwa, P. Viarouge and E.J. Dickinson, "Identification of Generalised Models of Synchronous Machines from Time-Domain Tests," IEE Proc. PtC, 138(6), pp. 485-498, Nov. 1991.

[89] M. Namba, T. Nishiwaki, S. Yokokawa, K. Ohtsuka, and Y. Ueki, "Identification of parameters for power system stability analysis using Kalman filter", IEEE Trans. on Power Apparatus and Systems, vol. PAS-100, no. 7, pp. 3304-3311, July 1981.

[90] P.K. Shadhu Khan, "Study of special features in transient performance of alternators", M.Sc. Engg. Thesis, BUET, 1987.

[91] I. Kamwa, P. Viarouge, E.J. Dickinson, "Direct Estimation of Generalized Equivalent Circuits of Synchronous Machines from Short-Circuit Oscillographs," IEE Proc. C.137(6), pp. 445-451, 1990.

[92] A.M. El-Serafi and J. Wu, "A New Method for Determining the Armature Leakage Reactance of Synchronous Machines", IEEE Trans. on Energy Conversion, vol. 6, no. 1, pp. 120-125, March 1991.

[93] W.W. Xu, H.W. Dommel and J.R. Marti, " A Synchronous Machine Model for Three-Phase Harmonic Analysis and EMTP initialization", IEEE Paper 91 WM 210-5 PWRS, Presented at IEEE/PES 1991, Winter Meeting, New York, February 3-7 1991.

[94]   R.E. Fairbairn and R.G. Harley, "On-line Measurement of Synchronous Machine Parameters", IEEE Transactions on Industry Applications, vol. 28, No. 3, pp. 639-645, May/June 1992.

[95]   C.A. Nickle and C.A. Pierce, "Stability of Synchronous Machine-Effect of Armature Circuit Resistance", AIEE Transactions, vol. 49, pp. 338-350, January 1930.

[96]   C.F. Wagner, "Effect of Armature Resistance Upon Hunting of Synchronous Machines", AIEE Trans, pp. 1011-1026, July 1930.

[97]   J.C. Prescott and J.E. Richardson, "The Inherent Instability of Synchronous Machinery", Journal IEE, vol. 75, pp. 497-511, 1934.

[98]   A.H. Lauder, "Salient Pole Motors Out of Synchronism", AIEE Transactions, vol 55, pp. 536-549, June section, 1936.

[99]   G. Kron, "A New Theory of Hunting", AIEE Trans. vol. 71, part 1, pp. 859-866, 1952.

[100]   G. Kron, "The Application of Tensors to the Analysis of Rotating Electrical Machinery", General Electric Review, Schenectady, N.Y., vol. 38, pp. 181-191, 1935 and vol. 39, pp. 108-116, 1936.

[101]   G. Kron, "Equivalent Circuit of the Salient-Pole Synchronous Machine", General Electric Review, Schenectady, N.Y., vol 44, pp. 679-683, 1941.

[102]   G. Kron, "Equivalent Circuit of the Primitive Machines with Asymmetrical Stator and Rotor", AIEE Transactions, vol 44, pp. 679-683, 1941.

[103]   M.M. Liwschitz, "Positive and Negative Damping in Synchronous Machines," Electrical Engineering (AIEE Transactions), vol. 60, pp. 210-13, May 1941.

[104]   C. Concordia and K. Carter, "Negative Damping of Electrical Machinery," AIEE Transactions, vol. 60, pp. 116-19, 1941.

[105]   T. Warming, "Power Pulsations Between Synchronous Generators", Transactions, American Society of Mechanical Engineers, New York,N.Y., pp. 165-176, 1943.

[106]   C. Concordia and G. Kron, "Damping and Synchronizing Torques of Power Systems", AIEE Transactions, vol 59, pp. 366-371, 1945.

[107]   C. Concordia, "Synchronous Machine Damping Torque at Low Speeds", AIEE Transactions, vol 69, pp. 1550-1553, 1950.

[108]   L.A. Kilgore and E.C. Whitney, "Spring and Damping Coefficients of Synchronous Machines and Their Application", AIEE Transactions, vol. 69, pp. 226-230, 1950.

[109]   C. Concordia, "Synchronous Machine Damping and Synchronizing Torques", AIEE Transactions, vol 70, part 1, pp. 731-737, 1951.

[110]   R.V. Shepherd, "Synchronizing and Damping Torque Coefficients of Synchronous Machines", AIEE Trans. pp. 180-189, June 1961.

[111]   C. Concordia, S.B. Cray, C.E. Kilbourne and C.N. Weygandt, Jr. "Synchronous Starting of Generator and Motor", Electrical Engineering (AIEE Transaction), vol 59, pp. 629-634, 1945.

[112]   R.A. Turton and G.R. Slemon, "Stability of synchronous motor drive using a current source inverter with power factor control", IEEE Trans. on Power Apparatus and Systems, vol. PAS-98, no. 5, pp. 1617-1620, Sept/Oct. 1979.

[113]   M.A. Rahman, J.E. Quaicoe and M.A. Choudhury, "Performance analysis of delta pwm inverters", IEEE Trans. on Power Electronics, vol. PE-2, pp. 227-233, July 1987.

[114]   J.L. Malsa and S.K. Jones, "Computer Programs for Computational Assistance in the Study of Linear Control Theory", McGraw-Hill Book Co., New York, N.Y., 1970.

[115]   Matlab software, Mathwork Inc. U.S.A.

[116]   M.S. Islam, "Analysis and implementation of microcomputer control of PWM rectifier", M.Sc. Engg. Thesis (in progress), EEE Department, BUET, Dhaka, 1995.

[117]   M. Nazmul Anwar, "On-line microcomputer control of delta modulated inverters", M.Sc. Engg. Thesis (in progress), EEE Department, BUET, Dhaka, 1995.

[118]   A.D. Esmail, M.A. Rahman, J.E. Quaicoe and M.A. Choudhury, "High performance three phase rectifier using delta PWM technique", Conference proceedings of ISEDCS (International symposium on Electronic Devices, Circuits and Systems), India, 1987, pp. 578-580.

[119]   M.A. Rahman, J.E. Quaicoe and M.A. Choudhury, "An optimum delta modulation strategy for inverter operation", Conference proceedings of IEEE PESC, Vancouver, B.C., Canada, 1986, pp. 410-416.

[120]   R.C. Winchester and W.B. Jackson, "Direct and quadrature axis equivalent circuits for solid-rotor turbogenerators", IEEE Transactions on Power Apparatus and Systems Vol. PAS 85, No. 7, pp. 1121-1136, July 1969 .

[121]   Task force on definition and procedures (IEEE Committee report), "Current usage & suggested practices in power system stability simulations for synchronous machines", IEEE Transactions on Energy Conversion, Vol., EC.,No. 1, pp. 77-93, March,1986.

[122]   H.S. Khalil, "The Applications of the Fast Fourier Transform for the Computation of Synchronous Machine Dynamic Behaviour", M.Sc.Thesis, University of Saskatchewan, 1972.

Appendix A

Simulated Waveforms and Spectra of Pulse Width Modulation

Waveform analyses of triangular sine pulse width modulation and delta modulation for single phase inverter output have been presented in sections 2.4 and 2.6, respectively. Section 2.7 covers the analyses of three-phase inverter output waveforms for pulsewidth modulation. Some of the results in details are given in this appendix.

Simulated waveforms of 30 Hz operating frequency for single phase inverter output is depicted in Fig. 2.6 of chapter 2 showing the change of modulation index. The corresponding spectra are shown in Fig. 2.7. Detailed variational effects of other parameters are shown in Figs. A.1 to A.6 of this appendix. Similarly, simulated waveforms of single phase delta modulated inverter output for 30 Hz operating frequency of two different magnitudes of modulating waves are shown in Fig. 2.15 for constant slope and window width. The spectra of these waveforms are shown in Fig. 2.16. The effects of variation of operating frequency, slope of the carrier wave and window width are presented in Figs. A.7 to A.16. Three phase waveforms of pulsewidth modulated inverter output have been shown in Figs. 2.26 and 2.27. These waveforms of the line and phase voltages and d-q axes voltages are obtained for 30 Hz operating frequency and 1.2 kHz carrier frequency. The influence of change of the parameters on the waveforms of three-phase inverter output are presented in Figs. A.17 to A.26 of this appendix.
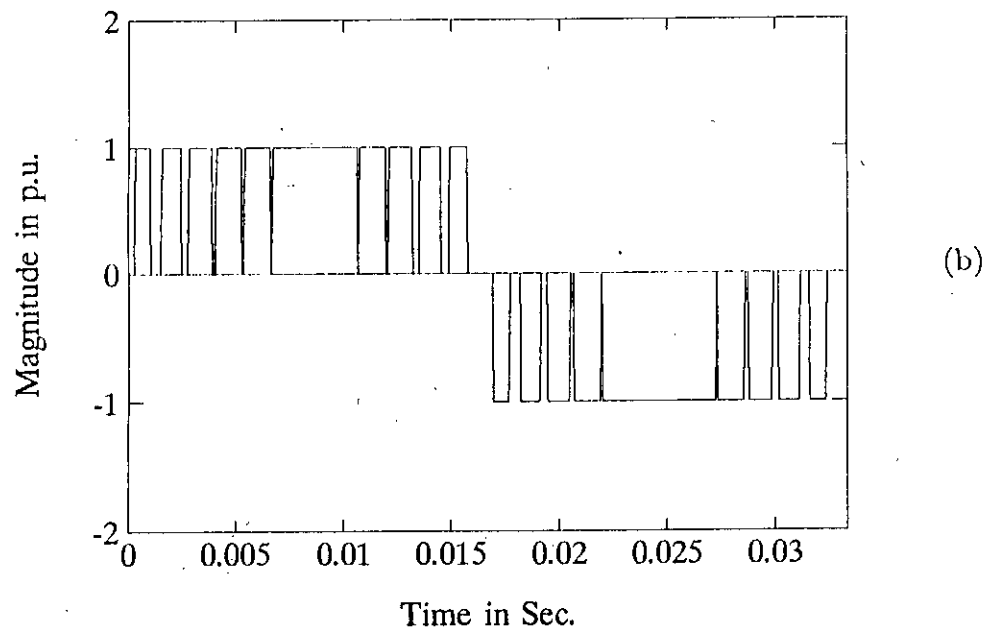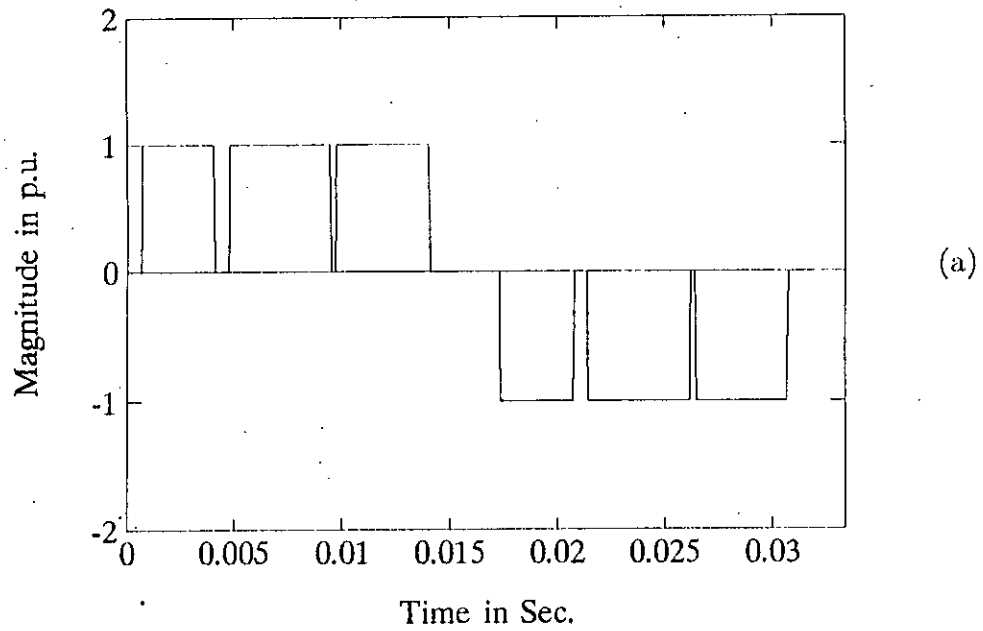
Figure A.1: Simulated single-phase triangular SPWM inverter wavforms for $f = 30$ Hz: (a) $N = 7$;(b) $N = 25$. (modulation index constant)

146
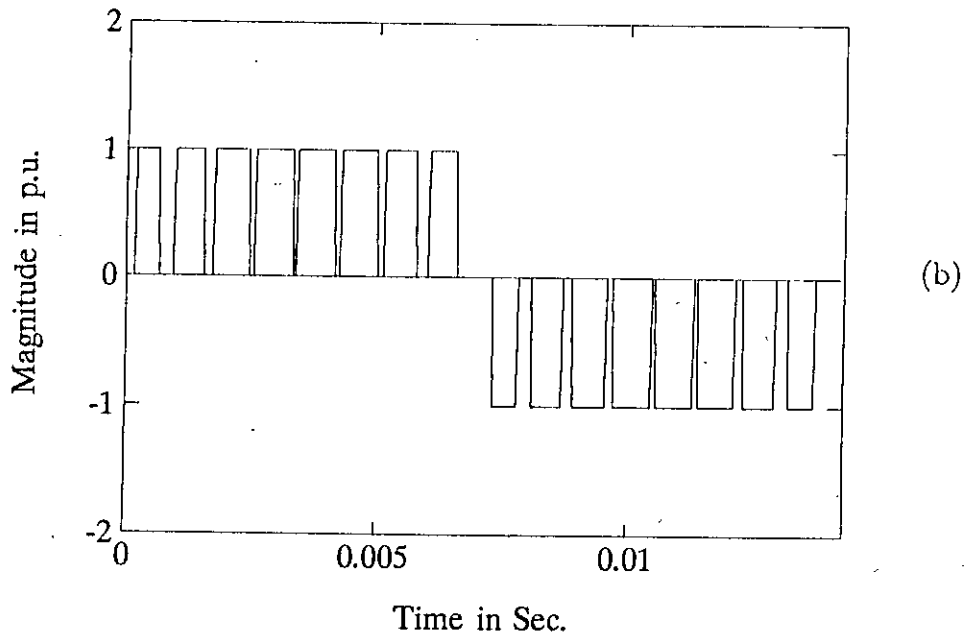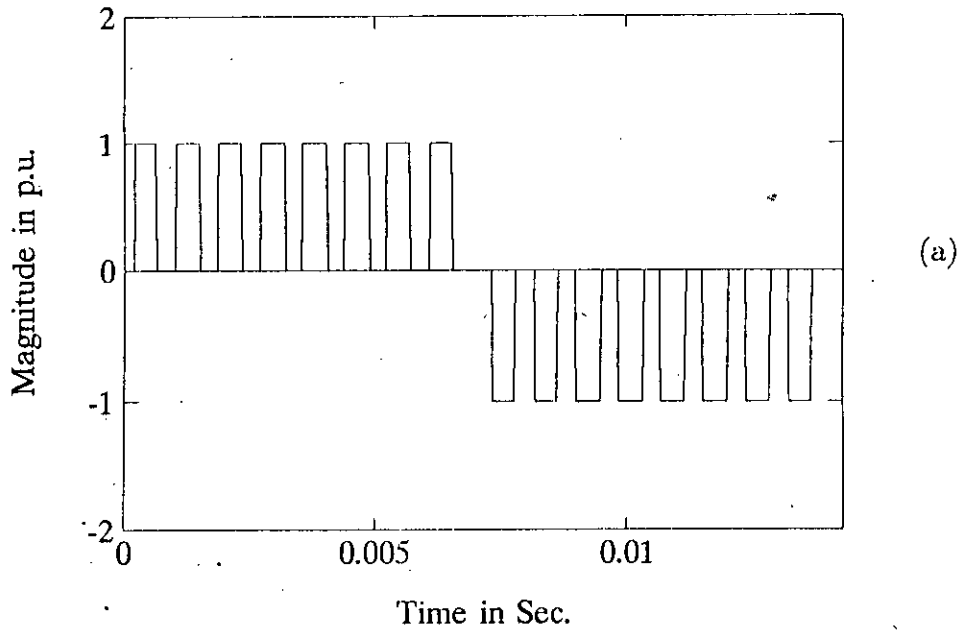
Figure A.2: Simulated single-phase triangular SPWM inverter waveforms for $f = 70$ Hz: (a) $m = 0.2$; (b) $m = 0.8$. (no. of pulse/cycle constant)

147
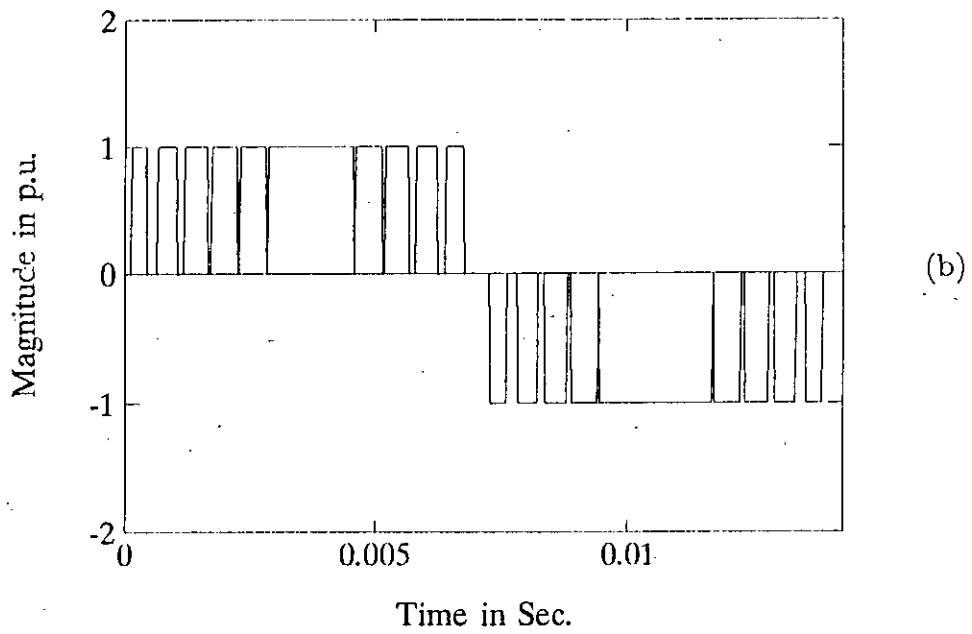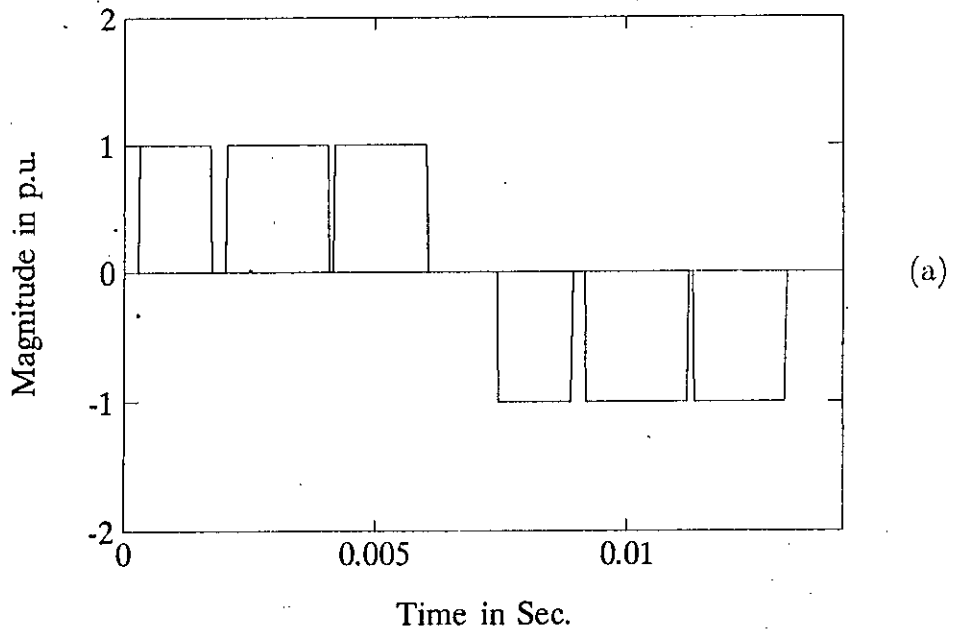
Figure A.3: Simulated single-phase triangular SPWM inverter wavforms for $f = 70$ Hz: (a) $N = 7$; (b) $N = 25$. (modulation index constant)

(a)

(b)
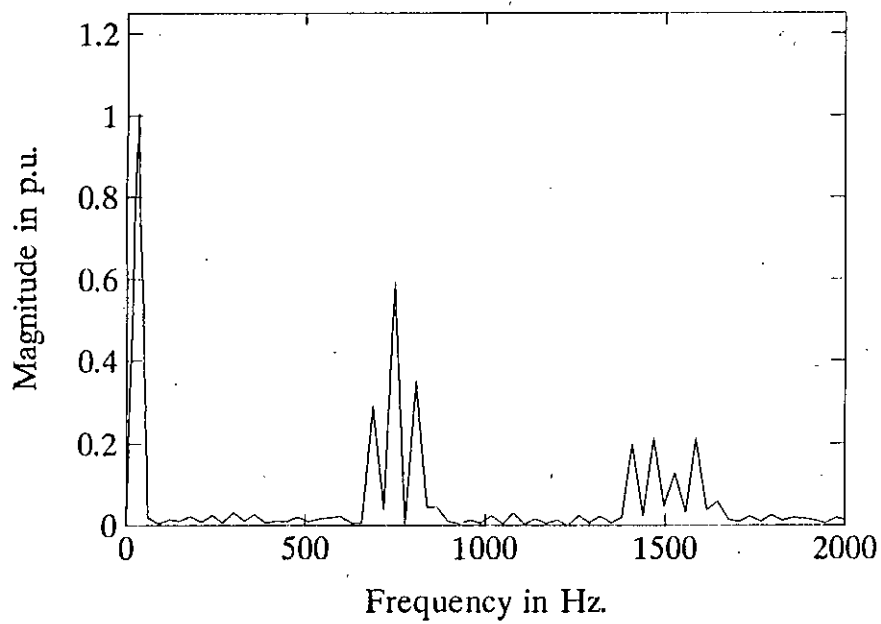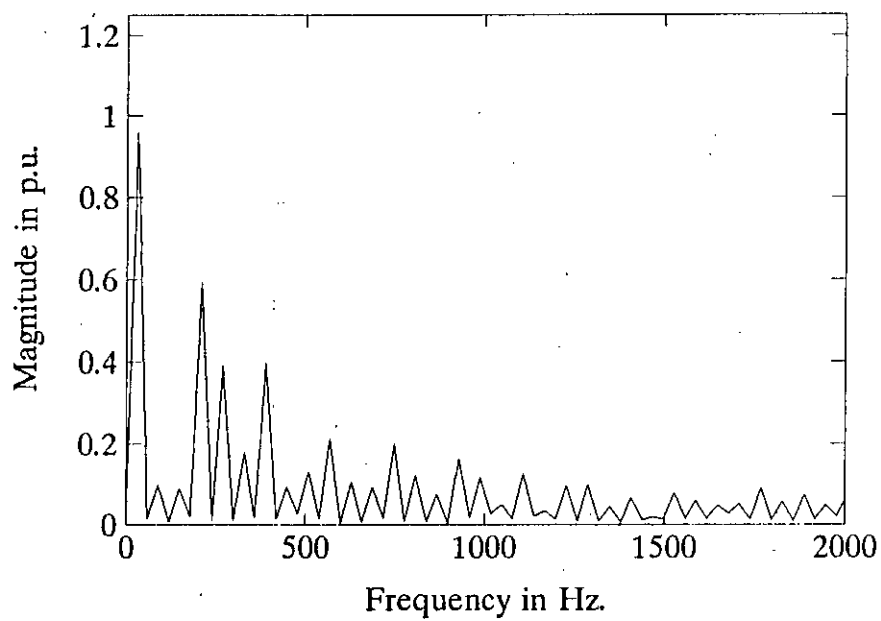
Figure A.4: Spectrum corresponding to simulated waveforms of Fig. A.1:(a) $N = 7$; (b) $N = 25$. (modulation index constant)

149
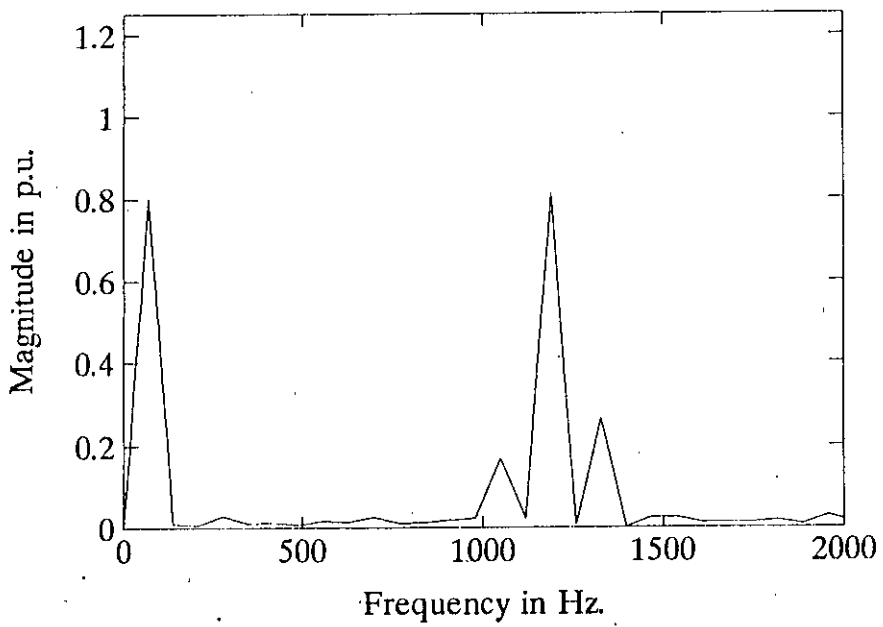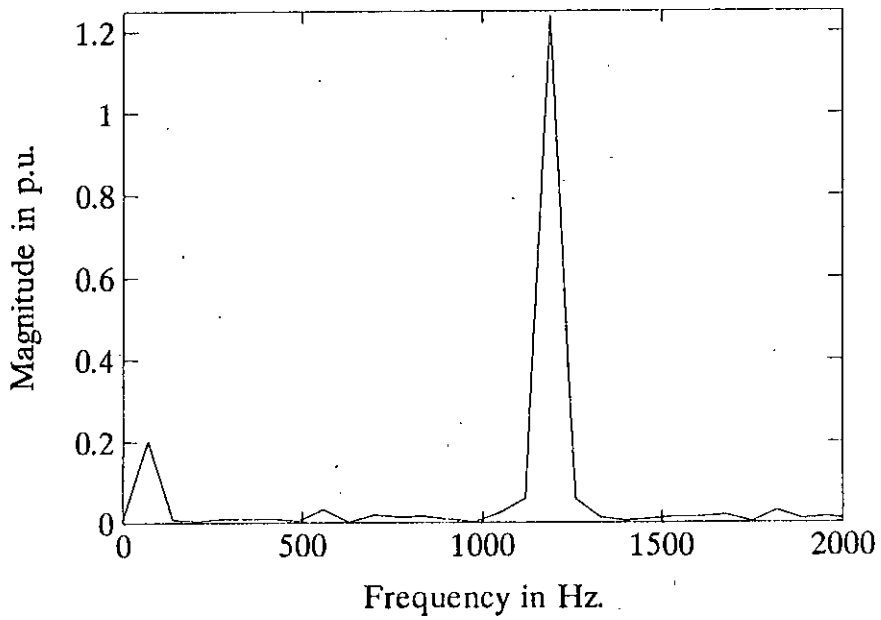
Figure A.5: Spectrum corresponding to simulated waveforms
of Fig. A.2:(a) $m = 0.2$; (b) $m = 0.8$.
(no. of pulse/cycle constant)
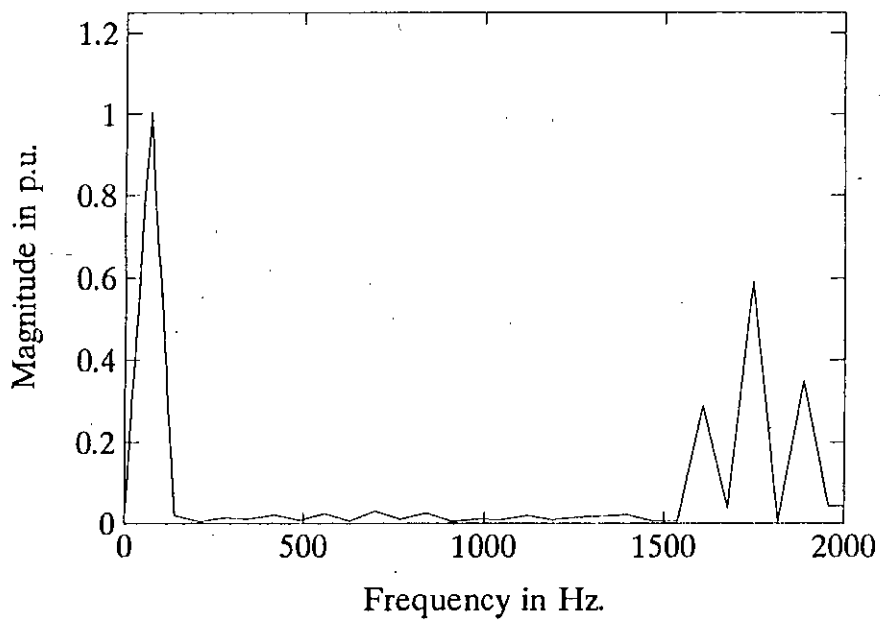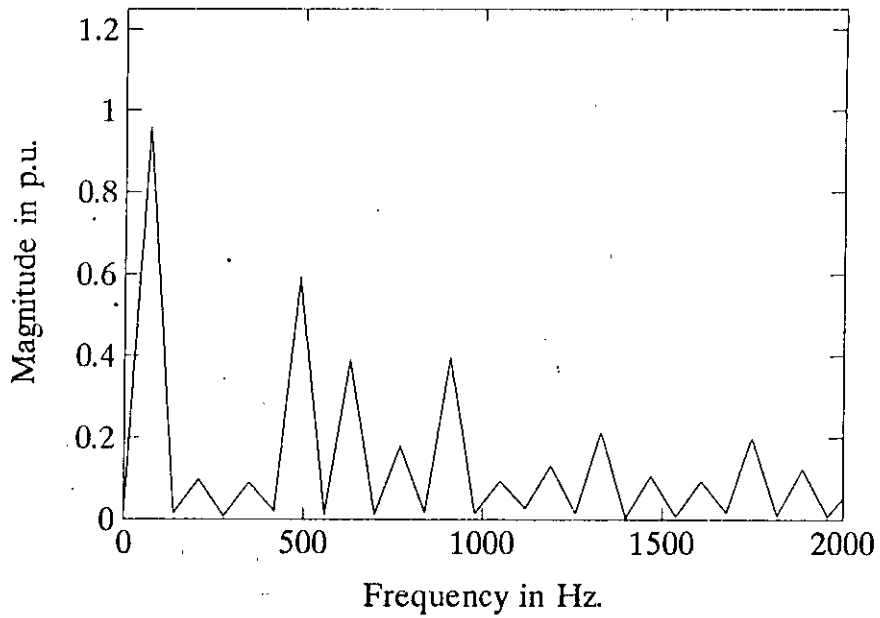
Figure A.6: Spectrum corresponding to simulated waveforms of Fig. A.3:(a) $N = 7$; (b) $N = 25$. (modulation index constant)

151

(a)

(b)
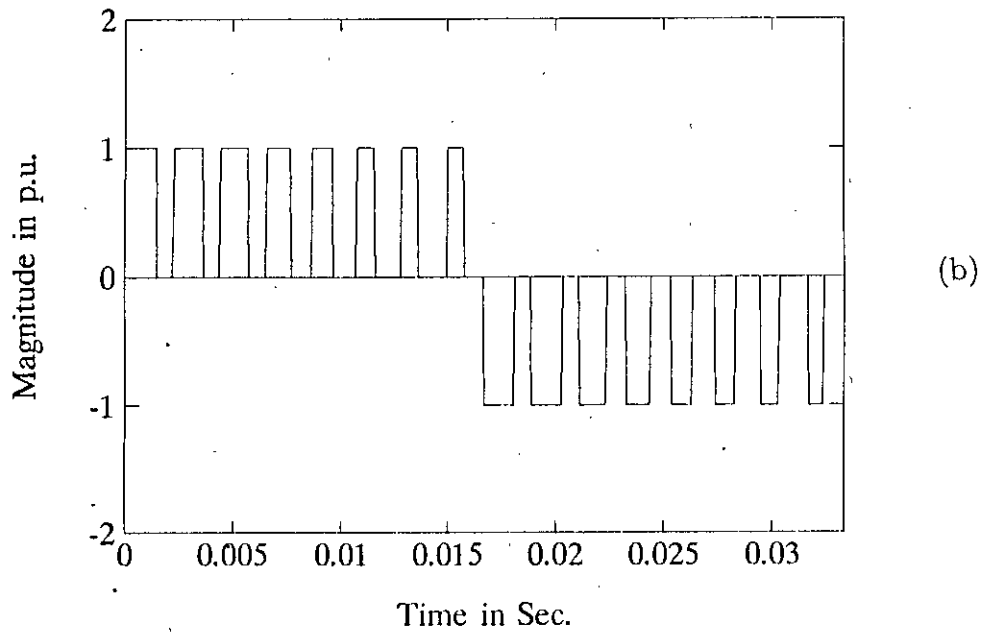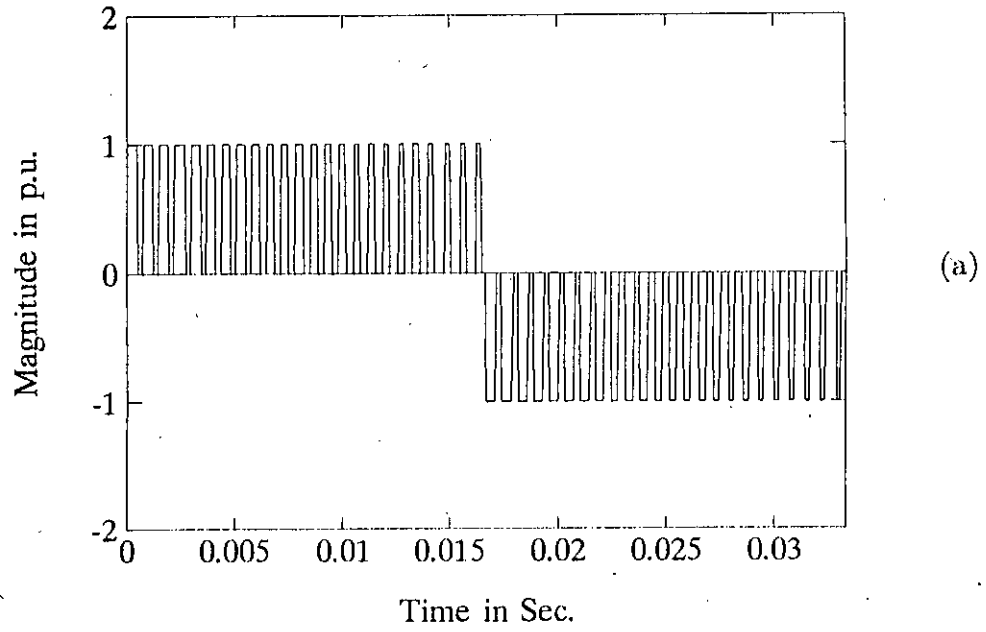
Figure A.7: Simulated single-phase DM inverter waveforms
for $f = 30$ Hz: (a) $\Delta V = 0.5$; (b) $\Delta V = 1.5$.
(slope and reference voltage constant)
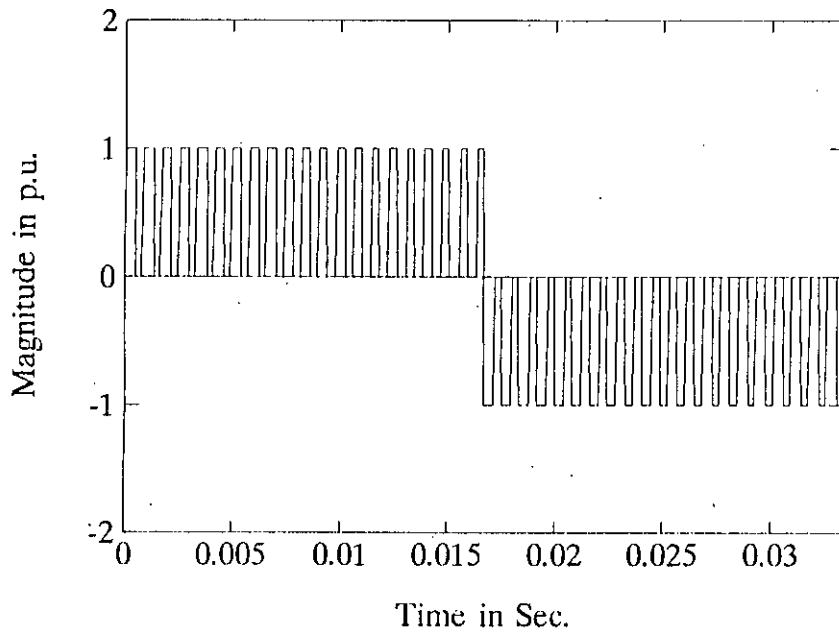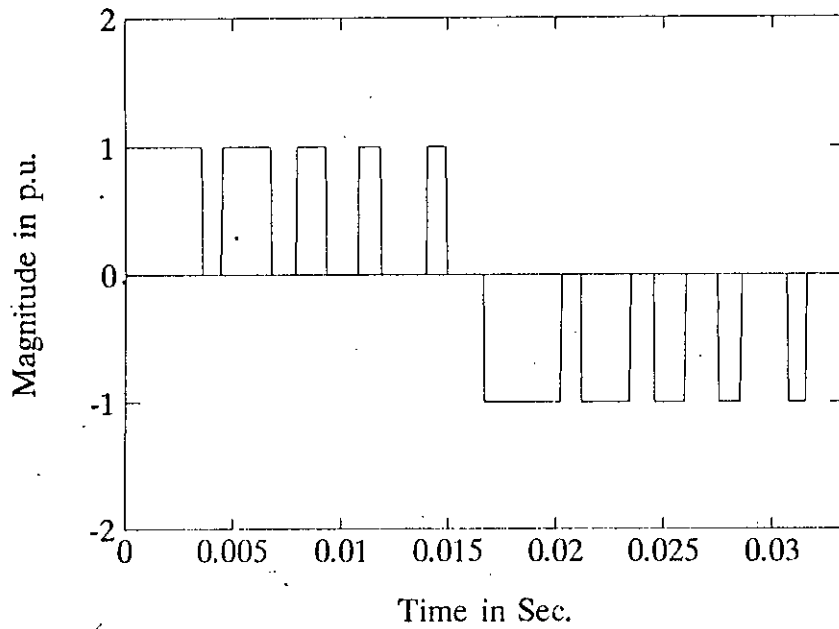
Figure A.8: Simulated single-phase DM inverter waveforms
for $f = 30$ Hz: (a) $S = 1500$; (b) $S = 5000$.
(window width and reference voltage constant)

(a)

(b)
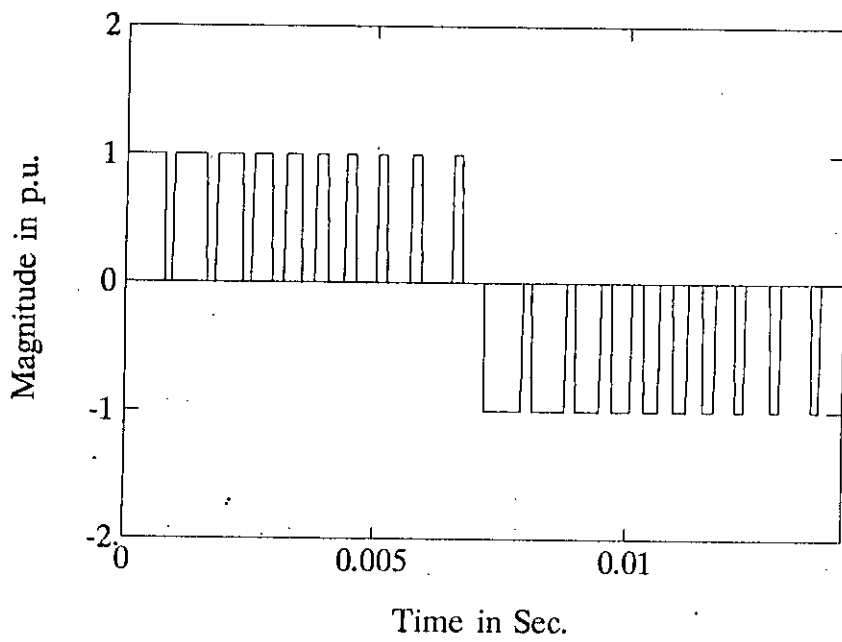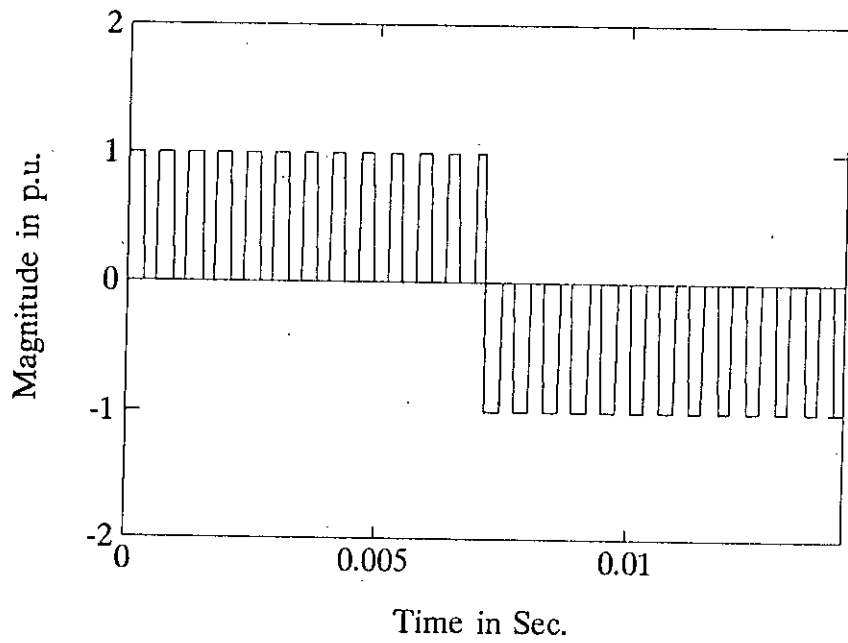
Figure A.9: Simulated single-phase DM inverter waveforms
for $f = 70$ Hz: (a) $V_m = 2$; (b) $V_m = 10$.
(slope and window width constant)

154
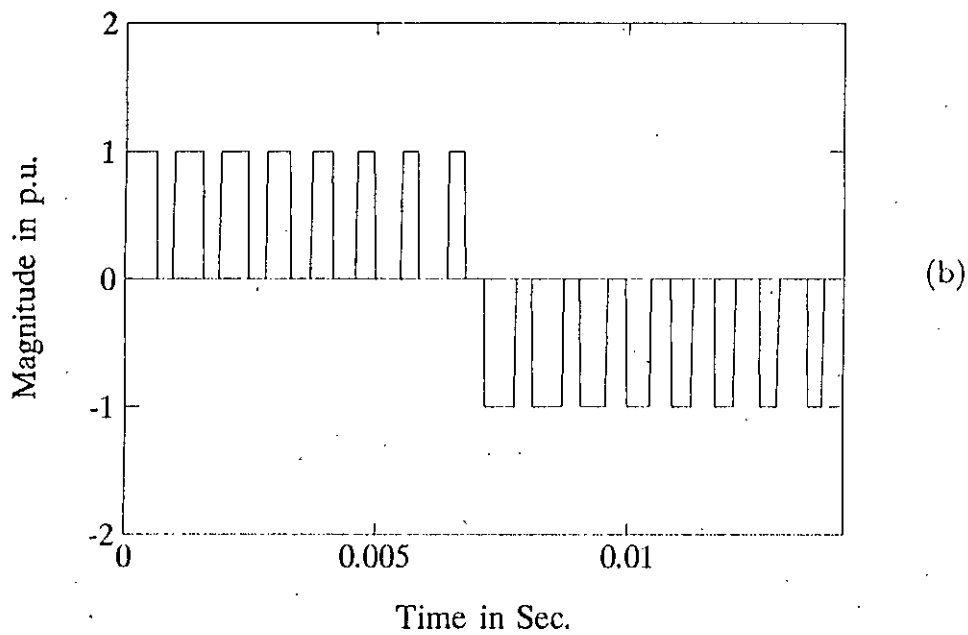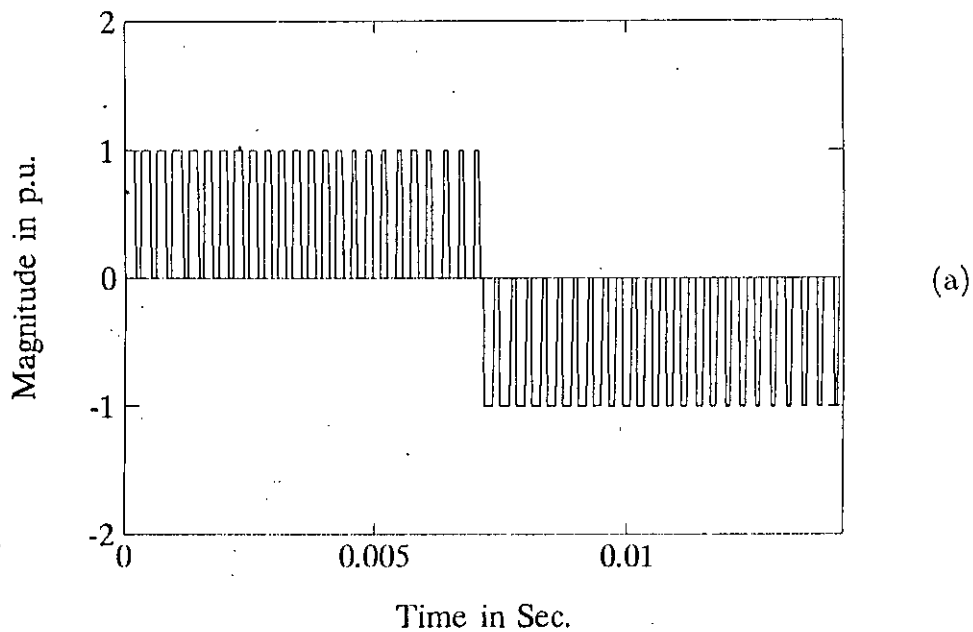
Figure A.10: Simulated single-phase DM inverter waveforms
for $f = 70$ Hz: (a) $\Delta V = 0.5$; (b) $\Delta V = 1.5$.
(slope and reference voltage constant)

(a)

(b)
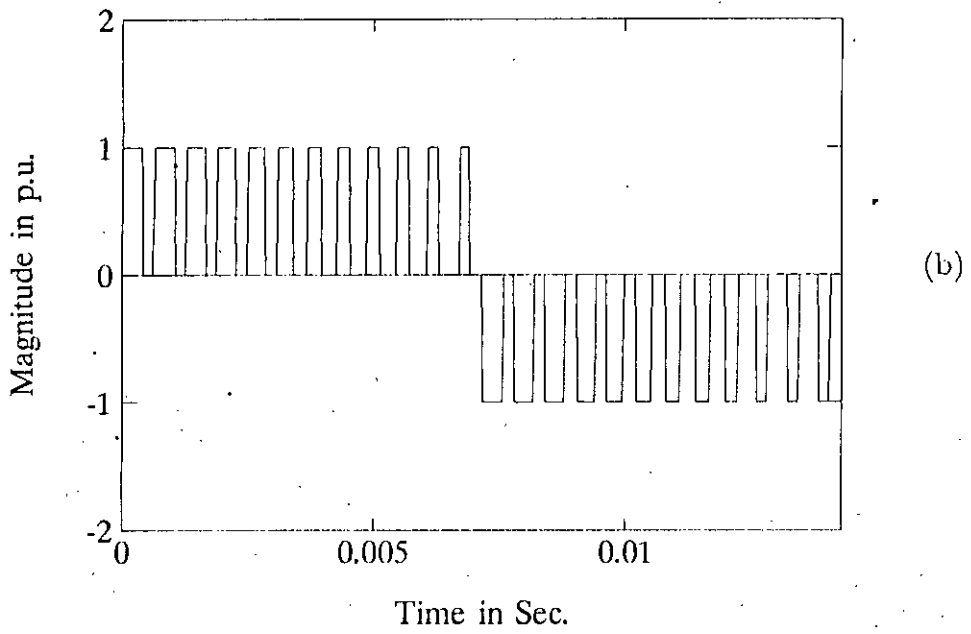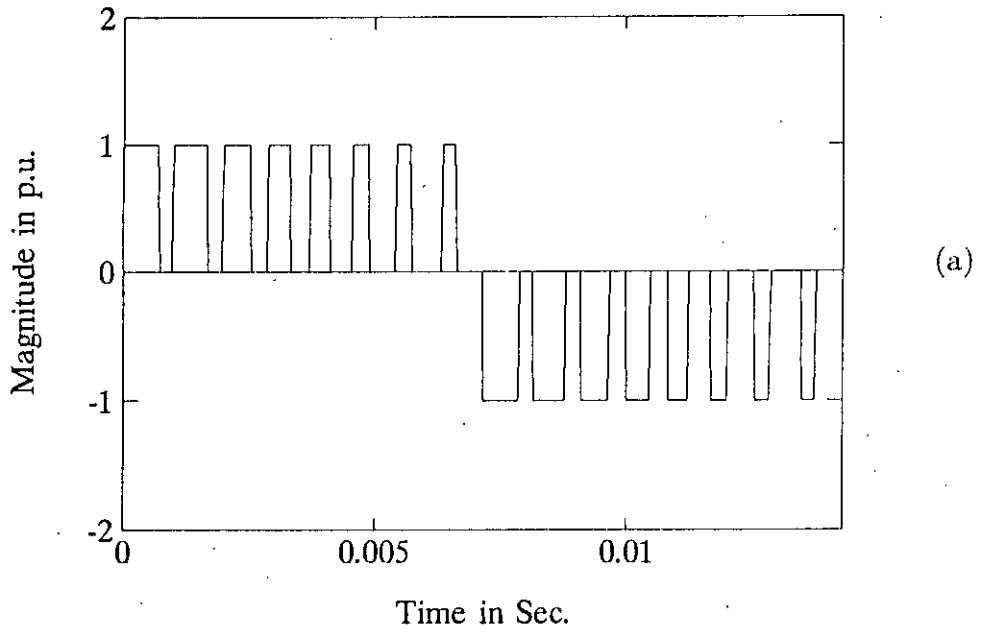
Figure A.11: Simulated single-phase DM inverter waveforms
for $f = 70$ Hz: (a) $S = 5000$; (b) $S = 7000$.
(window width and reference voltage constant)

156

(a)

(b)
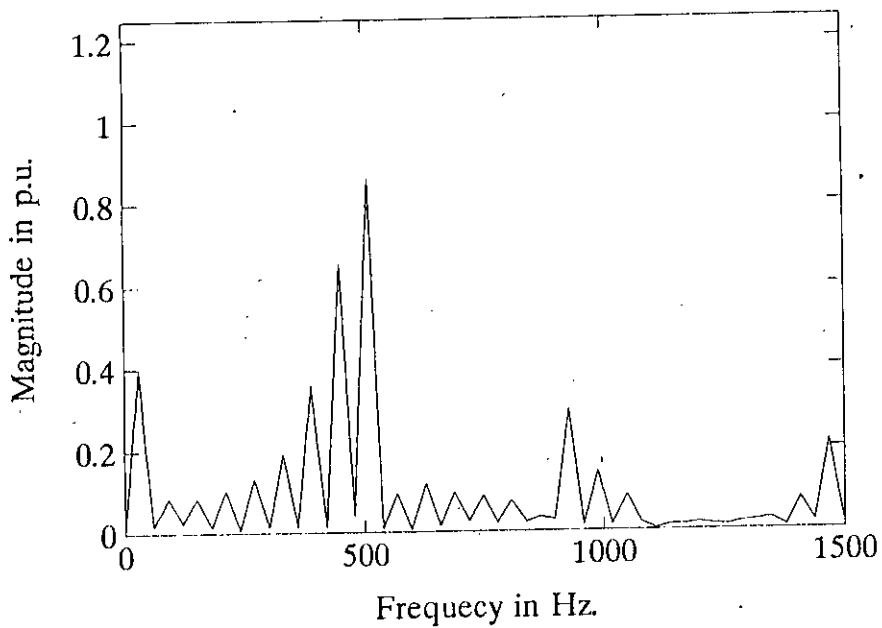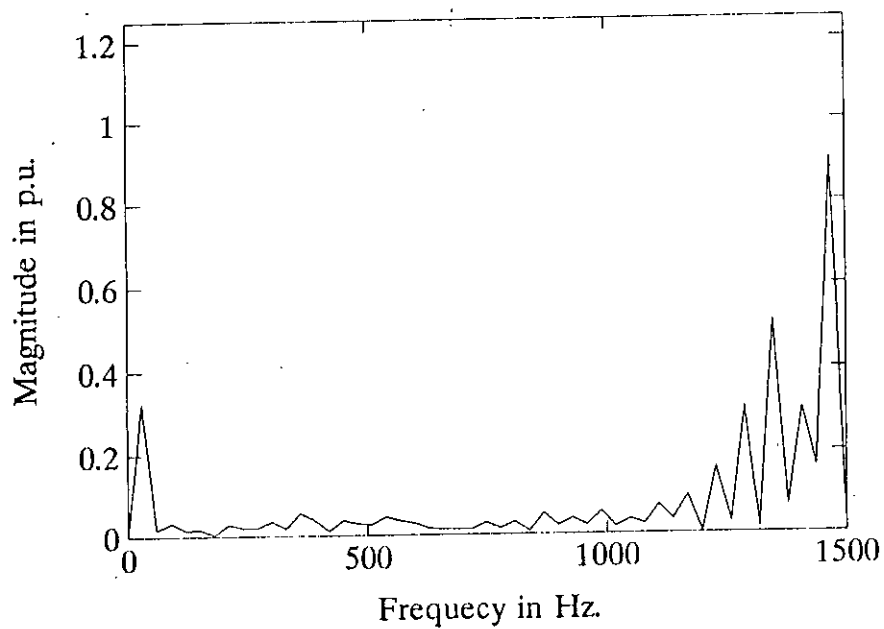
Figure A.12: Spectrum corresponding to simulated waveforms
of Fig. A.7: (a) $\Delta V = 0.5$; (b) $\Delta V = 1.5$.
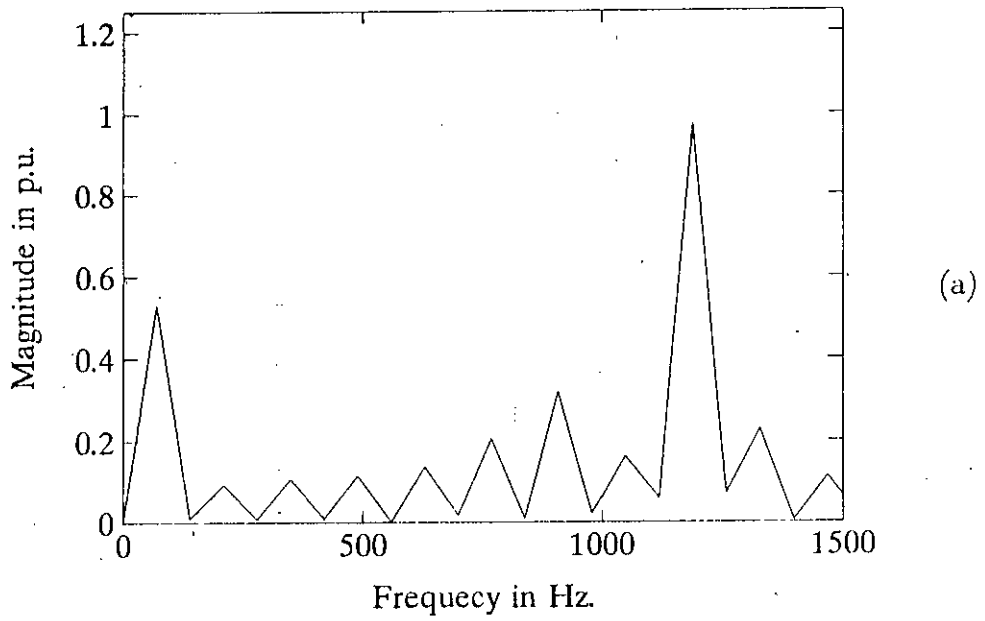(slope and reference voltage constant)
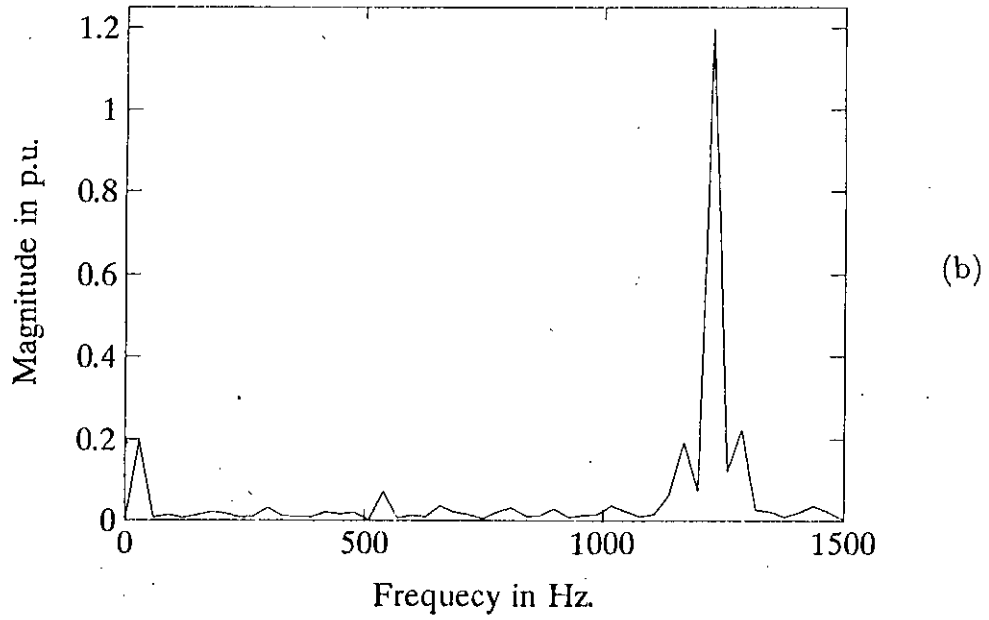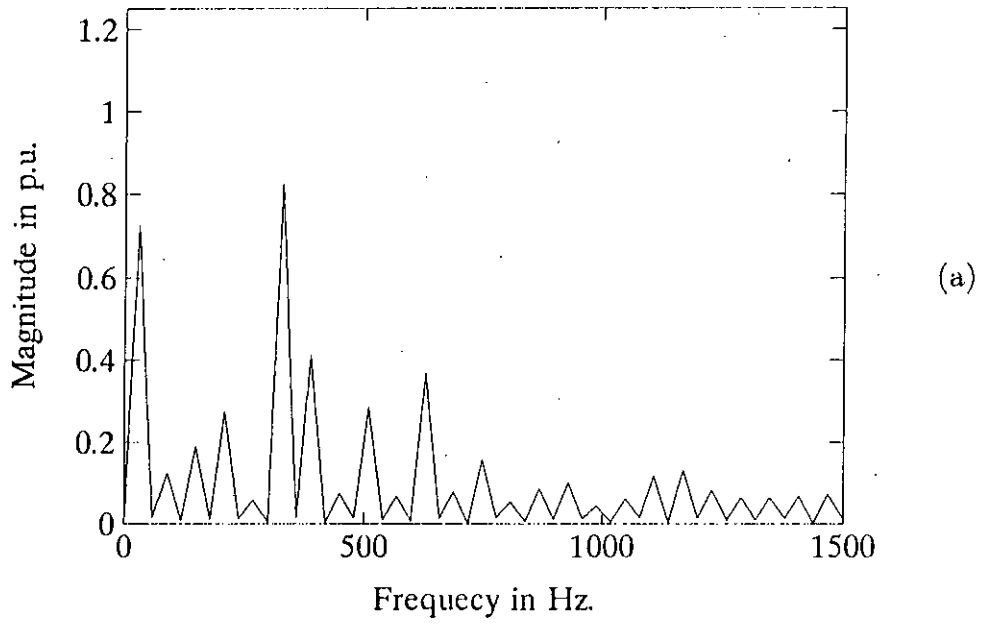
Figure A.13: Spectrum corresponding to simulated waveforms
of Fig. A.8: (a) $S = 1500$; (b) $S = 5000$..
(window width and reference voltage constant)
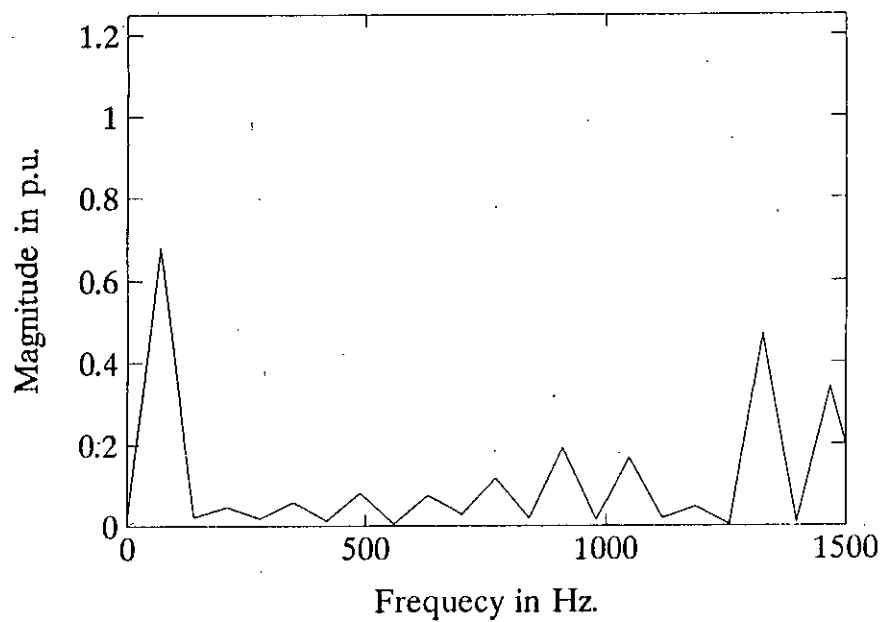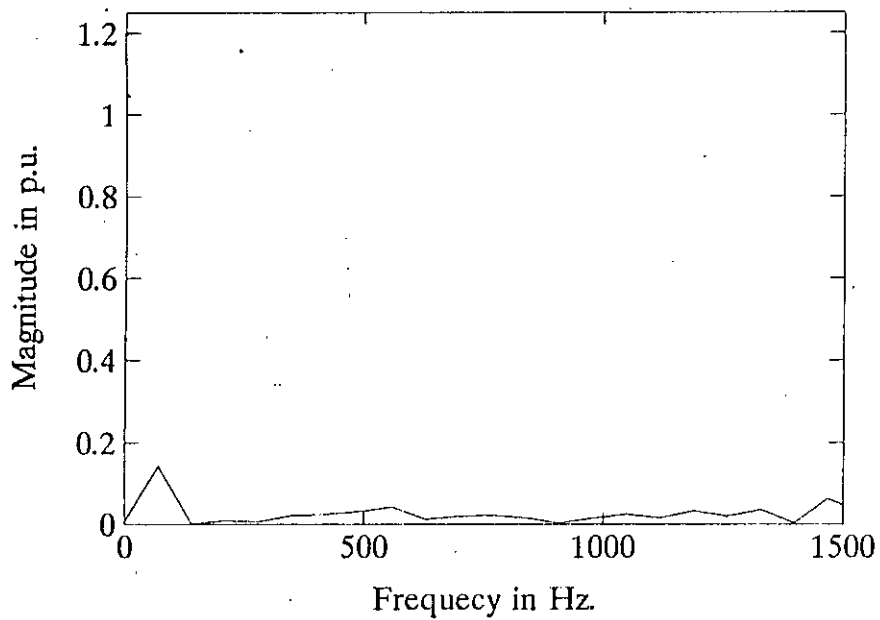
Figure A.14: Spectrum corresponding to simulated waveforms of Fig. A.9: (a) $V_m = 2$; (b) $V_m = 10$. (slope and window width constant)

(a)

(b)
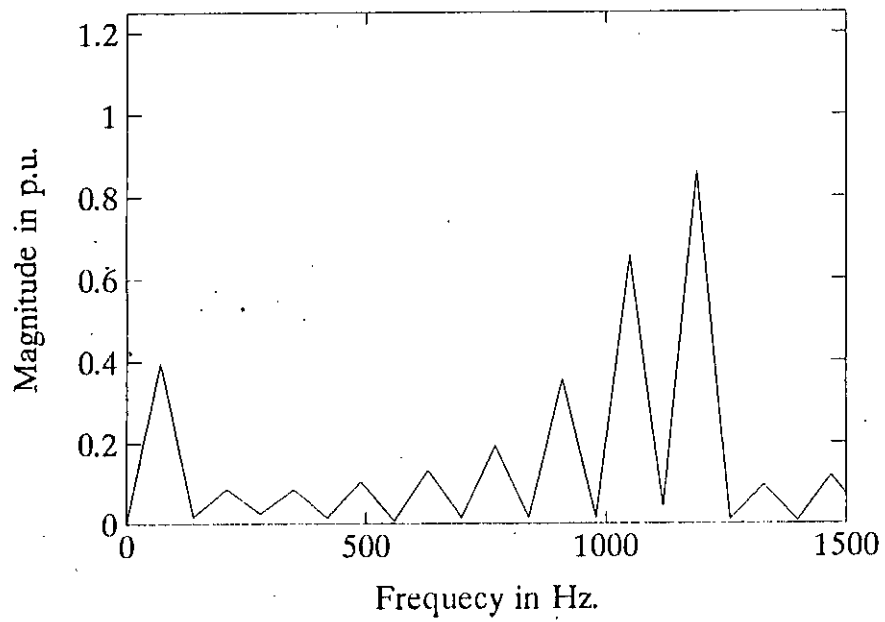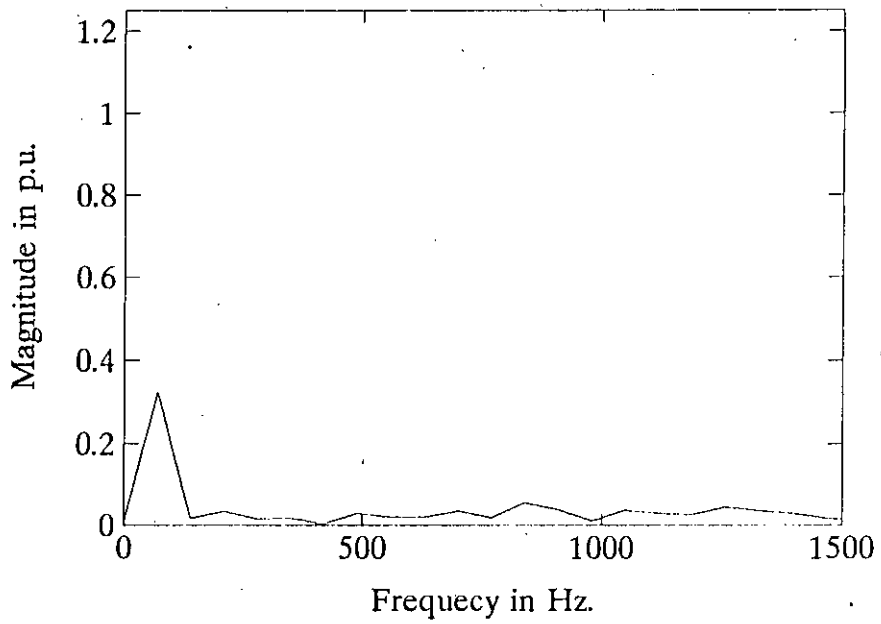
Figure A.15: Spectrum corresponding to simulated waveforms
of Fig. A.10: (a) $\Delta V = 0.5$; (b) $\Delta V = 1.5$.
(slope and reference voltage constant)

(a)

(b)
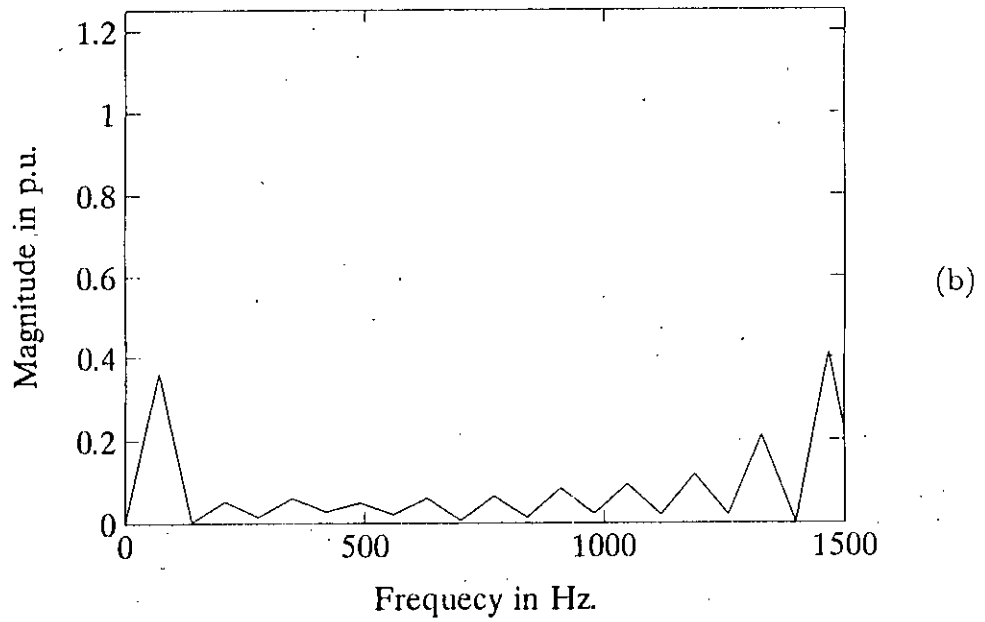
Figure A.16: Spectrum corresponding to simulated waveforms
of Fig. A.11: (a) $S = 5000$; (b) $S = 7000$..
(window width and reference voltage constant)

161

(a)

(b)
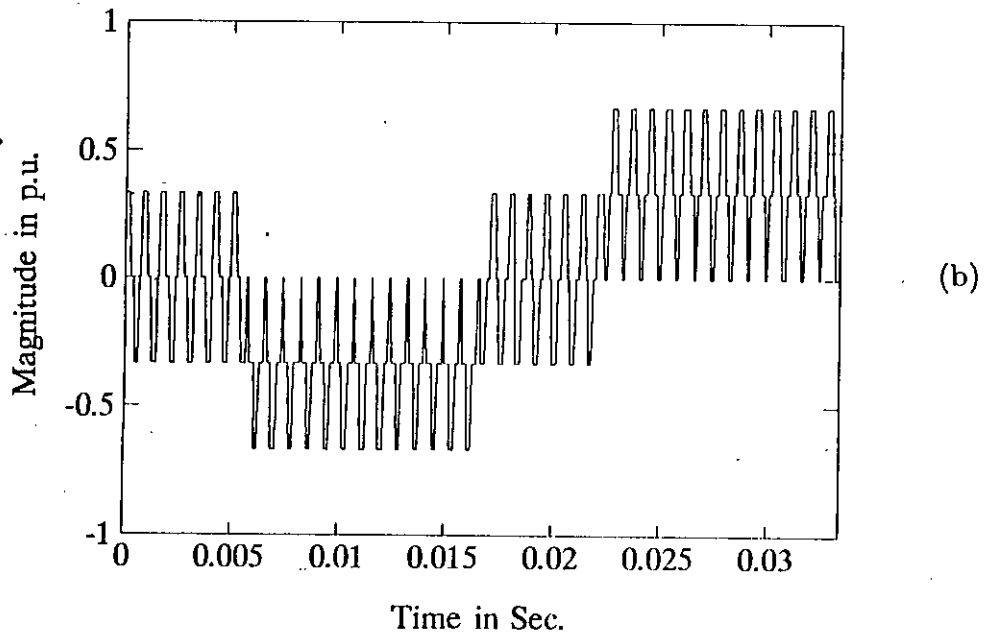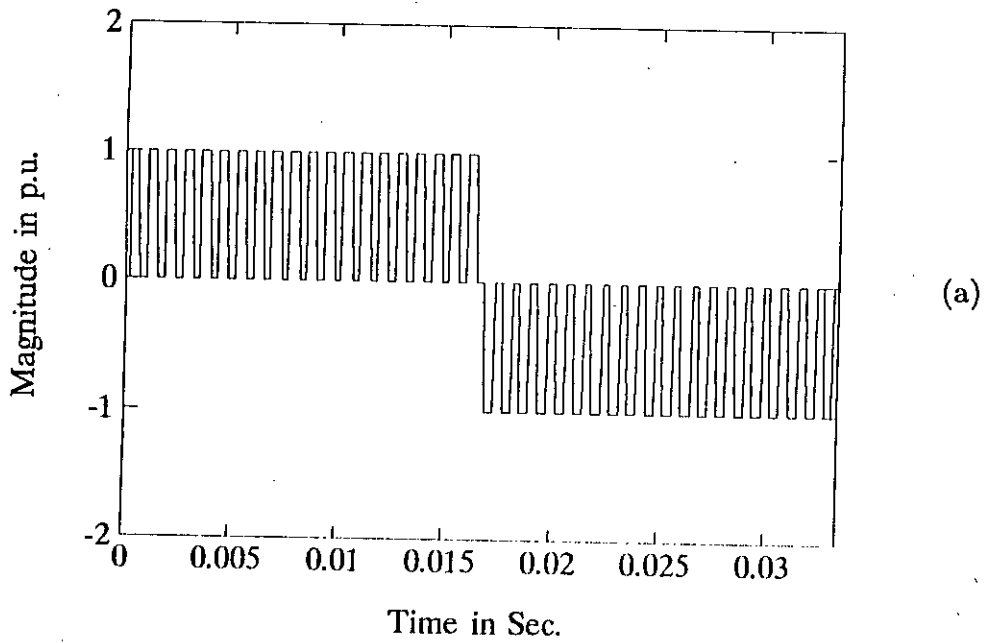
Figure A.17: Simulated waveforms of three phase PWM
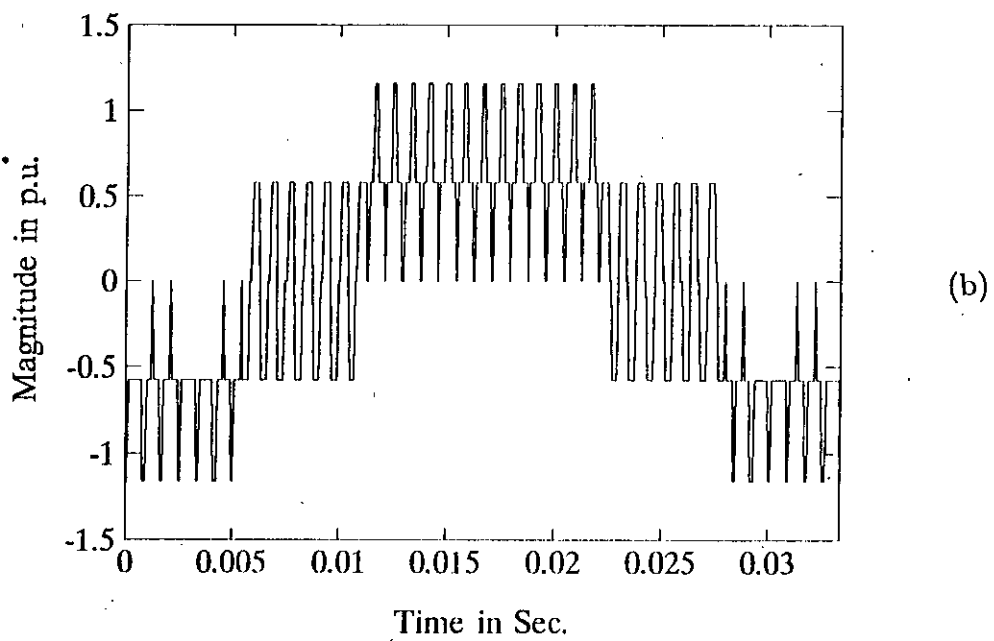inverter for $f = 30$ Hz, $m = 0.2$ and $N = 40$:
(a) line voltage; (b) phase voltage.

(a)

(b)
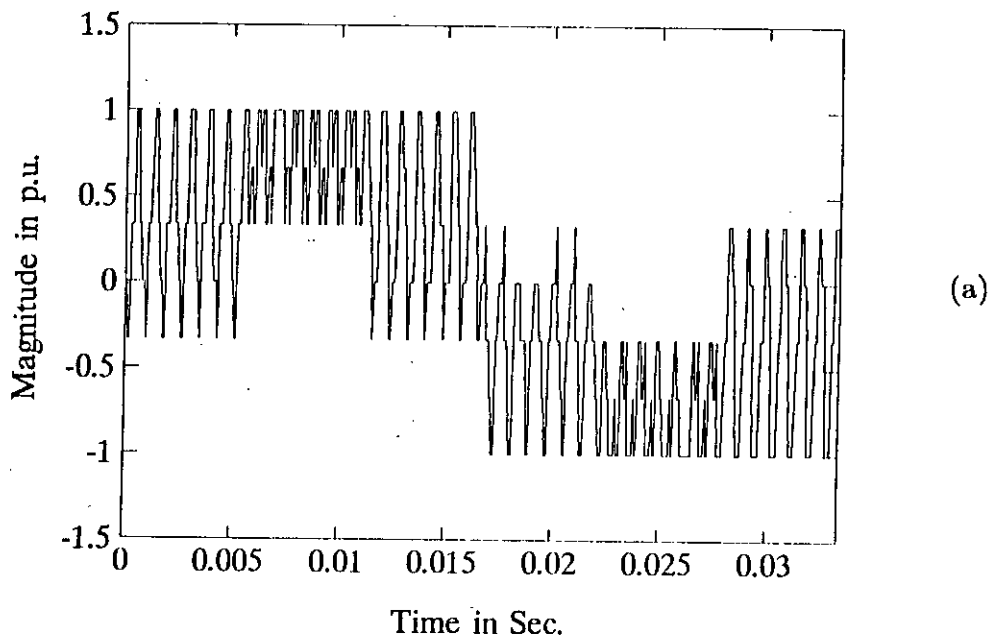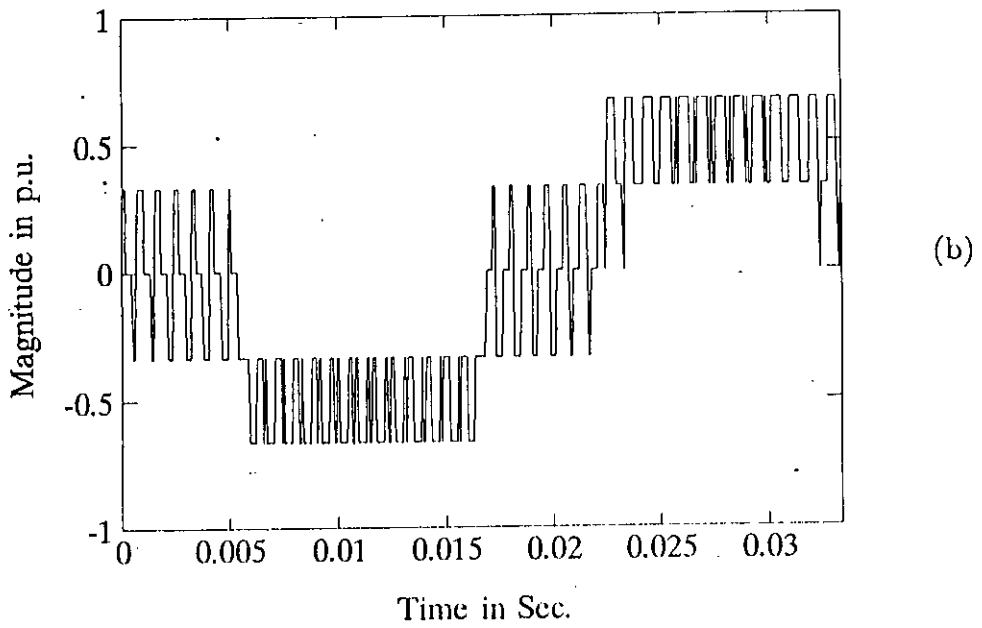
Figure A.18: Simulated waveforms of three phase PWM
inverter for $f = 30$ Hz, $m = 0.2$ and $N = 40$:
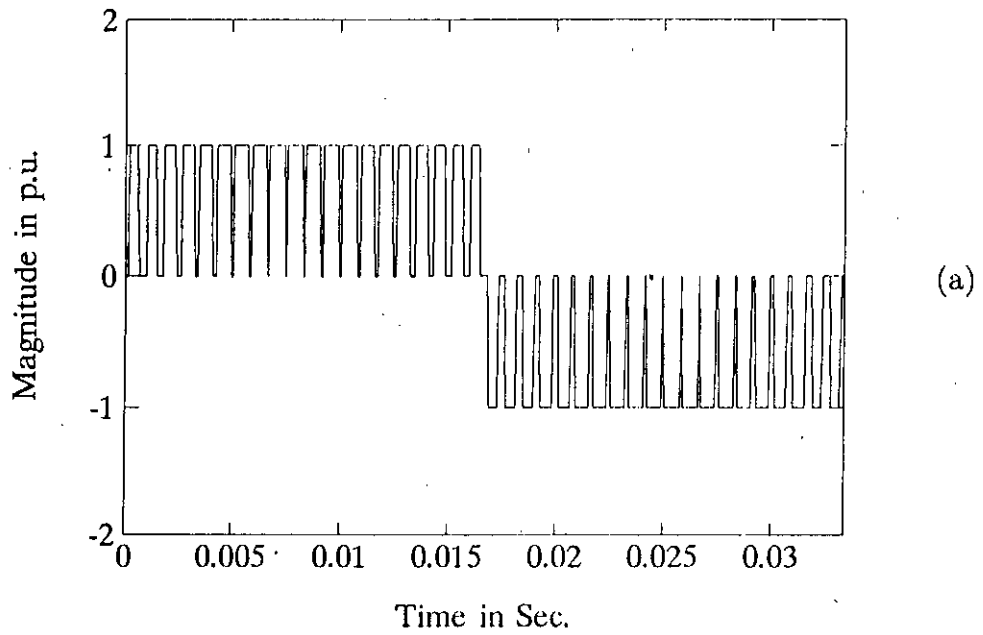(a) d-axis voltage; (b) q-axis voltage.

(a)

(b)

Figure A.19: Simulated waveforms of three phase PWM
inverter for $f = 30$ Hz, $m = 0.8$ and $N = 40$:
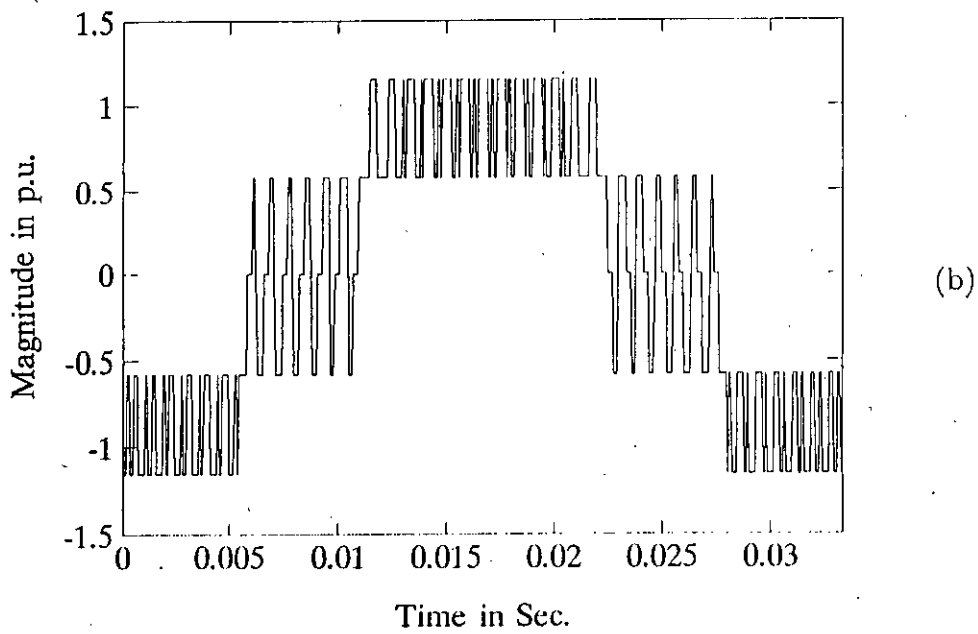(a) line voltage; (b) phase voltage.

Figure A.20: Simulated waveforms of three phase PWM
inverter for $f = 30$ Hz, $m = 0.8$ and $N = 40$:
(a) d-axis voltage; (b) q-axis voltage.

(a)

(b)

Figure A.21: Simulated waveforms of three phase PWM inverter for $f = 70$ Hz, $m = 0.2$ and $N = 40$: (a) line voltage; (b) phase voltage.
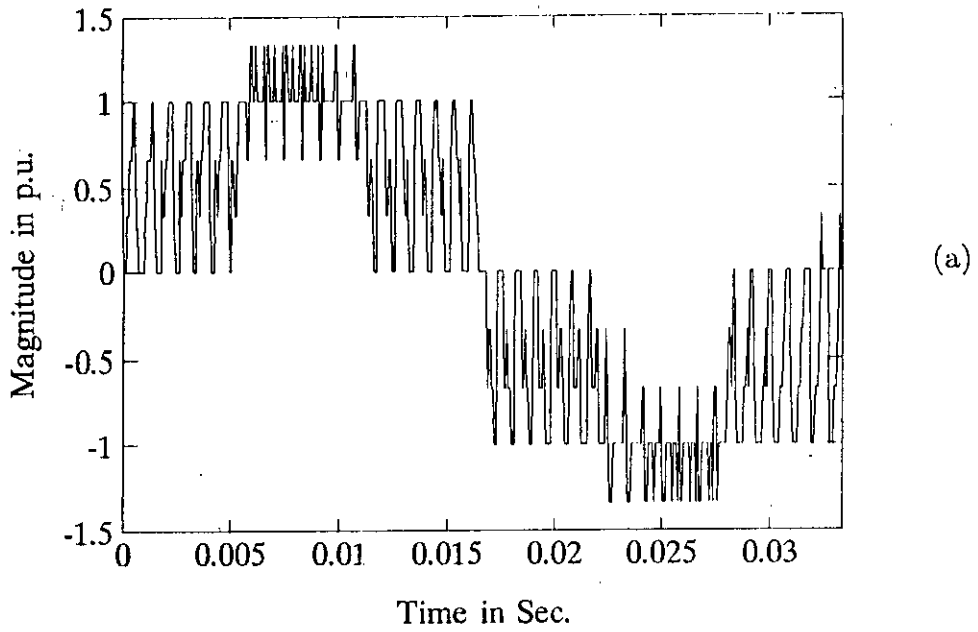
Figure A.22: Simulated waveforms of three phase PWM
inverter for $f = 70$ Hz, $m = 0.2$ and $N = 40$:
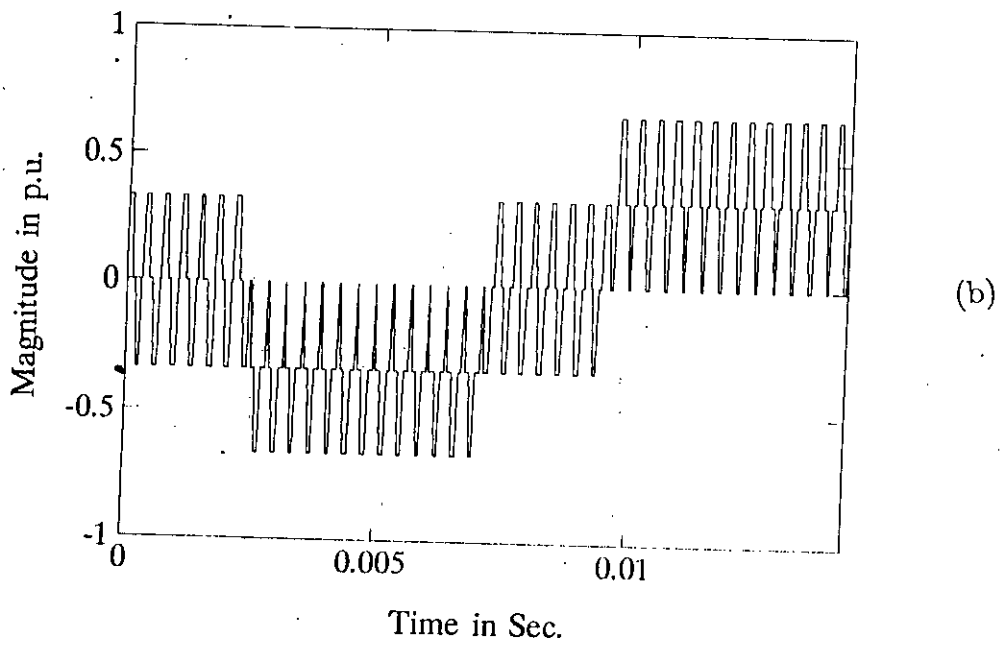(a) d-axis voltage; (b) q-axis voltage.

(a)

(b)

Figure A.23: Simulated waveforms of three phase PWM
inverter for $f = 70$ Hz, $m = 0.8$ and $N = 40$:
(a) line voltage; (b) phase voltage.

168

Figure A.24 Simulated waveforms of three phase PWM
inverter for $f = 70$ Hz, $m = 0.8$ and $N = 40$:
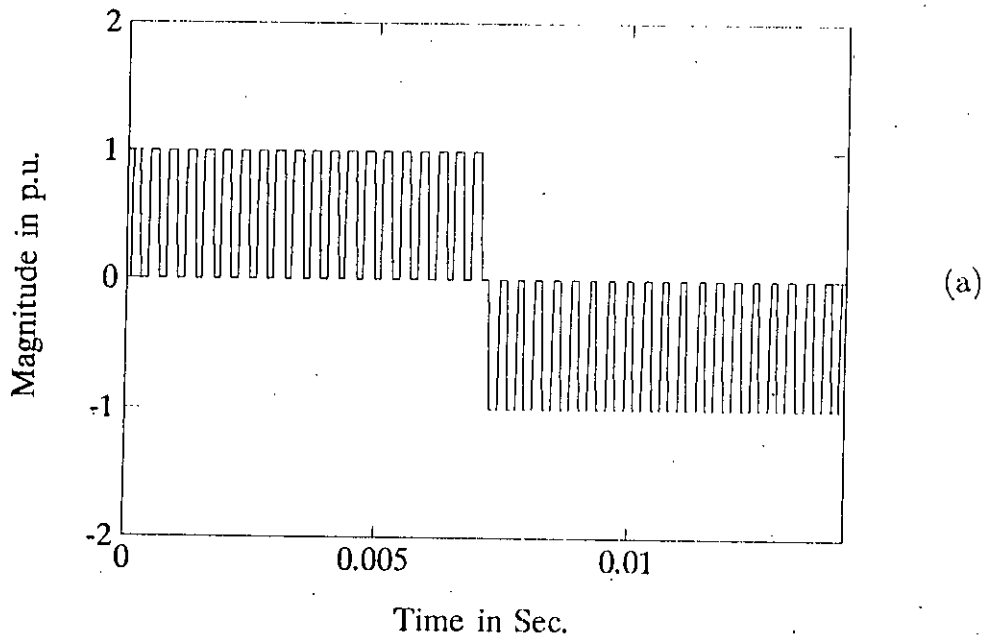(a) d-axis voltage; (b) q-axis voltage.

(a)

(b)

Figure A.25 Simulated waveforms of three phase PWM
inverter for $f = 50$ Hz, $m = 0.8$ and $N = 30$:
(a) line voltage; (b) phase voltage.

170
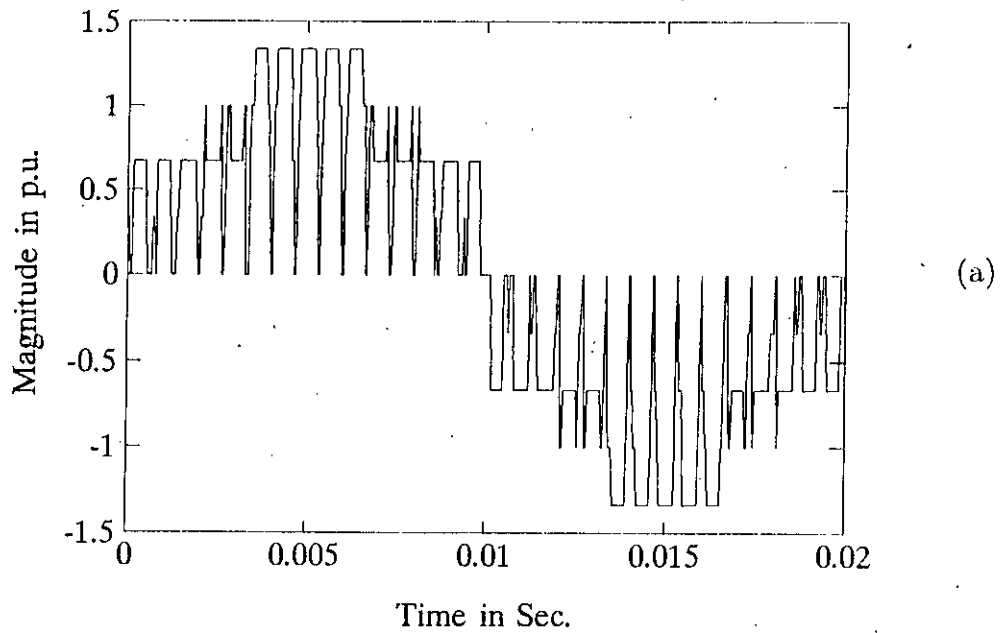
Figure A.26 Simulated waveforms of three phase PWM
inverter for $f = 50$ Hz, $m = 0.8$ and $N = 30$:
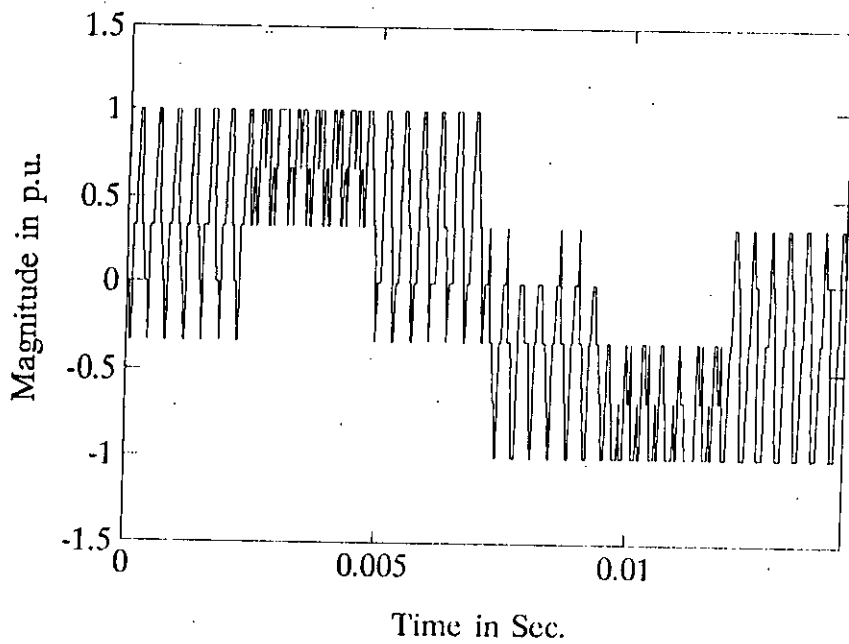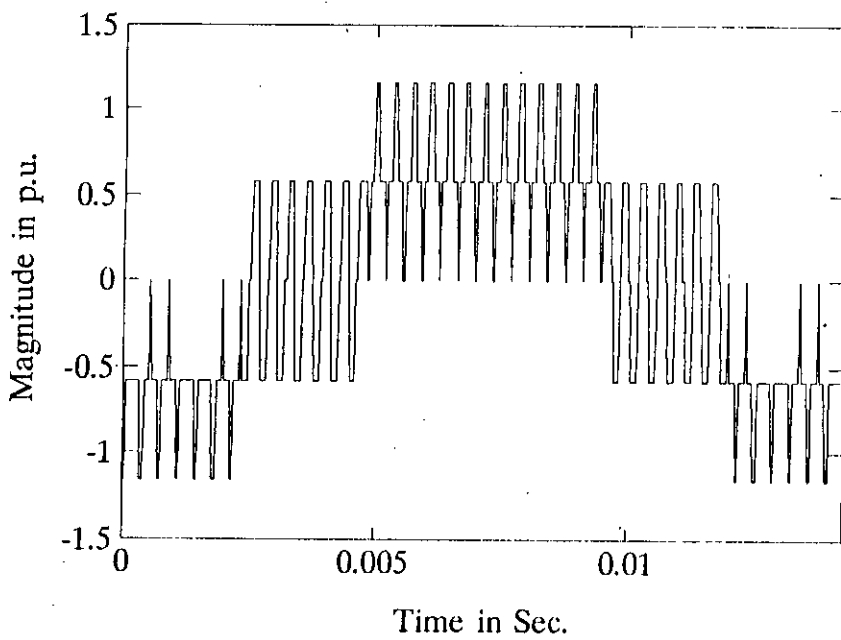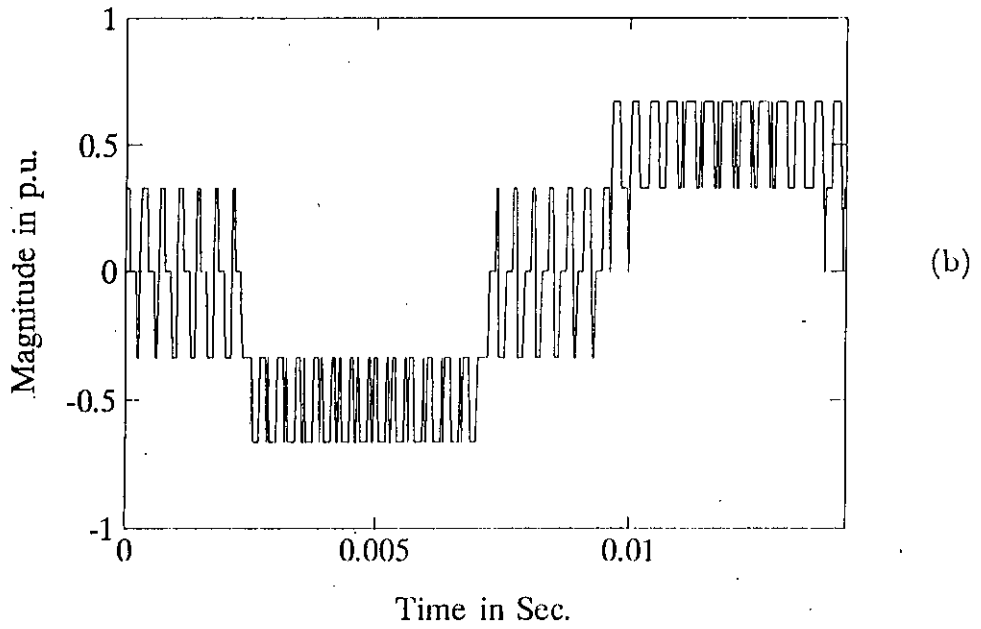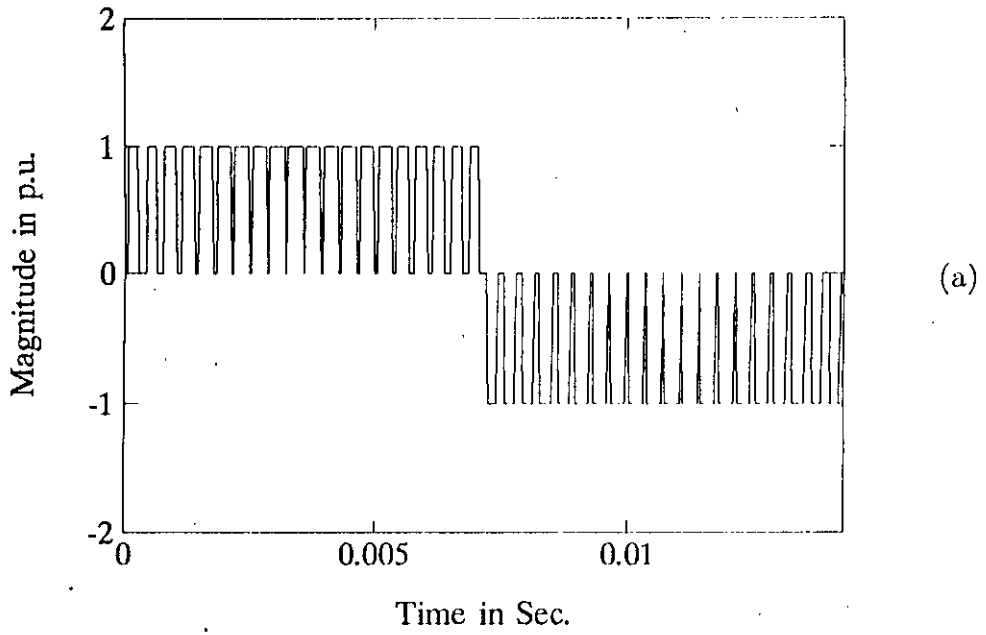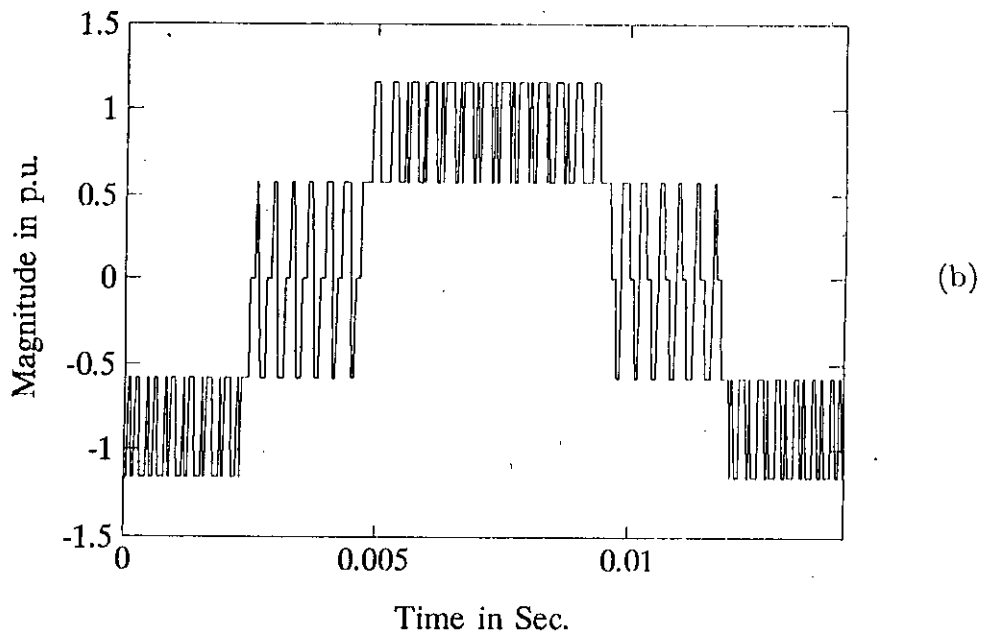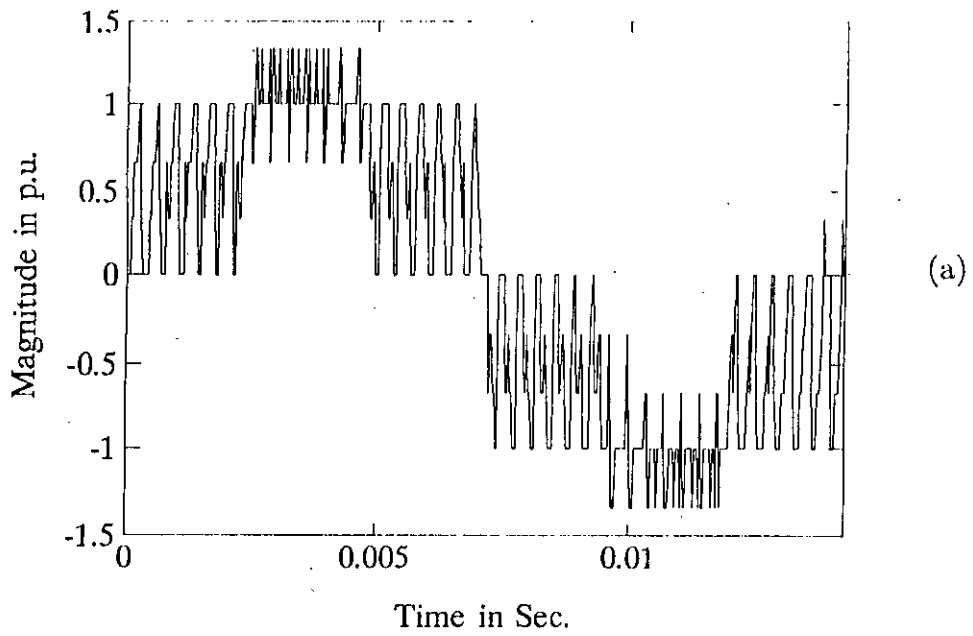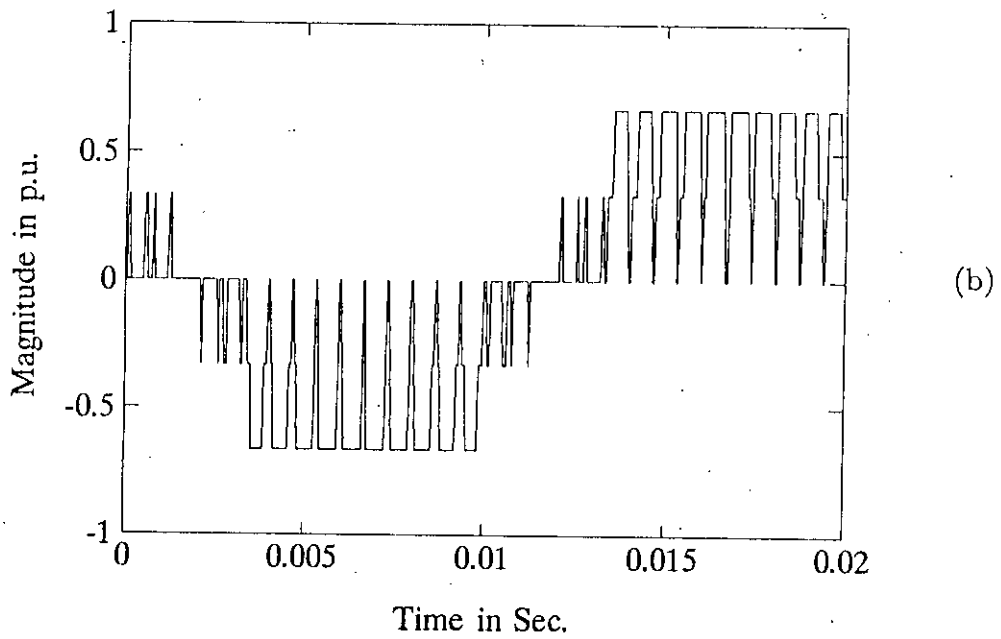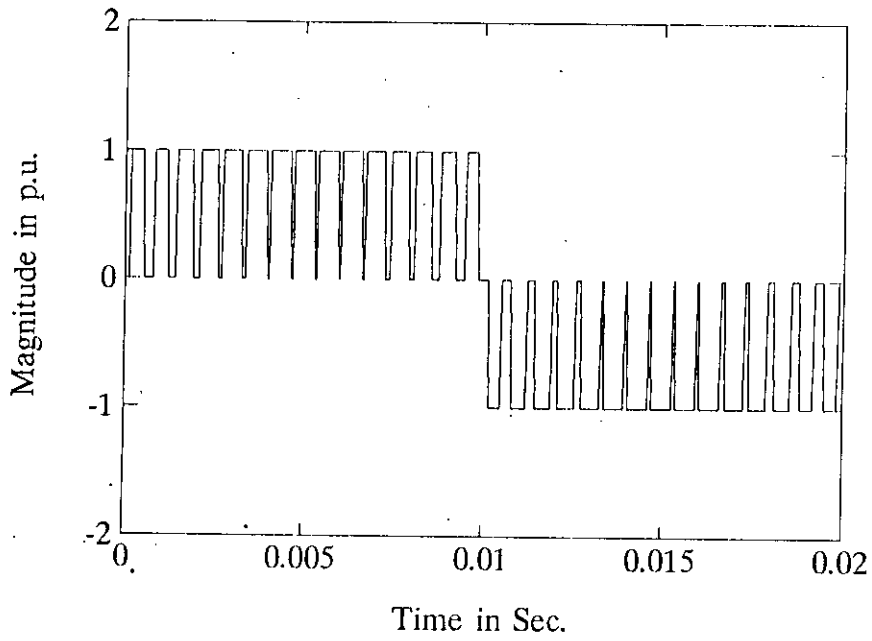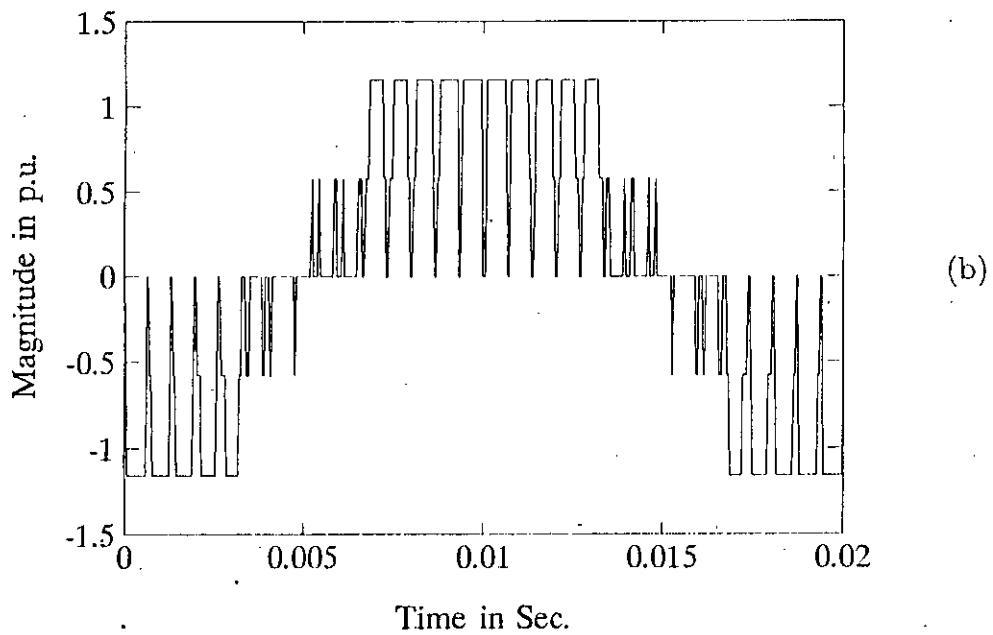(a) d-axis voltage; (b) q-axis voltage.

171

Appendix B

Synchronous Machine Parameter Identification by Stand-Still Tests

B.1   Introduction:

Machine modeling is a major area of research in the study of synchronous machine performance, specially for studying transient and stability phenomena of machines. Accurate representation of a machine by its parameters is necessary because these parameters are responsible for shaping the steady-state performance, transient response and stability patterns of the machine. The synchronous machine representation in d-q axes equivalent circuits is widely used [60]. In linear machine modeling equivalent circuits are drawn in terms of direct and quadrature axes parameters [61,120]. Two of these models are Park's two-reaction model and Canay's model. Modification of these models are also considered to solve more sophisticated problems. Continued research as indicated by works reported in literature highlights the need, diversity and complexity of the subject [78]. A considerable amount of research has so far been carried out to validate several proposed machine models and determination of the parameters of the models [61,62,121]. Parameters for models can be obtained either in the design and construction stage of the machine from design data or by means of analytical solution and experimental tests. Methods of parameter estimation include transient short-circuit test, slip test,

stand-still frequency response and stand-still time-domain identification methods etc. Among the analytical methods, frequency response method is based on mathematically involved parameter estimation technique requiring expensive experimental data acquisition instrumentation [65,122]. Analytical methods based on stand-still time-domain identification require experimental readings from simple instrumentation, but subsequent analytical and computational procedure are complex [86-88]. One of the main drawbacks of the conventional methods is that these methods make assumptions which are not completely valid for machines of all sizes. As a result, each method has specific area of use as pointed out by reference [78]. Practical difficulties are encountered in the case of small synchronous machines where the stator and rotor winding resistances are comparable to machine reactances.

Standard tests of synchronous machine parameters rely heavily on measurements of large transients as noted in reference [83]. As such they are susceptible to changes in saturation during measurements. Further, the accuracy and resolution with which a single transient can be measured are doubtful and insufficient to provide details required to model solid-rotors of synchronous machines [81]. Subsequent researchers focused attention towards frequency response and time-domain identification methods as stated. The frequency tests require sinusoidal sources having sufficient level of current with range of frequency varying from 0.001 to 200 Hz [80]. The results obtained by such tests have to be corrected for saturation [81] and overall method depends on curve-fitting techniques based on bode plots and statistical procedures [78]. The time-domain identifications rely on the transfer function simulation and noise free stand-still measurements [86]. The accuracy of this method also depends on arithmetic precessions during computation. The computational burden for time domain analysis is also considerable because it uses identification of multivariable system technique (i.e., q-axis identification required 24 second CPU time in high-speed VAX11/750 computer) [86].

As a part of this research a test method based on stand-still measurements is developed

to identify the parameters of Park's model of synchronous machines. The proposed method can identify parameters of both the direct and quadrature axes models and require several simple tests involving inexpensive instrumentation.

B.2 D-Q axis Input Impedance Relationship From Test Measurements

Equivalent impedance of a network of passive linear components can be obtained from voltage and current measurements at input and output terminals. If values of the elements in the network can be measured by standard tests, rest of the elements can be separated by applying phasor algebra. Such a procedure can be used for determining the rotor circuit parameters of a synchronous machine. The proposed method is based on the input impedance measurement technique applied to the test configurations of reference [81] for synchronous machines.

Two possible circuit configurations which represent the connections of stator and field coils of a synchronous machine are used for measuring the direct and quadrature axes input impedances as shown in Figs. B.1 and B.2. The derivations of the equations for evaluating d and q axes input impedances in terms of measured quantities are illustrated for both the test configurations of Fig. B.1. The stator and field coil connections shown in Fig. B.2 represent the same circuit configuration except the field winding is rotated through an angle of 90^0.

B.2.1 Connection-I

For direct axis measurement, the magnetic axes of phase 'a' and field windings are aligned, Hence from Fig. B.1(a), it is noted that

$$V_a = V_c \qquad \text{(B.1)}$$

$$V_s = V_a - V_b \tag{B.2}$$

$$I_s = -I_a \tag{B.3}$$

Because of the symmetry of the stator windings

$$I_b = I_c = -\frac{1}{2}I_a = \frac{1}{2}I_s \tag{B.4}$$

$$I_d = \frac{2}{3}[I_a \cos\theta + I_b \cos(\theta - 120) + I_c \cos(\theta + 120)] \tag{B.5}$$

$$= -I_s \tag{B.6}$$

$$I_q = \frac{2}{3}[I_a \sin\theta + I_b \sin(\theta - 120) + I_c \sin(\theta + 120)] = 0 \tag{B.7}$$

$$I_o = \frac{1}{3}(I_a + I_b + I_c) = 0 \tag{B.8}$$

$$V_d = \frac{2}{3}[V_a \cos\theta + V_b \cos(\theta - 120) + V_c \cos(\theta + 120)] \tag{B.9}$$

$$= \frac{2}{3}V_s \tag{B.10}$$

$$V_q = \frac{2}{3}[V_a \sin\theta + V_b \sin(\theta - 120) + V_c \sin(\theta + 120)] = 0 \tag{B.11}$$

Input impedance of the circuit is

$$Z_s = \frac{V_s}{I_s} \tag{B.12}$$

$$\text{Again,} \quad \frac{V_d}{I_d} = \frac{2}{3}\frac{V_s}{I_s} = -\frac{2}{3}Z_s \tag{B.13}$$

$$\tag{B.14}$$

For quadrature axis measurement, the rotor is rotated 90° electrically. Then

$$I_d = \frac{2}{3}\left[I_a \cos(90) - \frac{1}{2}I_a \cos(-30) - \frac{1}{2}I_a \cos(210)\right] = 0 \tag{B.15}$$

$$I_q = -\frac{2}{3}\left[I_a \sin(90) - \frac{1}{2}I_a \sin(-30) - \frac{1}{2}I_a \sin(210)\right] \tag{B.16}$$

$$= I_s \tag{B.17}$$

$$I_o = \frac{1}{3}\left(I_a - \frac{1}{2}I_a - \frac{1}{2}I_a\right) = 0 \tag{B.18}$$

$$V_d = \frac{2}{3}[V_a \cos(90) + V_b \cos(-30) + V_b \cos(210)] = 0 \tag{B.19}$$
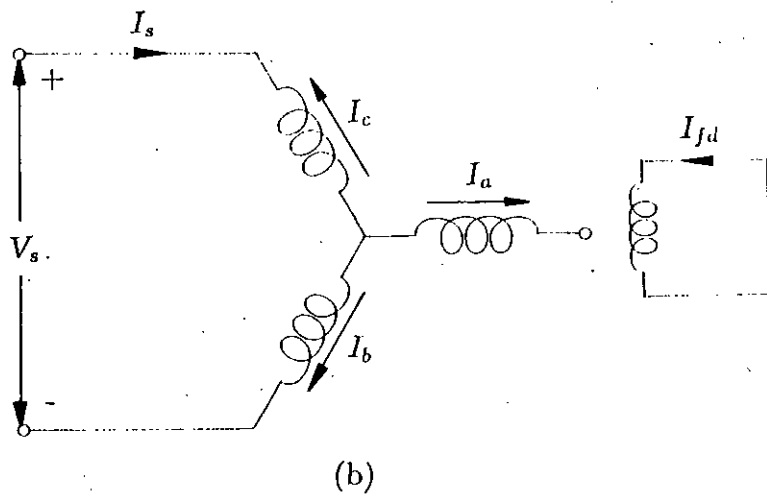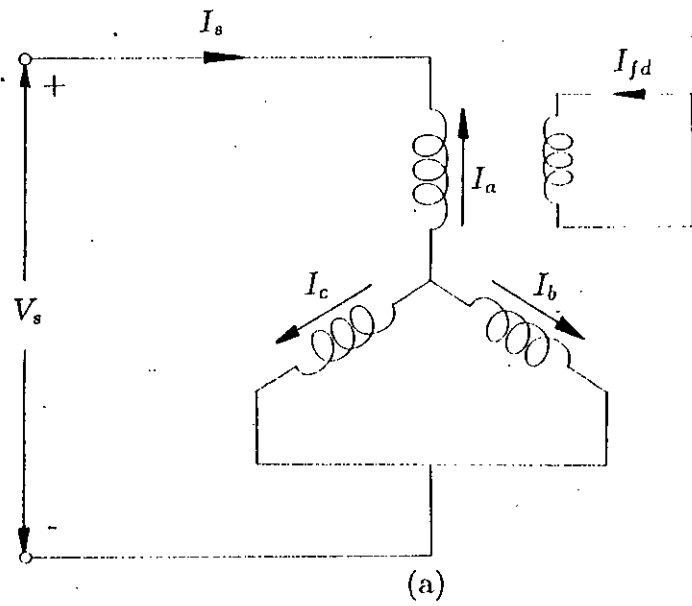
175

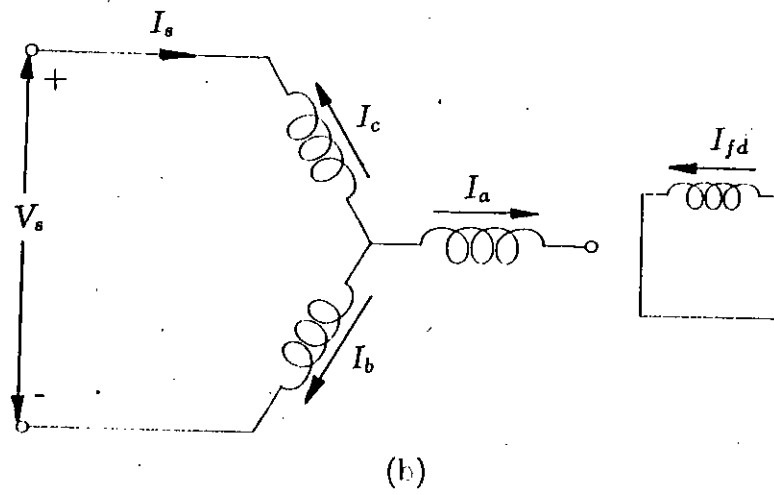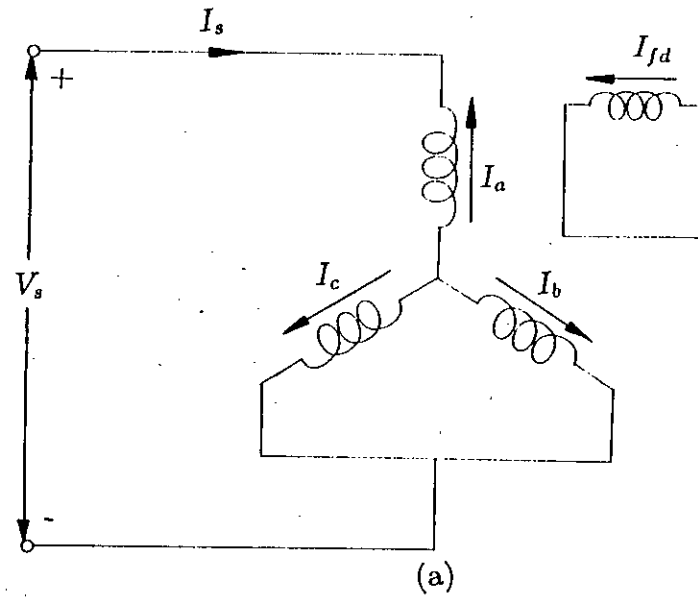Figure B.1: Test configurations for measuring d-q axes impedances: (a) connection-I; (b) connection-II.

176

Figure B.2: Test configurations for measuring d-q axes impedances: (a) connection-I; (b) connection-II.

$$V_q = -\frac{2}{3}[V_a\sin(90) + V_b\sin(-30) + V_b\sin(210)] \tag{B.20}$$

$$= -\frac{2}{3}V_s \tag{B.21}$$

$$\frac{V_q}{I_q} = -\frac{2}{3}\frac{V_s}{I_s} = -\frac{2}{3}Z_s \tag{B.22}$$

B.2.2　Connection-II

In the configuration of Fig. B.1(b), the following relations hold,

$$I_s = I_b = -I_c \tag{B.23}$$

$$I_a = 0 \tag{B.24}$$

$$V_s = V_c = -V_b \tag{B.25}$$

For direct axis measurement, the magnetic axis of the field winding is at 90° to that of phase 'a'. Because of symmetry $V_b = -V_c$, $V_a = 0$ since $I_a = 0$. The voltage and current equations can be written as,

$$I_d = \frac{2}{3}[I_a\cos(90) + I_b\cos(-120) + I_c\cos(210)] \tag{B.26}$$

$$= \frac{2}{\sqrt{3}}I_s \tag{B.27}$$

$$I_q = \frac{2}{3}[I_a\sin(90) + I_b\sin(-30) + I_c\sin(210)] = 0 \tag{B.28}$$

$$I_o = \frac{1}{3}(0 - I_s + I_s) = 0 \tag{B.29}$$

$$V_d = \frac{2}{3}[V_a\cos(90) + V_b\cos(-30) - V_b\cos(210)] \tag{B.30}$$

$$= \frac{4}{3}V_b\cos(30) = -\frac{1}{\sqrt{3}}V_s \tag{B.31}$$

$$V_q = -\frac{2}{3}[V_a\sin(90) + V_b\sin(-30) + V_c\sin(210)] = 0 \tag{B.32}$$

$$V_o = \frac{1}{3}(0 + V_b - V_b) = 0 \tag{B.33}$$

$$z_s = \frac{V_s}{I_s} \tag{B.34}$$

$$\frac{V_d}{I_d} = -\frac{1}{\sqrt{3}}\frac{\sqrt{3}V_s}{2I_s} = -\frac{1}{2}\frac{V_s}{I_s} \tag{B.35}$$

For quadrature axis measurement, the magnetic axis of the field windings is aligned with that of phase 'a', and

$$I_d = \frac{2}{3}\left[I_a\cos(0) + I_b\cos(-120) + I_c\cos(120)\right] = 0 \tag{B.36}$$

$$I_q = -\frac{2}{3}\left[I_a\sin(0) + I_b\sin(-120) + I_c\sin(120)\right] \tag{B.37}$$

$$= \frac{2}{\sqrt{3}}I_s \tag{B.38}$$

$$I_o = \frac{1}{3}(0 + I_s - I_s) = 0 \tag{B.39}$$

$$V_d = \frac{2}{3}\left[V_a\cos(0) + V_b\cos(-120) + -V_c\cos(120)\right] = 0 \tag{B.40}$$

$$V_q = -\frac{2}{3}\left[V_a\sin(0) + V_b\sin(-120) + V_c\sin(120)\right] \tag{B.41}$$

$$= -\frac{1}{3}V_s \tag{B.42}$$

$$\frac{V_q}{I_q} = -\frac{1}{\sqrt{3}}\frac{\sqrt{3}V_s}{2I_s} = -\frac{1}{2}\frac{V_s}{I_s} \tag{B.43}$$

As evident from the above analysis, the $d - q$ axes equivalent impedances of a synchronous machine can be obtained from test measurements of either of the two configurations. In this thesis synchronous machine parameters required for stability analysis have been determined by this input impedance measurement technique.

B.3 Test Procedure

Most of the synchronous machine problems are studied with simplified rotor circuits consisting of one damper coil on the direct axis and one damper coil on the quadrature axis except for special cases, where, more than one damper coils are provided in each axis. Although this simplification is based on certain assumptions, the results obtained with simplified rotor circuit are accurate enough for most purposes. Especially, use of a simplified rotor circuit is conventionally followed in the stability study with small perturbation technique. Therefore, one damper coil on direct axis and one damper coil on quadrature axis are considered for parameter identification as shown in Park's model

of Fig. 3.1 in chapter 3.

In the proposed method the input impedances derived in the previous section are determined by the measurements made at the machine terminals. The stator and field windings are connected according to the arrangements shown in Fig. B.3 for direct axis and for quadrature axis measurements. For better resolution, average impedance can be obtained using both the connections. Direct and quadrature axes are realized through the rotor alignment. The stator leakage inductance and direct and quadrature axes mutual inductances are obtained from the Potier triangle and slip test methods, respectively. The rest of the parameters are derived from the simple stand-still tests by measuring voltages, currents, phase angles, etc. at the stator terminals of the machine. Measurements are carried out by applying a sinusoidal supply voltage having a frequency of 50 Hz.

B.4 · Measurement of Direct and Quadrature axes Quantities

A sinusoidal voltage is applied between the terminals 'b' and 'c' and the terminal 'a' is kept open. The experimental connection is shown in Fig. B.3. The rotor is then rotated until the induced voltage in the field circuit reaches its maximum value. The rotor at this position is considered to be aligned along direct axis of the stator magnetic field. The voltage, current, and phase angle measured in this position are the direct axis quantities. These quantities are recorded for both the open-circuit and short-circuit field terminals. The open circuit measurements include the effect of the damper windings of the rotor circuits only , whereas, short-circuit condition takes into account of both the damper and field windings. Voltages, currents and phase angles are also recorded for direct axis measurement by applying voltage between phase 'a' and the terminals 'b' and 'c' connected together.

Measurements for quadrature axis quantities are performed using the same circuit con-
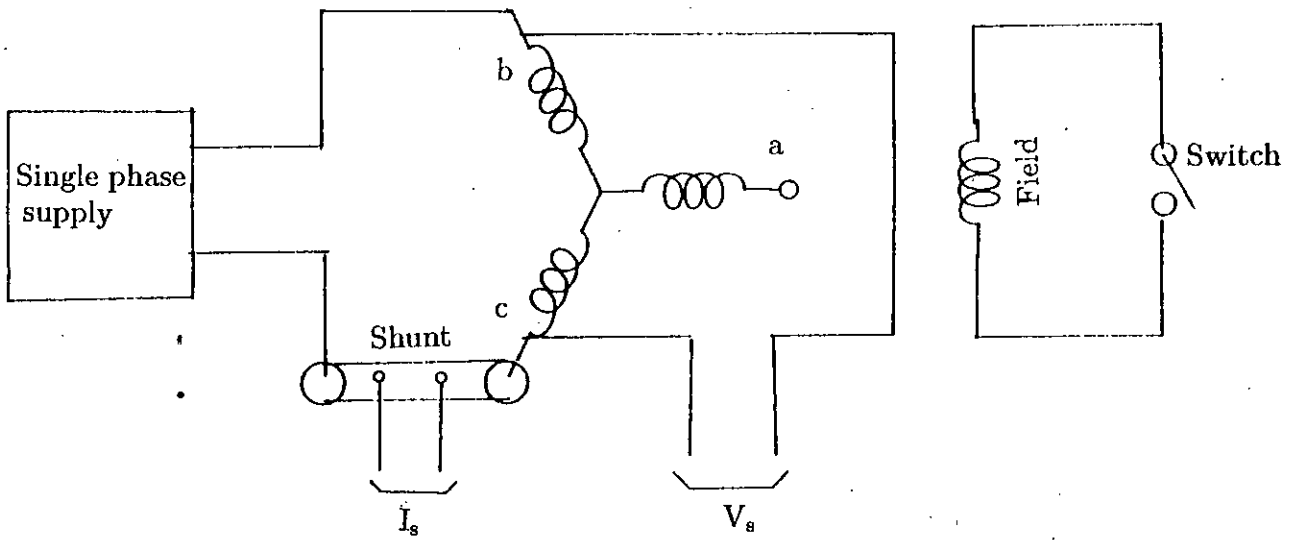
Figure B.3: Experimental connection diagram for measuring
direct and quadrature axes impedances.

nections as in Fig. B.3. In this measurement the rotor is aligned along the quadrature axis, which is realized by rotating the rotor until zero voltage is observed at the terminals of the field winding. The voltage, current, and phase angles recorded in this position are the quadrature axis quantities.

The fundamental components of measured quantities are used for parameter determination. For the sake of better resolution, average values of input impedances are considered. The measured direct and quadrature axes quantities are referred to the stator circuit of the machine.

B.5 Analytical Procedure

Applying the method of phasor algebra, the resistances and reactances of the equivalent circuits for d and q axes are calculated. The fundamental components of the measured quantities are used for the determination of the input impedances. The elements of equivalent circuits shown in Figs. B.4(a), B.4(b) and B.4(c) are all referred to the stator winding. Using these equivalent circuits the unknown parameters are calculated in terms of input impedance and known parameters as follows,

For open-circuited field winding,

$$Z_{d(oc)} = R_s + jX_{ls} + \frac{jX_{md}(R_{kd} + jX_{kd})}{jX_{md} + (R_{kd} + jX_{kd})} \tag{B.44}$$

$$Z_{d(oc)} = R_s + jX_{ls} + \frac{jX_{md}Z_{kd}}{jX_{md} + Z_{kd}} \tag{B.45}$$

where, $Z_{kd} = R_{kd} + jX_{kd}$

$$R_{kd} + jX_{kd} = Z_{kd} = \frac{jX_{md}(Z_{d(oc)} - R_s - jX_{ls})}{R_s + jX_{ls} + jX_{md} - Z_{d(oc)}} \tag{B.46}$$

Knowing all other variables in equation (B.46), the direct axis damper resistance and reactance can be determined by equating the real and imaginary parts.
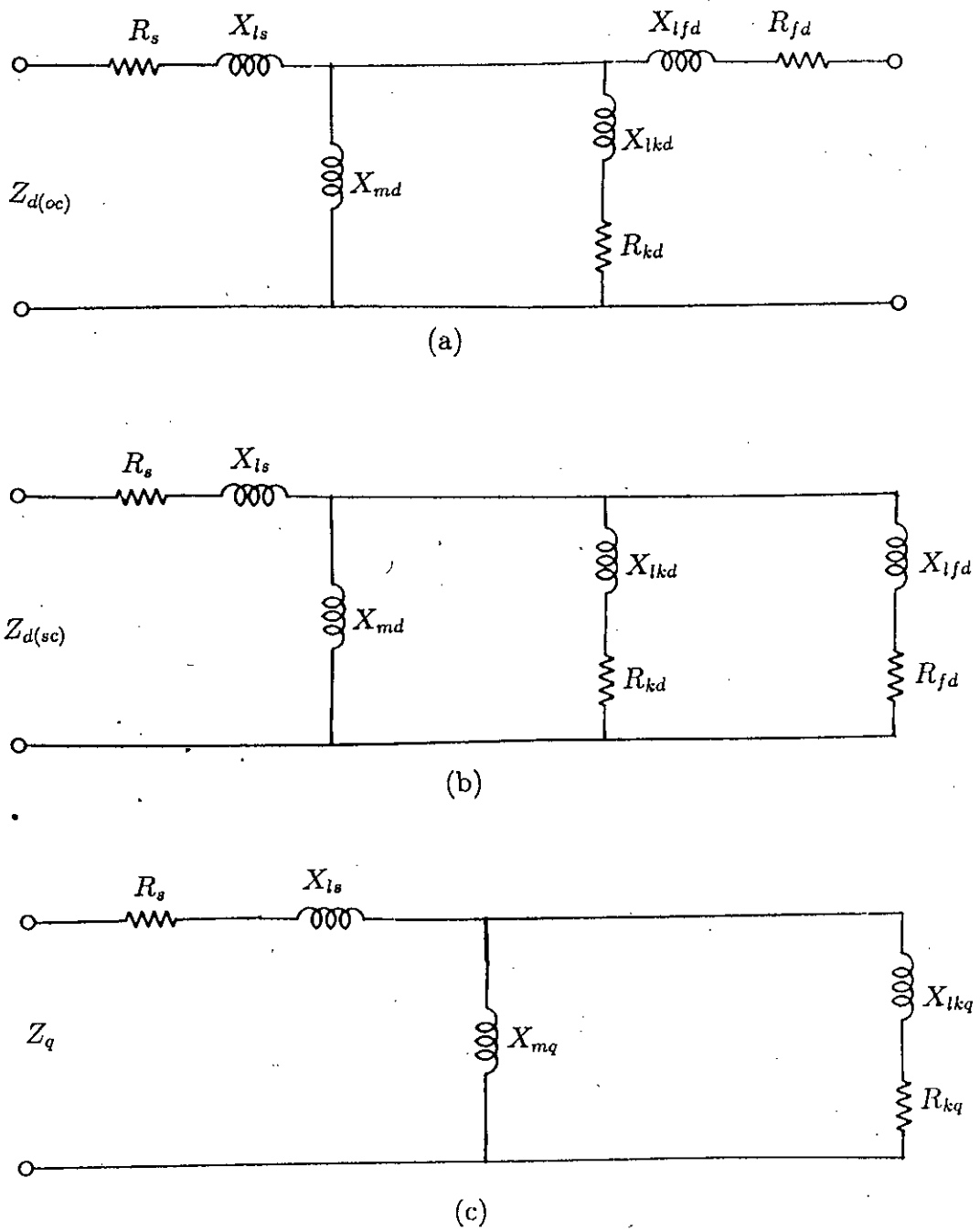
Figure B.4: Equivalent circuit for input impedance calculation:
(a)d-axis impedance from open-circuited field;
(b)d-axis impedance from short-circuited field;
(c) q-axis impedance.

For short-circuited field winding,

$$Z_{d(sc)} = R_s + jX_{ls} + \frac{jX_{md}(R_{kd} + jX_{kd})(R_{fd} + jX_{fd})}{jX_{md} + (R_{kd} + jX_{kd}) + (R_{fd} + jX_{fd})} \quad \text{(B.47)}$$

$$= R_s + jX_{ls} + \frac{jX_{md}Z_{kd}Z_{fd}}{jX_{md} + Z_{kd} + Z_{fd}} \quad \text{(B.48)}$$

where, $Z_{fd} = R_{fd} + jX_{fd}$

$$R_{fd} + jX_{fd} = Z_{fd} = \frac{jX_{md}Z_{kd}(R_s - jX_{ls} - Z_{d(sc)})}{Z_{d(sc)}(jX_{md} + Z_{kd}) - (R_s - jX_{ls})(jX_{md} + Z_{kd}) - jX_{md}Z_{kd}} \quad \text{(B.49)}$$

The resistance and reactance of the field winding can thus be found by equating the real and imaginary parts of Equation (B.49).

For quadrature axis parameters,

$$Z_q = R_s + jX_{ls} + \frac{jX_{mq}(R_{kq} + jX_{kq})}{jX_{mq} + (R_{kq} + jX_{kq})} \quad \text{(B.50)}$$

$$= R_s + jX_{ls} + \frac{jX_{mq}Z_{kq}}{jX_{mq} + Z_{kq}} \quad \text{(B.51)}$$

where, $Z_{kq} = R_{kq} + jX_{kq}$

$$R_{kq} + jX_{kq} = Z_{kq} = \frac{jX_{md}(Z_q - R_s - jX_{ls})}{R_s + jX_{ls} + jX_{md} - Z_q} \quad \text{(B.52)}$$

The quadrature axis damper resistance and reactance can be determined by equating the real and imaginary parts of equation (B.52).

The elements of the equivalent circuits are all referred to the stator winding of the synchronous machine.

The proposed tests have been performed in the laboratory on two synchronous machines, one 1/4 HP and another 9 KVA and the results obtained for 1/4 HP machine are presented for observation. The parameters of the machine determined using the proposed method are given in table B.1.

Table B.1: Synchronous machine ratings and parameters

Volts	380 V (L-L)
VA	175 VA
Frequency	50 Hz.
No. of Poles	4
Rotor inertia, J	2.81×10^{-3} kg-m^2
Stator resistance, R_s	51.25
Stator leakage reactance, X_{ls}	50.03
Q-axis mutual reactance, X_q	452.29
D-axis mutual reactance, X_d	45.22
Q-axis damper resistance, R_{kq}	31.395
Q-axis damper reactance, X_{lkq}	45.22
D-axis damper resistance, R_{kd}	21.85
D-axis damper reactance, X_{lkd}	48.72
Field circuit resistance, R_{fd}	36.99
Field circuit reactance, X_{lfd}	457.84

Table B.2: Time constants of the synchronous machine

Short-circuit time constants		
Time constants	Calculated vaules in msec.	Experimental values in msec.
τ_d'	38.00	40.00
τ_d''	13.03	15

B.6 Experimental Results

In order to show the validity of the method described in this appendix, it is considered convenient to calculate the time constants associated with the synchronous machine. The direct axis transient and subtransient time constants are expressed in terms of machine parameters as given in reference [80],

$$\tau_d' = \frac{1}{\omega_b R_{fd}} \left(X_{lfd} + \frac{X_{md} X_{ls}}{X_{ls} + X_{md}} \right) \tag{B.53}$$

$$\tau_d'' = \frac{1}{\omega_b R_{kd}} \left(X_{lkd} + \frac{X_{md} X_{ls} X_{lfd}}{X_{md} X_{ls} + X_{md} X_{lfd} + X_{ls} X_{lfd}} \right) \tag{B.54}$$

Three phase short-circuit tests have been carried out in the laboratory on the synchronous machine, the oscilloscope record of which is shown in Fig. B.6. The transient and subtransient time constants determined from the oscilloscope trace are compared with those obtained from equations (B.53) and (B.54) and are given in table B.2. A reasonably good agreement is found between the experimental and calculated results.

An indirect verification method is provided through the study of the starting performance of the synchronous machine. A computer program has been developed to investigate the starting performance using equations (3.34) to (3.43). The program is executed using the machine parameters obtained from the proposed test method. The simulated starting performance is shown in Fig. B.7. The starting performance of the machine is also obtained experimentally and the oscilloscope trace is shown in Fig. B.8. The magnitude of the starting current and time taken to reach the steady-state condition are noted for the experimental trace as well as for theoretical output. Comparison of the results of the starting performances indicates that the proposed parameter estimation method in this appendix is valid for synchronous machines. Also simulated short-circuit test result as obtained by solution of differential equations of the synchronous machine using fourth order Runge-Kutta method is provided in Fig. B.5. The simulated short-

circuit trace of the stator current justifies the time constants of experimental result with theoretical ones, indicating the validity of the method to close proximity.
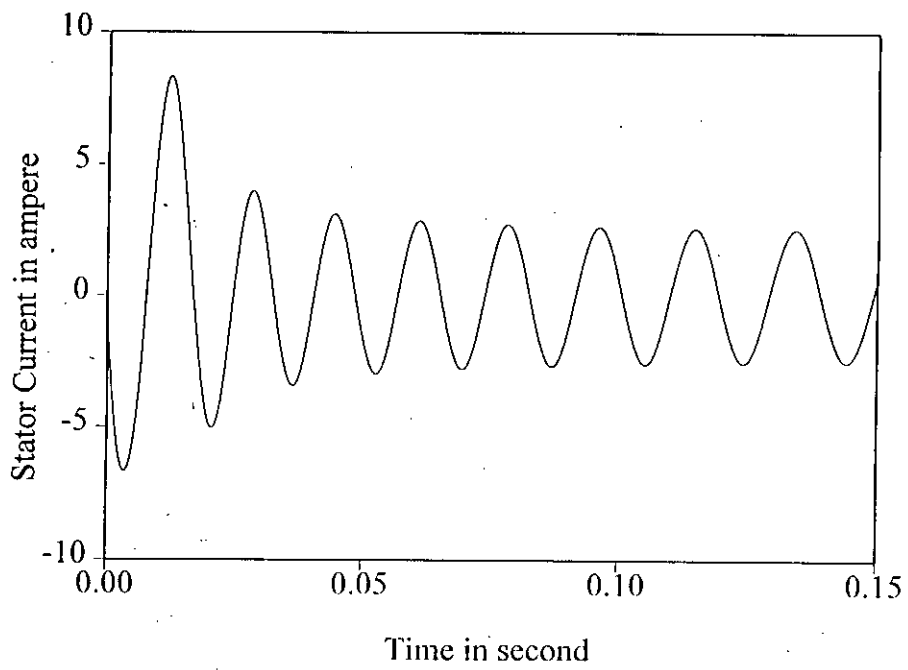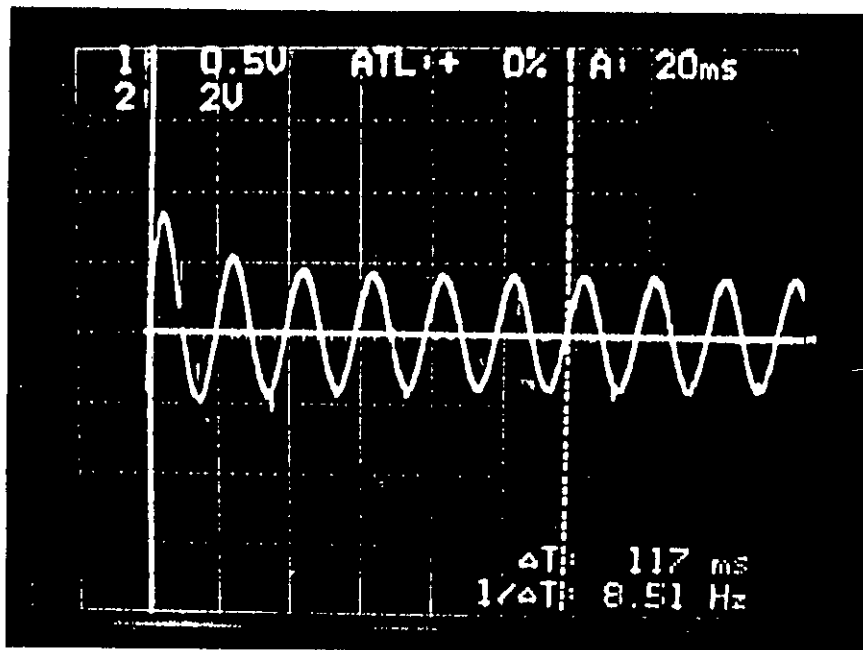
Figure B.5: Simulation of 3ϕ short-circuit current

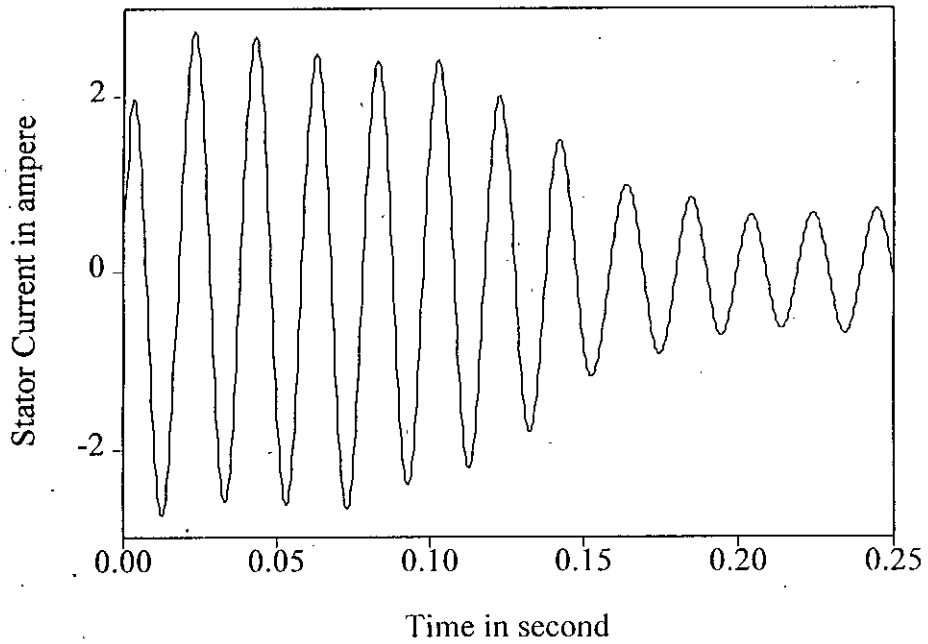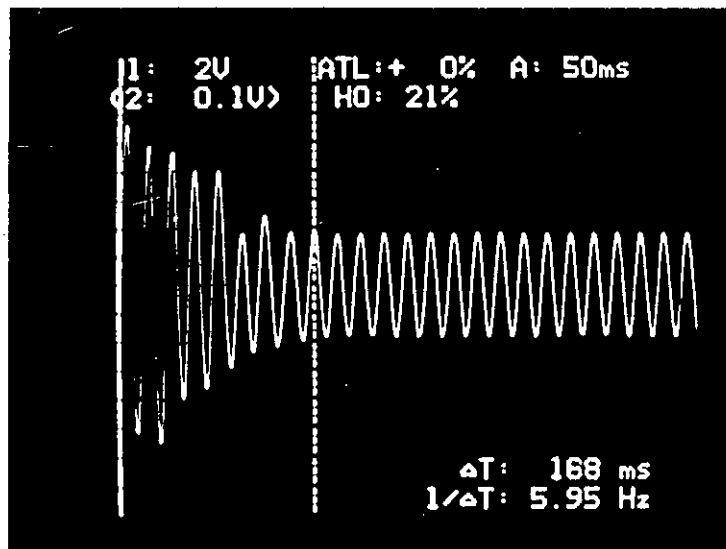Figure B.6: Oscilloscope record of 3ϕ short-circuit current

Figure B.7: Simulation of starting current

Figure B.8: Osilloscope trace of starting current